

SYNTHESIS OF SULFONAMIDE CHALCONES AS α -GLUCOSIDASE INHIBITORS



A Thesis Submitted in Partial Fulfillment of the Requirements
for the Degree of Master of Science in Chemistry

Department of Chemistry

FACULTY OF SCIENCE

Chulalongkorn University

Academic Year 2020

Copyright of Chulalongkorn University

การสังเคราะห์สัลโฟนามีดแคลโคนเพื่อเป็นสารยับยั้งแอลฟาไกลูโคซิเดส



วิทยานิพนธ์นี้เป็นส่วนหนึ่งของการศึกษาตามหลักสูตรปริญญาวิทยาศาสตรมหาบัณฑิต
สาขาวิชาเคมี ภาควิชาเคมี
คณะวิทยาศาสตร์ จุฬาลงกรณ์มหาวิทยาลัย
ปีการศึกษา 2563
ลิขสิทธิ์ของจุฬาลงกรณ์มหาวิทยาลัย

ไอ พุต สุคนาติ : การสังเคราะห์ซัลโฟนามิดแคลโคนเพื่อเป็นสารยับยั้งแอลฟาไกลูโคซิเดส.
(SYNTHESIS OF SULFONAMIDE CHALCONES AS α -GLUCOSIDASE INHIBITORS) อ.ที่ปรึกษาหลัก : วรินทร์ ขวศิริ

โรคเบาหวานเกิดจากภาวะการหลั่งอินซูลินที่ไม่เพียงพอหรือภาวะดื้อต่ออินซูลิน ทำให้เกิดภาวะแทรกซ้อนของโรคที่เกิดกับเส้นเลือดขนาดใหญ่และขนาดเล็กในระยะยาว พบโรคเบาหวานแบบที่สองมากกว่าร้อยละ 90 ทั่วโลก วิธีการหนึ่งในการบำบัดความผิดปกตินี้คือ การใช้ตัวยับยั้งแอลฟาไกลูโคซิเดส มีรายงานว่าซัลโฟนามิดและแคลโคนบางชนิดมีประสิทธิภาพในการลดภาวะน้ำตาลในเลือดสูง ได้สังเคราะห์สารในกลุ่มซัลโฟนามิดแคลโคนสี่สิบเจ็ดตัวด้วยปฏิกิริยา Claisen-Schmidt โดยมีหมู่แทนที่บนวงแหวน A, B, และ C หลากชนิดด้วยร้อยละผลผลิต 50-95 และได้ทดสอบฤทธิ์ยับยั้งแอลฟาไกลูโคซิเดส พบว่าสารยี่สิบเก้าตัวแสดงฤทธิ์ยับยั้งสูงมากด้วยค่า IC_{50} ต่ำกว่า $10 \mu M$ สารสิบเอ็ดตัวแสดงฤทธิ์ยับยั้งสูง (IC_{50} 10-49.9 μM) สารแปดตัวแสดงฤทธิ์ยับยั้งปานกลาง (IC_{50} 50-99.9 μM) สารห้าตัวแสดงฤทธิ์อ่อน (IC_{50} 100-199.9 μM) และสารสองตัวไม่แสดงฤทธิ์ (IC_{50} >200 μM) ซัลโฟนามิดแคลโคนที่มีหมู่ NHR บนวงแหวน A ที่ตำแหน่งพารา (62) แสดงฤทธิ์ยับยั้งแอลฟาไกลูโคซิเดสสูงเช่นเดียวกับสารที่มีหมู่ 3-methoxy (65) บนวงแหวน B สารที่มีหมู่แทนที่แอลคิลบนวงแหวน B (67-72) แสดงฤทธิ์ยับยั้งที่สูงมาก เช่นเดียวกับสารที่มีหมู่แทนที่ไฮโลเจน (73-75) นำประหลาดใจที่สารที่ไม่มีหมู่แทนที่ใด (63) ก็แสดงฤทธิ์ยับยั้งที่สูงมากด้วยค่า IC_{50} $0.07 \pm 0.01 \mu M$ นอกจากนั้นสารที่มีหมู่แทนที่สองหมู่บนวงแหวน B เช่น 3-hydroxy-4-methoxy (86) แสดงฤทธิ์ที่ตีมากด้วยค่า IC_{50} $0.12 \pm 0.01 \mu M$ โดยทั่วไปพบว่าหมู่แทนที่บนวงแหวน C เพิ่มฤทธิ์การยับยั้งแอลฟาไกลูโคซิเดสอย่างมีนัยสำคัญ หมู่แทนที่ 4-methoxy (94) มีฤทธิ์เพิ่มมากกว่าสารที่ไม่มีหมู่แทนที่ (92) 783 เท่า เมื่อเปรียบเทียบกับซัลโฟนามิดแอซิโทฟิโนน ซัลโฟนามิดแคลโคนมีฤทธิ์สูงกว่าในช่วง 4-38 เท่า จากการศึกษาลินเวอเวอร์-เบิร์กพล็อตสำหรับสาร 62 และ 86 พบว่ารูปแบบการยับยั้งเป็นแบบ uncompetitive ในขณะที่สาร 63 และ 94 เป็นตัวยับยั้งแบบ non-competitive และ mixed-mode ตามลำดับ.

จุฬาลงกรณ์มหาวิทยาลัย
CHULALONGKORN UNIVERSITY

สาขาวิชา เคมี
ปีการศึกษา 2563

ลายมือชื่อนิสิต

ลายมือชื่อ อ.ที่ปรึกษาหลัก

6270119523 : MAJOR CHEMISTRY

KEYWORD: Sulfonamide Chalcone α -Glucosidase Diabetes mellitus

I Putu Sukanadi : SYNTHESIS OF SULFONAMIDE CHALCONES AS α -GLUCOSIDASE INHIBITORS.

Advisor: Asst. Prof. Dr. WARINTHORN CHAVASIRI

Diabetes mellitus occurs from deficiencies in insulin secretion or insulin resistance which leads over time to high risk for long-term macro-and microvascular complications. Diabetes mellitus type 2 contributes to more than 90% of all cases worldwide. One approach of treatment for this disorder is utilizing α -glucosidase inhibitors. Certain sulfonamides and chalcones are considered as viable candidates that are effective in reducing hyperglycemia. Forty-seven sulfonamide chalcones were synthesized by the Claisen-Schmidt reaction with various substituents on the A, B, and C-rings furnishing the desired products with 50-95 %yield. All compounds were-tested for α -glucosidase inhibitory activity. Twenty-nine compounds exhibited a very strong inhibitory activity with IC_{50} below 10 μ M, eleven with strong activity (IC_{50} 10-49.9 μ M), eight with moderate activity (IC_{50} 50-99.9 μ M), five with weak activity (IC_{50} 100-199.9 μ M), and two not active (IC_{50} >200 μ M). The sulfonamide chalcones bearing *p*-NHR on the A-ring (62) strongly influenced α -glucosidase inhibition, as well as 3-methoxy (65) on the B-ring. The alkyl substituents (67-72) on the B-ring gave a very strong inhibitory activity and followed by the halogen substituents (73-75). Surprisingly, 63 without any substituent also displayed a very strong inhibitory activity with IC_{50} 0.07 \pm 0.01 μ M. Moreover, disubstituents on the B-ring such as 3-hydroxy-4-methoxy (86) revealed superior activity with IC_{50} 0.12 \pm 0.01 μ M. In general, the substituent on the C-ring gave a significant increment of the α -glucosidase inhibitory activity. The 4-methoxy substituent (94) increased the activity by 783 times more than the unsubstituent one (92). Comparing with sulfonamide acetophenones, the sulfonamide chalcones increased the activity by the value of 4-38 times. From Lineweaver-Burk plot for 62 and 86, the inhibition type was disclosed to be uncompetitive while those for 63 and 94 were non-competitive and mixed-mode inhibitors, respectively.

Field of Study: Chemistry

Student's Signature

Academic Year: 2020

Advisor's Signature

ACKNOWLEDGEMENTS

The author would like to express his gratitude, respect, and sincere appreciation to his advisor Assistant Professor Dr. Warinthorn Chavasiri who always encourages and takes care of the author from every difficult situation. Thanks to his advisor, the author was motivated and got out of difficult times, in consequence, he was able to maintain the confidence to do good research work. The author believes that "failure is a motivation and action is the solution", so there is no giving up in life.

The author is most grateful to Professor Dr. Khanitha Pudhom as chairman, and Professor Dr. Paitoon Rashatasakhon, and Dr. Poochit Nonejuie as the committees who provided suggestions and comments in the completion of this thesis thoroughly in the best way. The author would like to express his happiness for their attendance in the author's thesis defense.

The author would like to thank Mr. Ade Danova, a Ph.D. student who has helped the author in biological activity testing. In addition, he has also given advice and learning that supports the author in completing the research and writing a thesis.

On this opportunity, the author also would like to express his sincere thankfulness to all of the sponsors of ASEAN and Non-ASEAN scholarship who supported the author's tuition and living fees during the pursuit of a Master's degree at Chulalongkorn University.

Moreover, the author would like to thank all members of the WC lab, especially a Ph.D. student, Mr. Duy Vu Nguyen, and others who have always supported the author both academically and in research. Their care and friendliness make the author always in a state of excitement and happiness.

Finally, the author would like to express his sincere gratitude and respect to the author's parents. Thanks to their blessings and prayers, the author was able to go through the ups and downs in pursuing his master's degree abroad. In this world, there are no words that can describe the sincerity of their love and sacrifice for the author's success.

I Putu Sukanadi

TABLE OF CONTENTS

	Page
ABSTRACT (THAI).....	iii
ABSTRACT (ENGLISH).....	iv
ACKNOWLEDGEMENTS	v
TABLE OF CONTENTS	vi
LIST OF TABLES	x
LIST OF FIGURES	xi
LIST OF ABBREVIATIONS	xviii
CHAPTER I INTRODUCTION.....	1
1.1 Chalcones	2
1.2 Sulfonamides	4
1.3 Sulfonamide chalcones	7
1.4 Diabetes mellitus.....	8
1.4.1 Diabetes mellitus type 1	8
1.4.2 Diabetes mellitus type 2	9
1.5 α -Glucosidase inhibitors.....	10
1.6 Objective of this research.....	12
CHAPTER II EXPERIMENTAL	13
2.1 Instruments	13
2.2 General materials.....	13
2.3 Preparation of p-toluenesulfonyl aminoacetophenones ³⁷	13
2.4 Preparation of sulfonamide chalcones ³⁸	14

2.4.1 Preparation of sulfonamide chalcones (60-62)	15
2.4.2 Preparation of sulfonamide chalcones (63-76)	16
2.4.3 Preparation of sulfonamide chalcones with disubstituent on B-ring (77-83) 20	
2.4.4 Preparation of sulfonamide chalcones with disubstituent (OH, OCH ₃ , and OCH ₂ OCH ₂ CH ₃) on B-ring (84-88).....	23
2.4.4.1 Preparation of protected benzaldehydes.....	23
2.4.4.2 Preparation of sulfonamide chalcones bearing protecting groups and deprotecting groups from chalcones.....	23
2.4.5 Preparation of sulfonamide chalcones with dichloro substituent on B-ring (89-91) 25	
2.5 Preparation of sulfonamide chalcones with 3,4 dimethoxy on B-ring	26
2.5.1 Preparation of sulfonamide chalcones with unsubstituent and monosubstituent on C-ring (92-99).....	26
2.5.2 Preparation of sulfonamide chalcones with disubstituent on C-ring (100- 103) 29	
2.6 Preparation of benzenesulfonyl aminoacetophenones (104-111).....	31
2.7 Preparation of 4-acetyl- <i>N</i> -phenylbenzenesulfonamide with un- and monosubstituent.....	33
2.7.1 Preparation of benzenesulfonamide chalcones with 3,4-dimethoxy (112- 114) 34	
2.8 α -Glucosidase inhibitory activity	35
2.8.1 α -Glucosidase inhibitory assay ⁴⁰	35
2.8.2 Kinetic study of α -glucosidase inhibition ⁴⁰	36
CHAPTER III RESULTS AND DISCUSSION.....	37

3.1 Synthesis and evaluation of sulfonamide chalcones with <i>o</i> -, <i>m</i> -, and <i>p</i> - position of NHR and 3,4-dimethoxy group on B-ring.....	37
3.1.1 Synthesis and structural elucidation	37
3.1.2 α -Glucosidase inhibitory activity evaluation	38
3.2 Synthesis and evaluation of sulfonamide chalcones with un- and monosubstituent on B-ring	40
3.2.1 Synthesis and structural elucidation	40
3.2.2 α -Glucosidase inhibitory activity evaluation	40
3.3 Synthesis and evaluation of sulfonamide chalcones with disubstituent on B- ring	44
3.3.1 Synthesis and structural elucidation	44
3.3.2 α -Glucosidase inhibitory activity evaluation	45
3.4 Synthesis and evaluation of sulfonamide chalcones with un-, monosubstituent and disubstituent on C-ring	48
3.4.1 Synthesis and structural elucidation	48
3.4.2 α -Glucosidase inhibitory activity evaluation	48
3.5 Synthesis and evaluation of sulfonamide acetophenones.....	51
3.5.1 Synthesis and structural elucidation	51
3.5.2 α -Glucosidase inhibitory activity evaluation	51
3.6 Synthesis and evaluation of benzenesulfonamide chalcones with 3,4 dimethoxy in B-ring.....	54
3.6.1 Synthesis and structural elucidation	54
3.6.2 α -Glucosidase inhibitory activity evaluation	54
3.7 Kinetic study	56
CHAPTER 4 CONCLUSIONS	59

APPENDIX.....	61
REFERENCES	138
VITA.....	145



LIST OF TABLES

Table 3.1 Effects of the position of sulfonamide group on A-ring against α -glucosidase	39
Table 3.2 Effects of un- and monosubstituents on B-ring against α -glucosidase	41
Table 3.3 Effects of disubstituent on B-ring against α -glucosidase	45
Table 3.4 Effects of un-, monosubstituents and disubstituent on C-ring against α -glucosidase.....	49
Table 3.5 Effects of sulfonamide acetophenones against α -glucosidase.....	52
Table 3.6 Effects of benzenesulfonamide chalcones against α -glucosidase.....	55



LIST OF FIGURES

Figure 1.1	Core structure of chalcone.....	2
Figure 1.2	Reported chalcones 1-8 as α -glucosidase inhibitors	3
Figure 1.3	Reported chalcones 9-20 as α -glucosidase inhibitors.....	3
Figure 1.4	Reported chalcones 21-24 as α -glucosidase inhibitors	4
Figure 1.5	Intestinal metabolism of prontosil.....	4
Figure 1.6	Reported sulfonylureas 27-30 as anti-diabetes mellitus	5
Figure 1.7	Reported pyridine sulfonamide 31-39 as α -glucosidase inhibitors	6
Figure 1.8	Reported Chromone hydrazone sulfonamide 40-42 as α -glucosidase inhibitors.....	6
Figure 1.9	Reported piperazine sulfonamide 43-48 as α -amylase inhibitors.....	7
Figure 1.10	Reported chalcones and sulfonamide chalcones 49-56 as α -glucosidase inhibitors.....	7
Figure 1.11	Early stages of type 1 diabetes.....	9
Figure 1.12	Natural history and clinical staging of diabetes	10
Figure 1.13	Acarbose.....	11
Figure 1.14	Mechanism of action of acarbose.....	12
Figure 2.1	The structures of <i>p</i> -toluenesulfonyl aminoacetophenones (57-59)	14
Figure 2.2	The structures of synthesized sulfonamide chalcones (60-62).....	15
Figure 2.3	The structures of synthesized sulfonamide chalcones (63-76).....	16
Figure 2.4	The structures of synthesized sulfonamide chalcones with disubstituent on B-ring (77-83).....	20
Figure 2.5	The structures of synthesized sulfonamide chalcones (84-88).....	23
Figure 2.6	The structures of synthesized sulfonamide chalcones with dichlorosubstituent on B-ring (89-91).....	25
Figure 2.7	The structures of synthesized sulfonamide chalcones with unsubstituent and monosubstituents on C-ring (92-99)	27
Figure 2.8	The structures of synthesized sulfonamide chalcones with disubstituents on C-ring (100-103).....	30

Figure 2.9 The structures of synthesized benzenesulfonyl aminoacetophenones (104-111).....	32
Figure 2.10 The structures of synthesized 4-acetyl- <i>N</i> -phenylbenzenesulfonamide (112-114).....	34
Figure 3.1 Synthesis of sulfonamide chalcones (60-62).....	38
Figure 3.2 Synthesis of sulfonamide chalcones (63-76).....	40
Figure 3.3 The IC ₅₀ graph of α -glucosidase inhibitors 64-66.....	42
Figure 3.4 The IC ₅₀ graph of α -glucosidase inhibitors 64-72.....	43
Figure 3.5 Synthesis of sulfonamide chalcones (77-91).....	44
Figure 3.6 The IC ₅₀ graph of α -glucosidase inhibitors 62 and 77-81.....	46
Figure 3.7 The IC ₅₀ graph of α -glucosidase inhibitors 62 and 83-88.....	47
Figure 3.8 Synthesis of sulfonamide chalcones (92-103).....	48
Figure 3.9 The IC ₅₀ graph of α -glucosidase inhibitors 92-98 and 100-103.....	50
Figure 3.10 Synthesis of sulfonamide acetophenones (59, 104-111).....	51
Figure 3.11 The IC ₅₀ graph of α -glucosidase inhibitors 59 and 104-111.....	53
Figure 3.12 Graph of IC ₅₀ comparison between sulfonamide acetophenones and sulfonamide chalcones.....	53
Figure 3.13 Synthesis of benzenesulfonamide chalcones (112-114).....	54
Figure 3.14 Graph of IC ₅₀ comparison between general sulfonamide chalcones and benzenesulfonamide chalcones.....	55
Figure 3.15 Lineweaver–Burk plot analysis, K _m (μ M) and V _{max} (μ M/min) of 62 (A), 63 (B), 86 (C) and 94 (D).....	57
Figure 3.16 Lineweaver–Burk plots illustrating competitive, uncompetitive, and non-competitive inhibition.....	58
Figure A.1 The ¹ H NMR spectrum (DMSO- <i>d</i> ₆ , 500 MHz) of 57.....	61
Figure A.2 The ¹³ C NMR spectrum (DMSO- <i>d</i> ₆ , 125 MHz) of 57.....	61
Figure A.3 The ¹ H NMR spectrum (DMSO- <i>d</i> ₆ , 500 MHz) of 58.....	62
Figure A.4 The ¹³ C NMR spectrum (DMSO- <i>d</i> ₆ , 125 MHz) of 58.....	62
Figure A.5 The ¹ H NMR spectrum (DMSO- <i>d</i> ₆ , 500 MHz) of 59.....	63
Figure A.6 The ¹³ C NMR spectrum (DMSO- <i>d</i> ₆ , 125 MHz) of 59.....	63

Figure A.7	The ^1H NMR spectrum (DMSO- d_6 , 500 MHz) of 60	64
Figure A.8	The ^{13}C NMR spectrum (DMSO- d_6 , 125 MHz) of 60	64
Figure A.9	The ^1H NMR spectrum (DMSO- d_6 , 500 MHz) of 61	65
Figure A.10	The ^{13}C NMR spectrum (DMSO- d_6 , 125 MHz) of 61	65
Figure A.11	The ^1H NMR spectrum (DMSO- d_6 , 500 MHz) of 62	66
Figure A.12	The ^{13}C NMR spectrum (DMSO- d_6 , 125 MHz) of 62	66
Figure A.13	The ^1H NMR spectrum (DMSO- d_6 , 500 MHz) of 63	67
Figure A.14	The ^{13}C NMR spectrum (DMSO- d_6 , 125 MHz) of 63	67
Figure A.15	The ^1H NMR spectrum (DMSO- d_6 , 500 MHz) of 64	68
Figure A.16	The ^{13}C NMR spectrum (DMSO- d_6 , 125 MHz) of 64	68
Figure A.17	The ^1H NMR spectrum (DMSO- d_6 , 500 MHz) of 65	69
Figure A.18	The ^{13}C NMR spectrum (DMSO- d_6 , 125 MHz) of 65	69
Figure A.19	The ^1H NMR spectrum (DMSO- d_6 , 500 MHz) of 66	70
Figure A.20	The ^{13}C NMR spectrum (DMSO- d_6 , 125 MHz) of 66	70
Figure A.21	The ^1H NMR spectrum (DMSO- d_6 , 500 MHz) of 67	71
Figure A.22	The ^{13}C NMR spectrum (DMSO- d_6 , 125 MHz) of 67	71
Figure A.23	The ^1H NMR spectrum (DMSO- d_6 , 500 MHz) of 68	72
Figure A.24	The ^{13}C NMR spectrum (DMSO- d_6 , 125 MHz) of 68	72
Figure A.25	The ^1H NMR spectrum (DMSO- d_6 , 500 MHz) of 69	73
Figure A.26	The ^{13}C NMR spectrum (DMSO- d_6 , 125 MHz) of 69	73
Figure A.27	The ^1H NMR spectrum (DMSO- d_6 , 500 MHz) of 70	74
Figure A.28	The ^{13}C NMR spectrum (DMSO- d_6 , 125 MHz) of 70	74
Figure A.29	The ^1H NMR spectrum (DMSO- d_6 , 500 MHz) of 71	75
Figure A.30	The ^{13}C NMR spectrum (DMSO- d_6 , 125 MHz) of 71	75
Figure A.31	The ^1H NMR spectrum (DMSO- d_6 , 500 MHz) of 72	76
Figure A.32	The ^{13}C NMR spectrum (DMSO- d_6 , 125 MHz) of 72	76
Figure A.33	The ^1H NMR spectrum (DMSO- d_6 , 500 MHz) of 73	77
Figure A.34	The ^{13}C NMR spectrum (DMSO- d_6 , 125 MHz) of 73	77
Figure A.35	The ^1H NMR spectrum (DMSO- d_6 , 500 MHz) of 74	78
Figure A.36	The ^{13}C NMR spectrum (DMSO- d_6 , 125 MHz) of 74	78
Figure A.37	The ^1H NMR spectrum (DMSO- d_6 , 500 MHz) of 75	79

Figure A.38	The ^{13}C NMR spectrum (DMSO- d_6 , 125 MHz) of 75	79
Figure A.39	The ^1H NMR spectrum (DMSO- d_6 , 500 MHz) of 76	80
Figure A.40	The ^{13}C NMR spectrum (DMSO- d_6 , 125 MHz) of 76	80
Figure A.41	The ^1H NMR spectrum (DMSO- d_6 , 500 MHz) of 77	81
Figure A.42	The ^{13}C NMR spectrum (DMSO- d_6 , 125 MHz) of 77	81
Figure A.43	The ^1H NMR spectrum (DMSO- d_6 , 500 MHz) of 78	82
Figure A.44	The ^{13}C NMR spectrum (DMSO- d_6 , 125 MHz) of 78	82
Figure A.45	The ^1H NMR spectrum (DMSO- d_6 , 400 MHz) of 79	83
Figure A.46	The ^{13}C NMR spectrum (DMSO- d_6 , 100 MHz) of 79	83
Figure A.47	The ^1H NMR spectrum (DMSO- d_6 , 500 MHz) of 80	84
Figure A.48	The ^{13}C NMR spectrum (DMSO- d_6 , 125 MHz) of 80	84
Figure A.49	The ^1H NMR spectrum (DMSO- d_6 , 500 MHz) of 81	85
Figure A.50	The ^{13}C NMR spectrum (DMSO- d_6 , 125 MHz) of 81	85
Figure A.51	The ^1H NMR spectrum (DMSO- d_6 , 500 MHz) of 82	86
Figure A.52	The ^{13}C NMR spectrum (DMSO- d_6 , 125 MHz) of 82	86
Figure A.53	The ^1H NMR spectrum (DMSO- d_6 , 500 MHz) of 83	87
Figure A.54	The ^{13}C NMR spectrum (DMSO- d_6 , 125 MHz) of 83	87
Figure A.55	The ^1H NMR spectrum (DMSO- d_6 , 500 MHz) of 84	88
Figure A.56	The ^{13}C NMR spectrum (DMSO- d_6 , 125 MHz) of 84	88
Figure A.57	The ^1H NMR spectrum (DMSO- d_6 , 500 MHz) of 85	89
Figure A.58	The ^{13}C NMR spectrum (DMSO- d_6 , 125 MHz) of 85	89
Figure A.59	The ^1H NMR spectrum (DMSO- d_6 , 500 MHz) of 86	90
Figure A.60	The ^{13}C NMR spectrum (DMSO- d_6 , 125 MHz) of 86	90
Figure A.61	The ^1H NMR spectrum (DMSO- d_6 , 500 MHz) of 87	91
Figure A.62	The ^{13}C NMR spectrum (DMSO- d_6 , 125 MHz) of 87	91
Figure A.63	The ^1H NMR spectrum (DMSO- d_6 , 500 MHz) of 88	92
Figure A.64	The ^{13}C NMR spectrum (DMSO- d_6 , 125 MHz) of 88	92
Figure A.65	The ^1H NMR spectrum (DMSO- d_6 , 500 MHz) of 89	93
Figure A.66	The ^{13}C NMR spectrum (DMSO- d_6 , 125 MHz) of 89	93
Figure A.67	The ^1H NMR spectrum (DMSO- d_6 , 500 MHz) of 90	94
Figure A.68	The ^{13}C NMR spectrum (DMSO- d_6 , 125 MHz) of 90	94

Figure A.69	The ^1H NMR spectrum (DMSO- d_6 , 500 MHz) of 91	95
Figure A.70	The ^{13}C NMR spectrum (DMSO- d_6 , 125 MHz) of 91	95
Figure A.71	The ^1H NMR spectrum (DMSO- d_6 , 500 MHz) of 92	96
Figure A.72	The ^{13}C NMR spectrum (DMSO- d_6 , 125 MHz) of 92	96
Figure A.73	The ^1H NMR spectrum (DMSO- d_6 , 500 MHz) of 93	97
Figure A.74	The ^{13}C NMR spectrum (DMSO- d_6 , 125 MHz) of 93	97
Figure A.75	The ^1H NMR spectrum (DMSO- d_6 , 500 MHz) of 94	98
Figure A.76	The ^{13}C NMR spectrum (DMSO- d_6 , 125 MHz) of 94	98
Figure A.77	The ^1H NMR spectrum (DMSO- d_6 , 500 MHz) of 95	99
Figure A.78	The ^{13}C NMR spectrum (DMSO- d_6 , 125 MHz) of 95	99
Figure A.79	The ^1H NMR spectrum (DMSO- d_6 , 500 MHz) of 96	100
Figure A.80	The ^{13}C NMR spectrum (DMSO- d_6 , 125 MHz) of 96	100
Figure A.81	The ^1H NMR spectrum (DMSO- d_6 , 500 MHz) of 97	101
Figure A.82	The ^{13}C NMR spectrum (DMSO- d_6 , 125 MHz) of 97	101
Figure A.83	The ^1H NMR spectrum (DMSO- d_6 , 500 MHz) of 98	102
Figure A.84	The ^{13}C NMR spectrum (DMSO- d_6 , 125 MHz) of 98	102
Figure A.85	The ^1H NMR spectrum (DMSO- d_6 , 500 MHz) of 99	103
Figure A.86	The ^{13}C NMR spectrum (DMSO- d_6 , 125 MHz) of 99	103
Figure A.87	The ^1H NMR spectrum (DMSO- d_6 , 500 MHz) of 100	104
Figure A.88	The ^{13}C NMR spectrum (DMSO- d_6 , 125 MHz) of 100	104
Figure A.89	The ^1H NMR spectrum (DMSO- d_6 , 500 MHz) of 101	105
Figure A.90	The ^{13}C NMR spectrum (DMSO- d_6 , 125 MHz) of 101	105
Figure A.91	The ^1H NMR spectrum (DMSO- d_6 , 500 MHz) of 102	106
Figure A.92	The ^{13}C NMR spectrum (DMSO- d_6 , 125 MHz) of 102	106
Figure A.93	The ^1H NMR spectrum (DMSO- d_6 , 500 MHz) of 103	107
Figure A.94	The ^{13}C NMR spectrum (DMSO- d_6 , 125 MHz) of 103	107
Figure A.95	The ^1H NMR spectrum (DMSO- d_6 , 500 MHz) of 104	108
Figure A.96	The ^{13}C NMR spectrum (DMSO- d_6 , 125 MHz) of 104	108
Figure A.97	The ^1H NMR spectrum (DMSO- d_6 , 500 MHz) of 105	109
Figure A.98	The ^{13}C NMR spectrum (DMSO- d_6 , 125 MHz) of 105	109
Figure A.99	The ^1H NMR spectrum (DMSO- d_6 , 500 MHz) of 106	110

Figure A.100	The ^{13}C NMR spectrum (DMSO- d_6 , 125 MHz) of 106	110
Figure A.101	The ^1H NMR spectrum (DMSO- d_6 , 500 MHz) of 107	111
Figure A.102	The ^{13}C NMR spectrum (DMSO- d_6 , 125 MHz) of 107	111
Figure A.103	The ^1H NMR spectrum (DMSO- d_6 , 500 MHz) of 108	112
Figure A.104	The ^{13}C NMR spectrum (DMSO- d_6 , 125 MHz) of 108	112
Figure A.105	The ^1H NMR spectrum (DMSO- d_6 , 500 MHz) of 109	113
Figure A.106	The ^{13}C NMR spectrum (DMSO- d_6 , 125 MHz) of 109	113
Figure A.107	The ^1H NMR spectrum (DMSO- d_6 , 500 MHz) of 110	114
Figure A.108	The ^{13}C NMR spectrum (DMSO- d_6 , 125 MHz) of 110	114
Figure A.109	The ^1H NMR spectrum (DMSO- d_6 , 500 MHz) of 111	115
Figure A.110	The ^{13}C NMR spectrum (DMSO- d_6 , 125 MHz) of 111	115
Figure A.111	The ^1H NMR spectrum (DMSO- d_6 , 500 MHz) of 112	116
Figure A.112	The ^{13}C NMR spectrum (DMSO- d_6 , 125 MHz) of 112	116
Figure A.113	The ^1H NMR spectrum (DMSO- d_6 , 500 MHz) of 113	117
Figure A.114	The ^{13}C NMR spectrum (DMSO- d_6 , 125 MHz) of 113	117
Figure A.115	The ^1H NMR spectrum (DMSO- d_6 , 500 MHz) of 114	118
Figure A.116	The ^{13}C NMR spectrum (DMSO- d_6 , 125 MHz) of 114	118
Figure A.117	The HR-MS (ESI) of 60	119
Figure A.118	The HR-MS (ESI) of 61	119
Figure A.119	The HR-MS (ESI) of 62	120
Figure A.120	The HR-MS (ESI) of 64	120
Figure A.121	The HR-MS (ESI) of 65	121
Figure A.122	The HR-MS (ESI) of 68	121
Figure A.123	The HR-MS (ESI) of 69	122
Figure A.124	The HR-MS (ESI) of 70	122
Figure A.125	The HR-MS (ESI) of 72	123
Figure A.126	The HR-MS (ESI) of 77	123
Figure A.127	The HR-MS (ESI) of 78	124
Figure A.128	The HR-MS (ESI) of 79	124
Figure A.129	The HR-MS (ESI) of 80	125
Figure A.130	The HR-MS (ESI) of 81	125

Figure A.131 The HR-MS (ESI) of 82.....	126
Figure A.132 The HR-MS (ESI) of 83.....	126
Figure A.133 The HR-MS (ESI) of 85.....	127
Figure A.134 The HR-MS (ESI) of 86.....	127
Figure A.135 The HR-MS (ESI) of 87.....	128
Figure A.136 The HR-MS (ESI) of 88.....	128
Figure A.137 The HR-MS (ESI) of 89.....	129
Figure A.138 The HR-MS (ESI) of 90.....	129
Figure A.139 The HR-MS (ESI) of 91.....	130
Figure A.140 The HR-MS (ESI) of 92.....	130
Figure A.141 The HR-MS (ESI) of 93.....	131
Figure A.142 The HR-MS (ESI) of 94.....	131
Figure A.143 The HR-MS (ESI) of 95.....	132
Figure A.144 The HR-MS (ESI) of 96.....	132
Figure A.145 The HR-MS (ESI) of 98.....	133
Figure A.146 The HR-MS (ESI) of 99.....	133
Figure A.147 The HR-MS (ESI) of 100.....	134
Figure A.148 The HR-MS (ESI) of 101.....	134
Figure A.149 The HR-MS (ESI) of 102.....	135
Figure A.150 The HR-MS (ESI) of 103.....	135
Figure A.151 The HR-MS (ESI) of 112.....	136
Figure A.152 The HR-MS (ESI) of 113.....	136
Figure A.153 The HR-MS (ESI) of 114.....	137

LIST OF ABBREVIATIONS

CH ₂ Cl ₂	dichloromethane
d	doublet (NMR)
dd	doublet of doublets (NMR)
DMSO	dimethyl sulfoxide
eq/equiv	equivalent
EtOH	ethanol
EtOAc	ethyl acetate
EOM-Cl	chloroethyl methyl ether
ESI	electron spray ionization
g	gram (s)
h	hour (s)
HCl	hydrochloric acid
HRMS/HR-MS	High-resolution mass spectra
<i>J</i>	Coupling constant (NMR)
K ₂ CO ₃	potassium carbonate
K _m	Michaelis-Menten constant
m	multiplet (NMR)
<i>m</i> -	meta
M	molar (s)
MeOH	methanol
MHz	Mega Hertz
min	minute (s)
mL	milliliter (s)
mM	milimolar (s)
mmol	millimole (s)
N	mormalitas (s)
NaHCO ₃	sodium carbonate
NaOH	sodium hydroxide
Na ₂ SO ₄	sodium sulfate

NMR	Nuclear Magnetic Resonance
<i>o</i> -	ortho
<i>p</i> -	para
p	pentet (NMR)
ppm	part per million
q	quartet (NMR)
rt	room temperature
s	singlet (NMR)
SD	standard deviation
sx	sextet (NMR)
t	triplet (NMR)
TLC	Thin layer chromatography
U/mL	unit per milliliter (s)
V_{\max}	maximum enzyme velocity
$[M+Na]^+$	pseudomolecular ion
α	alpha
β	beta
π	phi
δ	chemical shift
μL	microliter (s)
μM	micromolar (s)
[I]	concentration of inhibitors

CHAPTER I

INTRODUCTION

Diabetes is a major health issue that has reached alarming levels, nearly half a billion people are living with diabetes worldwide. The International Diabetes Federation reported 463 million people with diabetes in 2019 and estimated an increase up to 51% (700 million) individuals with diabetes by 2045. Diabetes mellitus is a complex chronic illness associated with a state of elevated levels of blood glucose or hyperglycemia. Diabetes mellitus is occurring from deficiencies in insulin secretion or insulin resistance which leads over time to high risk for long-term macro-and microvascular complications, including elevated risk for cardiovascular diseases. Diabetes mellitus type 2 contributes to more than 90% of all cases worldwide than diabetes mellitus type 1 and gestational diabetes. One of the therapeutic strategies for suppressing hyperglycemia by retarding the absorption of glucose through the inhibition of the bio-catalyzers involved in carbohydrate digestion, namely α -amylase (EC 3.2.1.1) and α -glucosidase (EC 3.2.1.20). The α -glucosidase inhibitors seem to be the most effective in reducing hyperglycemia, because α -glucosidase inhibitor can inhibit the glucosidase in the intestinal cells to hydrolyze carbohydrates to simple sugars, so that α -glucosidase inhibitors reduce the impact of dietary carbohydrates on blood sugar. Some drugs for α -glucosidase inhibitors have been clinically used, such as acarbose, miglitol, and voglibose, but they have adverse effects (e.g. gastrointestinal symptoms). Therefore, it is imperative to find suitable medication for diabetes mellitus, specially α -glucosidase inhibitors. Thus, α -glucosidase inhibitors were considered as a potent target for drug design as anti-diabetic. Certain chalcones and sulfonamides have been reported to display anti-diabetic activity. As a result, the preparation of sulfonamide chalcones as α -glucosidase inhibitors would be an attractive direction for finding a new therapy for diabetes.

1.1 Chalcones

Chalcones (1,3-diphenyl-2-propene-1-ones), also known as chalconoid have a simple typical structure, providing two phenyls (rings A and B) mainly connected by *trans*-enone bonds [(α,β)-unsaturated bond and a carbonyl group] (Figure 1.1).¹ Chalcones are an early intermediate in the biosynthesis of all flavonoids. Chalcones are unstable and easily converted into flavanones in plant cells, but modified chalcones are more stable. They can play a key role in the ecophysiological system as pigments, phytoalexins, and symbiotic signals. They are also attracting attention as bioactive compounds having cytotoxic and chemoprotective properties.² This remarkable structure has been widely studied for its biological activities because the chalcone-based skeleton has appealed to intensive scientific studies throughout the world and its derivatives demonstrate a variety of promising biological activity such as α -glucosidase,^{3,4,5} anti-diabetic,⁶ anti-inflammatory,^{7,8} NF-KB inhibition,^{9,10,11} anticancer,^{7,9} and anti-oxidant.¹²

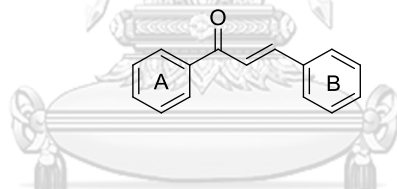


Figure 1.1 Core structure of chalcone.

The existence of double bonds in conjugation with carbonyl functionality is believed to be responsible for the biological activity of chalcones. Many chalcones have been prepared by Claisen-Schmidt reaction. In 2015, Sun *et al.*³ synthesized a series of chalcone-based compounds with different substituents on both rings such as prenyl, geranyl, hydroxy, and methoxy as α -glucosidase inhibitors (Figure 1.2). The A-ring with 2',4'-dihydroxy-5'-prenyl (**2**) and 2',4'-dihydroxy-5'-geranyl (**3**) substituent exhibited better activity than the unsubstituted compound (**1**). However, **4**, **5** and **7** exhibited significantly enhanced activity. Among them, **5** showed the strongest α -glucosidase inhibitors with IC_{50} 0.90 μ M, which was 100-fold more active than unsubstituted (**1**).

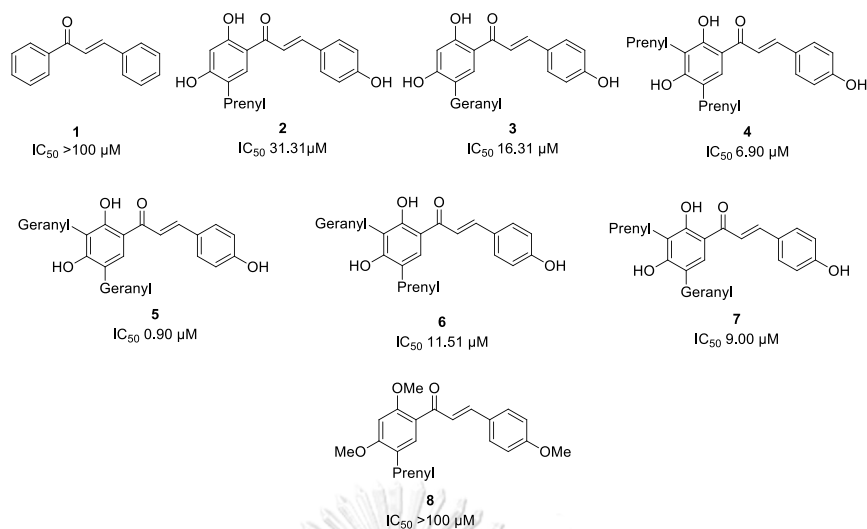


Figure 1.2 Reported chalcones 1-8 as α -glucosidase inhibitors

Chalcones as α -glucosidase inhibitors were also reported by Cai *et al.* in 2017.⁴ Chalcones with methoxy (9-14) groups showed lower inhibitory activity than those with hydroxy (15-20), and poor solubility. The activity increased for the hydroxy substituent, which was considered as the main key in α -glucosidase inhibitors. As shown in Figure 1.3, the A-ring with 4-hydroxy (17) had a stronger inhibitory activity than 3-hydroxy (18) with IC_{50} 13.4 ± 2.7 and $42.0 \pm 6.0 \mu M$, respectively. In addition, 2',4'-dihydroxy (17) was more effective than 3',4'-dihydroxy (16) in A-ring. This also applied to B-ring in 19 with increased activity ($12.5 \pm 2.1 \mu M$).

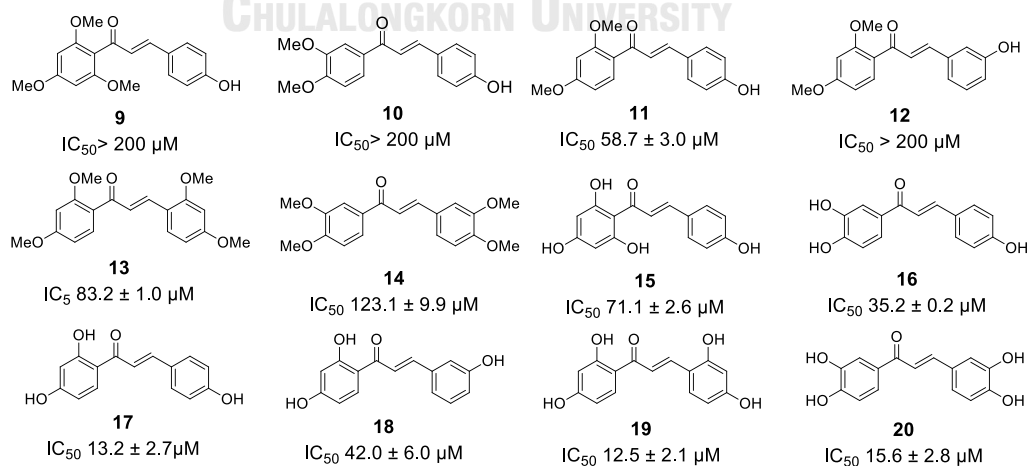


Figure 1.3 Reported chalcones 9-20 as α -glucosidase inhibitors

In 2019, Rocha *et al.*⁵ synthesized the chalcones with hydroxy, methyl, methoxy, nitro, and halogen substituents. The compounds with methyl, methoxy, fluoro and bromo substituents exhibited % inhibition less than 20%. Only four candidates exhibited % inhibition >85% (**Figure 1.4**). Those compounds contained hydroxy, nitro and chloro as substituents. The most potent inhibitors were butein (**21**) with IC_{50} $21.0 \pm 2.0 \mu M$. Besides that, 2-nitro (**23**) substituent with IC_{50} $41.0 \pm 1.0 \mu M$ revealed better activity than 4-nitro (**22**) and 2,4-dichloro substituents with IC_{50} 53.0 ± 1.0 and $87.0 \pm 3.0 \mu M$, respectively.

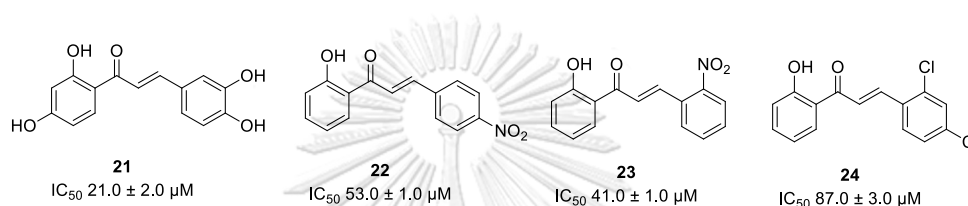


Figure 1.4 Reported chalcones **21-24** as α -glucosidase inhibitors

1.2 Sulfonamides

Sulfonamide is a sulfonyl group connected to an amine moiety. The general formula is RSO_2NH_2 , where R can be either alkyl or aryl groups. Sulfonamides are a class of synthetic bacteriostatic antibiotics used for the treatment of bacterial infections and those caused by other microorganisms. They are known as sulfa drugs and a major source therapy against bacterial infection before its introduction in 1941 as penicillin. Prontosil (**24**) was the first sulfonamide identified by Demagk *et al.* in 1935. It was metabolized by bacteria into sulfanilamide (**26**) which is an active metabolite (**Figure 1.5**). Sulfanilamide is an antibacterial agent synthesized in 1936.¹³ Since then there have been many analogies of sulfanilamide developed as pharmacological agents, for example as antidiabetic,¹⁴ α -glucosidase inhibitors,^{15,16,17} antibacterial,¹⁸ anti-inflammatory,¹⁹ antifungal,²⁰ and anticancer.²¹⁻²²

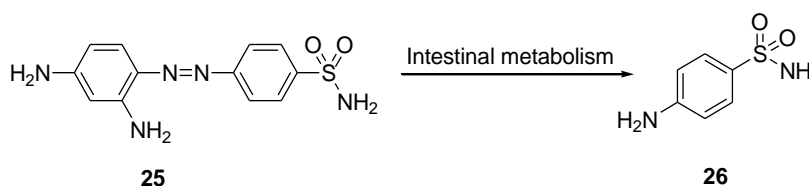


Figure 1.5 Intestinal metabolism of prontosil

The first sulfonylurea, VK 57 was concentrated in 1942. This compound exhibited to cause neofunctional insulin granules in mouse β -cells and since 1954, sulfonylureas used as an anti-diabetes mellitus drug. The first generation sulfonylurea was chlorpropamide, tolbutamide, tolazamide, and acetohexamide (**Figure 1.6**).¹⁴

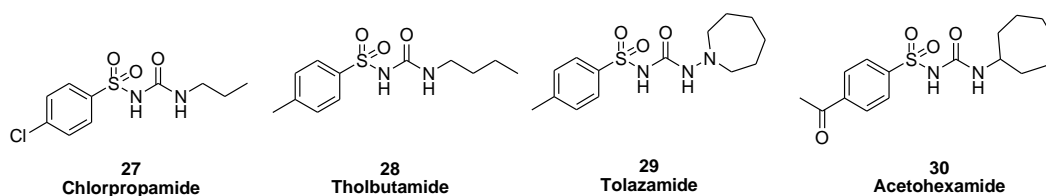
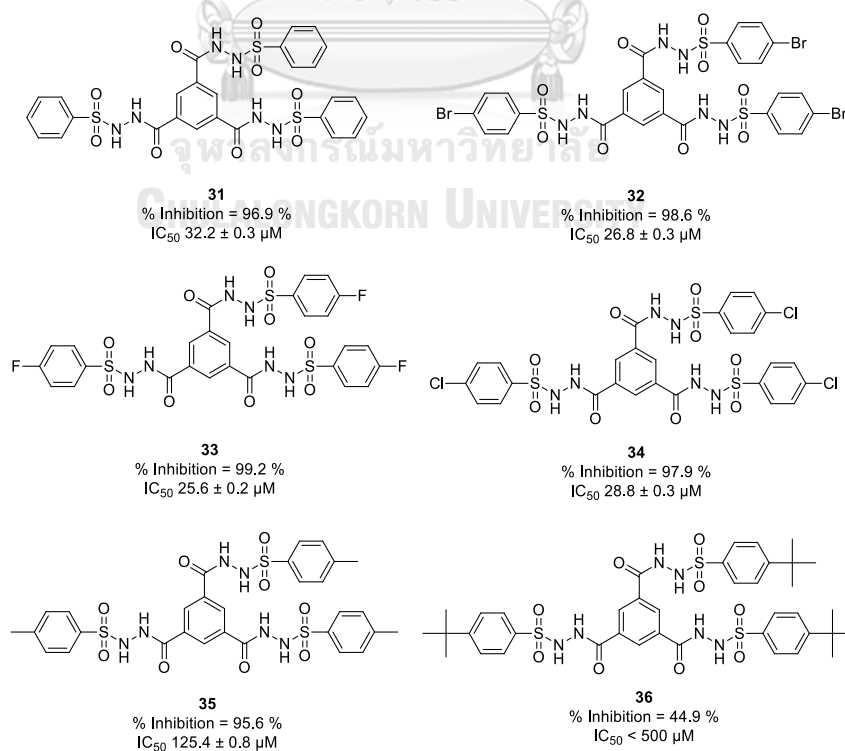


Figure 1.6 Reported sulfonylureas **27-30** as anti-diabetes mellitus

In 2015, Riaz *et al.*¹⁵ synthesized pyridine sulfonamide (**Figure 1.7**) as α -glucosidase inhibitors. Those compounds containing the halogen substituents (**32-34**) which were more active than unsubstituted (**31**). The better results may occur due to the polarity orientation of the halogen groups. Among these compounds, **33** had the strongest activity with IC_{50} 25.62±0.21 μ M.



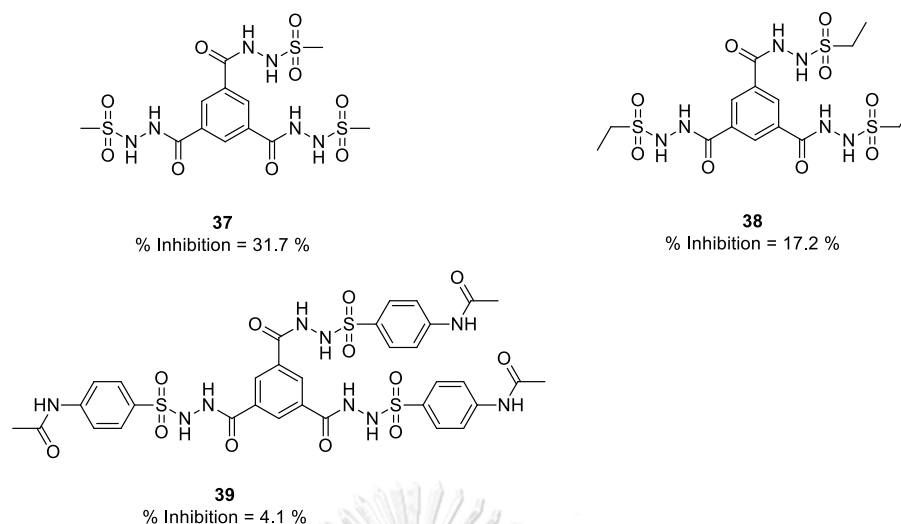


Figure 1.7 Reported pyridine sulfonamide **31-39** as α -glucosidase inhibitors

Chromone hydrazone containing sulfonamide (**Figure 1.8**) as α -glucosidase inhibitors were also reported by Wang *et al.* in 2017.¹⁶ Those with 4-sulfonamide substituents (**40** and **42**) at phenyl ring of hydrazone were the most active compounds. In addition, unsubstituted chromone (**40**) had better activity than that with hydroxy substituent (**42**), with IC_{50} 20.1 ± 0.19 and 25.2 ± 0.26 μM , respectively.

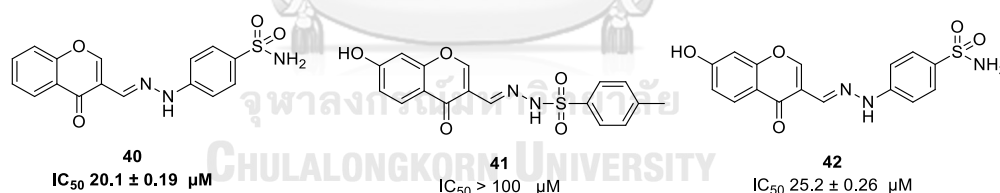


Figure 1.8 Reported chromone hydrazone sulfonamides **40-42** as α -glucosidase inhibitors

In 2017, Taha *et al.*¹⁷ synthesized piperazine sulfonamide as anti-diabetic mellitus II. Piperazine sulfonamide showed α -amylase inhibition with IC_{50} ranging between 1.57 ± 0.05 to 2.87 ± 0.40 μM (**Figure 1.9**). **45** revealed outstanding inhibition with IC_{50} 1.57 ± 0.05 μM compared with the standard acarbose (IC_{50} 1.35 ± 0.23 μM).

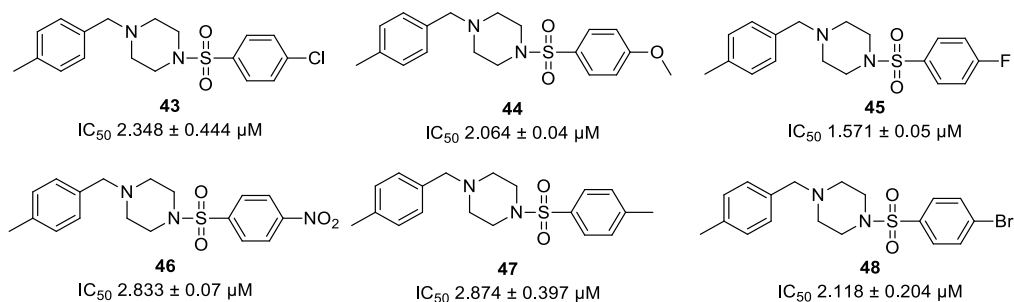


Figure 1.9 Reported piperazine sulfonamide **43-48** as α -amylase inhibitors

1.3 Sulfonamide chalcones

Sulfonamide chalcones comprise of sulfonamide and chalcone moieties. Their relationship is very important to increase the biological activity of these medicinal substances. In 2005, Seo *et al.*²³ synthesized aminochalcones (**49-52**) and sulfonamide chalcones (**53-56**) as α -glucosidase inhibitors (**Figure 1.10**). Sulfonamide chalcones **43-46** with IC_{50} values ranging between 0.40 to 15.6 μ M had improved progressively compared with chalcones **39-42** (IC_{50} 41.0-200 μ M). In addition, **56** with IC_{50} 0.40 μ M showed 150 times stronger inhibitory activity than acarbose (IC_{50} 60.8 μ M). Sulfonamide groups revealed an important role to increase the inhibitory activity. This effect was also found for the position of amine in chalcone.

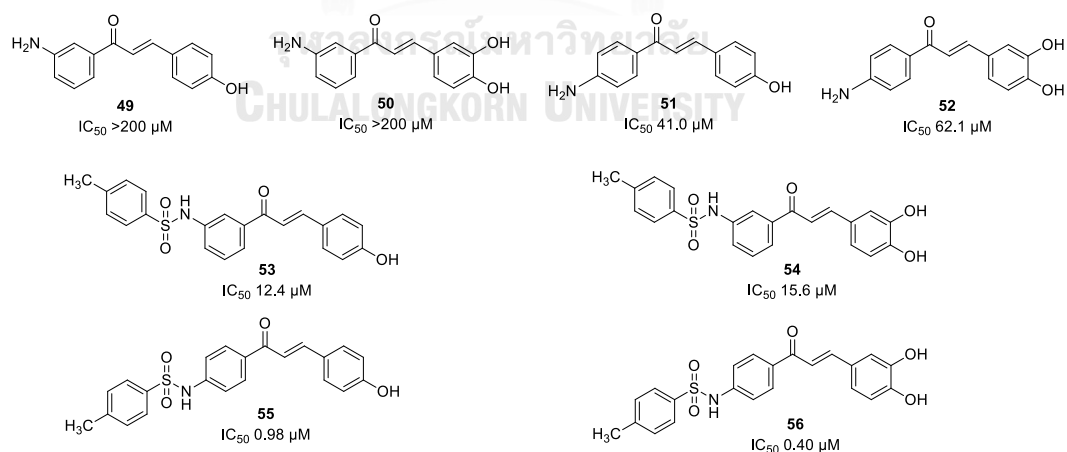


Figure 1.10 Reported chalcones and sulfonamide chalcones **49-56** as α -glucosidase inhibitors

1.4 Diabetes mellitus

In the 21st century diabetes had increased due to various sources such as an aging population, abundant nutrition, and an unhealthy lifestyle. Diabetes is a serious threat to global health, where people living with diabetes are at risk of various types of diseases, and causing an increase in demand for medical care, and decreased quality of life. Globally, diabetes is one of the top 10 causes of death. The estimated prevalence of types 1 and 2 diabetes, both diagnosed and undiagnosed in 2000, with an age range of 20-79 years has increased from 151 million (4.6% of the global population at that time) to 463 million (9.3%) in 2019. Without adequate action to tackle the disease, the *IDF Diabetes Atlas* estimates 578 million people (10.2% of the population) will suffer from diabetes by 2030. That number will jump to 700 million (10.9%) by 2045.²⁴

1.4.1 Diabetes mellitus type 1

Diabetes mellitus type 1 is a chronic autoimmune disease with genetic and environmental contributions resulting in decreased pancreatic cell function, leading to symptomatic diabetes and lifelong insulability.^{25,26} In children and adults, the rate of progression from autoimmunity to glucose intolerance can last from months to decades.²⁶ Diabetes mellitus type 1 can be diagnosed based on clinical symptoms related to hyperglycemia and metabolic imbalance. However, this disease can be identified at an earlier pre-symptomatic stage.²⁷

There are three stages of diabetes mellitus type 1, namely stage 1: autoimmunity +/-normoglycemia/presymptomatic diabetes mellitus type 1, representing individuals who have developed auto antibodies associated with type 1 diabetes mellitus but are hormoneoglycemic. Stage 2: autoimmunity +/-dysglycemia/presymptomatic diabetes mellitus type 1, at this stage is the same as stage 1, but the disease has progressed to glucose intolerance, or dysglycemia, due to loss of functional β -cell mass. Stage 3: autoimmunity +/-dysglycemia/symptoms of diabetes mellitus type 1, this stage is the result of clinical symptoms and signs of diabetes, which may include polyuria, polydipsia, weight loss, fatigue, diabeticketoacidosis (DKA), and others (**Figure 1.11**).²⁸

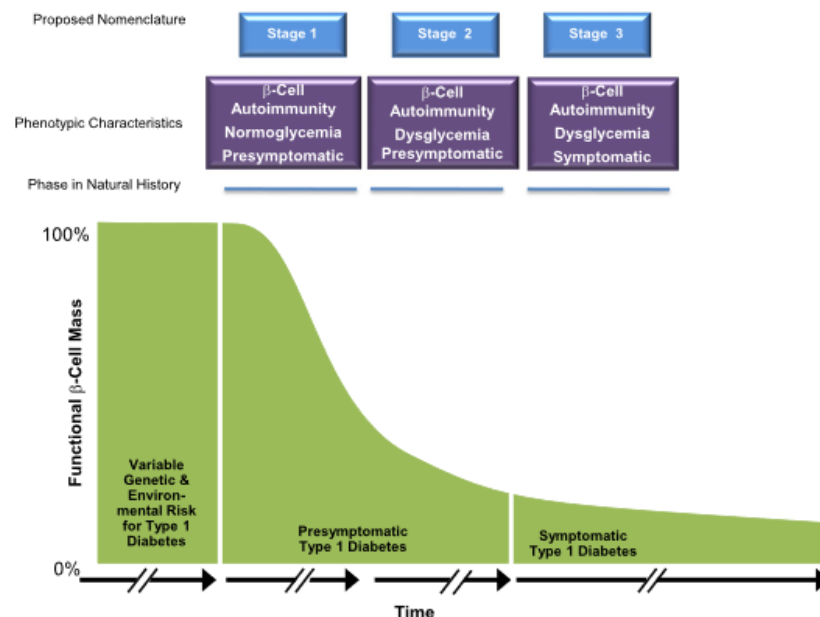


Figure 1.11 Early stages of type 1 diabetes

1.4.2 Diabetes mellitus type 2

Diabetes mellitus type 2 is classified as borderline diabetes or diabetes that does not require insulin, where insulin is used to control glycemic, and to survive. Diabetes mellitus type 2 occurs when the body's cells counter the normal effects of insulin which pushes glucose in the blood into the cells. This condition is called insulin resistance which causes glucose to start building up in the blood. It also occurs in the premature reduction of β -cell mass in patients with a pre-diabetic condition. even before diabetes was diagnosed, more than 50% of β -cells had disappeared in patients with pre-diabetes (IFG). Whereas with clear diabetes, more than 70% of β -cells have been reduced.²⁹ During the prediabetic stage, the remaining β -cells may be activated to compensate for the loss of cell function, but the β -cell overwork does not last long, and the patient eventually exhibits hyperglycemia sufficient to be diagnosed with diabetes. Therefore, the stage of diabetes may be determined by the number of β -cells lost, not only by insulin requirements or insulin secretion capacity (Figure 1.12).³⁰

Thus, the main cause of type 2 diabetes mellitus is the progressively disrupted secretion of insulin by pancreatic β -cells, against the backdrop of pre-existing insulin resistance in skeletal muscle, liver and adipose tissue. Prediabetes is characterized by

impaired fasting glucose levels (IFG), impaired glucose tolerance (IGT) or increased levels of glycated hemoglobin A1c (HbA1c). People with prediabetes have HbA1c levels between 5.7-6.4%. The annual conversion rate for prediabetes to diabetes mellitus type 2 ranges from 3% to 11% per year.³¹

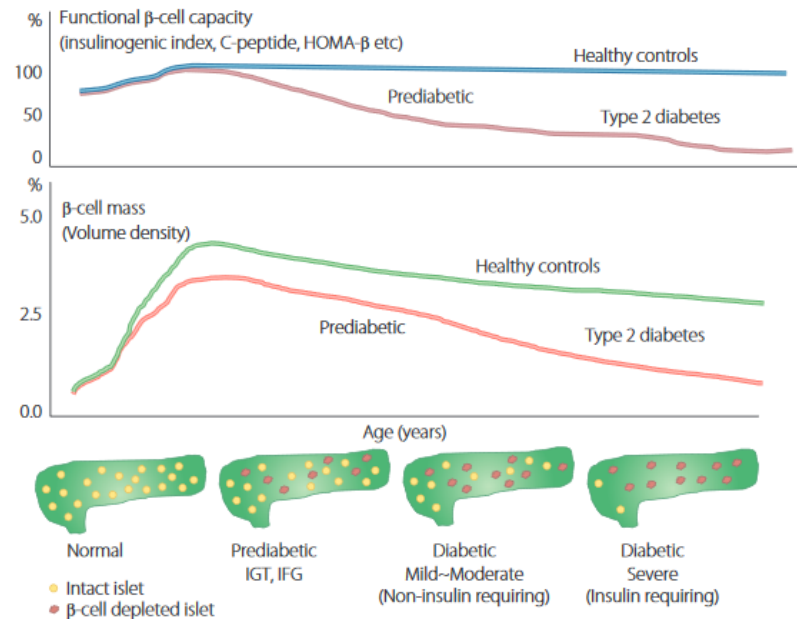


Figure 1.12 Natural history and clinical staging of diabetes

Thus, screening in persons at risk is very important, because prediabetes is common and more than 30% of people with type 2 diabetes mellitus are undiagnosed. Prevention of diabetes requires a life history of someone who has prediabetes and intervention, with lifestyle modifications such as weight loss and exercise, plus anti-diabetic and anti-obesity drugs.³²

1.5 α -Glucosidase inhibitors

Diabetes mellitus is a global problem that is well developed clinically and economic terms. Treatment of diabetes mellitus by means of oral α -glucosidase inhibitors are limited to acarbose, miglitol, and voglibose. One therapy diabetes treatment is by slowing down the absorption of glucose in the body, through the enzyme glucosidase in the body. α -Glucosidase is exo type carbohydrates which are

widely distributed in microorganism, plant, and animal tissues, which hydrolyze carbohydrate to α -glucose from the non-reducing end of the substrate.^{33,34} In humans this enzyme is bound to a membrane epithelium of the small intestine, which serves to facilitate absorption of glucose by the small intestine by hydrolysis oligosaccharides become monosaccharides so that they can be absorbed.³⁵

Inhibition of α -glucosidase in the intestine can suppress the rate of oligosaccharide and hydrolytic cleavage in the digestion process of carbohydrates. This slow digestion can slow down the rate of overall glucose absorption into the blood. This has been proven to be one strategy to reduce the postprandial increase in blood glucose, thereby helping to avoid diabetes complications.³⁵

Acarbose (**Figure 1.13**) is produced by fermentation using strains derived from *Actinoplanes* sp. SE50. Acarbose has been used since 1990 as diabetes therapy for type II, which allows the patient to better control blood sugar.³⁶

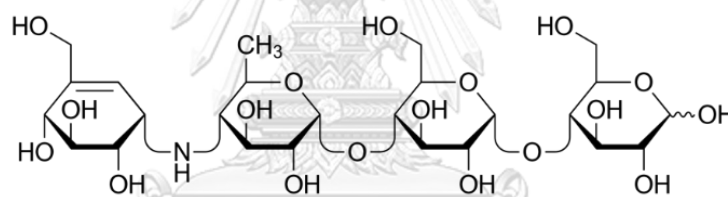


Figure 1.13 Acarbose

Acarbose delays the digestion of carbohydrates by inhibiting the hydrolysis of carbohydrates in a competitive and unaffected manner absorption of glucose. Acarbose inhibits α -glucosidase located in the brush border of the enterocytes lining of intestine and pancreatic α -amylase which is located in the intestinal lumen (**Figure 1.14**). Pancreatic α -amylase helps digest complex starch into oligosaccharides, while maltase, and isomaltase hydrolyze oligosaccharides, trisaccharides, and disaccharides to simple sugars.

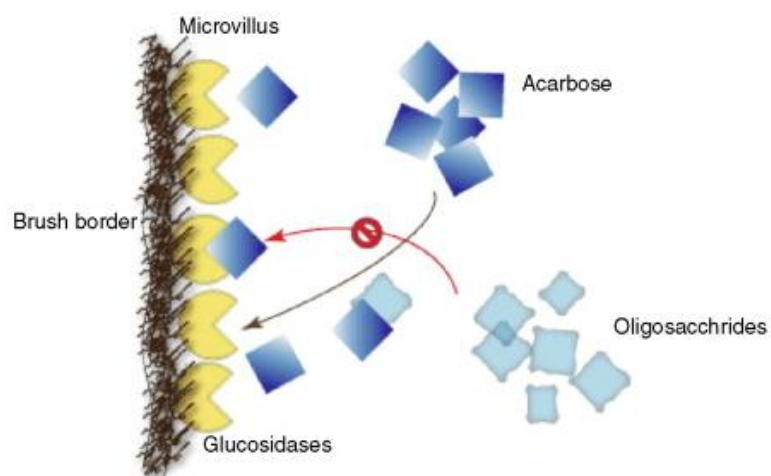


Figure 1.14 Mechanism of action of acarbose

1.6 Objective of this research

The series of sulfonamide chalcones were synthesized with various substituents on the A, B, and C-rings. All compounds were elucidated by NMR, and mass-spectra for new compounds. Furthermore, sulfonamide chalcones have synthesized and characterized was tested as α -glucosidase inhibitory activity and studied their structure-activity relationship. In addition, the selected candidates were studied the underlying mechanism of α -glucosidase inhibition by kinetic studies.

CHAPTER II EXPERIMENTAL

The synthesis of sulfonamide chalcones was carried out in two steps. The first step was sulfonation of aminoacetophenone using benzenesulfonyl chloride while the second step was conducted through Claisen-Schmidt condensation using sulfonamide acetophenone and selected benzaldehyde. Various substituents of benzenesulfonyl chloride and benzaldehyde were reacted to manipulate sulfonamide acetophenones and sulfonamide chalcones.

2.1 Instruments

The ^1H and ^{13}C NMR spectra were recorded in $\text{DMSO}-d_6$ using a Bruker Ultrashield 400 Plus NMR spectrometer and a JEOL JNM-EC500R/S1 NMR. High-resolution mass spectra (HRMS) were recorded on a Bruker Daltonics microTOF using electron spray ionization (ESI).

2.2 General materials

All solvents used in this study were distilled before use except for the high grade solvents. Aluminum sheet coated with silica gel (Kieselgel 60 PF254) was used as thin layer chromatography (TLC). In open column chromatography, silica gel (No. 7734 and 9385, Merck) was used as the stationary phase.

2.3 Preparation of *p*-toluenesulfonyl aminoacetophenones³⁷

Aminoacetophenone (7.4 mmol) was dissolved in 50 mL CH_2Cl_2 . *p*-Toluenesulfonyl chloride (8.2 mmol) in pyridine was then added. The reaction was maintained while stirring at room temperature (27-30 °C) for 24 h and monitored by TLC. Saturated NaHCO_3 solution was added to make the pH become 8 and extracted with CH_2Cl_2 . The organic layer was evaporated and the residue was recrystallized with a mixture of CH_2Cl_2 and hexane to obtain a target compound of about 95%. Three *p*-toluenesulfonyl aminoacetophenones (**57-59**) are described in **Figure 2.1**.

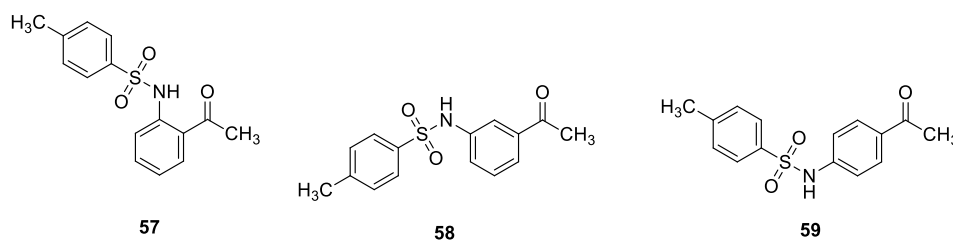


Figure 2.1 The structures of *p*-toluenesulfonyl aminoacetophenones (**57-59**)

N-(2-Acetylphenyl)-4-methylbenzenesulfonamide (**57**) $^1\text{H-NMR}$ (DMSO- d_6 , 500 MHz) δ 11.34 (s, 1H, N-H), 7.96 (dd, $J = 8.0, 1.5$ Hz, 1H, ArH), 7.68 (d, $J = 8.5$ Hz, 2H, ArH), 7.55-7.52 (m, 1H, ArH), 7.42 (dd, $J = 8.5, 1.0$ Hz, 1H, ArH), 7.35 (d, $J = 8.5$ Hz, 2H, ArH), 7.18-7.15 (m, 1H, ArH), 2.59 (s, 3H, CH₃), 2.32 (s, 3H, CH₃) ppm. $^{13}\text{C-NMR}$ (DMSO- d_6 , 125 MHz) δ 203.3, 144.1, 138.4, 135.7, 134.8, 132.6, 130.0, 127.0, 123.8, 123.5, 118.8, 28.6, 21.0 ppm.

N-(3-Acetylphenyl)-4-methylbenzenesulfonamide (**58**) $^1\text{H-NMR}$ (DMSO- d_6 , 500 MHz) δ 10.50 (s, 1H, N-H), 7.65 (d, $J = 8.5$ Hz, 2H, ArH), 7.64-7.61 (m, 2H, ArH), 7.38 (t, $J = 7.5$ Hz, 1H, ArH), 7.35-7.33 (m, 3H, ArH), 2.49 (s, 3H, CH₃), 2.31 (s, 3H, CH₃) ppm. $^{13}\text{C-NMR}$ (DMSO- d_6 , 125 MHz) δ 197.4, 143.5, 138.4, 137.6, 136.4, 129.8, 129.7, 126.8, 124.2, 124.1, 118.4, 26.8, 21.0 ppm.

N-(4-Acetylphenyl)-4-methylbenzenesulfonamide (**59**) $^1\text{H-NMR}$ (DMSO- d_6 , 500 MHz) δ 10.82 (s, 1H, N-H), 7.82 (d, $J = 9.0$ Hz, 2H, ArH), 7.71 (d, $J = 8.0$ Hz, 2H, ArH), 7.35 (d, $J = 8.0$ Hz, 2H, ArH), 7.20 (d, $J = 8.5$ Hz, 2H, ArH), 2.45 (s, 3H, CH₃), 2.31 (s, 3H, CH₃) ppm. $^{13}\text{C-NMR}$ (DMSO- d_6 , 125 MHz) δ 196.6, 143.8, 142.4, 136.5, 131.9, 130.0, 129.9, 126.8, 117.9, 26.5, 21.0 ppm.

2.4 Preparation of sulfonamide chalcones³⁸

Sulfonamide chalcones were synthesized by Claisen–Schmidt reaction as previously reported with some modifications. *p*-Toluenesulfonyl aminoacetophenones (0.5 mmol) and selected aromatic aldehydes (1.0 mmol) were dissolved in 10 mL EtOH. Afterward, NaOH (2 eq) was added and stirred at room temperature for 24 h. 10% HCl was added to the reaction mixture to adjust pH to 5 and extracted with EtOAc twice.

The organic portion was evaporated and purified using column chromatography or recrystallization using a suitable solvent.

2.4.1 Preparation of sulfonamide chalcones (60-62)

Three sulfonamide chalcones (**60-62**) with 3,4-dimethoxy substituent on B-ring and different positions of NHR (*o*-, *m*-, and *p*-) were synthesized (**Figure 2.2**). The new obtained products were presented with HRMS data shown below.

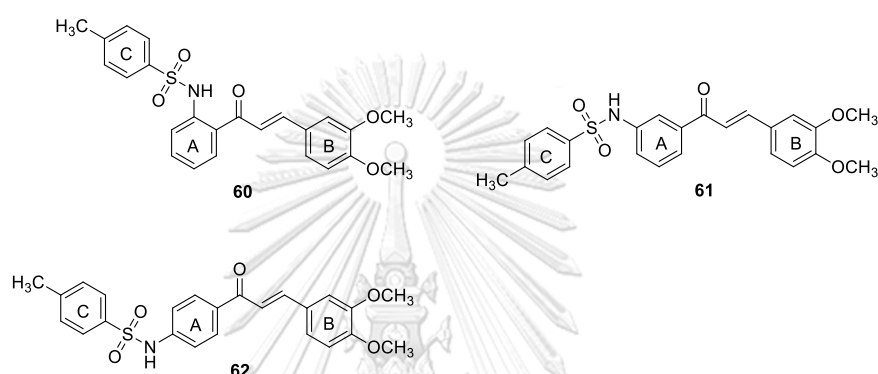


Figure 2.2 The structures of synthesized sulfonamide chalcones (**60-62**)

N-[2-(3-(3,4-dimethoxyphenyl)acryloyl)-phenyl]-4-methylbenzenesulfonamide (**60**) $^1\text{H-NMR}$ (DMSO- d_6 , 500 MHz) δ 11.26 (s, 1H, N-H), 8.06 (dd, J = 8.0, 1.5 Hz, 1H, ArH), 7.54 (s, 3H), 7.52 (s, 1H), 7.49-7.45 (m, 1H, ArH), 7.39 (d, J = 2.0 Hz, 1H, ArH), 7.37 (dd, J = 8.0, 1.0 Hz, 1H, ArH), 7.27 (dd, J = 8.5, 2.0 Hz, 1H, ArH), 7.20 (d, J = 8.0 Hz, 2H, ArH), 7.17-7.14 (m, 1H, ArH), 6.93 (d, J = 8.0 Hz, 1H, ArH), 3.74 (s, 3H, OCH₃), 3.72 (s, 3H, OCH₃), 2.13 (s, 3H, CH₃) ppm. $^{13}\text{C-NMR}$ (DMSO- d_6 , 125 MHz) δ 192.7, 151.8, 149.1, 146.2, 144.1, 138.6, 135.8, 134.3, 131.5, 130.0, 127.3, 127.0, 126.1, 124.7, 124.1, 120.5, 120.4, 111.6, 110.8, 55.8, 55.7, 21.0 ppm. HRMS (ESI, m/z): calculated for C₂₄H₂₃NNaO₅S [M+Na]⁺ 460.11946, found 460.11966.

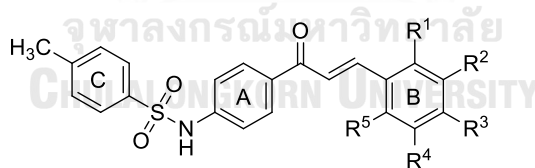
N-[3-(3-(3,4-dimethoxyphenyl)acryloyl)-phenyl]-4-methylbenzenesulfonamide (**61**) $^1\text{H-NMR}$ (DMSO- d_6 , 500 MHz) δ 10.45 (s, 1H, N-H), 7.84 (d, J = 8.0 Hz, 1H, ArH), 7.67 (d, J = 19.0 Hz, 1H, β -H), 7.67 (d, J = 19.0 Hz, 1H, α -H), 7.64 (d, J = 8.5 Hz, 2H, ArH), 7.62 (s, 1H, ArH), 7.46 (d, J = 1.5 Hz, 1H, ArH), 7.41 (t, J = 7.5 Hz, 1H, ArH), 7.34 (dd, J = 7.5, 1.5 Hz, 2H, ArH), 7.31 (d, J = 8.0 Hz, 2H, ArH), 7.00 (d, J = 8.5 Hz, 1H, ArH),

3.81 (s, 3H, OCH₃), 3.78 (s, 3H, OCH₃), 2.28 (s, 3H, CH₃) ppm. ¹³C-NMR (DMSO-*d*₆, 125 MHz) δ 188.7, 151.4, 149.0, 144.9, 143.5, 138.8, 138.5, 136.5, 129.8, 129.6, 127.4, 126.7, 124.3, 123.9, 123.9, 119.6, 119.0, 111.6, 110.8, 55.7, 55.6, 21.0 ppm. HRMS (ESI, *m/z*): calculated for C₂₄H₂₃NNaO₅S [M+Na]⁺ 460.11946, found 460.11913.

N-[4-(3-(3,4-dimethoxyphenyl)-acryloyl)-phenyl]-4-methylbenzenesulfonamide (**62**) ¹H-NMR (DMSO-*d*₆, 500 MHz) δ 10.80 (s, 1H, N-H), 8.01 (d, *J* = 9.0 Hz, 2H, ArH), 7.70 (d, *J* = 15.5 Hz, 1H, β -H), 7.70 (d, *J* = 8.0 Hz, 2H, ArH), 7.61 (d, *J* = 15.5 Hz, 1H, α -H), 7.46 (d, *J* = 1.5 Hz, 1H, ArH), 7.34 (d, *J* = 8.5 Hz, 2H, ArH), 7.31 (dd, *J* = 8.5, 2.0 Hz, 1H, ArH), 7.22 (d, *J* = 8.5 Hz, 2H, ArH), 6.82 (d, *J* = 8.5 Hz, 1H, ArH), 3.81 (s, 3H, OCH₃), 3.77 (s, 3H, OCH₃), 2.29 (s, 3H, CH₃) ppm. ¹³C-NMR (DMSO-*d*₆, 125 MHz) δ 187.4, 151.20, 149.0, 144.0, 143.8, 142.2, 136.5, 132.8, 130.1, 129.9, 127.5, 126.8, 123.9, 119.4, 118.0, 111.6, 110.6, 55.7, 55.6, 21.0 ppm. HRMS (ESI, *m/z*): calculated for C₂₄H₂₄NO₅S [M+H]⁺ 438.13752, found 438.13720.

2.4.2 Preparation of sulfonamide chalcones (63-76)

Fourteen sulfonamide chalcones (**63-76**) with unsubstituted and monosubstituted (OCH₃, alkyl, F, Cl, Br, and NO₂) on B-ring were attained following the procedure described in 2.4 (Figure 2.3).



- | | |
|--|--|
| 63. R ¹ = R ² = R ³ = R ⁴ = R ⁵ = H | 70. R ¹ = R ² = R ⁴ = R ⁵ = H, R ³ = CH ₂ CH ₂ CH ₂ CH ₃ |
| 64. R ² = R ³ = R ⁴ = R ⁵ = H, R ¹ = OCH ₃ | 71. R ¹ = R ² = R ⁴ = R ⁵ = H, R ³ = CH(CH ₃) ₂ |
| 65. R ¹ = R ³ = R ⁴ = R ⁵ = H, R ² = OCH ₃ | 72. R ¹ = R ² = R ⁴ = R ⁵ = H, R ³ = C(CH ₃) ₃ |
| 66. R ¹ = R ² = R ⁴ = R ⁵ = H, R ³ = OCH ₃ | 73. R ¹ = R ² = R ⁴ = R ⁵ = H, R ³ = F |
| 67. R ¹ = R ² = R ⁴ = R ⁵ = H, R ³ = CH ₃ | 74. R ¹ = R ² = R ⁴ = R ⁵ = H, R ³ = Cl |
| 68. R ¹ = R ² = R ⁴ = R ⁵ = H, R ³ = CH ₂ CH ₃ | 75. R ¹ = R ² = R ⁴ = R ⁵ = H, R ³ = Br |
| 69. R ¹ = R ² = R ⁴ = R ⁵ = H, R ³ = CH ₂ CH ₂ CH ₃ | 76. R ¹ = R ² = R ⁴ = R ⁵ = H, R ³ = NO ₂ |

Figure 2.3 The structures of synthesized sulfonamide chalcones (**63-76**)

N-[4-(3-(phenyl)-acryloyl)-phenyl]-4-methylbenzenesulfonamide (**63**) $^1\text{H-NMR}$ (DMSO- d_6 , 500 MHz) δ 10.83 (s, 1H, N-H), 8.01 (d, J = 8.5 Hz, 2H, ArH), 7.82 (d, J = 15.5 Hz, 1H, β -H), 7.81 (d, J = 4.0 Hz, 2H, ArH), 7.70 (d, J = 8.5 Hz, 2H, ArH), 7.65 (d, J = 15.5 Hz, 1H, α -H), 7.41 (d, J = 4.0 Hz, 2H, ArH), 7.40 (t, J = 2.5 Hz, 1 H, ArH), 7.33 (d, J = 8.5 Hz, 2H, ArH), 7.22 (d, J = 9.0 Hz, 2H, ArH), 2.29 (s, 3H, CH₃) ppm. $^{13}\text{C-NMR}$ (DMSO- d_6 , 125 MHz) δ 187.6, 143.8, 143.5, 142.5, 136.4, 134.7, 132.5, 130.6, 130.2, 129.9, 128.9, 128.8, 126.8, 121.9, 117.9, 21.0 ppm.

N-[4-(3-(2-methoxyphenyl)-acryloyl)-phenyl]-4-methylbenzenesulfonamide (**64**) $^1\text{H-NMR}$ (DMSO- d_6 , 500 MHz) δ 10.83 (s, 1H, N-H), 8.00 (d, J = 8.0 Hz, 2H, ArH), 7.96 (d, J = 16.0 Hz, 1H, β -H), 7.89 (d, J = 8.0 Hz, 1H, ArH), 7.78 (d, J = 16.0 Hz, 1H, α -H), 7.71 (d, J = 8.0 Hz, 2H, ArH), 7.41 (t, J = 7.5 Hz, 1 H, ArH), 7.34 (d, J = 8.0 Hz, 2H, ArH), 7.23 (d, J = 8.0 Hz, 2H, ArH), 7.07 (d, J = 8.5 Hz, 1H, ArH), 6.99 (t, J = 7.5 Hz, 1H, ArH), 3.85 (s, 3H, OCH₃), 2.30 (s, 3H, CH₃) ppm. $^{13}\text{C-NMR}$ (DMSO- d_6 , 125 MHz) δ 187.6, 158.2, 143.7, 142.3, 138.0, 136.4, 132.7, 132.2, 130.1, 129.9, 128.5, 126.8, 122.9, 121.6, 120.7, 118.0, 111.8, 55.7, 21.0 ppm. HRMS (ESI, m/z): calculated for C₂₃H₂₂NO₄S [M+H]⁺ 408.12695, found 408.12658.

N-[4-(3-(3-methoxyphenyl)-acryloyl)-phenyl]-4-methylbenzenesulfonamide (**65**) $^1\text{H-NMR}$ (DMSO- d_6 , 500 MHz) δ 10.85 (s, 1H, N-H), 8.04 (d, J = 9.0 Hz, 2H, ArH), 7.84 (d, J = 15.5 Hz, 1H, β -H), 7.72 (d, J = 8.5 Hz, 2H, ArH), 7.63 (d, J = 15.5 Hz, 1H, α -H), 7.42 (s, 1H, ArH), 7.37 (d, J = 9.5 Hz, 1H, ArH), 7.35 (d, J = 9.0 Hz, 2H, ArH), 7.33 (t, J = 8.0 Hz, 1H, ArH), 7.24 (d, J = 9.0 Hz, 2H, ArH), 6.68 (dd, J = 8.0, 3.0 Hz, 1H, ArH), 3.79 (s, 3H, OCH₃), 2.31 (s, 3H, CH₃) ppm. $^{13}\text{C-NMR}$ (DMSO- d_6 , 125 MHz) δ 187.5, 159.6, 143.8, 143.5, 142.5, 136.4, 136.1, 132.5, 130.2, 129.9, 126.8, 122.1, 121.6, 117.9, 116.7, 113.2, 55.3, 21.0 ppm. HRMS (ESI, m/z): calculated for C₂₃H₂₂NO₄S [M+H]⁺ 408.12695, found 408.12647.

N-[4-(3-(4-methoxyphenyl)-acryloyl)-phenyl]-4-methylbenzenesulfonamide (**66**) $^1\text{H-NMR}$ (DMSO- d_6 , 500 MHz) δ 10.83 (s, 1H, N-H), 8.02 (d, J = 9.0 Hz, 2H, ArH), 7.80 (d, J = 9.0 Hz, 2H, ArH), 7.73 (d, J = 8.5 Hz, 2H, ArH), 7.71 (d, J = 15.5 Hz, 1H, β -H), 7.65 (d, J = 15.5 Hz, 1H, α -H), 7.37 (d, J = 8.5 Hz, 2 H, ArH), 7.24 (d, J = 8.5 Hz, 2H, ArH), 7.00 (d, J = 9.0 Hz, 2H, ArH), 3.81 (s, 3H, OCH₃), 2.32 (s, 3H, CH₃) ppm. $^{13}\text{C-NMR}$ (DMSO- d_6 ,

125 MHz) δ 187.5, 161.4, 143.8, 143.5, 142.3, 136.5, 132.8, 130.8, 130.1, 129.9, 127.4, 126.8, 119.3, 118.0, 114.5, 55.4, 21.0 ppm.

N-[4-(3-(4-methylphenyl)-acryloyl)-phenyl]-4-methylbenzenesulfonamide (**67**)

$^1\text{H-NMR}$ (DMSO- d_6 , 500 MHz) δ 10.81 (s, 1H, N-H), 8.00 (d, J = 8.5 Hz, 2H, ArH), 7.76 (d, J = 15.5 Hz, 1H, β -H), 7.70 (d, J = 8.5 Hz, 2H, ArH), 7.69 (d, J = 8.0 Hz, 2H, ArH), 7.61 (d, J = 15.5 Hz, 1H, α -H), 7.33 (d, J = 8.5 Hz, 2H, ArH), 7.22 (d, J = 8.0 Hz, 2H, ArH), 7.21 (d, J = 8.5 Hz, 2H, ArH), 2.30 (s, 3H, CH₃), 2.29 (s, 3H, CH₃) ppm. $^{13}\text{C-NMR}$ (DMSO- d_6 , 125 MHz) δ 187.5, 143.8, 143.6, 142.4, 140.6, 136.5, 132.6, 132.0, 130.2, 129.9, 129.6, 128.9, 126.8, 120.8, 118.0, 21.1, 21.0 ppm.

N-[4-(3-(4-ethylphenyl)-acryloyl)-phenyl]-4-methylbenzenesulfonamide (**68**)

$^1\text{H-NMR}$ (DMSO- d_6 , 500 MHz) δ 10.82 (s, 1H, N-H), 8.00 (d, J = 8.5 Hz, 2H, ArH), 7.76 (d, J = 15.5 Hz, 1H, β -H), 7.72 (d, J = 7.5 Hz, 2H, ArH), 7.70 (d, J = 8.0 Hz, 2H, ArH), 7.62 (d, J = 15.5 Hz, 1H, α -H), 7.33 (d, J = 8.5 Hz, 2H, ArH), 7.24 (d, J = 8.0 Hz, 2H, ArH), 7.22 (d, J = 8.5 Hz, 2H, ArH), 2.59 (q, J = 7.5 Hz, 2H, CH₂), 2.29 (s, 3H, CH₃), 1.15 (t, J = 7.5 Hz, 3H, CH₃) ppm. $^{13}\text{C-NMR}$ (DMSO- d_6 , 125 MHz) δ 187.5, 146.8, 143.8, 143.6, 142.4, 136.5, 132.6, 132.3, 130.2, 129.9, 129.0, 128.4, 126.8, 120.9, 118.0, 28.2, 21.0, 15.4 ppm. HRMS (ESI, m/z): calculated for C₂₄H₂₃NNaO₃S [M+Na]⁺ 428.12963, found 428.12702.

N-[4-(3-(4-propylphenyl)-acryloyl)-phenyl]-4-methylbenzenesulfonamide (**69**)

$^1\text{H-NMR}$ (DMSO- d_6 , 500 MHz) δ 10.84 (s, 1H, N-H), 8.01 (d, J = 9.0 Hz, 2H, ArH), 7.78 (d, J = 15.5 Hz, 1H, β -H), 7.73 (d, J = 7.0 Hz, 2H, ArH), 7.71 (d, J = 7.0 Hz, 2H, ArH), 7.64 (d, J = 15.5 Hz, 1H, α -H), 7.35 (d, J = 8.0 Hz, 2H, ArH), 7.24 (d, J = 6.0 Hz, 2H, ArH), 7.22 (d, J = 7.0 Hz, 2H, ArH), 2.56 (t, J = 7.5 Hz, 2H, CH₂), 2.30 (s, 3H, CH₃), 1.57 (sx, 2H, CH₂), 0.86 (t, J = 7.0 Hz, 3H, CH₃) ppm. $^{13}\text{C-NMR}$ (DMSO- d_6 , 125 MHz) δ 187.5, 145.2, 143.8, 143.6, 142.4, 136.4, 132.6, 132.3, 130.2, 129.9, 128.9, 128.9, 126.8, 120.9, 117.9, 37.2, 23.9, 21.0, 13.6 ppm. HRMS (ESI, m/z): calculated for C₂₅H₂₅NNaO₃S [M+Na]⁺ 442.14528, found 442.14383.

N-[4-(3-(4-butylphenyl)-acryloyl)-phenyl]-4-methylbenzenesulfonamide (**70**)

$^1\text{H-NMR}$ (DMSO- d_6 , 500 MHz) δ 10.81 (s, 1H, N-H), 8.00 (d, J = 8.5 Hz, 2H, ArH), 7.75 (d, J = 15.5 Hz, 1H, β -H), 7.70 (d, J = 8.5 Hz, 2H, ArH), 7.69 (d, J = 8.5 Hz, 2H, ArH), 7.61 (d, J = 15.5 Hz, 1H, α -H), 7.33 (d, J = 8.0 Hz, 2H, ArH), 7.22 (d, J = 8.0 Hz, 2H, ArH), 7.21 (d, J =

8.5 Hz, 2H, ArH), 2.56 (t, $J = 7.5$ Hz, 2H, CH₂), 2.28 (s, 3H, CH₃), 1.51 (p, $J = 7.0$ Hz, 2H, CH₂), 1.25 (sx, $J = 7.5$ Hz, 2H, CH₂), 0.84 (t, $J = 7.5$ Hz, 3H, CH₃) ppm. ¹³C-NMR (DMSO-*d*₆, 125 MHz) δ 187.5, 145.5, 143.8, 143.6, 142.4, 136.5, 132.6, 132.3, 130.2, 129.9, 128.9, 126.8, 120.9, 118.0, 34.8, 32.9, 21.8, 21.0, 13.8 ppm. HRMS (ESI, m/z): calculated for C₂₆H₂₈NO₃S [M+H]⁺ 434.17899, found 434.17692.

N-[4-(3-(4-isopropylphenyl)-acryloyl)-phenyl]-4-methylbenzenesulfonamide

(71) ¹H-NMR (DMSO-*d*₆, 500 MHz) δ 10.82 (s, 1H, N-H), 8.00 (d, $J = 9.0$ Hz, 2H, ArH), 7.75 (d, $J = 15.5$ Hz, 1H, β -H), 7.71 (d, $J = 9.0$ Hz, 2H, ArH), 7.69 (d, $J = 8.5$ Hz, 2H, ArH), 7.61 (d, $J = 15.5$ Hz, 1H, α -H), 7.32 (d, $J = 8.0$ Hz, 2H, ArH), 7.26 (d, $J = 8.5$ Hz, 2H, ArH), 7.21 (d, $J = 8.5$ Hz, 2H, ArH), 2.87 (p, $J = 7.0$ Hz, 1H, CH), 2.28 (s, 3H, CH₃), 1.17 (s, 3H, CH₃), 1.15 (s, 3H, CH₃) ppm. ¹³C-NMR (DMSO-*d*₆, 125 MHz) δ 187.5, 151.4, 143.8, 143.6, 142.4, 136.5, 132.6, 132.4, 130.2, 129.9, 129.0, 126.9, 126.8, 120.9, 118.0, 33.5, 23.6, 21.0 ppm.

N-[4-(3-(4-tert-butylphenyl)-acryloyl)-phenyl]-4-methylbenzenesulfonamide

(72) ¹H-NMR (DMSO-*d*₆, 500 MHz) δ 10.85 (s, 1H, N-H), 8.03 (d, $J = 8.5$ Hz, 2H, ArH), 7.79 (d, $J = 15.5$ Hz, 1H, β -H), 7.75 (d, $J = 8.5$ Hz, 2H, ArH), 7.74 (d, $J = 8.5$ Hz, 2H, ArH), 7.66 (d, $J = 15.5$ Hz, 1H, α -H), 7.45 (d, $J = 8.0$ Hz, 2H, ArH), 7.37 (d, $J = 8.5$ Hz, 2H, ArH), 7.25 (d, $J = 8.5$ Hz, 2H, ArH), 2.32 (s, 3H, CH₃), 1.28 (s, 9H, CH₃) ppm. ¹³C-NMR (DMSO-*d*₆, 125 MHz) δ 187.6, 153.6, 143.8, 143.5, 142.4, 136.5, 132.6, 132.0, 130.2, 129.9, 128.7, 126.8, 125.7, 121.0, 118.0, 34.7, 30.9, 21.0 ppm. HRMS (ESI, m/z): calculated for C₂₆H₂₈NO₃S [M+H]⁺ 434.17899, found 434.17831.

N-[4-(3-(4-fluorophenyl)-acryloyl)-phenyl]-4-methylbenzenesulfonamide (73)

¹H-NMR (DMSO-*d*₆, 500 MHz) δ 10.83 (s, 1H, N-H), 8.00 (d, $J = 8.5$ Hz, 2H, ArH), 7.89 (dd, $J = 9.0, 6.0$ Hz, 2H, ArH), 7.78 (d, $J = 15.5$ Hz, 1H, β -H), 7.69 (d, $J = 8.0$ Hz, 2H, ArH), 7.64 (d, $J = 15.5$ Hz, 1H, α -H), 7.33 (d, $J = 8.0$ Hz, 2H, ArH), 7.24 (t, $J = 9.0$ Hz, 2H, ArH), 7.20 (d, $J = 9.0$ Hz, 2H, ArH), 2.28 (s, 3H, CH₃) ppm. ¹³C-NMR (DMSO-*d*₆, 125 MHz) δ 187.5, 164.4, 162.4, 143.8, 142.5, 142.3, 136.4, 132.5, 131.4, 131.2, 131.1, 130.2, 129.9, 126.8, 121.8, 117.9, 116.0, 115.9, 21.0 ppm.

N-[4-(3-(4-chlorophenyl)-acryloyl)-phenyl]-4-methylbenzenesulfonamide (74)

¹H-NMR (DMSO-*d*₆, 500 MHz) δ 10.85 (s, 1H, N-H), 8.02 (d, $J = 9.0$ Hz, 2H, ArH), 7.86 (d, $J = 8.5$ Hz, 2H, ArH), 7.85 (d, $J = 16.5$ Hz, 1H, β -H), 7.71 (d, $J = 8.0$ Hz, 2H, ArH), 7.64 (d,

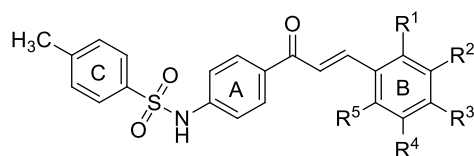
$J = 15.5$ Hz, 1H, α -H), 7.48 (d, $J = 8.5$ Hz, 2H, ArH), 7.34 (d, $J = 8.0$ Hz, 2H, ArH), 7.22 (d, $J = 9.0$ Hz, 2H, ArH), 2.30 (s, 3H, CH₃) ppm. ¹³C-NMR (DMSO-*d*₆, 125 MHz) δ 187.4, 143.8, 142.5, 142.0, 136.4, 135.0, 133.7, 132.4, 130.5, 130.3, 129.9, 128.9, 126.8, 122.6, 117.9, 21.0 ppm.

N-[4-(3-(4-bromophenyl)-acryloyl)-phenyl]-4-methylbenzenesulfonamide (**75**) ¹H-NMR (DMSO-*d*₆, 500 MHz) δ 10.85 (s, 1H, N-H), 8.02 (d, $J = 8.5$ Hz, 2H, ArH), 7.86 (d, $J = 15.5$ Hz, 1H, β -H), 7.79 (d, $J = 9.0$ Hz, 2H, ArH), 7.71 (d, $J = 8.0$ Hz, 2H, ArH), 7.62 (d, $J = 15.5$ Hz, 1H, α -H), 7.62 (d, $J = 8.5$ Hz, 2H, ArH), 7.34 (d, $J = 8.0$ Hz, 2H, ArH), 7.22 (d, $J = 8.5$ Hz, 2H, ArH), 2.30 (s, 3H, CH₃) ppm. ¹³C-NMR (DMSO-*d*₆, 125 MHz) δ 187.4, 143.8, 142.5, 142.1, 136.4, 134.0, 132.4, 131.9, 130.7, 130.3, 129.9, 126.8, 123.9, 122.7, 117.9, 21.0 ppm.

N-[4-(3-(4-nitrophenyl)-acryloyl)-phenyl]-4-methylbenzenesulfonamide (**76**) ¹H-NMR (DMSO-*d*₆, 500 MHz) δ 10.88 (s, 1H, N-H), 8.26 (d, $J = 8.5$ Hz, 2H, ArH), 8.12 (d, $J = 9.0$ Hz, 2H, ArH), 8.08 (d, $J = 8.5$ Hz, 2H, ArH), 8.04 (d, $J = 15.5$ Hz, 1H, β -H), 7.75 (d, $J = 15.0$ Hz, 1H, α -H), 7.74 (d, $J = 8.5$ Hz, 2H, ArH), 7.37 (d, $J = 8.5$ Hz, 2H, ArH), 7.26 (d, $J = 9.0$ Hz, 2H, ArH), 2.28 (s, 3H, CH₃) ppm. ¹³C-NMR (DMSO-*d*₆, 125 MHz): δ 187.4, 148.0, 143.8, 142.8, 141.2, 140.6, 136.4, 132.1, 130.5, 129.9, 129.8, 126.8, 125.9, 123.9, 117.9, 21.0 ppm.

2.4.3 Preparation of sulfonamide chalcones with disubstituent on B-ring (77-83)

Seven sulfonamide chalcones (**77-83**) with disubstituent (OCH₃, OCH₂O, and Cl) on B-ring were obtained following the procedure described in 2.4 (Figure 2.4).



- | | |
|---|---|
| 77. R ³ = R ⁴ = R ⁵ = H, R ¹ = R ² = OCH ₃ | 81. R ¹ = R ³ = R ⁴ = H, R ² = R ⁵ = OCH ₃ |
| 78. R ² = R ⁴ = R ⁵ = H, R ¹ = R ³ = OCH ₃ | 82. R ³ = R ⁴ = R ⁵ = H, R ¹ = R ² = OCH ₂ O |
| 79. R ² = R ³ = R ⁵ = H, R ¹ = R ⁴ = OCH ₃ | 83. R ¹ = R ⁴ = R ⁵ = H, R ² = R ³ = OCH ₂ O |
| 80. R ² = R ³ = R ⁴ = H, R ¹ = R ⁵ = OCH ₃ | |

Figure 2.4 The structures of synthesized sulfonamide chalcones with disubstituent on B-ring (**77-83**)

N-[4-(3-(2,3-dimethoxyphenyl)acryloyl)-phenyl]-4-methylbenzenesulfonamide (**77**) $^1\text{H-NMR}$ (DMSO- d_6 , 500 MHz) δ 10.84 (s, 1H, N-H), 8.01 (d, J = 8.0 Hz, 2H, ArH), 7.90 (d, J = 16.0 Hz, 1H, β -H), 7.78 (d, J = 15.5 Hz, 1H, α -H), 7.72 (d, J = 7.5 Hz, 2H, ArH), 7.54 (t, J = 4.5 Hz, 1H, ArH), 7.35 (d, J = 8.0 Hz, 2H, ArH), 7.23 (d, J = 8.0 Hz, 2H, ArH), 7.15 (d, J = 4.5 Hz, 2H, ArH), 3.80 (s, 3H, OCH₃), 3.75 (s, 3H, OCH₃), 2.30 (s, 3H, CH₃) ppm. $^{13}\text{C-NMR}$ (DMSO- d_6 , 125 MHz) δ 187.6, 152.8, 148.2, 143.8, 142.4, 137.5, 136.4, 132.5, 130.2, 129.9, 128.2, 126.8, 124.3, 122.7, 119.1, 118.0, 114.9, 61.0, 55.8, 21.0 ppm. HRMS (ESI, m/z): calculated for C₂₄H₂₄NO₅S [M+H]⁺ 438.13752, found 438.13683.

N-[4-(3-(2,4-dimethoxyphenyl)acryloyl)-phenyl]-4-methylbenzenesulfonamide (**78**) $^1\text{H-NMR}$ (DMSO- d_6 , 500 MHz) δ 10.80 (s, 1H, N-H), 7.98 (d, J = 9.0 Hz, 2H, ArH), 7.92 (d, J = 15.5 Hz, 1H, β -H), 7.85 (d, J = 8.5 Hz, 1H, ArH), 7.73 (d, J = 8.5 Hz, 2H, ArH), 7.67 (d, J = 15.5 Hz, 1H, α -H), 7.36 (d, J = 8.5 Hz, 2H, ArH), 7.24 (d, J = 8.5 Hz, 2H, ArH), 6.63 (d, J = 2.5 Hz, 1H, ArH), 6.61 (d, J = 2.5 Hz, 1H, ArH), 3.88 (s, 3H, OCH₃), 3.83 (s, 3H, OCH₃), 2.32 (s, 3H, CH₃) ppm. $^{13}\text{C-NMR}$ (DMSO- d_6 , 125 MHz) δ 187.5, 163.1, 159.9, 143.7, 142.1, 138.3, 136.5, 133.0, 130.1, 129.9, 126.8, 118.8, 118.0, 115.9, 106.3, 98.3, 55.8, 55.5, 21.0 ppm. HRMS (ESI, m/z): calculated for C₂₄H₂₄NO₅S [M+H]⁺ 438.13752, found 438.13751.

N-[4-(3-(2,5-dimethoxyphenyl)acryloyl)-phenyl]-4-methylbenzenesulfonamide (**79**) $^1\text{H-NMR}$ (DMSO- d_6 , 400 MHz) δ 7.92 (d, J = 8.8 Hz, 2H, ArH), 7.85 (d, J = 15.6 Hz, 1H, β -H), 7.69 (d, J = 15.6 Hz, 1H, α -H), 7.62 (d, J = 8.0 Hz, 2H, ArH), 7.37 (s, 1H, ArH), 7.24 (d, J = 8.0 Hz, 2H, ArH), 7.13 (d, J = 8.8 Hz, 2H, ArH), 6.89 (s, 2H, ArH), 3.69 (s, 3H, OCH₃), 3.66 (s, 3H, OCH₃), 2.20 (s, 3H, CH₃) ppm. $^{13}\text{C-NMR}$ (DMSO- d_6 , 100 MHz) δ 187.7, 153.3, 152.7, 143.8, 142.4, 137.9, 136.5, 132.7, 130.2, 129.9, 126.8, 123.6, 121.9, 118.2, 118.0, 113.1, 112.6, 56.2, 55.7, 21.0 ppm. HRMS (ESI, m/z): calculated for C₂₄H₂₄NO₅S [M+H]⁺ 438.13752, found 438.13598.

N-[4-(3-(2,6-dimethoxyphenyl)acryloyl)-phenyl]-4-methylbenzenesulfonamide (**80**) $^1\text{H-NMR}$ (DMSO- d_6 , 500 MHz) δ 10.81 (s, 1H, N-H), 8.05 (d, J = 15.5 Hz, 1H, β -H), 7.93 (d, J = 15.5 Hz, 1H, α -H), 7.88 (d, J = 8.5 Hz, 2H, ArH), 7.71 (d, J = 8.0 Hz, 2H, ArH), 7.36 (t, J = 8.5 Hz, 1H, ArH), 7.34 (d, J = 8.5 Hz, 2H, ArH), 7.25 (d, J = 8.5 Hz, 2H, ArH), 6.71 (d, J = 8.0 Hz, 2H, ArH), 3.88 (s, 6H, OCH₃), 2.30 (s, 3H, CH₃) ppm. $^{13}\text{C-NMR}$

(DMSO- d_6 , 125 MHz) δ 188.5, 160.0, 143.7, 142.1, 136.5, 134.4, 133.0, 132.3, 129.9, 129.8, 126.7, 123.3, 118.1, 111.5, 104.2, 56.0, 21.0 ppm. HRMS (ESI, m/z): calculated for $C_{24}H_{24}NO_5S$ $[M+H]^+$ 438.13752, found 438.13630.

N-[4-(3-(3,5-dimethoxyphenyl)-acryloyl)-phenyl]-4-methylbenzenesulfonamide (**81**) 1H -NMR (DMSO- d_6 , 500 MHz) δ 10.89 (s, 1H, N-H), 8.05 (d, J = 8.5 Hz, 2H, ArH), 7.84 (d, J = 15.5 Hz, 1H, β -H), 7.73 (d, J = 8.5 Hz, 2H, ArH), 7.60 (d, J = 15.5 Hz, 1H, α -H), 7.37 (d, J = 8.5 Hz, 2H, ArH), 7.25 (d, J = 8.5 Hz, 2H, ArH), 7.02 (d, J = 2.5 Hz, 2H, ArH), 6.56 (t, J = 2.5 Hz, 1H, ArH), 3.79 (s, 6H, OCH₃), 2.32 (s, 3H, CH₃) ppm. ^{13}C -NMR (DMSO- d_6 , 125 MHz) δ 187.7, 160.8, 143.9, 143.7, 142.6, 136.7, 136.5, 132.5, 130.4, 130.0, 126.8, 122.4, 118.0, 106.7, 102.9, 55.5, 21.0 ppm. HRMS (ESI, m/z): calculated for $C_{24}H_{24}NO_5S$ $[M+H]^+$ 438.13752, found 438.13424.

N-[4-(3-(2,3-methylenedioxyphenyl)-acryloyl)-phenyl]-4-methylbenzenesulfonamide (**82**) 1H -NMR (DMSO- d_6 , 500 MHz) δ 10.86 (s, 1H, N-H), 7.94 (d, J = 9.0 Hz, 2H, ArH), 7.78 (d, J = 15.5 Hz, 1H, β -H), 7.72 (d, J = 8.5 Hz, 2H, ArH), 7.61 (d, J = 15.5 Hz, 1H, α -H), 7.35 (d, J = 8.5 Hz, 2H, ArH), 7.28 (d, J = 8.5 Hz, 1H, ArH), 7.24 (d, J = 9.0 Hz, 2H, ArH), 6.97 (d, J = 7.5 Hz, 1H, ArH), 6.88 (t, J = 8.0 Hz, 1H, ArH), 6.14 (s, 2H, CH₂), 2.31 (s, 3H, CH₃) ppm. ^{13}C -NMR (DMSO- d_6 , 125 MHz) δ 187.5, 147.7, 146.7, 143.8, 142.5, 137.1, 136.4, 132.4, 130.1, 129.9, 126.8, 123.4, 122.0, 118.0, 117.1, 110.1, 101.7, 21.0 ppm. HRMS (ESI, m/z): calculated for $C_{23}H_{20}NO_5S$ $[M+H]^+$ 422.10622, found 422.1543.

N-[4-(3-(3,4-methylenedioxyphenyl)-acryloyl)-phenyl]-4-methylbenzenesulfonamide (**83**) 1H -NMR (DMSO- d_6 , 500 MHz) δ 10.80 (s, 1H, N-H), 8.00 (d, J = 8.5 Hz, 2H, ArH), 7.69 (d, J = 8.0 Hz, 2H, ArH), 7.69 (d, J = 15.5 Hz, 1H, β -H), 7.57 (d, J = 15.5 Hz, 1H, α -H), 7.55 (d, J = 1.5 Hz, 1H, ArH), 7.33 (d, J = 8.5 Hz, 2H, ArH), 7.25 (dd, J = 8.0, 1.0 Hz, 1H, ArH), 7.20 (d, J = 8.5 Hz, 2H, ArH), 6.93 (d, J = 8.0 Hz, 1H, ArH), 6.06 (s, 2H, CH₂), 2.29 (s, 3H, CH₃) ppm. ^{13}C -NMR (DMSO- d_6 , 125 MHz) δ 187.4, 149.5, 148.1, 143.8, 143.6, 142.3, 136.4, 132.8, 130.1, 129.9, 129.3, 126.8, 125.9, 119.8, 117.9, 108.5, 106.9, 101.7, 21.0 ppm. HRMS (ESI, m/z): calculated for $C_{23}H_{20}NO_5S$ $[M+H]^+$ 422.10622, found 422.10617.

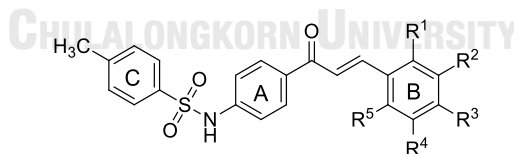
2.4.4 Preparation of sulfonamide chalcones with disubstituent (OH, OCH₃, and OCH₂OCH₂CH₃) on B-ring (84-88)

2.4.4.1 Preparation of protected benzaldehydes

The synthesis of EOM-protected benzaldehydes was followed the procedure from Kim *et. al.*³⁹ 3,4-Dihydroxybenzaldehyde (21.71 mmol) and K₂CO₃ (217.20 mmol) in 100 mL acetone were cooled to 0° C and EOM-Cl (93.65 mmol) was then added dropwise. The resulting mixture was stirred at room temperature for 24 h and then, diluted with water (100 mL) and extracted with EtOAc. The organic layer was dried over with Na₂SO₄ and evaporated to dryness to yield crude EOM-protected benzaldehyde which was purified by silica gel column chromatography.

2.4.4.2 Preparation of sulfonamide chalcones bearing protecting groups and deprotecting groups from chalcones

Sulfonamide chalcones **85**, **87** and **89** were obtained by following the general procedure 2.4. For sulfonamide chalcones **84** and **86** (Figure 2.5), the synthesis was conducted following the methodology reported by Kim *et al.*³⁹ To deprotect EOM groups, **85** and **87** were added 10% HCl (1 mL) and the mixture was further stirred 60° C for 30 min. Subsequently, the whole mixture was diluted with water (20 mL) and its pH was adjusted to 5 with 6N NaOH and purified using column chromatography or recrystallization using a suitable solvent.



- 84.** R¹ = R⁴ = R⁵ = H, R² = OCH₃, R³ = OH
85. R¹ = R⁴ = R⁵ = H, R² = OCH₃, R³ = OCH₂OCH₂CH₃
86. R¹ = R⁴ = R⁵ = H, R² = OH, R³ = OCH₃
87. R¹ = R⁴ = R⁵ = H, R² = OCH₂OCH₂CH₃, R³ = OCH₃
88. R¹ = R⁴ = R⁵ = H, R² = R³ = OCH₂OCH₂CH₃

Figure 2.5 The structures of synthesized sulfonamide chalcones (84-88)

N-[4-(3-(3-methoxy-4-hydroxyphenyl)-acryloyl)-phenyl]-4-methylbenzene sulfonamide (**84**) ¹H-NMR (DMSO-*d*₆, 500 MHz) δ 9.66 (s, 1H, N-H), 7.94 (d, *J* = 8.5 Hz, 2H, ArH), 7.65 (d, *J* = 8.5 Hz, 2H, ArH), 7.59 (d, *J* = 15.0 Hz, 1H, β -H), 7.52(d, *J* =15.0 Hz,

1H, α -H), 7.38 (d, J = 2.0 Hz, 1 H, ArH), 7.28 (d, J = 8.5 Hz, 2H, ArH), 7.16 (d, J = 8.5 Hz, 2H, ArH), 7.13 (d, J = 2.0 Hz, 1H, ArH), 6.74 (d, J = 8.0 Hz, 1H, ArH), 3.76 (s, 3H, OCH₃), 2.24 (s, 3H, CH₃) ppm. ¹³C-NMR (DMSO-*d*₆, 125 MHz) δ 187.4, 149.7, 148.0, 144.5, 143.7, 142.4, 136.6, 132.9, 130.1, 129.9, 126.8, 126.3, 124.2, 118.4, 118.0, 115.6, 111.5, 55.9, 21.0 ppm.

N-[4-(3-(3-methoxy-4-ethoxymethoxyphenyl)-acryloyl)-phenyl]-4-methyl benzenesulfonamide (**85**) ¹H-NMR (DMSO-*d*₆, 500 MHz) δ 10.78 (s, 1H, N-H), 7.97 (d, J = 9.0 Hz, 2 H, ArH), 7.68 (d, J = 15.5 Hz, 1H, β -H), 7.66 (d, J = 8.5 Hz, 2 H, ArH), 7.56 (d, J = 15.5 Hz, 1H, α -H), 7.45 (d, J = 2.0 Hz, 1H, ArH), 7.30 (d, J = 8.5 Hz, 2H, ArH), 7.26 (dd, J = 8.5, 2.0 Hz, 1H, ArH), 7.18 (d, J = 9.0 Hz, 2H, ArH), 7.03 (d, J = 8.5 Hz, 1H, ArH), 5.19 (s, 2H, CH₂), 3.79 (s, 3H, OCH₃), 3.59 (q, J = 7.0, 2H, CH₂), 2.26 (s, 3H, CH₃), 1.05 (t, J = 7.0, 3H, CH₃) ppm. ¹³C-NMR (DMSO-*d*₆, 125 MHz) δ 187.5, 149.8, 148.4, 143.8, 142.3, 136.5, 132.8, 130.2, 130.0, 128.9, 126.8, 123.4, 120.0, 118.0, 115.8, 111.5, 93.2, 64.0, 55.9, 21.0, 15.0 ppm. HRMS (ESI, m/z): calculated for C₂₆H₂₇NNaO₆S [M+Na]⁺ 504.14568, found 504.14362.

N-[4-(3-(3-hydroxy-4-methoxyphenyl)-acryloyl)-phenyl]-4-methylbenzene sulfonamide (**86**) ¹H-NMR (DMSO-*d*₆, 500 MHz) δ 10.82 (s, 1H, N-H), 9.15 (d, J = 1.0 Hz, 1H, Ar-OH), 8.01 (d, J = 8.5 Hz, 2H, ArH), 7.73 (d, J = 8.5 Hz, 2H, ArH), 7.60 (d, J = 15.5 Hz, 1H, β -H), 7.55 (d, J = 15.0 Hz, 1H, α -H), 7.37 (d, J = 8.0 Hz, 2H, ArH), 7.27 (d, J = 2.0 Hz, 1H, ArH), 7.25 (d, J = 2.0 Hz, 1H, ArH), 7.22 (d, J = 8.5 Hz, 2H, ArH), 6.98 (d, J = 8.5 Hz, 1H, ArH), 3.83 (s, 3H, OCH₃), 2.33 (s, 3H, CH₃) ppm. ¹³C-NMR (DMSO-*d*₆, 125 MHz) δ 187.4, 150.3, 146.6, 144.0, 143.8, 142.2, 136.5, 132.9, 130.0, 129.9, 127.7, 126.8, 122.0, 119.2, 118.0, 114.8, 111.9, 55.7, 21.0 ppm. HRMS (ESI, m/z): calculated for C₂₃H₂₂NO₅S [M+H]⁺ 424.12187, found 424.11965.

N-[4-(3-(3-ethoxymethoxy-4-methoxyphenyl)-acryloyl)-phenyl]-4-methyl benzenesulfonamide (**87**) ¹H-NMR (DMSO-*d*₆, 500 MHz) δ 10.84 (s, 1H, N-H), 8.02 (d, J = 8.5 Hz, 2 H, ArH), 7.73 (d, J = 8.5 Hz, 2 H, ArH), 7.68 (d, J = 15.5 Hz, 1H, β -H), 7.61 (d, J = 15.0 Hz, 1H, α -H), 7.56 (d, J = 2.5 Hz, 1H, ArH), 7.44 (dd, J = 8.0, 2.0 Hz, 1H, ArH), 7.37 (d, J = 8.0 Hz, 2H, ArH), 7.24 (d, J = 9.0 Hz, 2H, ArH), 7.05 (d, J = 8.5 Hz, 1H, ArH), 5.28 (s, 2H, CH₂), 3.82 (s, 3H, OCH₃), 3.69 (q, J = 7.5 Hz, 2H, CH₂), 2.33 (s, 3H, CH₃), 1.13

(t, $J = 7.0$, 3H, CH₃) ppm. ¹³C-NMR (DMSO-*d*₆, 125 MHz) δ 187.4, 152.3, 146.0, 143.7, 142.3, 136.5, 132.8, 130.1, 129.9, 127.5, 126.8, 124.9, 119.6, 118.0, 116.0, 112.3, 93.4, 64.0, 55.8, 21.0, 15.0 ppm. HRMS (ESI, m/z): calculated for C₂₆H₂₇NNaO₆S [M+Na]⁺ 504.14568, found 504.14389.

N-[4-(3-(3,4-ethoxymethoxyphenyl)-acryloyl)-phenyl]-4-methylbenzene sulfonamide (**88**) ¹H-NMR (DMSO-*d*₆, 500 MHz) δ 10.85 (s, 1H, N-H), 8.02 (d, $J = 9.0$ Hz, 2 H, ArH), 7.73 (d, $J = 8.5$ Hz, 2 H, ArH), 7.70 (d, $J = 16.0$ Hz, 1H, β -H), 7.60 (d, $J = 15.0$ Hz, 1H, α -H), 7.58 (d, $J = 1.5$ Hz, 1H, ArH), 7.43 (dd, $J = 8.5$, 2.5 Hz, 1H, ArH), 7.37 (d, $J = 8.5$ Hz, 2H, ArH), 7.24 (d, $J = 9.0$ Hz, 2H, ArH), 7.15 (d, $J = 8.5$ Hz, 1H, ArH), 5.31 (s, 2H, CH₂), 5.29 (s, 2H, CH₂), 3.70 (q, $J = 7.0$ Hz, 2H, CH₂), 3.67 (q, $J = 7.0$ Hz, 2H, CH₂), 2.33 (s, 3H, CH₃), 1.12 (td, $J = 7.0$, 3.0 Hz, 6H, CH₃) ppm. ¹³C-NMR (DMSO-*d*₆, 125 MHz) δ 18.5, 149.5, 146.8, 143.8, 143.5, 142.3, 136.5, 132.7, 130.1, 129.9, 128.7, 126.8, 124.3, 120.2, 118.0, 116.6, 116.3, 93.4, 93.2, 64.0, 21.0, 15.0, 15.0 ppm. HRMS (ESI, m/z): calculated for C₂₈H₃₁NNaO₇S [M+Na]⁺ 548.17189, found 548.17143.

2.4.5 Preparation of sulfonamide chalcones with dichloro substituent on B-ring (89-91)

Three sulfonamide chalcones (**89-91**) with dichloro substituents on B-ring were attained following the procedure described in 2.4 (Figure 2.6).

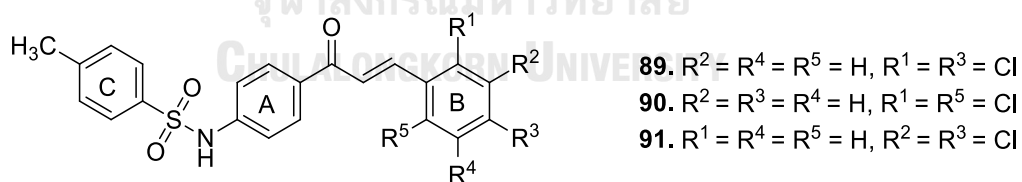


Figure 2.6 The structures of synthesized sulfonamide chalcones with dichlorosubstituent on B-ring (**89-91**)

N-[4-(3-(2,4-dichlorophenyl)-acryloyl)-phenyl]-4-methylbenzenesulfonamide (**89**) ¹H-NMR (DMSO-*d*₆, 500 MHz) δ 10.90 (s, 1H, N-H), 8.18 (d, $J = 9.0$ Hz, 1H, ArH), 8.05 (d, $J = 9.0$ Hz, 2H, ArH), 7.93 (d, $J = 15.5$ Hz, 1H, β -H), 7.88 (d, $J = 15.5$ Hz, 1H, α -H), 7.74 (d, $J = 8.5$ Hz, 2H, ArH), 7.72 (d, $J = 2.0$ Hz, 1H, ArH), 7.52 (dd, $J = 9.0$, 2.5 Hz, 1H, ArH), 7.37 (d, $J = 9.0$ Hz, 2H, ArH), 7.25 (d, $J = 9.0$ Hz, 2H, ArH), 2.32 (s, 3H, CH₃) ppm.

^{13}C -NMR (DMSO- d_6 , 125.7 MHz) δ 187.2, 143.9, 142.8, 136.8, 136.4, 135.6, 135.1, 132.1, 131.4, 130.5, 130.0, 129.8, 129.5, 128.0, 126.8, 125.2, 117.9, 21.0 ppm. HRMS (ESI, m/z): calculated for $\text{C}_{22}\text{H}_{16}\text{Cl}_2\text{NNa}_2\text{O}_3\text{S}$ [$\text{M}+2\text{Na}-\text{H}$] $^+$ 490.00178, found 490.0005.

N-[4-(3-(2,6-dichlorophenyl)acryloyl)-phenyl]-4-methylbenzenesulfonamide

(90) ^1H -NMR (DMSO- d_6 , 500 MHz) δ 10.93 (s, 1H N-H), 7.96 (d, J = 9.0 Hz, 2H, ArH), 7.74 (d, J = 8.5 Hz, 2H, ArH), 7.72 (d, J = 16.0 Hz, 1H, β -H), 7.63 (d, J = 16.0 Hz, 1H, α -H), 7.57 (d, J = 8.5 Hz, 2H, ArH), 7.41 (t, J = 8.0 Hz, 1H, ArH), 7.36 (d, J = 8.0 Hz, 2H, ArH), 7.26 (d, J = 9.0 Hz, 2H, ArH), 2.32 (s, 3H, CH_3) ppm. ^{13}C -NMR (DMSO- d_6 , 125 MHz) δ 187.3, 143.9, 142.9, 136.4, 134.1, 132.2, 131.8, 131.1, 130.4, 130.4, 130.0, 129.2, 126.8, 118.0, 21.0 ppm. HRMS (ESI, m/z): calculated for $\text{C}_{22}\text{H}_{18}\text{Cl}_2\text{NO}_3\text{S}$ [$\text{M}+\text{H}$] $^+$ 446.03844, found 446.0481.

N-[4-(3-(3,4-dichlorophenyl)acryloyl)-phenyl]-4-methylbenzenesulfonamide

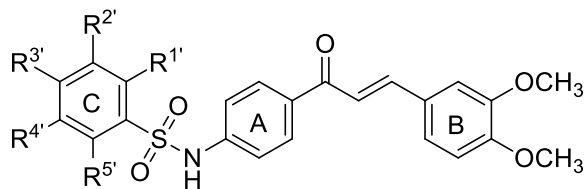
(91) ^1H -NMR (DMSO- d_6 , 500 MHz) δ 10.89 (s, 1H, N-H), 8.23 (d, J = 2.0 Hz, 1H, ArH), 8.06 (d, J = 9.0 Hz, 2H, ArH), 7.95 (d, J = 16.0 Hz, 1H, β -H), 7.82 (dd, J = 8.0, 2.0 Hz, 1H, ArH), 7.74 (d, J = 8.0 Hz, 2H, ArH), 7.69 (d, J = 8.5 Hz, 1H, ArH), 7.63 (d, J = 15.5 Hz, 1H, α -H), 7.37 (d, J = 8.5 Hz, 2H, ArH), 7.25 (d, J = 8.5 Hz, 2H, ArH), 2.32 (s, 3H, CH_3) ppm. ^{13}C -NMR (DMSO- d_6 , 125 MHz) δ 187.3, 143.9, 142.7, 140.7, 136.4, 135.7, 132.7, 132.3, 131.9, 131.0, 130.4, 130.1, 130.0, 129.1, 126.8, 124.0, 117.9, 21.0 ppm. HRMS (ESI, m/z): calculated for $\text{C}_{22}\text{H}_{18}\text{Cl}_2\text{NO}_3\text{S}$ [$\text{M}+\text{H}$] $^+$ 446.03844, found 446.03866.

2.5 Preparation of sulfonamide chalcones with 3,4 dimethoxy on B-ring

2.5.1 Preparation of sulfonamide chalcones with unsubstituent and monosubstituent on C-ring (92-99)

Eight sulfonamide chalcones (92-99) (Figure 2.7) were synthesized by dissolving 4-aminochalcone (0.6 mmol) in 10 mL CH_2Cl_2 in ice bath. Benzenesulfonyl chloride derivative (1.2 mmol) in pyridine (1.2 eq) was added. The reaction was maintained while stirring at room temperature for 24 h and monitored by TLC. The resulting mixture was added saturated NaHCO_3 to adjust the pH to 8 and extracted with CH_2Cl_2 . The organic layer was evaporated and recrystallized with a mixture of CH_2Cl_2 and

hexane. The solid obtained was slowly washed using MeOH to obtain a target compound of about 56-90%.



- 92.** $R^1 = R^2 = R^3 = R^4 = R^5 = H$ **96.** $R^1 = R^2 = R^4 = R^5 = H, R^3 = F$
93. $R^1 = R^2 = R^4 = R^5 = H, R^3 = NH_2$ **97.** $R^1 = R^2 = R^4 = R^5 = H, R^3 = Cl$
94. $R^1 = R^2 = R^4 = R^5 = H, R^3 = OCH_3$ **98.** $R^1 = R^2 = R^4 = R^5 = H, R^3 = NO_2$
95. $R^1 = R^2 = R^4 = R^5 = H, R^3 = CH_3CO$ **99.** 1-naphthalene

Figure 2.7 The structures of synthesized sulfonamide chalcones with unsubstituent and monosubstituent on C-ring (**92-99**)

N-[4-(3-(3,4-dimethoxyphenyl)acryloyl)-phenyl]-benzenesulfonamide (**92**) 1H -NMR (DMSO- d_6 , 500 MHz) δ 10.91 (s, 1H, N-H), 8.05 (d, $J = 8.5$ Hz, 2 H, ArH), 7.86 (d, $J = 7.5$ Hz, 2H, ArH), 7.73 (d, $J = 15.0$ Hz, 1H, β -H), 7.64 (t, $J = 8.0$ Hz, 2 H, ArH), 7.58 (d, $J = 15.0$ Hz, 1H, α -H), 7.58 (t, $J = 8.0$ Hz, 1H, ArH), 7.49 (d, $J = 2.0$ Hz, 1H, ArH), 7.34 (dd, $J = 8.5, 2.0$ Hz, 1H, ArH), 7.26 (d, $J = 8.5$ Hz, 2H, ArH), 7.00 (d, $J = 8.5$ Hz, 1H, ArH), 3.84 (s, 3H, OCH₃), 3.80 (s, 3H, OCH₃) ppm. ^{13}C -NMR (DMSO- d_6 , 125 MHz) δ 187.4, 151.2, 149.0, 144.0, 142.1, 139.3, 133.3, 133.0, 130.1, 129.5, 127.5, 126.7, 123.9, 119.4, 118.1, 111.6, 110.6, 55.7, 55.6 ppm. HRMS (ESI, m/z): calculated for C₂₃H₂₂NO₅S [M+H]⁺ 424.12187, found 424.12078.

N-[4-(3-(3,4-dimethoxyphenyl)acryloyl)-phenyl]-4-aminobenzenesulfonamide (**93**) 1H -NMR (DMSO- d_6 , 500 MHz) δ 10.51 (s, 1H, N-H), 8.03 (d, $J = 8.5$ Hz, 2H, ArH), 7.75 (d, $J = 15.5$ Hz, 1H, β -H), 7.63 (d, $J = 15.5$ Hz, 1H, α -H), 7.49 (d, $J = 1.5$ Hz, 1H, ArH), 7.48 (d, $J = 9.0$ Hz, 2H, ArH), 7.34 (dd, $J = 8.5, 2.0$ Hz, 1H, ArH), 7.21 (d, $J = 8.5$ Hz, 2H, ArH), 7.00 (d, $J = 8.5$ Hz, 1H, ArH), 6.56 (d, $J = 9.0$ Hz, 2H, ArH), 6.05 (s, 2H, NH₂), 3.84 (s, 3H, OCH₃), 3.80 (s, 3H, OCH₃) ppm. ^{13}C -NMR (DMSO- d_6 , 125 MHz) δ 187.4, 153.3, 151.2, 149.1, 143.9, 143.0, 132.2, 130.1, 128.9, 127.6, 124.0, 123.9, 119.5, 117.4, 112.7,

111.6, 110.6, 55.8, 55.7 ppm. HRMS (ESI, m/z): calculated for $C_{23}H_{23}N_2O_5S$ $[M+H]^+$ 439.13277, found 439.12965.

N-[4-(3-(3,4-dimethoxyphenyl)acryloyl)-phenyl]-4-methoxybenzenesulfonamide (**94**) 1H -NMR (DMSO- d_6 , 500 MHz) δ 10.77 (s, 1H, N-H), 8.05 (d, $J = 8.5$ Hz, 2H, ArH), 7.78 (d, $J = 8.5$ Hz, 2H, ArH), 7.76 (d, $J = 15.5$ Hz, 1H, β -H), 7.64 (d, $J = 15.0$ Hz, 1H, α -H) 7.49 (d, $J = 2.0$ Hz, 1H, ArH), 7.34 (dd, $J = 8.5, 2.0$ Hz, 1H, ArH), 7.25 (d, $J = 9.0$ Hz, 2H, ArH), 7.08 (d, $J = 9.0$ Hz, 2H, ArH), 7.00 (d, $J = 8.0$ Hz, 1H, ArH), 3.84 (s, 3H, OCH₃), 3.81 (s, 3H, OCH₃), 3.79 (s, 3H, OCH₃) ppm. ^{13}C -NMR (DMSO- d_6 , 125 MHz) δ 187.4, 162.7, 151.2, 149.0, 144.0, 142.3, 132.7, 130.8, 130.1, 129.0, 127.5, 123.9, 119.4, 117.9, 114.6, 111.5, 110.6, 55.7, 55.7, 55.6 ppm. HRMS (ESI, m/z): calculated for $C_{24}H_{24}NO_6S$ $[M+H]^+$ 454.13243, found 454.13117.

N-[4-(3-(3,4-dimethoxyphenyl)acryloyl)-phenyl]-4-Acetylbenzenesulfonamide (**95**) 1H -NMR (DMSO- d_6 , 500 MHz) δ 11.06 (s, 1H, N-H), 8.10 (d, $J = 8.5$ Hz, 2H, ArH), 8.05 (d, $J = 9.0$ Hz, 2H, ArH), 7.97 (d, $J = 8.5$ Hz, 2H, ArH), 7.73 (d, $J = 15.5$ Hz, 1H, β -H), 7.64 (d, $J = 15.5$ Hz, 1H, α -H), 7.48 (d, $J = 2.5$ Hz, 1H, ArH), 7.34 (dd, $J = 8.5, 2.5$ Hz, 1H, ArH), 7.27 (d, $J = 9.0$ Hz, 2H, ArH), 7.00 (d, $J = 8.0$ Hz, 1H, ArH), 3.84 (s, 3H, OCH₃), 3.80 (s, 3H, OCH₃), 2.58 (s, 3H, CH₃) ppm. ^{13}C -NMR (DMSO- d_6 , 125 MHz) δ 197.3, 187.5, 151.3, 149.0, 144.2, 142.9, 141.7, 140.0, 133.3, 130.2, 129.3, 127.5, 127.1, 124.0, 119.3, 118.4, 111.6, 110.6, 55.7, 55.6, 27.0 ppm. HRMS (ESI, m/z): calculated for $C_{25}H_{23}NNaO_6S$ $[M+Na]^+$ 488.11438, found 488.11401.

N-[4-(3-(3,4-dimethoxyphenyl)acryloyl)-phenyl]-4-fluorobenzenesulfonamide (**96**) 1H -NMR (DMSO- d_6 , 500 MHz) δ 10.89 (s, 1H, N-H), 8.03 (d, $J = 9.0$ Hz, 2H, ArH), 7.88 (dd, $J = 9.0, 5.5$ Hz, 2H, ArH), 7.71 (d, $J = 15.5$ Hz, 1H, β -H), 6.17 (d, $J = 15.5$ Hz, 1H, α -H), 7.47 (d, $J = 2.0$ Hz, 1H, ArH), 7.40 (t, $J = 8.5$ Hz, 2H, ArH), 7.32 (dd, $J = 8.5, 2.0$ Hz, 1H, ArH), 7.23 (d, $J = 8.5$ Hz, 2H, ArH), 6.97 (d, $J = 8.5$ Hz, 1H, ArH), 3.82 (s, 3H, OCH₃), 3.78 (s, 3H, OCH₃) ppm. ^{13}C -NMR (DMSO- d_6 , 125 MHz) δ 187.4, 165.5, 163.5, 151.3, 149.0, 144.1, 141.9, 135.7, 133.1, 130.1, 129.9, 129.8, 127.5, 123.9, 119.4, 118.3, 116.8, 116.6, 111.6, 110.6, 55.7, 55.6 ppm. HRMS (ESI, m/z): calculated for $C_{23}H_{20}FNNaO_5S$ $[M+Na]^+$ 464.09439, found 464.1548.

N-[4-(3-(3,4-dimethoxyphenyl)acryloyl)-phenyl]-4-chlorobenzenesulfonamide

(97) ¹H-NMR (DMSO-*d*₆, 500 MHz) δ 10.95 (s, 1H, N-H), 8.04 (d, *J* = 9.0 Hz, 2H, ArH), 7.82 (d, *J* = 9.0 Hz, 2H, ArH), 7.72 (d, *J* = 15.5 Hz, 1H, β -H), 7.64 (d, *J* = 9.0 Hz, 2H, ArH), 7.62 (d, *J* = 15.5 Hz, 1H, α -H), 7.47 (d, *J* = 2.0 Hz, 1H, ArH), 7.32 (dd, *J* = 8.5, 2.5 Hz, 1H, ArH), 7.23 (d, *J* = 8.5 Hz, 2H, ArH), 6.98 (d, *J* = 8.5 Hz, 1H, ArH), 3.82 (s, 3H, OCH₃), 3.78 (s, 3H, OCH₃) ppm. ¹³C-NMR (DMSO-*d*₆, 125 MHz) δ 187.4, 151.3, 149.0, 144.1, 141.7, 138.2, 138.1, 133.2, 130.1, 129.7, 128.7, 127.5, 124.0, 119.3, 118.4, 111.5, 110.6, 55.7, 55.6 ppm.

N-[4-(3-(3,4-dimethoxyphenyl)acryloyl)-phenyl]-4-nitrobenzenesulfonamide

(98) ¹H-NMR (DMSO-*d*₆, 500 MHz) δ 11.15 (s, 1H, N-H), 8.34 (d, *J* = 8.5 Hz, 2H, ArH), 8.03 (d, *J* = 8.5 Hz, 2H, ArH), 8.02 (d, *J* = 8.5 Hz, 2H, ArH), 7.68 (d, *J* = 15.5 Hz, 1H, β -H), 7.59 (d, *J* = 15.5 Hz, 1H, α -H), 7.43 (s, 1H, ArH), 7.28 (d, *J* = 8.5 Hz, 1H, ArH), 7.23 (d, *J* = 8.0 Hz, 2H, ArH), 6.94 (d, *J* = 7.5 Hz, 1H, ArH), 3.78 (s, 3H, OCH₃), 3.75 (s, 3H, OCH₃) ppm. ¹³C-NMR (DMSO-*d*₆, 125 MHz) δ 187.5, 151.3, 150.1, 149.0, 144.6, 144.3, 141.3, 133.6, 130.2, 128.4, 127.5, 124.9, 124.0, 119.3, 118.7, 111.6, 110.6, 55.7, 55.6 ppm. HRMS (ESI, *m/z*): calculated for C₂₃H₂₁N₂O₇S [M+H]⁺ 469.10695, found 469.10504.

N-[4-(3-(3,4-dimethoxyphenyl)acryloyl)-phenyl]-1-naphthalenesulfonamide

(99) ¹H-NMR (DMSO-*d*₆, 500 MHz) δ 11.32 (s, 1H, N-H), 8.74 (d, *J* = 9.0 Hz, 1H, ArH), 8.35 (d, *J* = 7.0 Hz, 1H, ArH), 8.24 (d, *J* = 8.5 Hz, 1H, ArH), 8.08 (d, *J* = 8.0 Hz, 1H, ArH), 7.98 (d, *J* = 8.5 Hz, 2H, ArH), 7.77 (t, *J* = 9.0 Hz, 1H, ArH), 7.68 (d, *J* = 16.0 Hz, 1H, β -H), 7.67 (t, *J* = 9.0 Hz, 2H, ArH), 7.60 (d, *J* = 15.5 Hz, 1H, α -H), 7.47 (d, *J* = 2.5 Hz, 1H, ArH), 7.31 (dd, *J* = 8.0, 2.0 Hz, 1H, ArH), 7.20 (d, *J* = 8.5 Hz, 2H, ArH), 6.98 (d, *J* = 8.0 Hz, 1H, ArH), 3.83 (s, 3H, OCH₃), 3.79 (s, 3H, OCH₃) ppm. ¹³C-NMR (DMSO-*d*₆, 125 MHz) δ 187.3, 151.2, 149.0, 143.9, 141.9, 134.9, 133.9, 133.8, 132.5, 130.3, 130.1, 129.2, 128.4, 127.5, 127.3, 127.1, 124.5, 124.0, 123.9, 119.3, 117.1, 111.5, 110.6, 55.7, 55.6 ppm. HRMS (ESI, *m/z*): calculated for C₂₇H₂₃NNaO₅S [M+Na]⁺ 496.11946, found 496.11846.

2.5.2 Preparation of sulfonamide chalcones with disubstituent on C-ring (100-103)

Four sulfonamide chalcones (100-103) with disubstituent (Cl, NO₂ and OCH₂CH₃) on C-ring were attained following the procedure described in 2.4 (Figure 2.8).

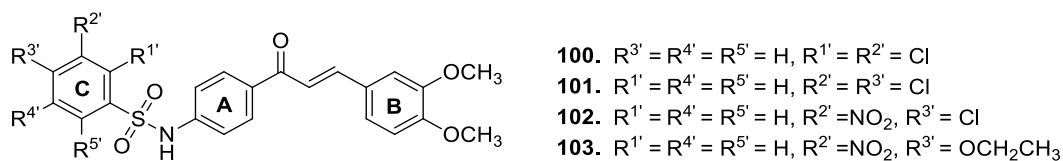


Figure 2.8 The structures of synthesized sulfonamide chalcones with disubstituent on C-ring (**100-103**)

N-[4-(3-(3,4-dimethoxyphenyl)-acryloyl)-phenyl]-2,3-dichlorobenzenesulfonamide (**100**) ¹H-NMR (DMSO-*d*₆, 500 MHz) δ 11.38 (s, 1H, N-H), 8.14 (dd, *J* = 8.0, 1.0 Hz, 1H, ArH), 8.03 (d, *J* = 9.0 Hz, 2H, ArH), 7.93 (dd, *J* = 8.5, 1.0 Hz, 1H, ArH), 7.71 (d, *J* = 15.5 Hz, 1H, β -H), 7.61 (d, *J* = 15.5 Hz, 1H, α -H), 7.58 (t, *J* = 8.5 Hz, 1H, ArH), 7.47 (d, *J* = 1.5 Hz, 1H, ArH), 7.31 (dd, *J* = 8.5, 1.5 Hz, 1H, ArH), 7.22 (d, *J* = 8.5 Hz, 2H, ArH), 6.97 (d, *J* = 8.5 Hz, 1H, ArH), 3.82 (s, H, OCH₃), 3.78 (s, H, OCH₃) ppm. ¹³C-NMR (DMSO-*d*₆, 125 MHz) δ 187.4, 151.2, 149.0, 144.1, 141.1, 138.4, 135.4, 134.4, 133.1, 130.6, 130.2, 128.8, 127.5, 124.0, 119.3, 117.6, 111.5, 110.6, 55.7, 55.6 ppm. HRMS (ESI, *m/z*): calculated for C₂₃H₁₈Cl₂NNa₂O₅S [M+2Na-H]⁺ 536.00726, found 536.00668.

N-[4-(3-(3,4-dimethoxyphenyl)-acryloyl)-phenyl]-3,4-dichlorobenzenesulfonamide (**101**) ¹H-NMR (DMSO-*d*₆, 500 MHz) δ 11.00 (s, 1H, N-H), 8.05 (d, *J* = 9.0 Hz, 2H, ArH), 8.00 (d, *J* = 2.0 Hz, 1H, ArH), 7.84 (d, *J* = 8.5 Hz, 1H, ArH), 7.74 (dd, *J* = 8.5, 2.0 Hz, 1H, ArH), 7.72 (d, *J* = 15.5 Hz, 1H, β -H), 7.62 (d, *J* = 15.5 Hz, 1H, α -H), 7.47 (d, *J* = 1.5 Hz, 1H, ArH), 7.32 (dd, *J* = 8.5, 1.5 Hz, 1H, ArH), 7.25 (d, *J* = 9.0 Hz, 2H, ArH), 6.98 (d, *J* = 8.0 Hz, 1H, ArH), 3.82 (s, H, OCH₃), 3.78 (s, H, OCH₃) ppm. ¹³C-NMR (DMSO-*d*₆, 125 MHz) δ 187.5, 151.3, 149.0, 144.2, 141.4, 139.5, 136.5, 133.5, 132.4, 132.0, 130.2, 128.4, 127.5, 126.8, 124.0, 119.3, 118.7, 111.6, 110.6, 55.7, 55.6 ppm. HRMS (ESI, *m/z*): calculated for C₂₃H₂₀Cl₂NO₅S [M+H]⁺ 492.04392, found 492.03667.

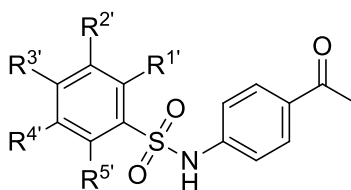
N-[4-(3-(3,4-dimethoxyphenyl)-acryloyl)-phenyl]-4-chloro-3-nitrobenzenesulfonamide (**102**) ¹H-NMR (DMSO-*d*₆, 500 MHz) δ 11.12 (s, 1H, N-H), 8.47 (s, 1H, ArH), 8.04 (d, *J* = 7.5 Hz, 2H, ArH), 8.01 (s, 1H, ArH), 7.95 (dd, *J* = 8.5, 1.0 Hz, 1H, ArH), 7.70 (d, *J* = 15.5 Hz, 1H, β -H), 7.61 (d, *J* = 15.5 Hz, 1H, α -H), 7.45 (s, 1H, ArH), 7.30 (d, *J* = 8.0 Hz, 1H, ArH), 7.24 (d, *J* = 7.5 Hz, 2H, ArH), 6.96 (d, *J* = 8.5 Hz, 1H, ArH), 3.80 (s, 3H, OCH₃),

3.76 (s, 3H, OCH₃) ppm. ¹³C-NMR (DMSO-*d*₆, 125 MHz) δ 187.5, 151.3, 149.0, 147.5, 144.3, 141.1, 139.4, 133.7, 133.5, 131.4, 130.4, 130.3, 127.5, 124.3, 124.0, 119.3, 119.0, 111.6, 110.7, 55.7, 55.6 ppm. HRMS (ESI, *m/z*): calculated for C₂₃H₁₈ClN₂Na₂O₇S [M+2Na-H]⁺ 547.03132, found 547.03172.

N-[4-(3-(3,4-dimethoxyphenyl)-acryloyl)-phenyl]-4-ethoxy-3-nitrobenzene sulfonamide (**103**) ¹H-NMR (DMSO-*d*₆, 500 MHz) δ 10.92 (s, 1H N-H), 8.28 (d, *J* = 2.5 Hz, 1H, ArH), 8.03 (d, *J* = 9.0 Hz, 2H, ArH), 7.98 (dd, *J* = 9.0, 2.0 Hz, 1H, ArH), 7.70 (d, *J* = 15.5 Hz, 1H, β -H), 7.60 (d, *J* = 15.0 Hz, 1H, α -H), 7.47 (d, *J* = 9.0 Hz, 1H, ArH), 7.45 (d, *J* = 2.0 Hz, 1H, ArH), 7.30 (dd, *J* = 8.5, 2.0 Hz, 1H, ArH), 7.24 (d, *J* = 9.0 Hz, 2H, ArH), 6.96 (d, *J* = 8.5 Hz, 1H, ArH), 4.22 (q, *J* = 7.0 Hz, 2H, CH₂), 3.80 (s, 3H, OCH₃), 3.76 (s, 3H, OCH₃), 1.27 (t, *J* = 7.0 Hz, 3H, CH₃) ppm. ¹³C-NMR (DMSO-*d*₆, 125 MHz) δ 187.5, 154.5, 151.3, 149.0, 144.2, 141.6, 138.8, 133.3, 132.6, 130.6, 130.2, 127.5, 124.1, 124.0, 119.4, 118.5, 116.2, 111.6, 110.7, 66.1, 55.7, 55.6, 14.2 ppm. HRMS (ESI, *m/z*): calculated for C₂₅H₂₄N₂NaO₈S [M+Na]⁺ 535.11511, found 535.11347.

2.6 Preparation of benzenesulfonyl aminoacetophenones (**104-111**)

Following the procedure in 2.3, sulfonamide acetophenones were synthesized by treating 4-aminoacetophenone (3.2 mmol) in CH₂Cl₂ (25 mL) in ice bath. Selected benzenesulfonyl chloride derivative (4.1 mmol) in pyridine (1.2 eq) was added. The reaction was maintained while stirring at room temperature for 24 h and monitored by TLC. The resulting composite was added saturated NaHCO₃ to alter the pH to 8 and extracted with CH₂Cl₂. The organic layer was evaporated and recrystallized with CH₂Cl₂ and hexane. The solid collected is slowly washed using MeOH to procure a target compound of around 68-97%. Eight benzenesulfonyl aminoacetophenones (**104-111**) are illustrated in **Figure 2.9**.



- 104.** $R^1 = R^2 = R^3 = R^4 = R^5 = H$ **108.** $R^1 = R^2 = R^4 = R^5 = H, R^3 = Cl$
105. $R^1 = R^2 = R^4 = R^5 = H, R^3 = OCH_3$ **109.** $R^1 = R^2 = R^4 = R^5 = H, R^3 = NO_2$
106. $R^1 = R^2 = R^4 = R^5 = H, R^3 = CH_3CO$ **110.** $R^3 = R^4 = R^5 = H, R^1 = R^2 = Cl$
107. $R^1 = R^2 = R^4 = R^5 = H, R^3 = F$ **111.** $R^1 = R^4 = R^5 = H, R^2 = NO_2, R^3 = Cl$

Figure 2.9 The structures of synthesized benzenesulfonyl aminoacetophenones (104-111)

N-(4-Acetylphenyl)-benzenesulfonamide (**104**) 1H -NMR (DMSO- d_6 , 500 MHz) δ 10.90 (s, 1H, N-H), 7.85-7.82 (m, 4H, ArH), 7.63 (t, $J = 7.5$ Hz, 1H, ArH), 7.57 (t, $J = 8.0$ Hz, 2H, ArH), 7.21 (d, $J = 9.0$ Hz, 2H, ArH), 2.46 (s, 3H, CH_3) ppm. ^{13}C -NMR (DMSO- d_6 , 125 MHz) δ 196.5, 142.2, 129.3, 133.3, 132.0, 129.9, 129.5, 126.7, 118.0, 26.5 ppm.

N-(4-Acetylphenyl)-4-methoxybenzenesulfonamide (**105**) 1H -NMR (DMSO- d_6 , 500 MHz) δ 10.74 (s, 1H, N-H), 7.82 (d, $J = 8.5$ Hz, 2H, ArH), 7.76 (d, $J = 8.5$ Hz, 2H, ArH), 7.20 (d, $J = 8.5$ Hz, 2H, ArH), 7.07 (d, $J = 9.0$ Hz, 2H, ArH), 3.79 (s, 3H, OCH_3), 2.46 (s, 3H, CH_3) ppm. ^{13}C -NMR (DMSO- d_6 , 125 MHz) δ 196.4, 162.7, 142.4, 131.8, 130.8, 129.8, 129.0, 117.7, 114.6, 55.7, 26.4 ppm.

N-(4-Acetylphenyl)-4-acetylbenzenesulfonamide (**106**) 1H -NMR (DMSO- d_6 , 500 MHz) δ 11.05 (s, 1H, N-H), 8.10 (d, $J = 8.5$ Hz, 2H, ArH), 7.96 (d, $J = 8.5$ Hz, 2H, ArH), 7.84 (d, $J = 9.0$ Hz, 2H, ArH), 7.23 (d, $J = 9.0$ Hz, 2H, ArH), 2.58 (s, 3H, CH_3), 2.46 (s, 3H, CH_3) ppm. ^{13}C -NMR (DMSO- d_6 , 125 MHz) δ 197.2, 196.5, 142.8, 141.9, 140.0, 132.3, 129.9, 129.3, 127.1, 118.2, 27.1, 26.5 ppm.

N-(4-Acetylphenyl)-4-fluorobenzenesulfonamide (**107**) 1H -NMR (DMSO- d_6 , 500 MHz) δ 10.89 (s, 1H, N-H), 7.89 (dd, $J = 8.5, 5.0$ Hz, 2H, ArH), 7.84 (d, $J = 8.5$ Hz, 2H, ArH), 7.42 (t, $J = 9.0$ Hz, 2H, ArH), 7.21 (d, $J = 8.5$ Hz, 2H, ArH), 2.47 (s, 3H, CH_3) ppm. ^{13}C -NMR (DMSO- d_6 , 125 MHz) δ 196.5, 165.5, 163.5, 142.0, 135.6, 132.2, 129.9, 118.2, 116.8, 116.6, 26.4 ppm.

N-(4-Acetylphenyl)-4-chlorobenzenesulfonamide (**108**) $^1\text{H-NMR}$ (DMSO- d_6 , 500 MHz) δ 10.95 (s, 1H, N-H), 7.84 (d, $J = 9.0$ Hz, 2H, ArH), 7.82 (d, $J = 8.5$ Hz, 2H, ArH), 7.65 (d, $J = 8.5$ Hz, 2H, ArH), 7.21 (d, $J = 8.5$ Hz, 2H, ArH), 2.47 (s, 3H, CH₃) ppm. $^{13}\text{C-NMR}$ (DMSO- d_6 , 125 MHz) δ 196.5, 141.9, 138.2, 138.1, 132.2, 129.9, 129.7, 128.6, 118.2, 26.4 ppm.

N-(4-Acetylphenyl)-4-nitrobenzenesulfonamide (**109**) $^1\text{H-NMR}$ (DMSO- d_6 , 500 MHz) δ 11.17 (s, 1H, N-H), 8.38 (d, $J = 9.0$ Hz, 2H, ArH), 8.07 (d, $J = 9.0$ Hz, 2H, ArH), 7.85 (d, $J = 9.0$ Hz, 2H, ArH), 7.23 (d, $J = 8.5$ Hz, 2H, ArH), 2.47 (s, 3H, CH₃) ppm. $^{13}\text{C-NMR}$ (DMSO- d_6 , 125 MHz) δ 196.5, 150.1, 144.6, 141.5, 132.6, 129.9, 128.3, 124.9, 118.6, 26.5 ppm.

N-(4-Acetylphenyl)-2,3-dichlorobenzenesulfonamide (**110**) $^1\text{H-NMR}$ (DMSO- d_6 , 500 MHz) δ 11.37 (s, 1H, N-H), 8.13 (dd, $J = 8.0, 1.5$ Hz, 1H, ArH), 7.93 (dd, $J = 8.0, 1.0$ Hz, 1H, ArH), 7.83 (d, $J = 8.5$ Hz, 2H, ArH), 7.58 (t, $J = 8.0$ Hz, 1H, ArH), 7.19 (d, $J = 8.5$ Hz, 2H, ArH), 2.45 (s, 3H, CH₃) ppm. $^{13}\text{C-NMR}$ (DMSO- d_6 , 125 MHz) δ 196.5, 141.2, 138.3, 135.4, 134.4, 132.1, 130.6, 129.9, 128.9, 128.8, 117.5, 26.4 ppm.

N-(4-Acetylphenyl)-3-nitro-4-chlorobenzenesulfonamide (**111**) $^1\text{H-NMR}$ (DMSO- d_6 , 500 MHz) δ 8.50 (d, $J = 2.0$ Hz, 1H, ArH), 8.05 (dd, $J = 8.5, 2.5$ Hz, 1H, ArH), 7.99 (d, $J = 8.5$ Hz, 1H, ArH), 7.86 (d, $J = 9.0$ Hz, 2H, ArH), 7.24 (d, $J = 8.5$ Hz, 2H, ArH), 2.48 (s, 3H, CH₃) ppm. $^{13}\text{C-NMR}$ (DMSO- d_6 , 125 MHz) δ 196.6, 147.5, 141.3, 139.3, 133.5, 132.7, 130.3, 130.0, 124.2, 118.8, 26.5 ppm.

2.7 Preparation of 4-acetyl-*N*-phenylbenzenesulfonamide with un- and monosubstituent

Following the procedure in 2.3, 4-acetyl-*N*-phenylbenzenesulfonamides were synthesized by treating aniline derivatives (3.2 mmol) in CH₂Cl₂ (25 mL) in ice bath. *p*-Acetylbenzenesulfonyl chloride (4.1 mmol) in pyridine (1.2 eq) was added. The reaction was continued while stirring at room temperature for 24 h and controlled by TLC. The resulting admixture was added saturated NaHCO₃ to change the pH to 8 and extracted with CH₂Cl₂. The organic layer was evaporated and recrystallized by a mixture

of CH_2Cl_2 and hexane. The solid collected is slowly washed using MeOH to procure a target compound of around 50-65%.

2.7.1 Preparation of benzenesulfonamide chalcones with 3,4-dimethoxy (112-114)

Following the procedure in 2.4, benzenesulfonamide chalcones **112-114** (Figure 2.10) were synthesized by Claisen–Schmidt reaction according to previous report with some modifications by reacting 4-acetyl-*N*-phenyl benzenesulfonamide (1 eq) and 3,4-dimethoxy benzaldehyde (1 eq) in EtOH. Subsequently, 6N NaOH (2 eq) was added and stirred at room temperature for 24 h. The resulting mixture was adjusted its pH to 5 by adding 10% HCl and extracted with EtOAc. The organic portion was dried over with anhydrous Na_2SO_4 and evaporated. The target compound was purified using column chromatography or recrystallization using a suitable solvent.

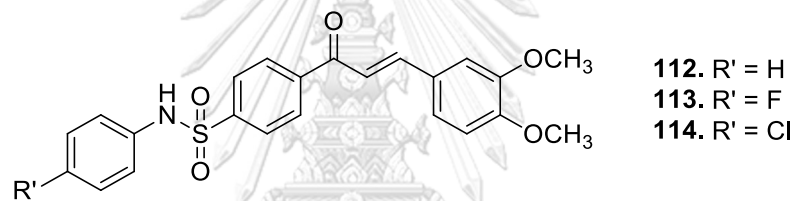


Figure 2.10 The structures of synthesized 4-acetyl-*N*-phenylbenzenesulfonamide (112-114)

N-(phenyl)-4-[1-oxo-3-(3,4-dimethoxyphenyl)-2-propen-1-yl]benzenesulfonamide (**112**) $^1\text{H-NMR}$ ($\text{DMSO-}d_6$, 500 MHz) δ 10.46 (s, 1H, N-H), 8.23 (d, $J = 8.0$ Hz, 2H, ArH), 7.90 (d, $J = 8.5$ Hz, 2H, ArH), 7.77 (d, $J = 15.5$ Hz, 1H, β -H), 7.71 (d, $J = 15.5$ Hz, 1H, α -H), 7.53 (d, $J = 1.5$ Hz, 1H, ArH), 7.39 (dd, $J = 8.5, 1.5$ Hz, 1H, ArH), 7.24 (t, $J = 7.5$ Hz, 1H, ArH), 7.23 (d, $J = 8.0$ Hz, 1H, ArH), 7.11 (d, $J = 8.0$ Hz, 2H, ArH), 7.05 (d, $J = 8.0$ Hz, 1H, ArH), 7.02 (d, $J = 8.5$ Hz, 1H, ArH), 3.84 (s, 3H, OCH_3), 3.81 (s, 3H, OCH_3) ppm. $^{13}\text{C-NMR}$ ($\text{DMSO-}d_6$, 125 MHz) δ 188.3, 151.7, 149.1, 145.8, 142.8, 141.1, 137.4, 129.3, 129.2, 127.3, 127.1, 124.5, 120.4, 119.3, 111.6, 110.8, 55.8, 55.7 ppm. HRMS (ESI, m/z): calculated for $\text{C}_{23}\text{H}_{21}\text{NNaO}_5\text{S}$ [$\text{M}+\text{Na}$] $^+$ 446.10381, found 446.10295.

N-(4-fluorophenyl)-4-[1-oxo-3-(3,4-dimethoxyphenyl)-2-propen-1-yl]benzenesulfonamide (**113**) $^1\text{H-NMR}$ ($\text{DMSO-}d_6$, 500 MHz) δ 10.39 (s, 1H, N-H), 8.22 (d, $J = 8.5$ Hz,

2H, ArH), 7.84 (d, $J = 8.5$ Hz, 2H, ArH), 7.76 (d, $J = 15.5$ Hz, 1H, β -H), 7.70 (d, $J = 15.5$ Hz, 1H, α -H), 7.51 (d, $J = 2.0$ Hz, 1H, ArH), 7.37 (dd, $J = 8.5, 2.0$ Hz, 1H, ArH), 7.09 (s, 2H, ArH), 7.08 (d, $J = 2.0$ Hz, 2H, ArH), 7.00 (d, $J = 8.0$ Hz, 1H, ArH), 3.82 (s, 3H, OCH₃), 3.79 (s, 3H, OCH₃) ppm. ¹³C-NMR (DMSO-*d*₆, 125 MHz) δ 188.3, 160.3, 158.3, 151.6, 149.0, 145.8, 142.5, 141.1, 133.5, 129.2, 127.3, 127.1, 124.5, 123.3, 123.2, 119.3, 116.1, 116.0, 111.6, 110.8, 56.8, 55.6 ppm. HRMS (ESI, m/z): calculated for C₂₃H₂₀FNNaO₅S [M+Na]⁺ 464.09439, found 464.09253.

N-(4-chlorophenyl)-4-[1-oxo-3-(3,4-dimethoxyphenyl)-2-propen-1-yl]benzene sulfonamide (**114**) ¹H-NMR (DMSO-*d*₆, 500 MHz) δ 10.55 (s, 1H, N-H), 8.17 (d, $J = 8.5$ Hz, 2H, ArH), 7.82 (d, $J = 8.5$ Hz, 2H, ArH), 7.70 (d, $J = 15.5$ Hz, 1H, β -H), 7.64 (d, $J = 15.5$ Hz, 1H, α -H), 7.45 (d, $J = 1.5$ Hz, 1H, ArH), 7.31 (dd, $J = 8.0, 1.5$ Hz, 1H, ArH), 7.23 (d, $J = 8.5$ Hz, 2H, ArH), 7.04 (d, $J = 9.0$ Hz, 2H, ArH), 6.94 (d, $J = 8.0$ Hz, 1H, ArH) 3.76 (s, 3H, OCH₃), 3.74 (s, 3H, OCH₃) ppm. ¹³C-NMR (DMSO-*d*₆, 125 MHz) δ 188.3, 151.7, 149.1, 145.8, 142.5, 141.3, 136.4, 129.3, 128.7, 127.3, 127.1, 124.5, 122.0, 119.4, 111.6, 110.8, 55.8, 55.7 ppm. HRMS (ESI, m/z): calculated for C₂₃H₁₉ClNNa₂O₅S [M+2Na-H]⁺ 502.04624, found 502.04479.

2.8 α -Glucosidase inhibitory activity

2.8.1 α -Glucosidase inhibitory assay⁴⁰

α -Glucosidase (0.1 U/mL) and the substrate (1 mM *p*-nitrophenyl- α -D-glucopyranoside) were dissolved in 0.1 M phosphate buffer (pH 6.9). 10 μ L of the test sample with 4 mM was added with 40 μ L of α -glucosidase and incubated at 37° C for 10 min. Then, 50 μ L of the substrate solution was added and incubated at 37° C for 20 min. It was ended by adding 1 solution of Na₂CO₃ (100 μ L). The final concentration of samples used was 200 μ M. Enzymatic activity was measured with the ALLSHENG AMR-100 microplate reader at 405 nm. The percentage of inhibitory activity was calculated as follows:

$$\% \text{ Inhibition} = \frac{(A_0 - A_1)}{A_0} \times 100 \%$$

A_0 = absorbance without the sample, A_1 = absorbance with the sample

The samples with %inhibition above 50% were further investigated for their IC_{50} . The IC_{50} value was deduced from the plot of % inhibition vs concentration of test sample. Acarbose was used as standard control and the experiment was performed in triplicate.

2.8.2 Kinetic study of α -glucosidase inhibition⁴⁰

In order to figure out α -glucosidase inhibition type, kinetic study was conducted according to procedure 2.8.1. The α -glucosidase inhibition type was determined at various concentrations of *p*-NPG substrate in the absence or presence of test compounds at different concentrations. The K_m and V_{max} values were calculated from Lineweaver-Burk plots of $1/V$ versus $1/[S]$.



CHAPTER III

RESULTS AND DISCUSSION

The synthesis of sulfonamide chalcones was achieved with %yield ranging from 50-95%. All compounds were well-characterized by ^1H and ^{13}C NMR and HR-MS for new compounds. All compounds were tested for %inhibition of α -glucosidase at 200 μM . The compounds with %inhibition above 50% were further investigated and determined their IC_{50} . The IC_{50} results were categorized as follows: very strong (<10 μM), strong (10-49.9 μM), moderate (50-99.9 μM), weak (100-199.9 μM), and not active (>200 μM). The structure-activity relationship was explored through α -glucosidase inhibitory activity test by comparing their IC_{50} values.

3.1 Synthesis and evaluation of sulfonamide chalcones with *o*-, *m*-, and *p*-position of NHR and 3,4-dimethoxy group on B-ring

3.1.1 Synthesis and structural elucidation

Following the procedure of Bahekar *et al.*³⁸, three mentioned sulfonamide chalcones (**60-62**) were fruitfully synthesized (**Figure 3.1**). All compounds were obtained as yellow powder with 67-81% yield. These compounds were purified by column chromatograph. All compounds are new. Nevertheless, the α -glucosidase inhibitory activity of these three compounds has not been addressed. Seo *et al.* in 2005 reported that the sulfonamide chalcones with -NHR at *p*-position exhibited better α -glucosidase inhibitory activity than those at *meta* position. However, that study did not discuss the structure-activity relationship. Thus further investigation was needed to observe the effect of -NHR at *o*-, *m*-, and *p*-positions on α -glucosidase inhibition.

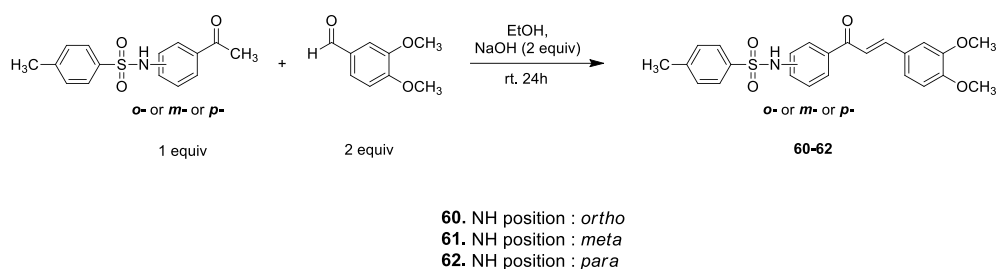


Figure 3.1 Synthesis of sulfonamide chalcones (**60-62**)

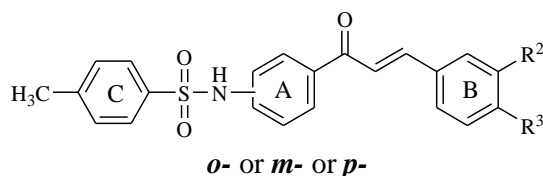
The structural identification of prepared compounds was carried out by ^1H and ^{13}C NMR analysis. The important signals of chalcones are two doublets of olefinic protons of α,β -unsaturated ketone around 7.61-7.70 ppm with coupling constant (J) around 15-19 Hz. The signals are much lower than those of normal ketones because of the conjugation.⁴¹

In the ^1H NMR spectrum, aromatic protons were observed in the range of 6.82-8.60 ppm. Besides, there was a secondary sulfonamide proton ($-\text{SO}_2\text{NH}$ exchangeable) as a singlet about δ 10.45-11.26 ppm. The ^{13}C NMR spectrum showed the number of resonances required with different signals for C=O (δ 187.4-192.9 ppm), aromatic carbons (δ 110.6-151.8 ppm), $-\text{OCH}_3$ (δ 55.6-55.8 ppm), and $-\text{CH}_3$ (δ 21.0 ppm). The structures were confirmed by HR-MS (ESI) with HRMS (m/z) calculated for $\text{C}_{24}\text{H}_{23}\text{NNaO}_5\text{S}$ $[\text{M}+\text{Na}]^+$ 460.11966 (**60**), $\text{C}_{24}\text{H}_{23}\text{NNaO}_5\text{S}$ $[\text{M}+\text{Na}]^+$ 460.11913 (**61**), and $\text{C}_{24}\text{H}_{24}\text{NO}_5\text{S}$ $[\text{M}+\text{H}]^+$ 438.13720 (**62**).

3.1.2 α -Glucosidase inhibitory activity evaluation

α -Glucosidase inhibitors are one of the steps to treat type 2 diabetes, which are effective in reducing postprandial hyperglycemia.⁴ Following the procedure from Ramadhan *et al.* in 2015, the IC_{50} value was inferred from a plot of % inhibition vs test sample concentration using acarbose as a standard control. Acarbose is an anti-diabetic drug used to treat diabetes mellitus type 2. The results are presented in **Table 3.1**.

Table 3.1 Effects of the position of sulfonamide group on A-ring against α -glucosidase



o- or *m*- or *p*-

Compound	-NHR	R ²	R ³	IC ₅₀ ± SD (μM)
60	<i>o</i> -	OCH ₃	OCH ₃	76.75 ± 5.99
61	<i>m</i> -	OCH ₃	OCH ₃	30.22 ± 4.40
62	<i>p</i> -	OCH ₃	OCH ₃	1.04 ± 0.19
acarbose				93.63 ± 0.49

All compounds were examined in a set of experiments repeated three times; Error is standard deviation (SD); IC₅₀ values of compounds represent the concentration that caused 50% enzyme activity loss.

Table 3.1 shows the IC₅₀ values of sulfonamide chalcones with three different positions of sulfonamide substituent (-NH-SO₂R-) against α -glucosidase. The sulfonamide substituent at the *p*-position (**62**) revealed a very strong inhibition with IC₅₀ 1.04±0.19 μM, where this value was 30 and 76 times more intense than those bearing at *m*- (**61**) and *o*- (**60**) positions, respectively. **62** revealed better activity because the sulfonamide was not close to the carbonyl group, there was no bond competency between the carbonyl group with the substituent in forming bonds with the enzyme. Whereas at *o*- and *m*- positions, the sulfonamide was closer to the carbonyl group which caused the sulfonamide and carbonyl to oppose or weaken each other in forming bonds with the enzyme. In 2008, Bharatham *et al.* addressed the validated docking results that the NHR group played an important role in the binding of sugar/non-sugar derivatives to the active site, where is the NHR group from sulfonamide interacts through an H-bond with Asp349, while the two oxygens in the SO₂ group form an H-bond with His348 and Arg212.⁴² Thus, the sulfonamide at *p*-position could be used as a guideline for determining the effect of other substituents on the B-ring of chalcone.

3.2 Synthesis and evaluation of sulfonamide chalcones with un- and monosubstituent on B-ring

3.2.1 Synthesis and structural elucidation

Fourteen sulfonamide chalcones with un- and monosubstituent (OCH₃, alkyl, F, Cl, Br, and NO₂) on B-ring (**63-76**) were synthesized by Claisen-Schmidt condensation reaction (Figure 3.2). All compounds were purified by column chromatograph to gain yellow powder (**63**, **67**, and **74**), yellow crystals (**64-72**), and white powder (**73**) with 45-74% yield.

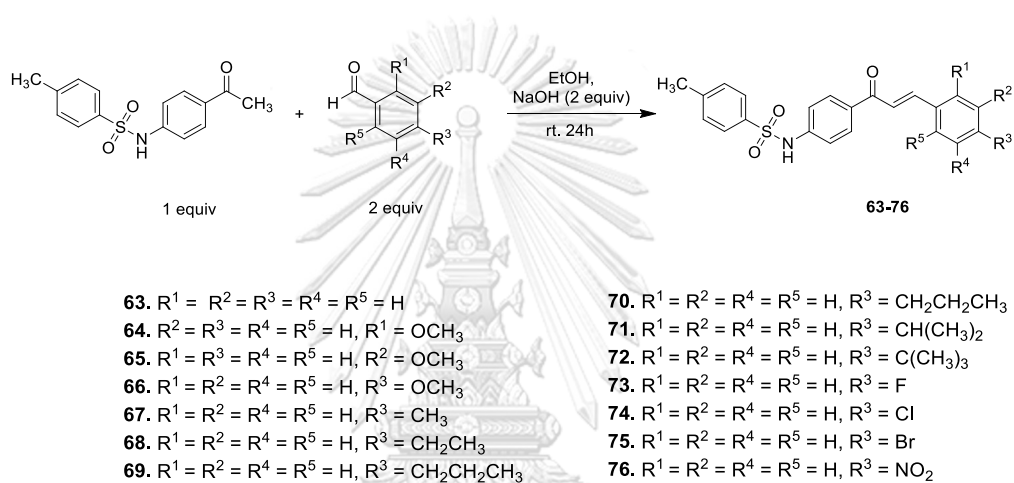
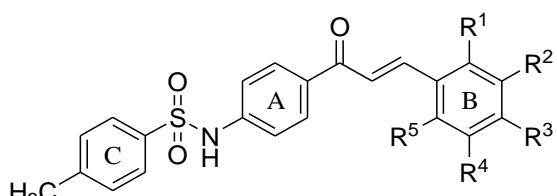


Figure 3.2 Synthesis of sulfonamide chalcones (**63-76**)

All compounds were characterized by ¹H and ¹³C NMR. The structures of new compounds were in addition confirmed by HR-MS (ESI) with HRMS (*m/z*) calculated for C₂₃H₂₃NO₄S [M+H]⁺ 408.12658 (**64**), C₂₃H₂₃NO₄S [M+H]⁺ 408.12647 (**65**), C₂₄H₂₃NNaO₃S [M+Na]⁺ 428.12702 (**68**), C₂₅H₂₅NNaO₃S [M+Na]⁺ 442.14383 (**69**), C₂₆H₂₈NO₃S [M+H]⁺ 434.17692 (**70**), and C₂₆H₂₈NO₃S [M+H]⁺ 434.17831 (**72**).

3.2.2 α-Glucosidase inhibitory activity evaluation

Table 3.1 reveals that the position of sulfonamide group expressed fairly large inhibitory activity. This model structure was used to explore the effects of the substituents on B-ring. The results are presented in Table 3.2.

Table 3.2 Effects of un- and monosubstituent on B-ring against α -glucosidase


Compound	R ¹	R ²	R ³	R ⁴	R ⁵	IC ₅₀ (μM) ± SD
63	H	H	H	H	H	0.07 ± 0.01
64	OCH ₃	H	H	H	H	28.66 ± 4.30
65	H	OCH ₃	H	H	H	4.82 ± 1.08
66	H	H	OCH ₃	H	H	10.55 ± 0.67
67	H	H	CH ₃	H	H	0.67 ± 0.06
68	H	H	CH ₂ CH ₃	H	H	0.58 ± 0.01
69	H	H	CH ₂ CH ₂ CH ₃	H	H	0.30 ± 0.01
70	H	H	CH ₂ CH ₂ CH ₂ CH ₃	H	H	1.34 ± 0.14
71	H	H	CH(CH ₃) ₂	H	H	0.80 ± 0.12
72	H	H	C(CH ₃) ₃	H	H	1.13 ± 0.01
73	H	H	F	H	H	15.54 ± 0.85
74	H	H	Cl	H	H	14.67 ± 0.76
75	H	H	Br	H	H	18.92 ± 0.46
76	H	H	NO ₂	H	H	80.30 ± 2.59
acarbose						93.63 ± 0.49

All compounds were examined in a set of experiments repeated three times; Error is standard deviation (SD); IC₅₀ values of compounds represent the concentration that caused 50% enzyme activity loss.

According to **Table 3.2**, most sulfonamide chalcones exhibited as good α -glucosidase inhibitors. The inhibitory activity was significantly affected by the position of the substituents on B-ring. In the case of methoxy substituent (**Figure 3.3**), the activity could be ranged in order of 3- (**65**) > 4- (**66**) > 2-methoxy (**64**).

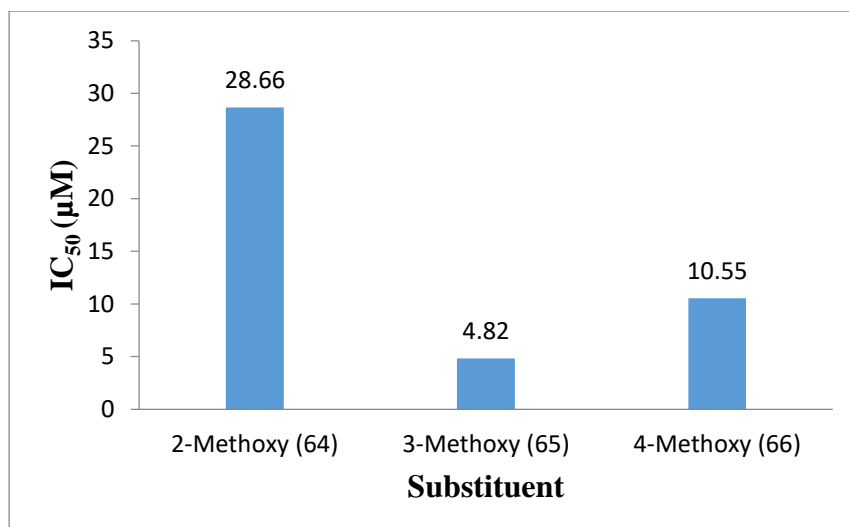


Figure 3.3 The IC₅₀ graph of α -glucosidase inhibitors **64-66**

Gani *et al.*⁴³ reported that the oxygen atom of the methoxy group performed the H-bond interaction with ASP327, this interaction created the methoxy substituent a role in α -glucosidase inhibition. **Figure 3.3** shows that 3-methoxy substituent had greater inhibitory activity than those at 2- and 4-positions. It is probably because 3-methoxy (*m*-) substituents only contributed the inductive effect, whereas 2- (*o*-) and 4-methoxy (*p*-) substituents did both inductive and resonant effects. In the *o*-/*p*-position, the lone pair of electrons on oxygen could donate back to the aryl ring through resonance giving rise to additional resonance structures, which may cause unstable H-bond interaction and led to the less inhibitory activity than the *m*-position.

Stemmed from the observation of 4-methyl substituent (**67**) that revealed anti- α -glucosidase activity, five alkyl derivatives were designed and synthesized to scrutinize the alkyl substituent effect on the activity as presented in **Figure 3.4**. Moreover, Nipun *et al.*⁴⁴, reported that alkyl groups could form π -alkyl interactions with α -glucosidase.⁴⁵ However, they did not explain the effect of alkyl group chains on this activity. Therefore, it is necessary to observe the optimum chain length of alkyl groups in sulfonamide chalcone for α -glucosidase inhibitory activity.

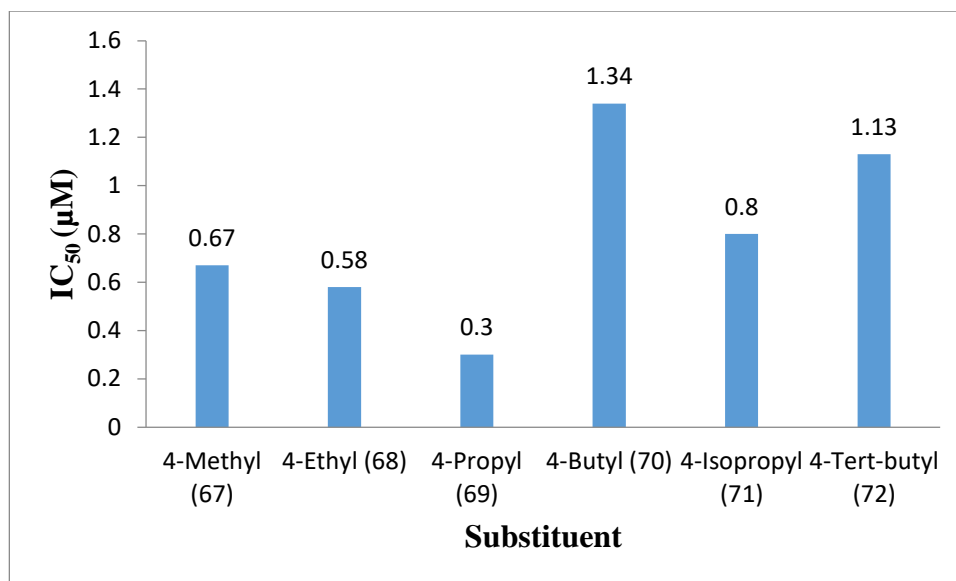


Figure 3.4 The IC₅₀ graph of α -glucosidase inhibitors 67-72

Figure 3.4 clearly shows the effect of alkyl substituents. The more carbon atoms in the chain increased the activity from 4-methyl (67) to 4-ethyl (68) and maximized at 4-propyl (69). Nonetheless, adding one more carbone atom as 4-*n*-butyl (70), the activity significantly dropped. Other isomers including 4-isopropyl (71) or 4-*tert*-butyl (72) also showed decreased the α -glucosidase inhibitory activity.

For B-ring halogen containing sulfonamide chalcones, the inhibitory activities of 4-fluoro (73) and 4-chloro (74) were almost the same, and decreased in 4-bromo (75) substituent. The halogens as electron-withdrawing groups furnished IC₅₀ in the range of 15-19 μ M. 4-Nitro (76) as an electron-withdrawing group also decreased the activity with an IC₅₀ value of $80.30 \pm 2.59 \mu$ M. This indicated that the electron-withdrawing group on B-ring at 4-position gave moderate inhibitory activity.

Furthermore, 63 without any substituent exhibited a very strong inhibitory activity with IC₅₀ $0.07 \pm 0.01 \mu$ M. Its inhibitory activity was about 69 times stronger than OCH₃, 4 times than alkyl, and 209 times than halogen substituents. According to Brylinski,⁴⁶ the key interactions between ligands and macromolecules are hydrogen bonds, π - π aromatic arrangement,⁴⁷ cation- π interactions, hydrophobic effects, halogen bonds, and salt bridges. Thus, the benzene ring on the B-ring allowed greater

interaction with α -glucosidase through aromatic-aromatic or π - π interactions and hydrogen bonds, thereby increasing the inhibitory activity.

3.3 Synthesis and evaluation of sulfonamide chalcones with disubstituent on B-ring

3.3.1 Synthesis and structural elucidation

To learn more about the effect of the substituent on B-ring on the inhibition of α -glucosidase, the following fifteen sulfonamide chalcones with disubstituent (OCH_3 , OCH_2O , OH , $\text{OCH}_2\text{OCH}_2\text{CH}_3$ and Cl) were synthesized (**Figure 3.5**). All compounds were purified using column chromatograph to furnish products in the form of yellow crystal (**77-82** and **88**), yellow powder (**83-85**, **89** and **91**), yellow oil (**87**), and white powder (**90**) with 50-91% yield. **78-82** and **85-91** are new, while **77**, **83** and **84** has been reported.

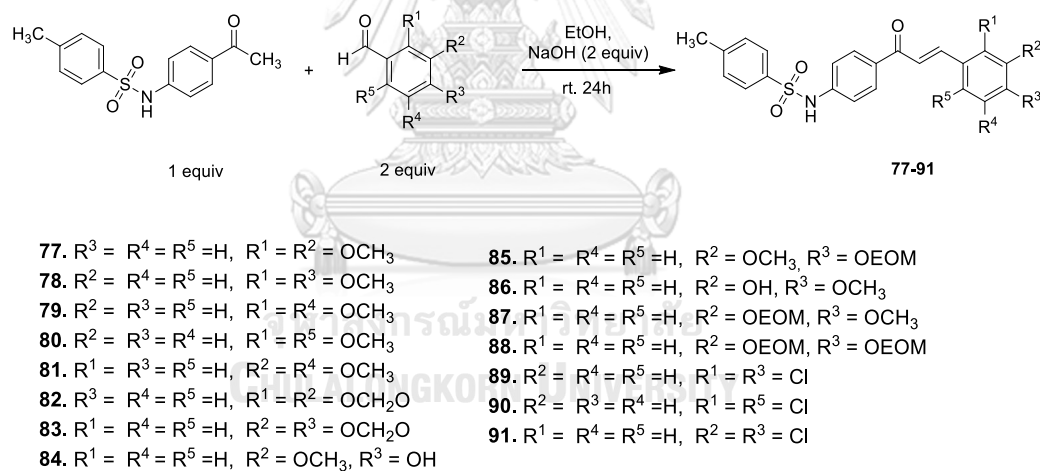


Figure 3.5 Synthesis of sulfonamide chalcones (**77-91**)

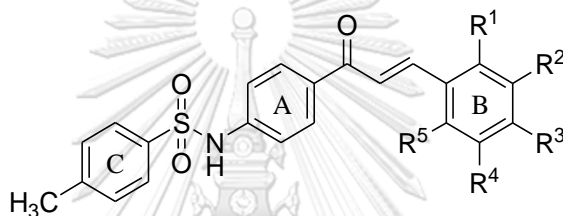
85, **87**, and **88** were obtained through the OH protection step (isovanillin, vanillin, and dihydroxybenzaldehyde). Meanwhile, **84** and **86** were obtained through the deprotection process of **85** and **87**, since **84** and **86** contained hydroxyl groups which reacted very easily with bases, so a protective group was needed. The synthesis of these series involved three steps with a protective group (ethyl methyl ether, EOM). After preparing the protected aromatic aldehyde (74% yield), it was reacted with

sulfonamide acetophenone to produce **85**, **87**, and **88** with 50-65% yield. Then the EOM group was deprotected by stirring **85** and **87** in 10% HCl at 60 °C for 15 minutes to obtain the target compounds with 80-95% yield.

3.3.2 α -Glucosidase inhibitory activity evaluation

Based on **Tables 3.1** and **3.2**, the substituent at positions 3 and 4 had very important role in α -glucosidase inhibition. The effects of disubstituent on B-ring is presented in **Table 3.3**.

Table 3.3 Effects of disubstituent on B-ring against α -glucosidase



Compound	R ¹	R ²	R ³	R ⁴	R ⁵	IC ₅₀ (μM) ± SD
77	OCH ₃	OCH ₃	H	H	H	2.47 ± 0.32
78	OCH ₃	H	OCH ₃	H	H	19.65 ± 2.55
79	OCH ₃	H	H	OCH ₃	H	46.91 ± 2.94
80	OCH ₃	H	H	H	OCH ₃	57.49 ± 8.26
81	H	OCH ₃	H	OCH ₃	H	1.81 ± 0.40
82		-OCH ₂ O-	H	H	H	76.47 ± 3.88
83	H	-OCH ₂ O-		H	H	0.32 ± 0.02
84	H	OCH ₃	OH	H	H	0.29 ± 0.04
85	H	OCH ₃	OEOM	H	H	10.5 ± 1.43
86	H	OH	OCH ₃	H	H	0.12 ± 0.01
87	H	OEOM	OCH ₃	H	H	0.19 ± 0.01
88	H	OEOM	OEOM	H	H	1.54 ± 0.19
89	Cl	H	Cl	H	H	84.89 ± 7.49
90	Cl	H	H	H	Cl	144.26 ± 4.29
91	H	Cl	Cl	H	H	102.44 ± 2.84

 acarbose

93.63 ± 0.49

All compounds were examined in a set of experiments repeated three times; Error is standard deviation (SD); IC₅₀ values of compounds represent the concentration that caused 50% enzyme activity loss.

For dimethoxy substituents, the inhibitory activity was evident in the order of 3,4-dimethoxy (**62**) > 3,5-dimethoxy (**81**) > 2,3-dimethoxy (**77**) > 2,4-dimethoxy (**78**) > 2,5-dimethoxy (**79**) > 2,6-dimethoxy (**80**). Where the compounds containing the substituent at the 3-position (**62**, **81** and **77**) had better activity than those without the substituent at 3-position (**78**, **79** and **80**). This phenomenon also applied to methylenedioxy and dichloro substituents, where 3,4-methylenedioxy (**83**) exhibited greater activity than 2,3-methylenedioxy (**82**) and 2,3-dichloro (**89**) > 3,4-dichloro (**91**) > 2,6-dichloro (**90**).

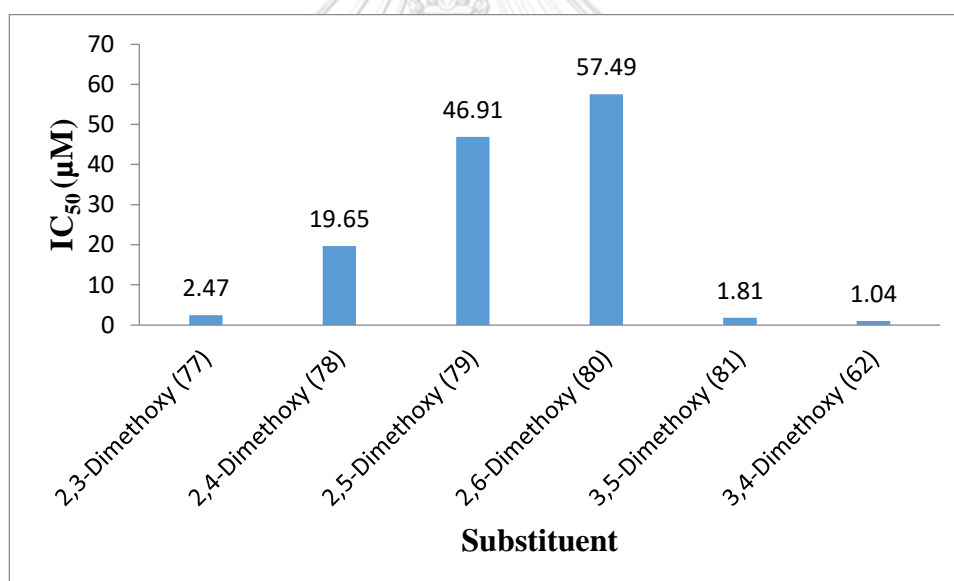


Figure 3.6 The IC₅₀ graph of α -glucosidase inhibitors **62** and **77-81**

The inhibitory effect of the dimethoxy substituent can be seen in **Figure 3.6**. The graph shows that the combination of 3-methoxy with 2-, 4- and 5-methoxy affected on the increment of α -glucosidase inhibitory activity with IC₅₀ below 3 µM. Moreover, the combination of 2,4-, 2,5- and 2,6-dimethoxy decreased inhibitory activity. An excellent combination in this series is a 3,4-dimethoxy substituent with IC₅₀ 1.04±0.19 M. Thus, 3,4-dimethoxy in the B-ring is interesting for further study.

Furthermore, apart from being influenced by the position of the substituent, the inhibition was influenced by the type of the substituent. When one or both of the methoxy groups were replaced with other groups, their activities could increase or decrease. For instance, the presence of hydroxy at 3-(**86**) and 4-position (**84**) increased the activity 4-9 times of 3,4-dimethoxy (**62**), as did the protected compounds at 3-position (**87**) and 3,4-methylenedioxy (**83**). Meanwhile, the protected compounds at 4-(**85**) and 3,4-positions (**88**) decreased the activity.

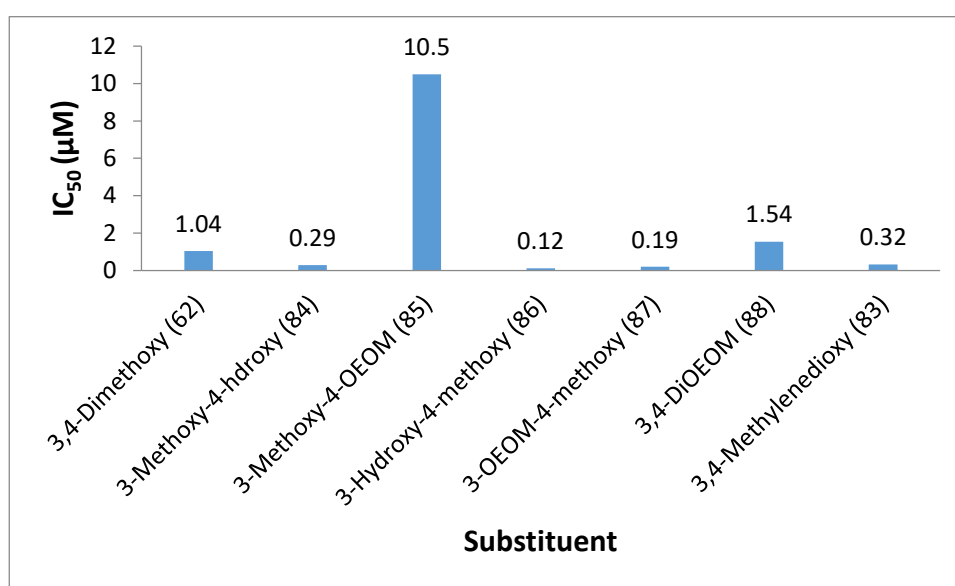


Figure 3.7 The IC₅₀ graph of α -glucosidase inhibitors **62** and **83-88**

Basically, the hydroxyl groups formed H-bonds with Arg212 and Arg439 and have an important role both in the catalytic mechanism and in the substrate bond.⁴² Thus, the presence of a hydroxy substituent could increase the inhibitory activity of α -glucosidase. Likewise, the methylenedioxy had influence at the 3,4-position. In addition, **Figure 3.7** shows the protected compound at 4- and 3,4-position caused the inhibitory activity decreased, otherwise, the protected compound at 3-position increased its activity around 5 times. This proved that the position and type of substituent also affected the effectiveness of α -glucosidase inhibition.

3.4 Synthesis and evaluation of sulfonamide chalcones with un-, monosubstituent and disubstituent on C-ring

3.4.1 Synthesis and structural elucidation

Sulfonamide chalcone with 3,4-dimethoxy group on B-ring (**62**) displayed a fairly good inhibitory activity. Thus, the 3,4-dimethoxy substituent on B-ring was used to examine the effect of the substituent on the sulfonamide ring (C-ring) with un-, monosubstituent (OCH₃, CH₃CO, F, and Cl) and disubstituent (Cl, NO₂, and OCH₂CH₃) (Figure 3.8).

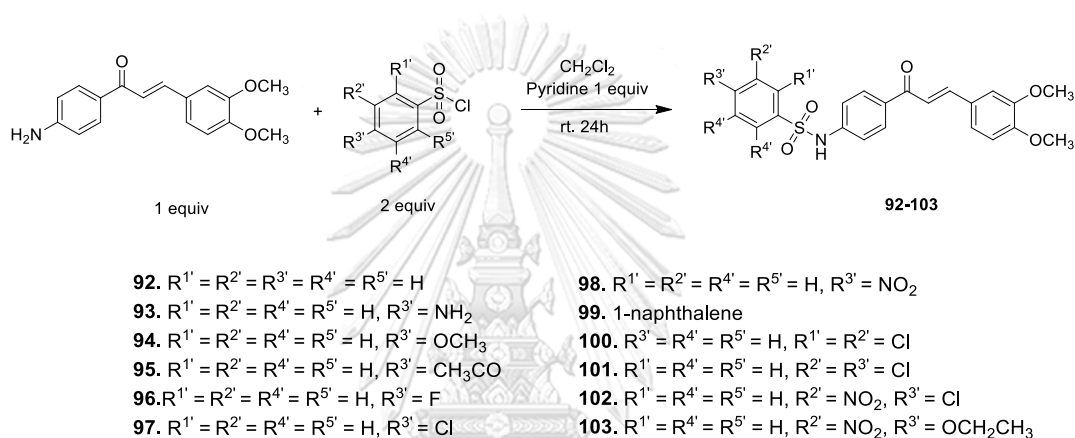


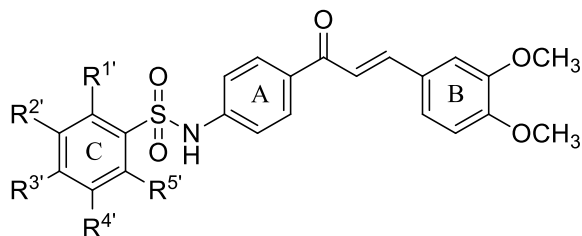
Figure 3.8 Synthesis of sulfonamide chalcones (92-103)

These compounds were synthesized following the procedure of Park, *et al.* (2007), amino chalcones were reacted with sulfonyl chloride in a solution of CH₂Cl₂ and pyridine (Figure 3.8). Twelve compounds were obtained with 37-84% yield and were purified by column chromatograph and recrystallization to obtain the desired products in the form of yellow crystals (**92**, **95-98**, and **103**), and yellow powder (**93**, **94**, and **99-102**). **93-95** and **97-103** are new, while **92** and **96** has been reported.

3.4.2 α -Glucosidase inhibitory activity evaluation

The sulfonamide chalcone (**62**) with methyl substituent on the sulfonamide ring opened the opportunity to learn more about the effect of the substituent on C-ring as α -glucosidase inhibition. The effects of un-, monosubstituent and disubstituent on C-ring are presented in Table 3.4.

Table 3.4 Effects of un-, monosubstituent and disubstituent on C-ring against α -glucosidase



Compound	R ^{1'}	R ^{2'}	R ^{3'}	R ^{4'}	R ^{5'}	IC ₅₀ (μM) ± SD
92	H	H	H	H	H	54.84 ± 5.04
93	H	H	NH ₂	H	H	4.10 ± 0.25
94	H	H	OCH ₃	H	H	0.07 ± 0.03
95	H	H	CH ₃ CO	H	H	0.18 ± 0.01
96	H	H	F	H	H	0.25 ± 0.14
97	H	H	Cl	H	H	0.18 ± 0.04
98	H	H	NO ₂	H	H	0.17 ± 0.01
99	1-naphthalene					158.63 ± 11.71
100	Cl	Cl	H	H	H	17.16 ± 1.66
101	H	Cl	Cl	H	H	0.31 ± 0.13
102	H	NO ₂	Cl	H	H	102.69 ± 4.97
103	H	NO ₂	OCH ₂ CH ₃	H	H	2.93 ± 0.57
acarbose						93.63 ± 0.49

All compounds were examined in a set of experiments repeated three times; Error is standard deviation (SD); IC₅₀ values of compounds represent the concentration that caused 50% enzyme activity loss.

In general, the presence of substituents in the sulfonamide ring could increase the α -glucosidase inhibitory activity. The very strong inhibitor could be observed in 4-OCH₃, 4-NO₂, 4-CH₃CO, 4-Cl, 4-F, and 3,4-diCl substituents with activity increasing more than 55 times. Moreover, 4-NH₂ and 3-NO₂-4-OCH₂CH₃ showed very strong inhibitory activity with increased activity around 13-18 times. The strong activity occurred in 2,3-diCl substituents with IC₅₀ 17.16±1.66 μM. However, 3-NO₂-4-Cl substituent and 1-naphthalene gave weak activity than unsubstituent (Figure 3.9).

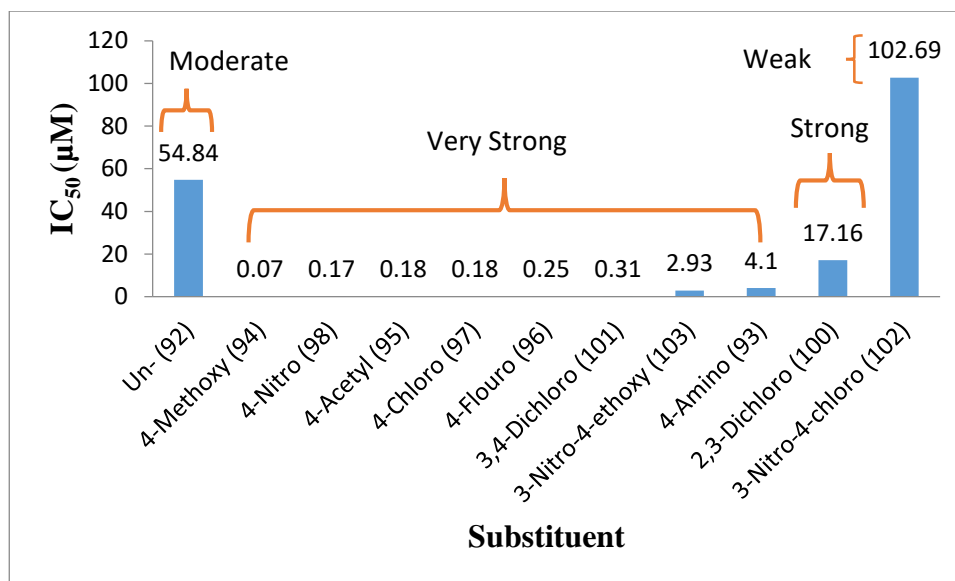


Figure 3.9 The IC₅₀ graph of α -glucosidase inhibitors **92-98** and **100-103**

Based on **Table 3.4**, without the substituent (**92**) has a fairly large IC₅₀ value ($54.84 \pm 5.04 \mu\text{M}$), as well as for 1-naphthalene (**99**). However, the presence of substituents on the sulfonamide ring could increase the inhibitory activity. The effect of the electron-donating group: 4-methoxy (**94**) exhibited an inhibitory activity 4 times better than 4-fluoro (**96**), 14 times than 4-methyl (**62**) and 58 times than 4-amino (**93**). Whereas for the electron-withdrawing group, the resulting IC₅₀ values were excellent in the same level of inhibition: 4-nitro (**98**) \geq 4-acetyl (**95**) = 4-chloro (**97**).

These findings indicated that the effect of the electron-donating group on the inhibition of α -glucosidase in the C-ring occurred based on the activation level of the substituent. When the activation was amplified on the sulfonamide ring, might cause the active side of sulfonamide weaken, likewise the weak activator could not activate the benzene ring on the sulfonamide. Thus, for electron-withdrawing groups, all revealed the same role. This may occur because the inductive effect made the active site more stable.

According to the obtained results, it could be seen that the substituent on sulfonamide is crucial to enhance the inhibitory activity of α -glucosidase, especially for the electron-withdrawing group. **101** with 3,4-dichloro (IC₅₀ $0.31 \pm 0.13 \mu\text{M}$) expressed an inhibitory activity 56 times greater than 2,3-dichloro (**100**) and when the

substituent at 3-position was replaced with nitro (**102**) the activity decreased. Whereas for 3-nitro-4-ethoxy substituent (**103**), the activity increased. Thus, the combination of the electron-donating and electron-withdrawing groups could increase the inhibitory activity of disubstituents.

3.5 Synthesis and evaluation of sulfonamide acetophenones

3.5.1 Synthesis and structural elucidation

In order to find out more sulfonamides as α -glucosidase inhibitor, nine sulfonamide acetophenones were synthesized using amino acetophenones reacting with sulfonyl chloride derivatives in CH_2Cl_2 and pyridine (**Figure 3.10**). All compounds are purified by recrystallization and washed using methanol to obtain white crystal of target product with 61-93% yield. Sulfonamide acetophenones are often used as intermediate compounds so that all are known.

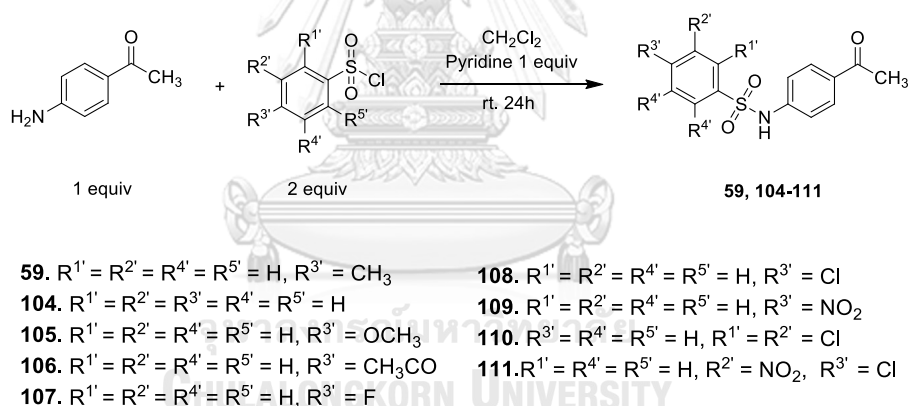
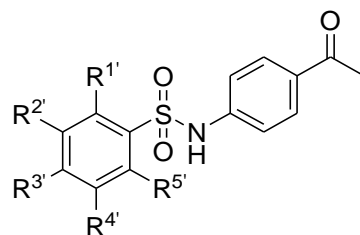


Figure 3.10 Synthesis of sulfonamide acetophenones (**59, 104-111**)

3.5.2 α -Glucosidase inhibitory activity evaluation

Sulfonamide chalcones have excellent α -glucosidase inhibitory activity, this is also seen in chalcones and sulfonylureas.^{3, 4, 14, 23} The synthesised sulfonamide acetophenones were tested for α -glucosidase inhibitory activity to observe if there was relationship between sulfonamide and chalcone. The α -glucosidase inhibitory activity of sulfonamide acetophenones is presented in **Table 3.5**.

Table 3.5 Effects of sulfonamide acetophenones against α -glucosidase

Compound	R ^{1'}	R ^{2'}	R ^{3'}	R ^{4'}	R ^{5'}	IC ₅₀ (μM) ± SD
104	H	H	H	H	H	24.53 ± 3.27
59	H	H	CH ₃	H	H	8.01 ± 0.27
105	H	H	OCH ₃	H	H	0.52 ± 0.07
106	H	H	CH ₃ CO	H	H	3.49 ± 0.32
107	H	H	F	H	H	3.80 ± 1.83
108	H	H	Cl	H	H	1.20 ± 0.29
109	H	H	NO ₂	H	H	7.56 ± 2.50
110	Cl	Cl	H	H	H	73.14 ± 3.02
111	H	NO ₂	Cl	H	H	69.65 ± 7.28
acarbose						93.63 ± 0.49

All compounds were examined in a set of experiments repeated three times; Error is standard deviation (SD); IC₅₀ values of compounds represent the concentration that caused 50% enzyme activity loss.

Based on the obtained results in **Table 3.5**, sulfonamide acetophenones showed better inhibitory activity than acarbose with IC₅₀ less than 73 μM. Most of the monosubstituents at 4-position, increased their inhibitory activity with IC₅₀ below 10 μM. However, a surprising decreased the activity occurred in 2,3-diCl and 3-NO₂-4-Cl substituents with IC₅₀ increasing above 70 μM (**Figure 3.11**). Thus, 2,3-diCl and 3-NO₂-4-Cl substituents had no potential. **105** bearing 4-methoxy substituent exhibited excellent inhibitory activity with IC₅₀ 0.52±0.07 μM, as did 4-chloro (**108**) with IC₅₀ 1.20±0.29 μM.

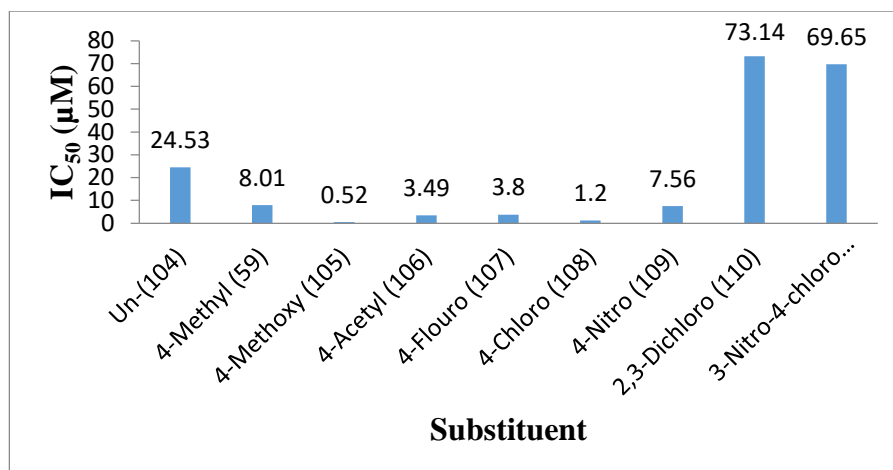


Figure 3.11 The IC₅₀ graph of α -glucosidase inhibitor for 59 and 104-111

Generally, comparing the results in **Tables 3.4**, sulfonamides increased the activity when combined with chalcone, for example, 4-CH₃, 4-OCH₃, 4-CH₃CO, 4-F, 4-Cl, 4-NO₂, and 2,3-diCl substituents displayed their activity to increase approximately 8, 5, 18, 13, 6, 38, and 4 times, respectively. However, the un- and 3-NO₂-4-Cl substituent decreased the sulfonamide activity when paired with chalcone 1-2 times (**Figure 3.12**). Thus, the presence of sulfonamides in chalcone ring enhanced the α -glucosidase inhibitory activity. This finding reinforced the reason that the inhibitory activity was increased because sulfonamides had substantially good inhibitory activity.

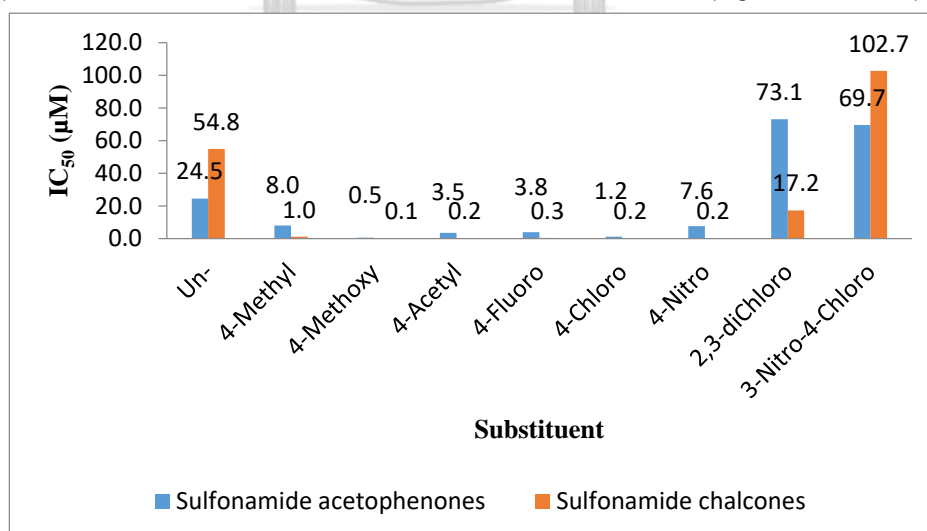


Figure 3.12 Graph of IC₅₀ comparison between sulfonamide acetophenones and sulfonamide chalcones

Based on the graph of comparison in **Figure 3.12**, the 4-OCH₃ and 4-Cl substituents significantly affected the inhibition of either sulfonamide acetophenone or sulfonamide chalcone with an IC₅₀ ranging from 0.1-1.2 μM. Thus, 4-OCH₃ and 4-Cl substituents could maintain the active site in both structures.

3.6 Synthesis and evaluation of benzenesulfonamide chalcones with 3,4-dimethoxy in B-ring

3.6.1 Synthesis and structural elucidation

Furthermore, three benzenesulfonamide chalcones with 3,4-dimethoxy in B-ring were synthesized through the Claisen-Schmidt condensation reaction. These compounds were not much different from previous synthesized sulfonamide chalcones. Benzenesulfonamide chalcones were purified using column chromatograph to obtain the desired products in the form of yellow crystals (**112**) and yellow powder (**113** and **114**) with 59-66% yield. All compounds has not yet been reported.

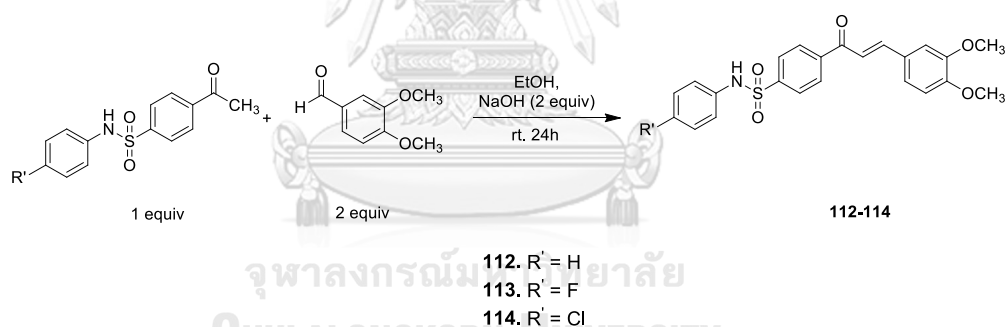
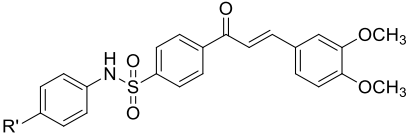


Figure 3.13 Synthesis of benzenesulfonamide chalcones (**112-114**)

3.6.2 α -Glucosidase inhibitory activity evaluation

Based on the general sulfonamide chalcone results, 3,4-dimethoxy substituent in the chalcone ring revealed good α -glucosidase inhibitory activity, likewise of 4-fluoro and chloro substituents. However, it is necessary to study the relationship between secondary amine and chalcone ring. The IC₅₀ of benzenesulfonamide chalcones is presented in **Table 3.6**.

Table 3.6 Effects of benzenesulfonamide chalcones against α -glucosidase


Compound	R'	IC ₅₀ (μM) ± SD
112	H	NA
113	F	135.90 ± 11.06
114	Cl	NA
acarbose		93.63 ± 0.49

All compounds were examined in a set of experiments repeated three times; Error is standard deviation (SD); IC₅₀ values of compounds represent the concentration that caused 50% enzyme activity loss ; NA is not active.

Based on **Table 3.6**, benzenesulfonamide chalcone with fluoro substituent in C-ring (**113**) provided weak inhibitory activity than acarbose with IC₅₀ > 100 μM, likewise, **112** and **114** were not active. These results indicated that secondary amines in the chalcone ring affected the inhibition of α -glucosidase. Bharatham *et al.*⁴² explained that NH formed H-bonds with carboxyl groups from Asp349 while SO₂ with Arg212 and His348/His111.

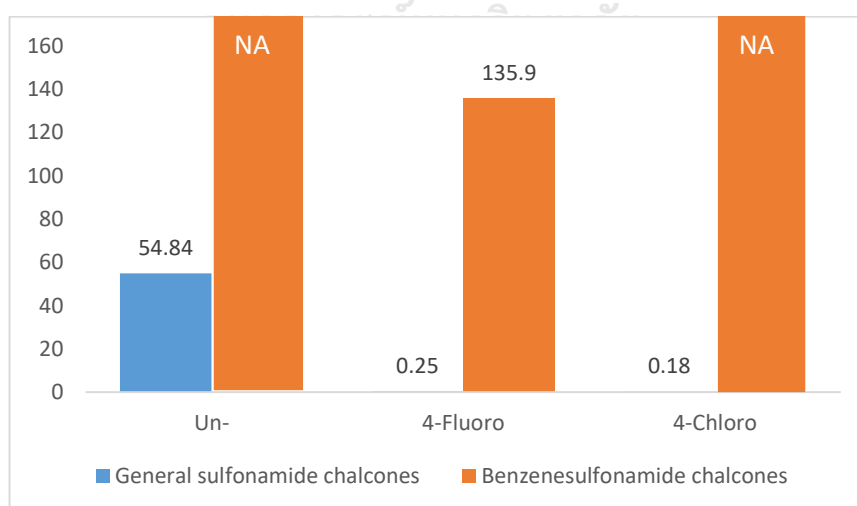
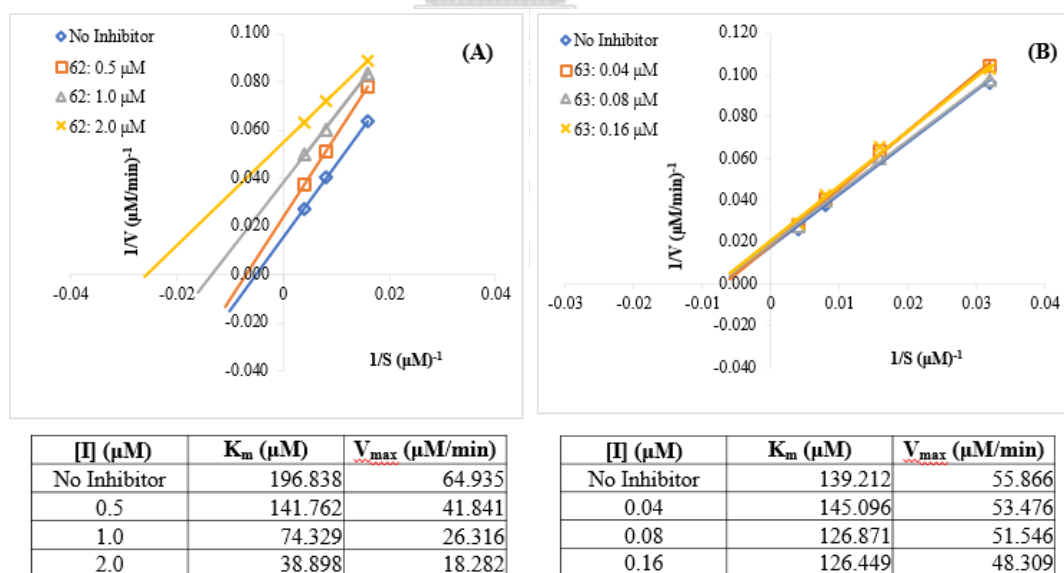


Figure 3.14 Graph of IC₅₀ comparison between general sulfonamide chalcones and benzenesulfonamide chalcones

Figure 3.14 shows that the position of NH and SO₂ on the sulfonamide chalcone greatly affected the IC₅₀ value. The unsubstituted (92) in general sulfonamide chalcones showed moderate activity, when the NH position was exchanged with SO₂ (112) the activity became not active. In addition, the 4-fluoro (96) and 4-chloro (97) substituents had very strong activity, moreover, their activity decreased (113) and not active (114) when the NH position was changed. This may occur because the sulfonyl group deactivated of chalcone ring and the bond between the sulfonyl with enzyme may be blocked by the benzene ring which bound to the secondary amine.

3.7 Kinetic study

To determine the mechanism underlying the inhibitory effect of α -glucosidase, a kinetic study was conducted. Based on the results obtained in testing the inhibitory activity of α -glucosidase, 62, 63, 86 and 94 exhibited a fairly good activity, were selected to examine for further kinetic study. The results of Lineweaver-Burk plot analysis are presented in Figure 3.15.



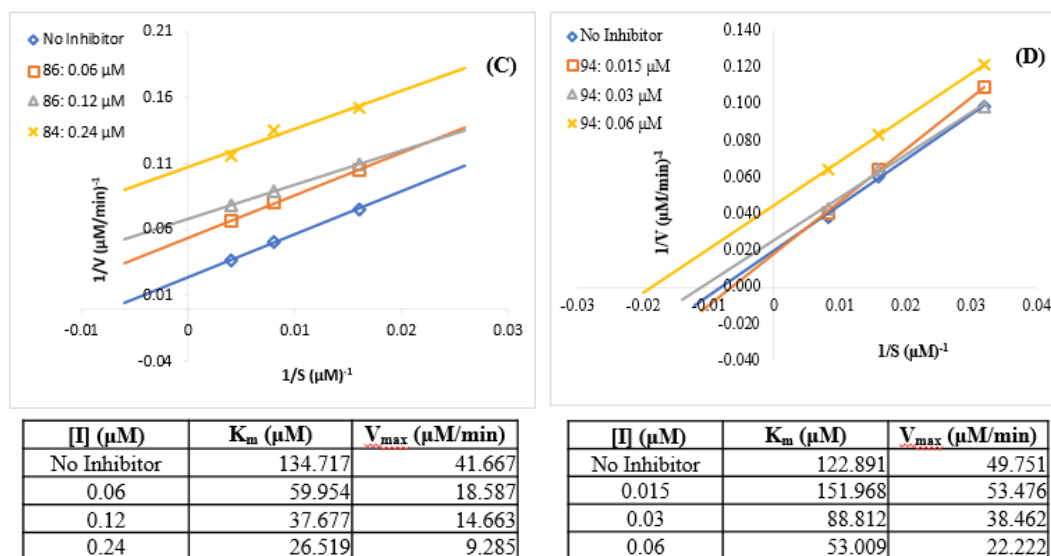


Figure 3.15 Lineweaver–Burk plot analysis, K_m (μM) and V_{max} ($\mu\text{M}/\text{min}$) of **62** (A), **63** (B), **86** (C) and **94** (D)

The kinetics evaluation was carried out using the Lineweaver–Burk plot, where the maximum enzyme velocity (V_{max}) and the Michaelis–Menten constant (K_m) were used to prove the inhibition model. Lineweaver–Burk plots of all compounds produced straight lines with different slopes. **62** and **86** clearly indicated the parallel or non-intersecting points of each concentration. This behavior indicated that **62** and **86** were uncompetitive inhibitors, as evidenced by a decrease in the values of K_m and V_{max} when the concentration increased (Figure 3.15, A and C). Meanwhile, **63** was a non-competitive inhibitor, where the straight lines of each concentration crossed and there was no significant change in V_{max} and K_m (Figure 3.15, B). However, **94** was a mixed inhibitor, because the straight line at a concentration of 0.015 μM intersected the control, while the other straight lines were parallel (Figure 3.15, D).

According to Roskoski (2007),⁴⁸ the key value generated by the Line-weaver Burk plot is V_{max} , where in competitive inhibition, V_{max} did not change (Figure 3.16, A), while the uncompetitive inhibitor V_{max} increased without changing the slope (Figure 3.16, B). However in non-competitive inhibition, the V-axis decreases and the lines intersected to the left of the y-axis because the slope corresponding to the increase in inhibitor concentration increased (Figure 3.16, C).

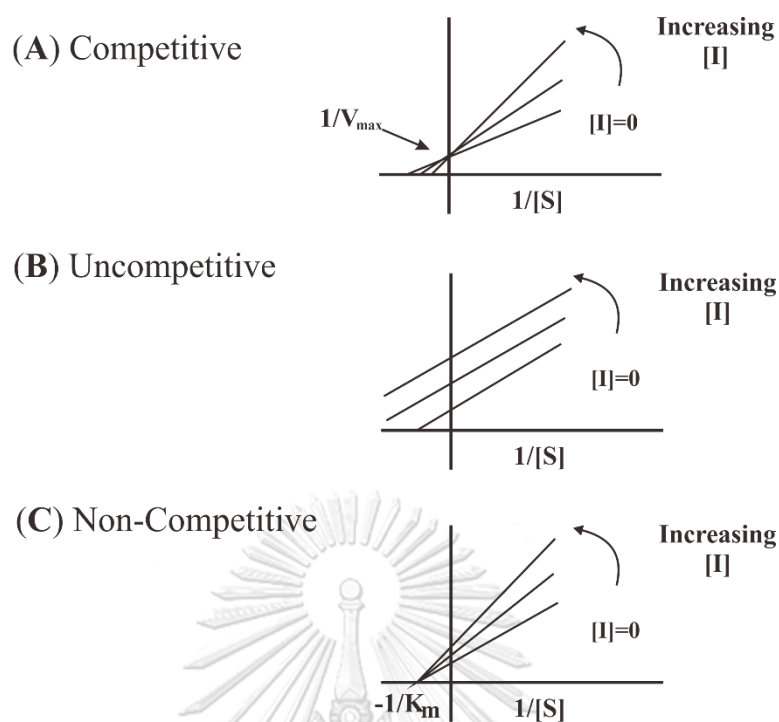


Figure 3.16 Lineweaver-Burk plots illustrating competitive, uncompetitive, and non-competitive inhibition

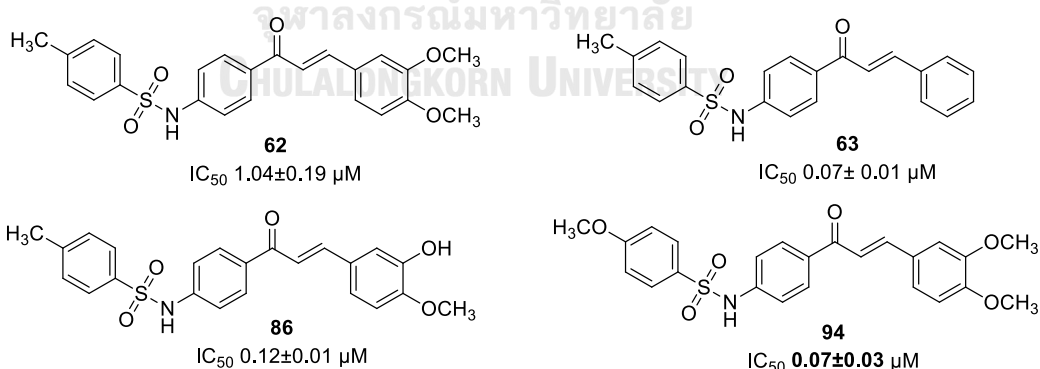
Knowing the type of inhibition produced by four sulfonamide chalcones, it could be concluded that **63** provided better inhibition effectiveness with uncompetitive inhibition and IC_{50} $0.07 \pm 0.01 \mu M$. Basically, non-competitive inhibitors bound to enzymes and enzyme-substrate complexes well. The presence of noncompetitive inhibitors would reduce V_{max} and would not affect K_m . The uncompetitive inhibitor only bound to the enzyme-substrate complex and reduced V_{max} and K_m . Furthermore, mixed inhibition was an inhibitor that bound to the enzyme at a different location from the substrate-binding site. This binding changes K_m and V_{max} . Mixed inhibition was similar to non-competitive inhibition except that the binding of a substrate or inhibitor affected the binding affinity of the enzyme to another. These different inhibitory mechanisms produced different relationships between inhibitory potential and substrate concentration.

CHAPTER 4

CONCLUSIONS

Forty-seven sulfonamide chalcones with various substituents on A, B, and C-rings were fruitfully synthesized, well characterized and tested for α -glucosidase inhibitory activity. Thirty-eight (**60-65**, **68-70**, **71**, **77-83**, **85-96**, **98-103** and **112-114**) new compounds were manipulated. Based on IC_{50} results, twenty-nine compounds exhibited as potent candidates with IC_{50} below 10 μ M. The structure relationship of *p*-NHR (**62**) in the sulfonamide chalcones was very important to enhance the α -glucosidase inhibitory activity. Moreover, the 3-position of substituent on B-ring gave remarkable effectiveness, as seen in **62**, **65**, **77**, **81**, and **83-88**, as well as the 4-alkyl substituents (**67-72**). Furthermore, the monosubstituent on the C-ring (**93-98**), significantly affected the α -glucosidase inhibition, both the electron-withdrawing and electron-donating groups.

Four excellent sulfonamide chalcones (**62**, **63**, **86** and **94**) were selected for kinetic examination for the mode of action. Through the Lineweaver–Burk plot, **62** and **86**, **63**, and **94** were uncompetitive, non-competitive and mixed inhibitors, respectively.



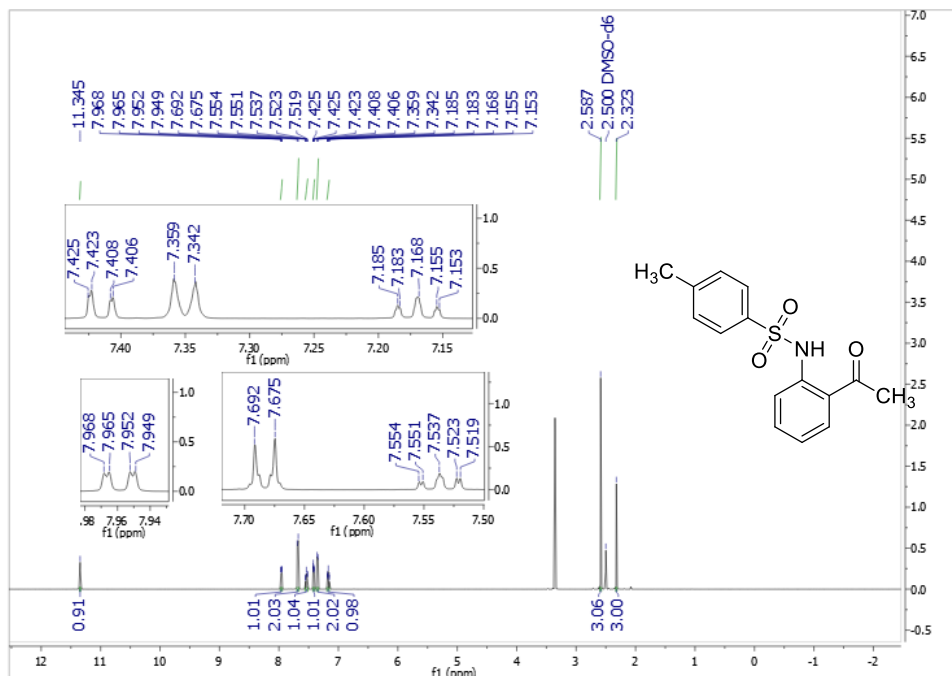
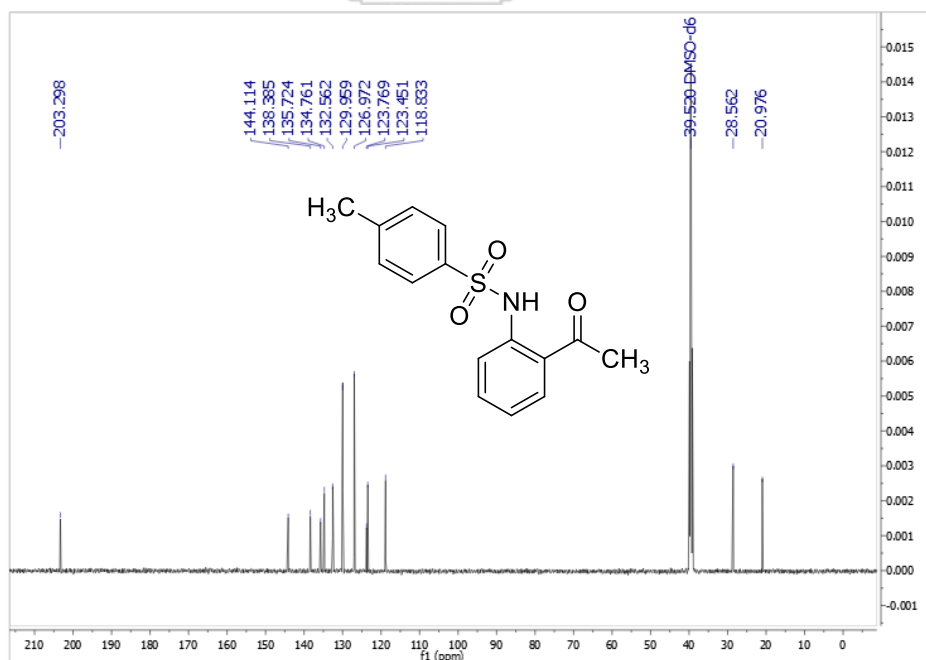
Suggestion for future work

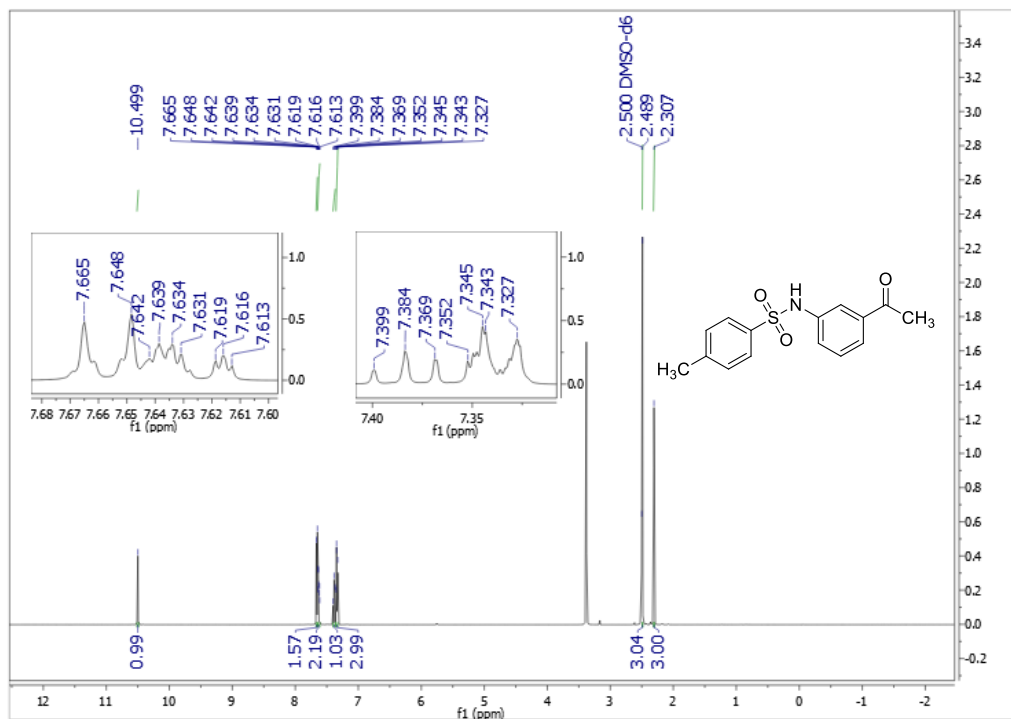
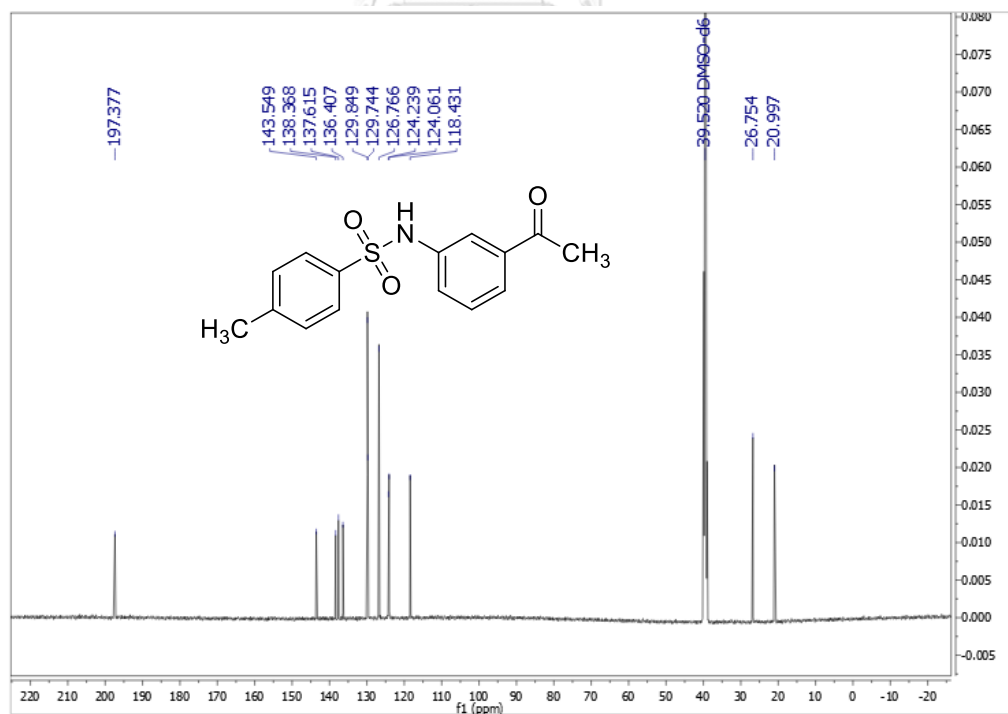
The toxicity test of sulfonamide chalcones is essentially needed to be evaluated, particularly for most potent inhibitors. Selected candidates should further be applied *in vivo* assays to study the mechanism, metabolism, and effects or

disturbances exerted by candidate compounds. Computational study would be a useful tool for scrutinizing the binding of the potent compounds with the active site which would lead to better understanding of their mechanism of action.



APPENDIX

Figure A.3 The ¹H NMR spectrum (DMSO-*d*₆, 500 MHz) of **57**Figure A.4 The ¹³C NMR spectrum (DMSO-*d*₆, 125 MHz) of **57**

Figure A.3 The ^1H NMR spectrum (DMSO- d_6 , 500 MHz) of **58**Figure A.4 The ^{13}C NMR spectrum (DMSO- d_6 , 125 MHz) of **58**

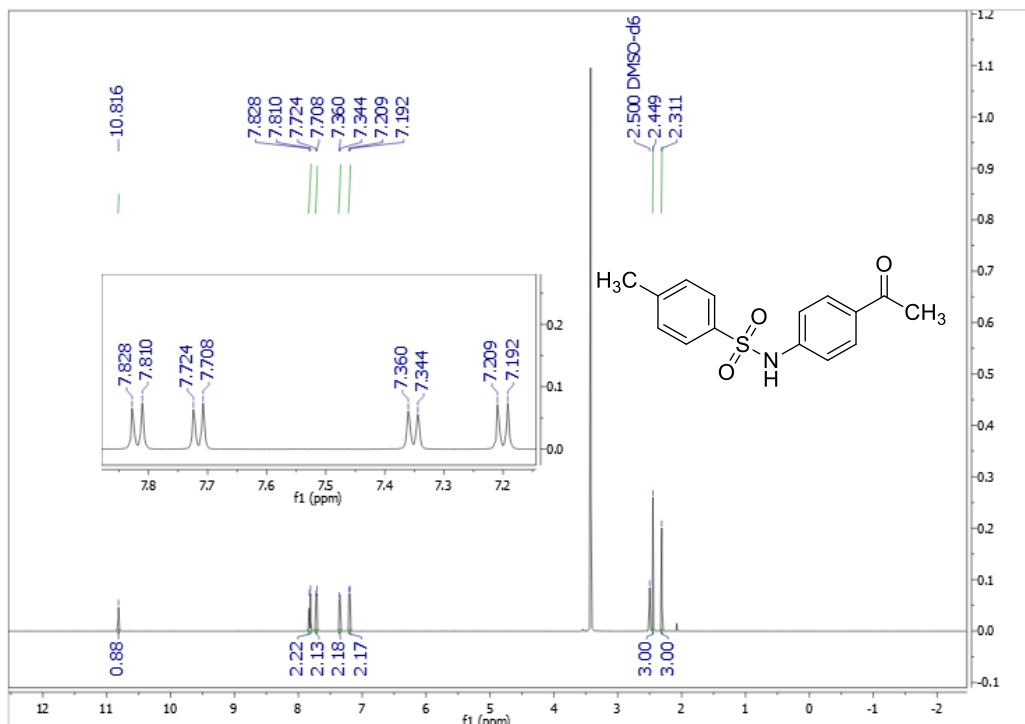


Figure A.5 The ^1H NMR spectrum (DMSO- d_6 , 500 MHz) of **59**

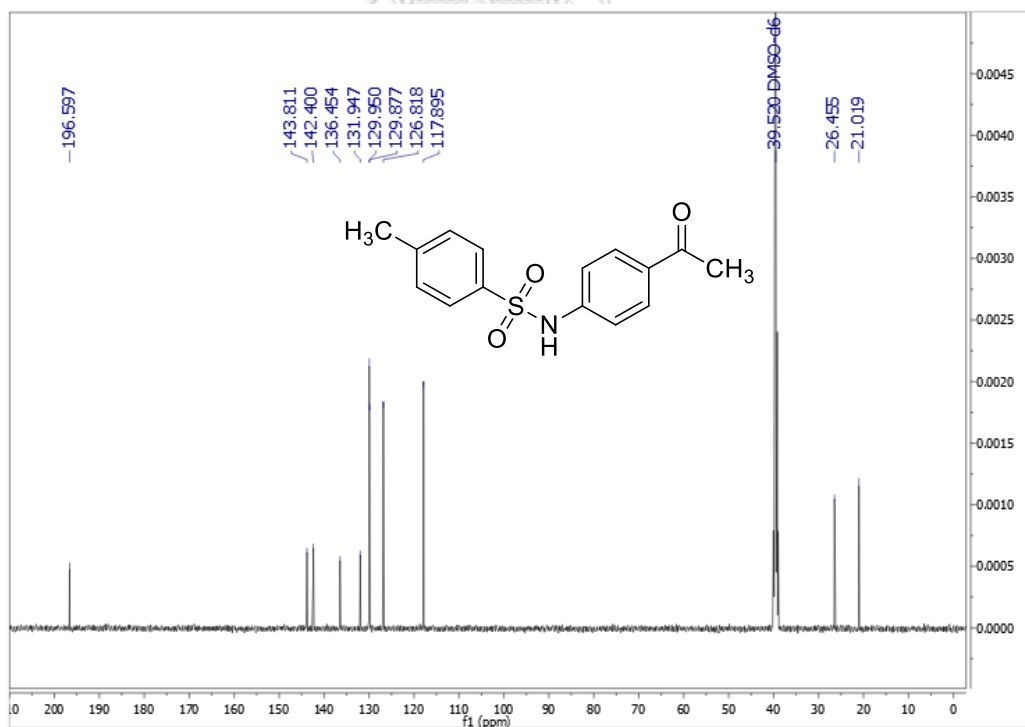


Figure A.6 The ^{13}C NMR spectrum (DMSO- d_6 , 125 MHz) of **59**

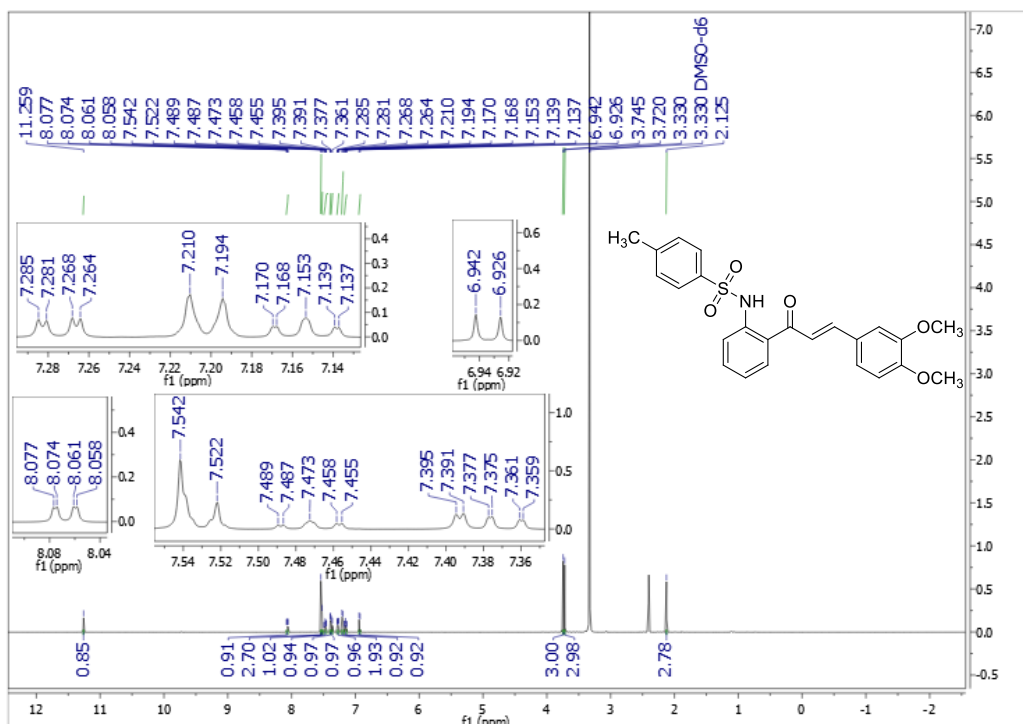


Figure A.7 The ^1H NMR spectrum (DMSO- d_6 , 500 MHz) of **60**

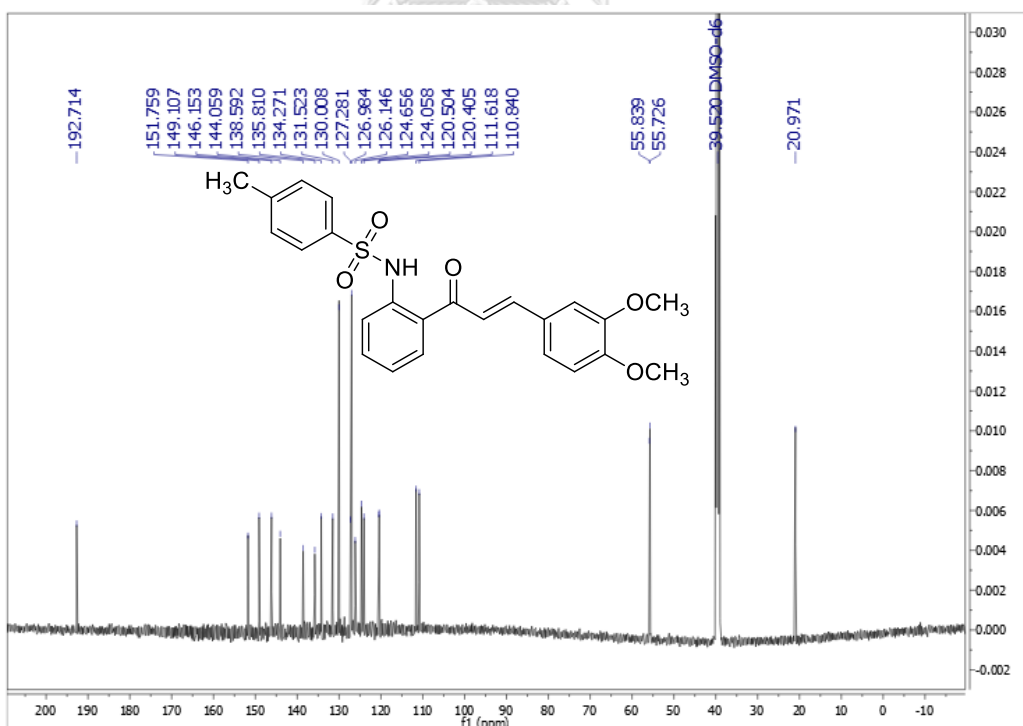


Figure A.8 The ^{13}C NMR spectrum (DMSO- d_6 , 125 MHz) of **60**

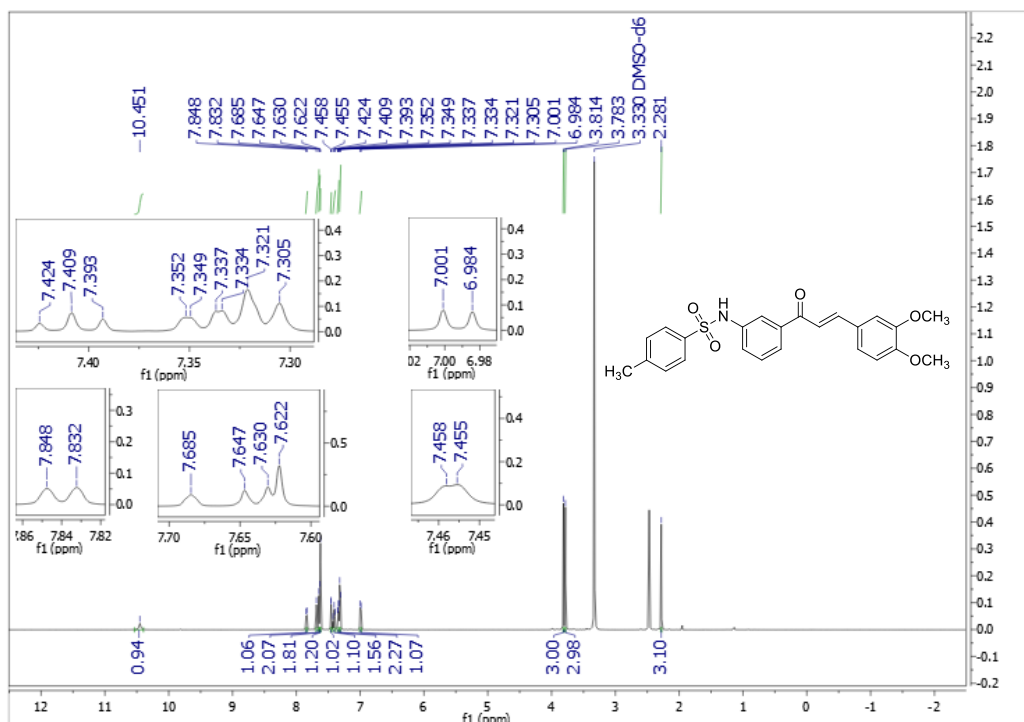


Figure A.9 The ¹H NMR spectrum (DMSO-*d*₆, 500 MHz) of **61**

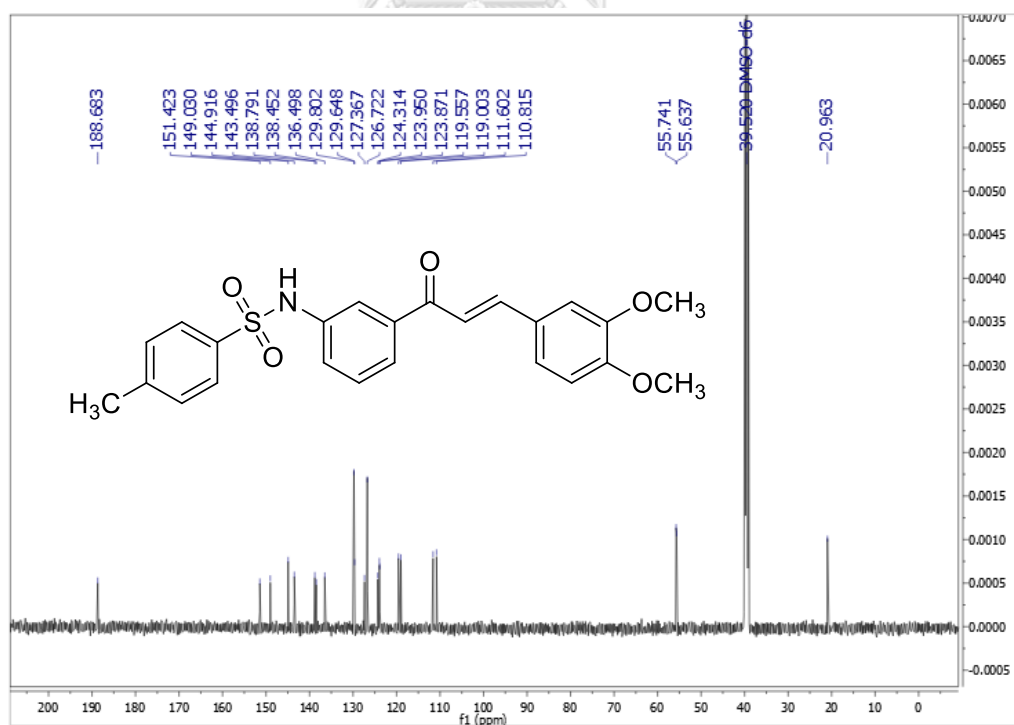


Figure A.10 The ¹³C NMR spectrum (DMSO-*d*₆, 125 MHz) of **61**

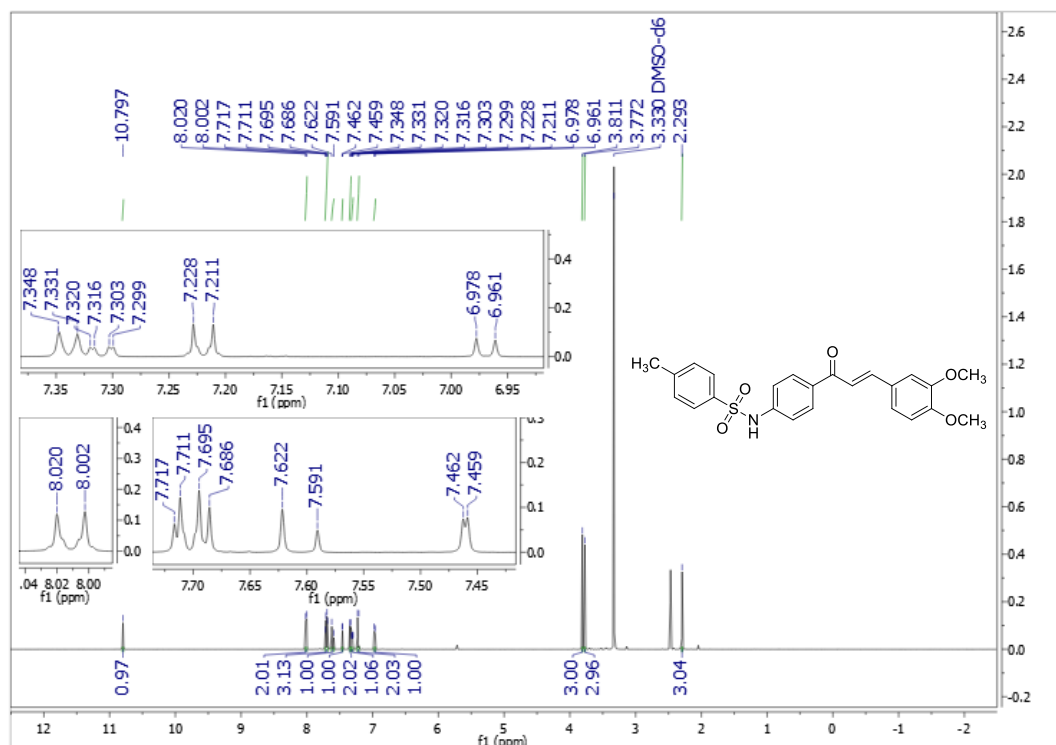


Figure A.11 The ¹H NMR spectrum (DMSO-*d*₆, 500 MHz) of **62**

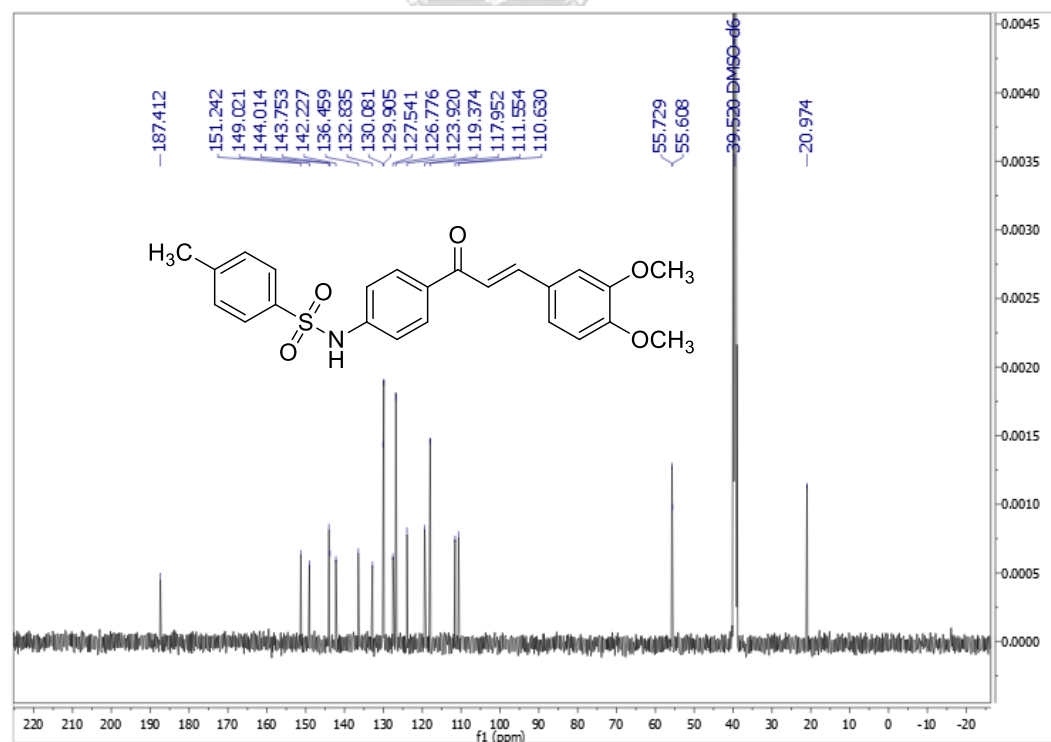
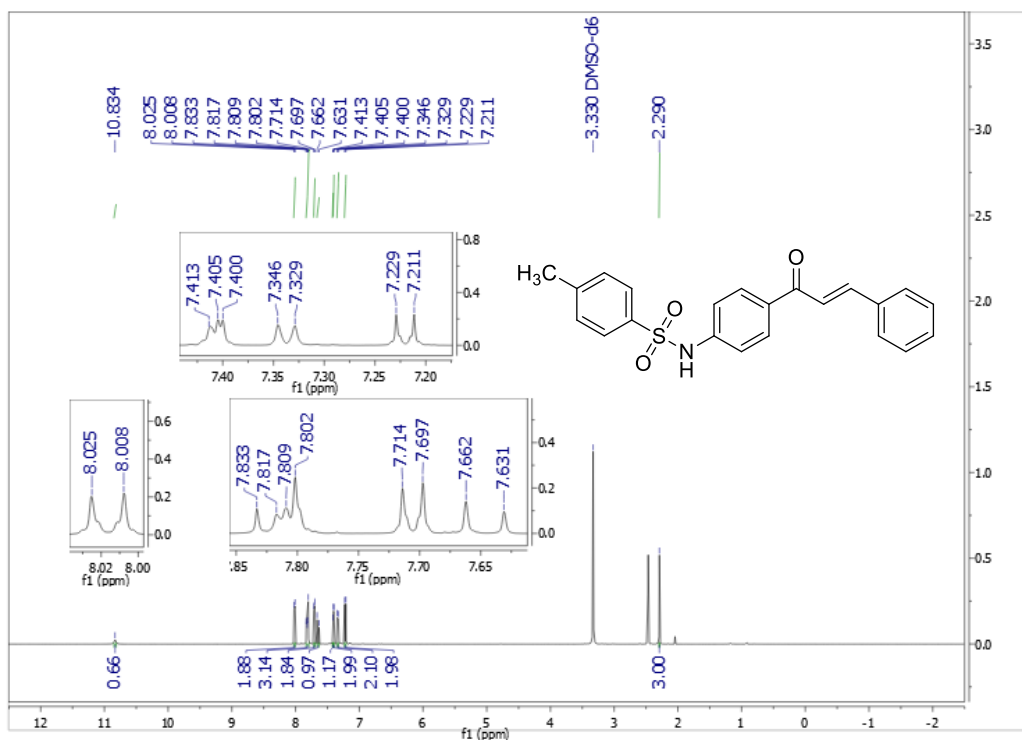
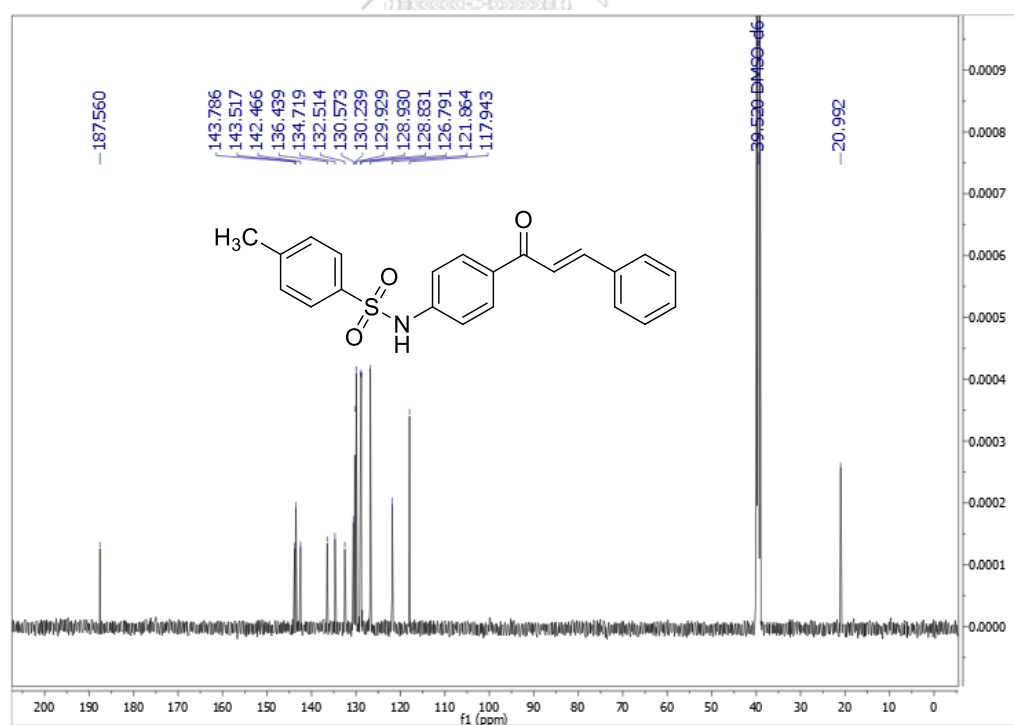


Figure A.12 The ¹³C NMR spectrum (DMSO-*d*₆, 125 MHz) of **62**

Figure A.13 The ¹H NMR spectrum (DMSO-*d*₆, 500 MHz) of 63Figure A.14 The ¹³C NMR spectrum (DMSO-*d*₆, 125 MHz) of 63

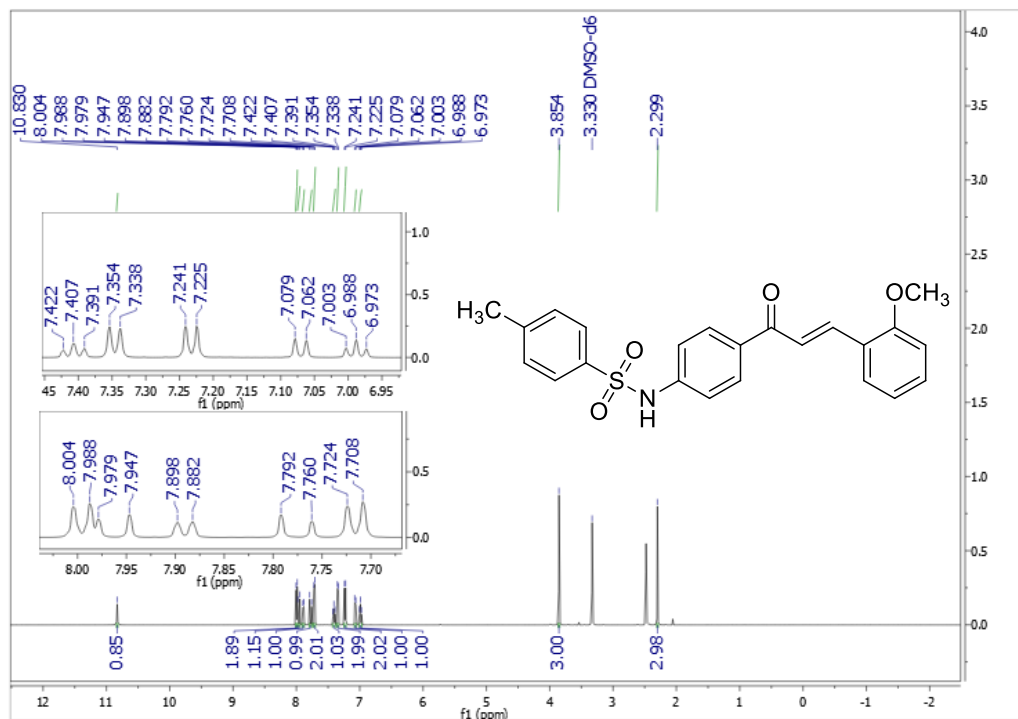


Figure A.15 The ¹H NMR spectrum (DMSO-*d*₆, 500 MHz) of **64**

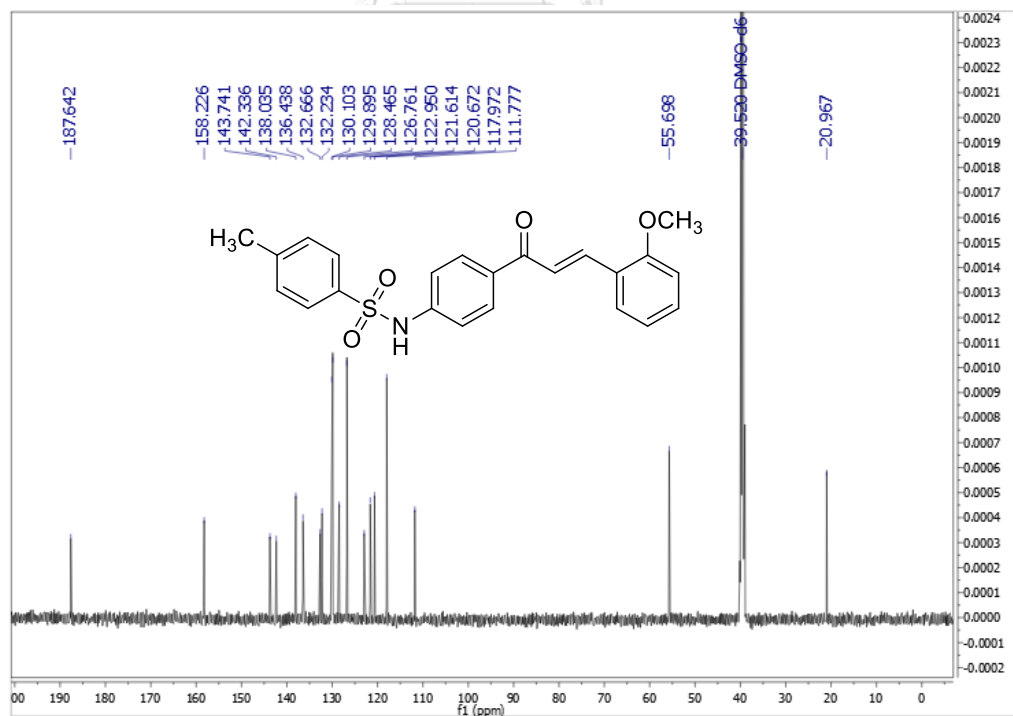


Figure A.16 The ¹³C NMR spectrum (DMSO-*d*₆, 125 MHz) of **64**

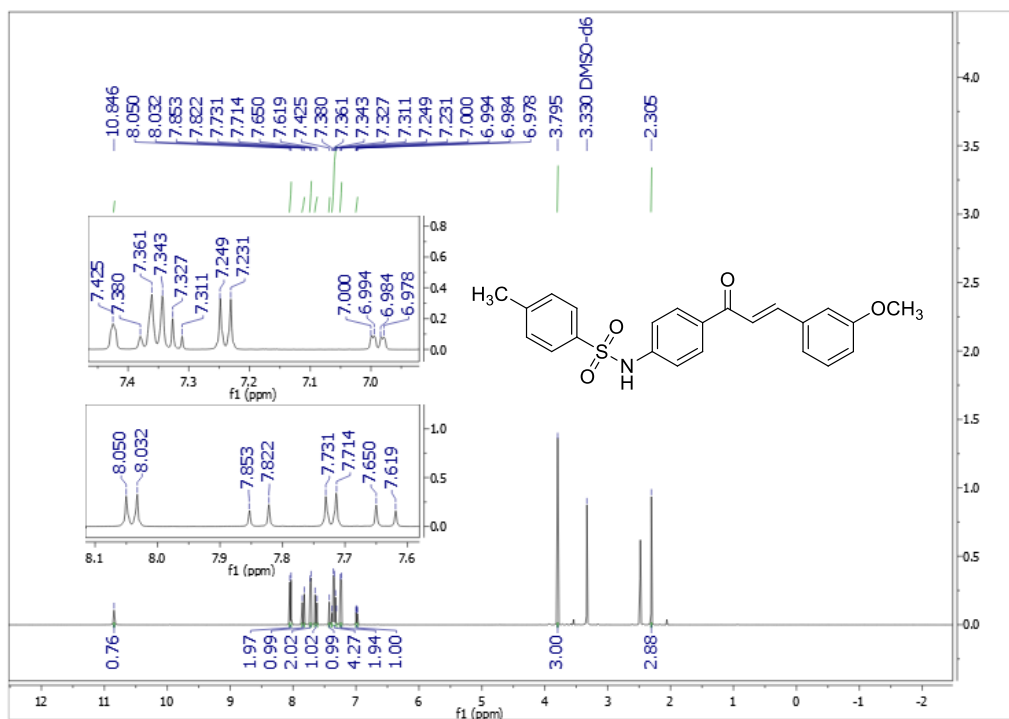


Figure A.17 The ^1H NMR spectrum (DMSO- d_6 , 500 MHz) of 65

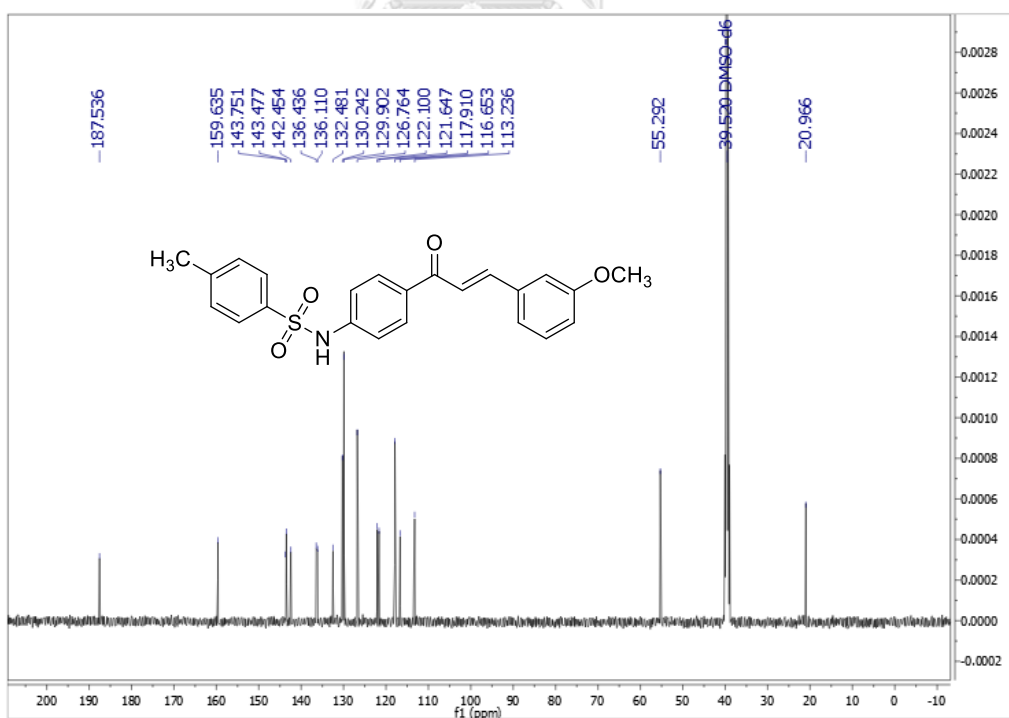


Figure A.18 The ^{13}C NMR spectrum (DMSO- d_6 , 125 MHz) of 65

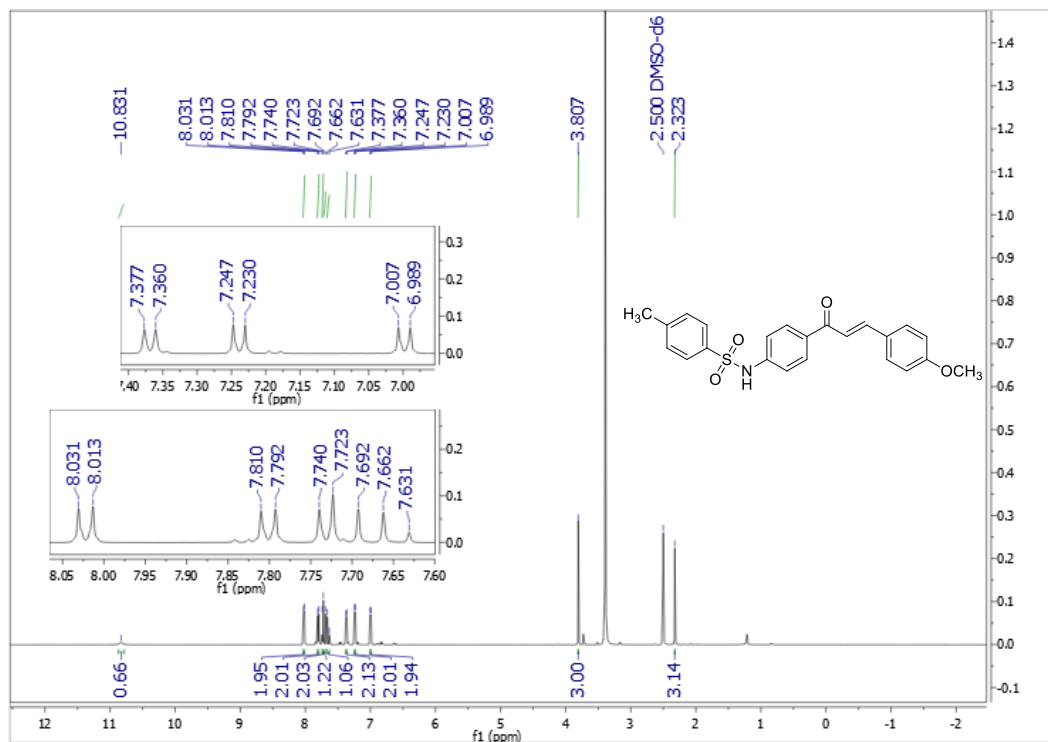


Figure A.19 The ^1H NMR spectrum (DMSO- d_6 , 500 MHz) of **66**

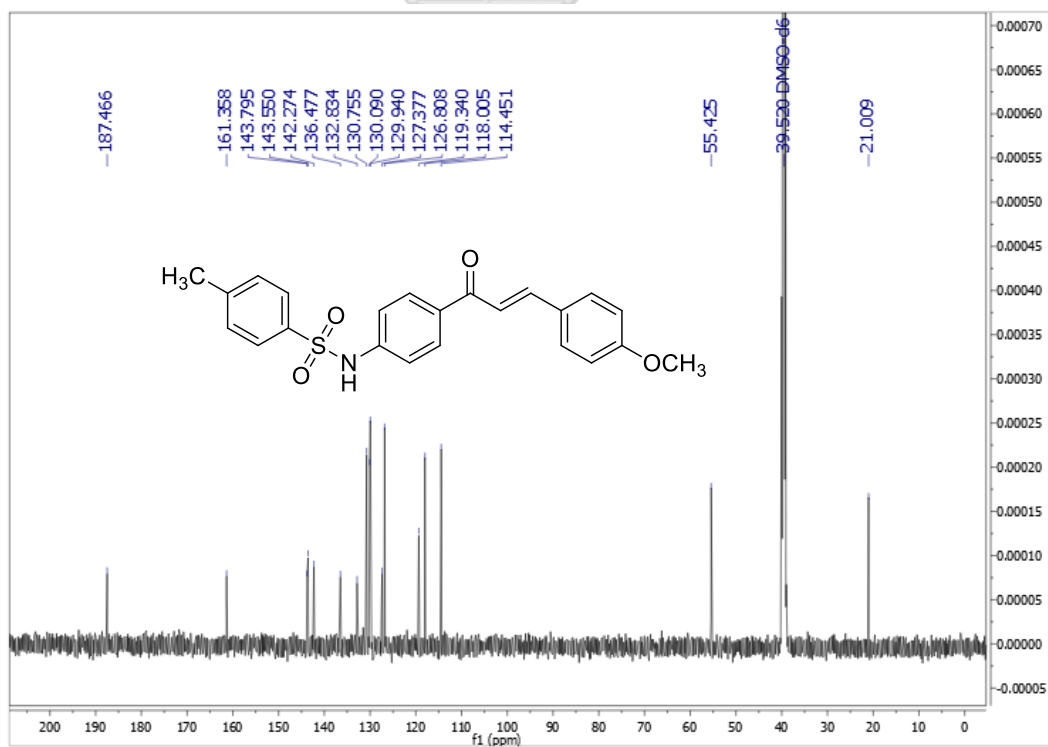


Figure A.20 The ^{13}C NMR spectrum (DMSO- d_6 , 125 MHz) of **66**

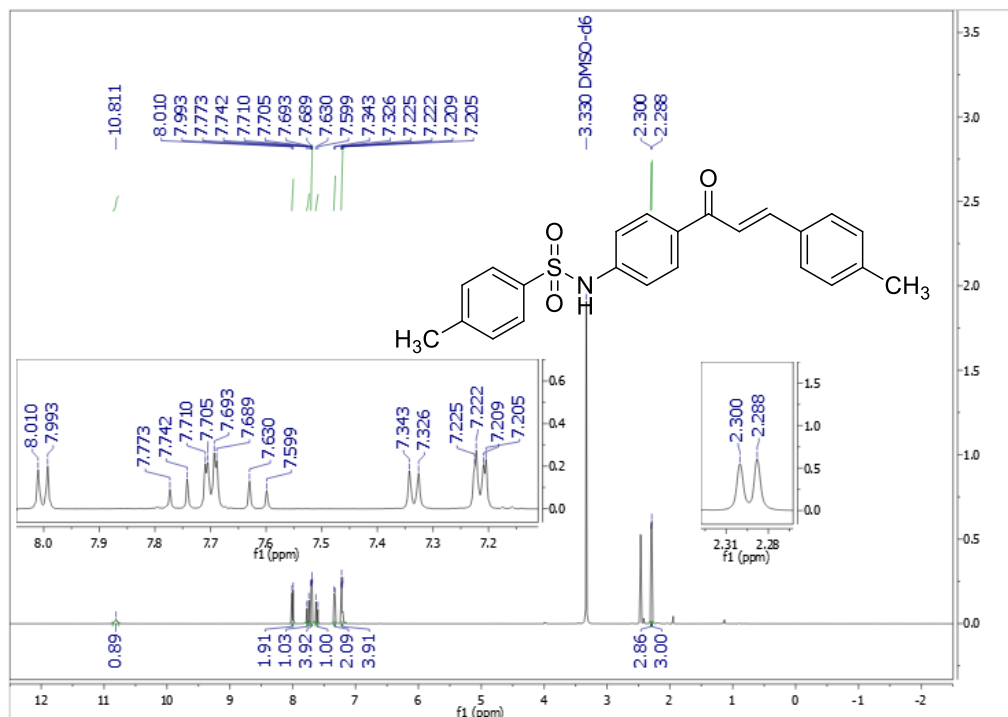


Figure A.21 The ^1H NMR spectrum (DMSO- d_6 , 500 MHz) of **67**

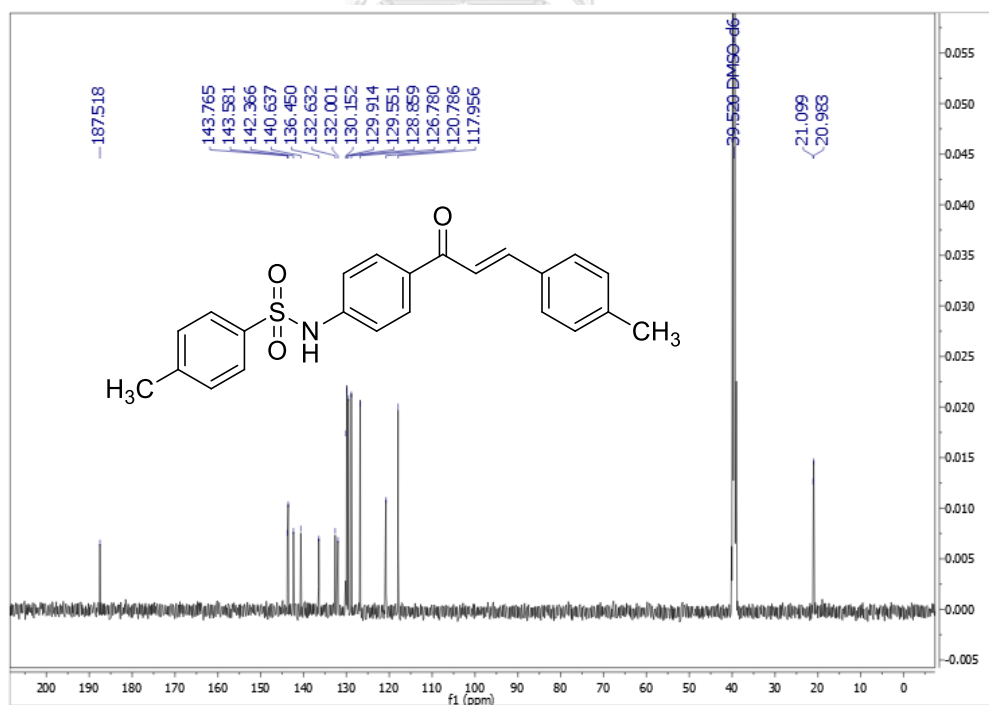


Figure A.22 The ^{13}C NMR spectrum (DMSO- d_6 , 125 MHz) of **67**

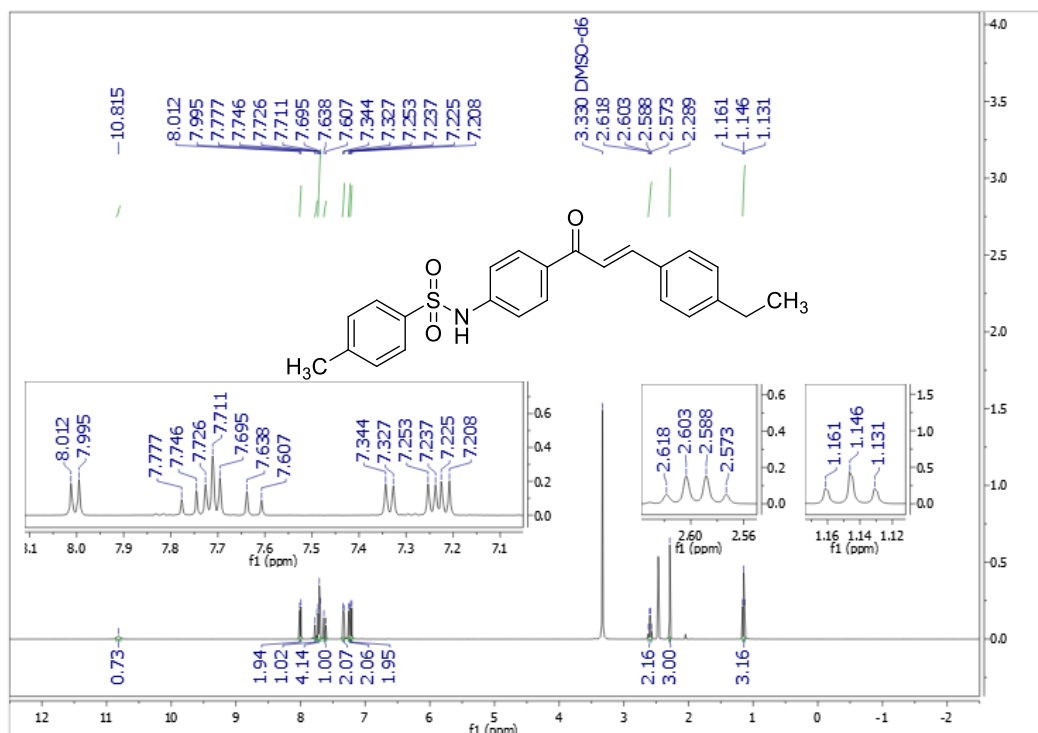


Figure A.23 The ¹H NMR spectrum (DMSO-*d*₆, 500 MHz) of 68

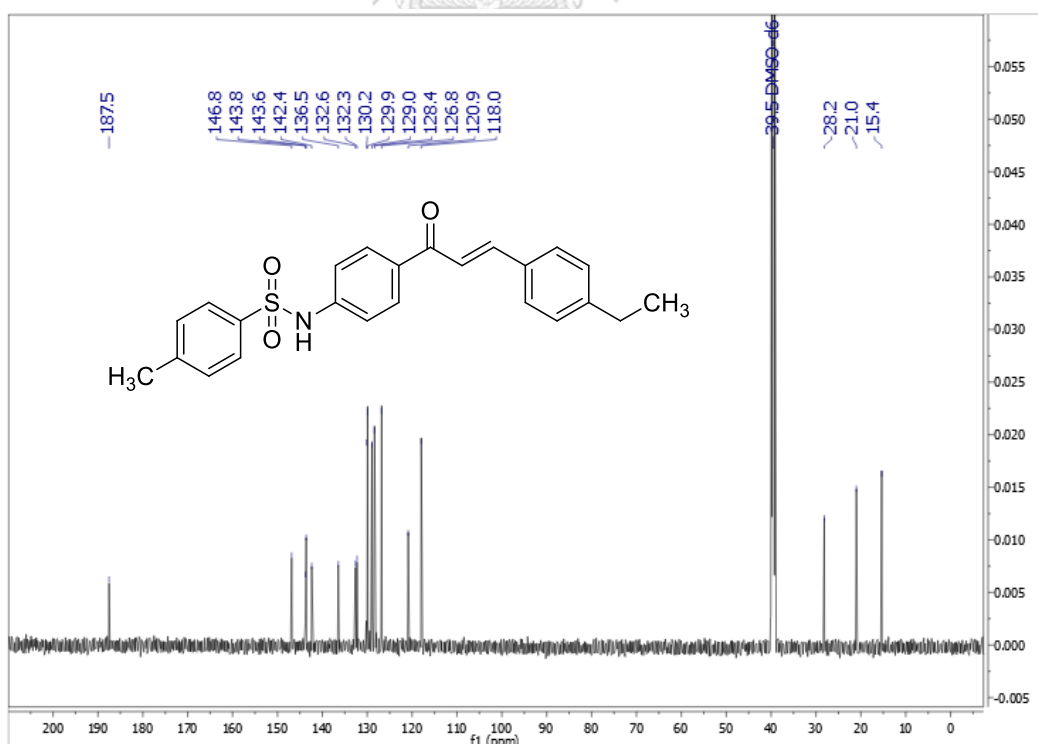


Figure A.24 The ¹³C NMR spectrum (DMSO-*d*₆, 125 MHz) of 68

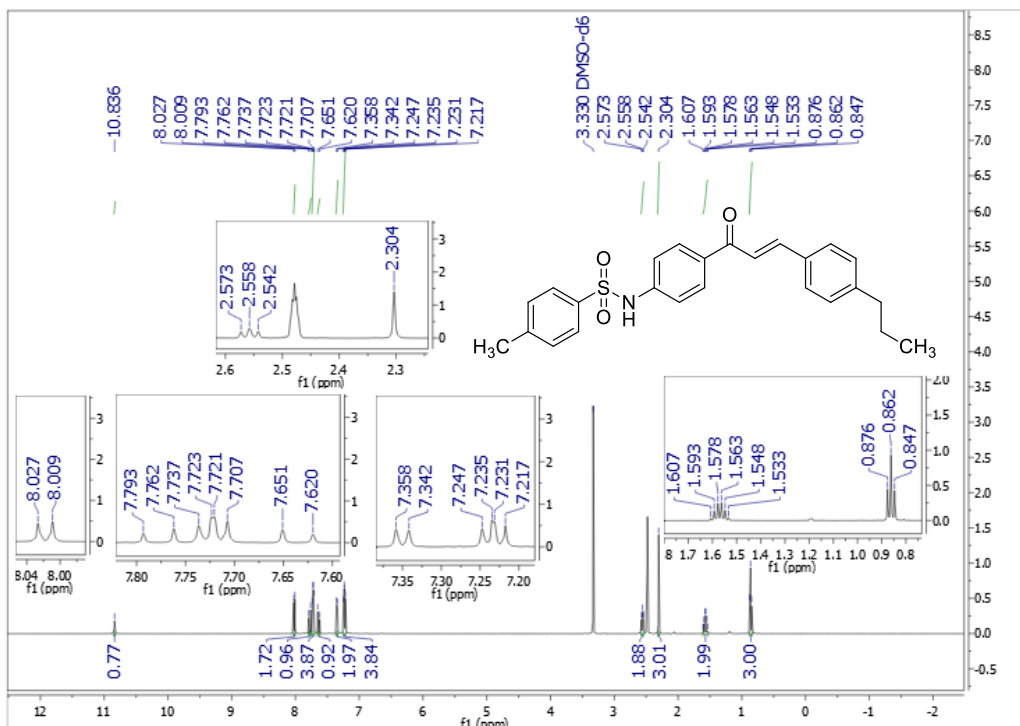


Figure A.25 The ^1H NMR spectrum (DMSO- d_6 , 500 MHz) of 69

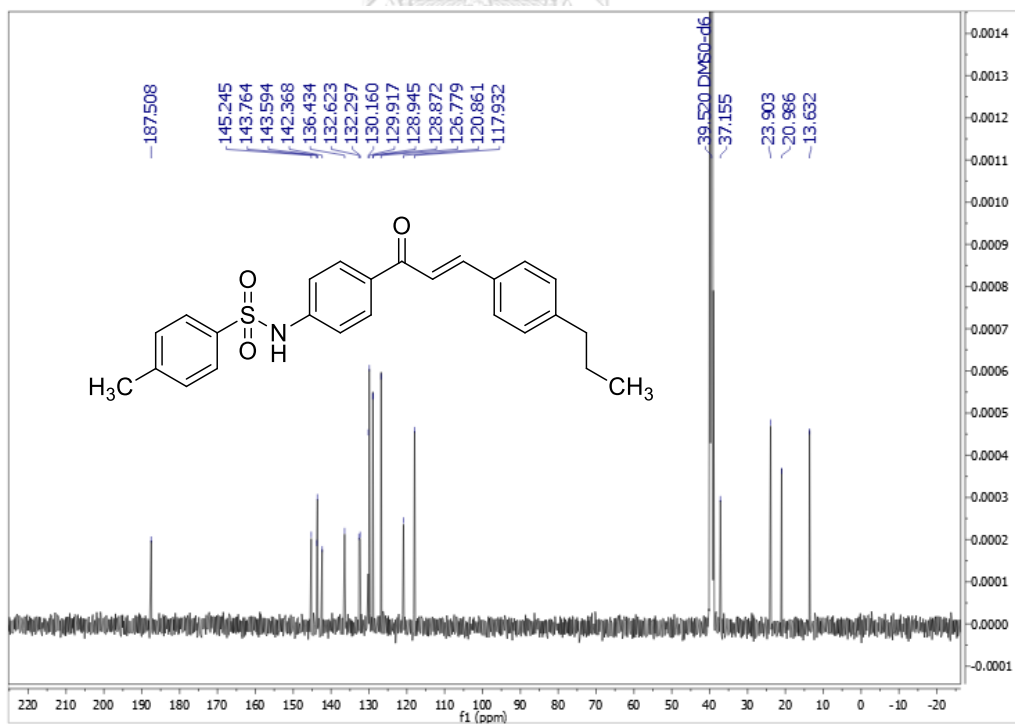


Figure A.26 The ^{13}C NMR spectrum (DMSO- d_6 , 125 MHz) of 69

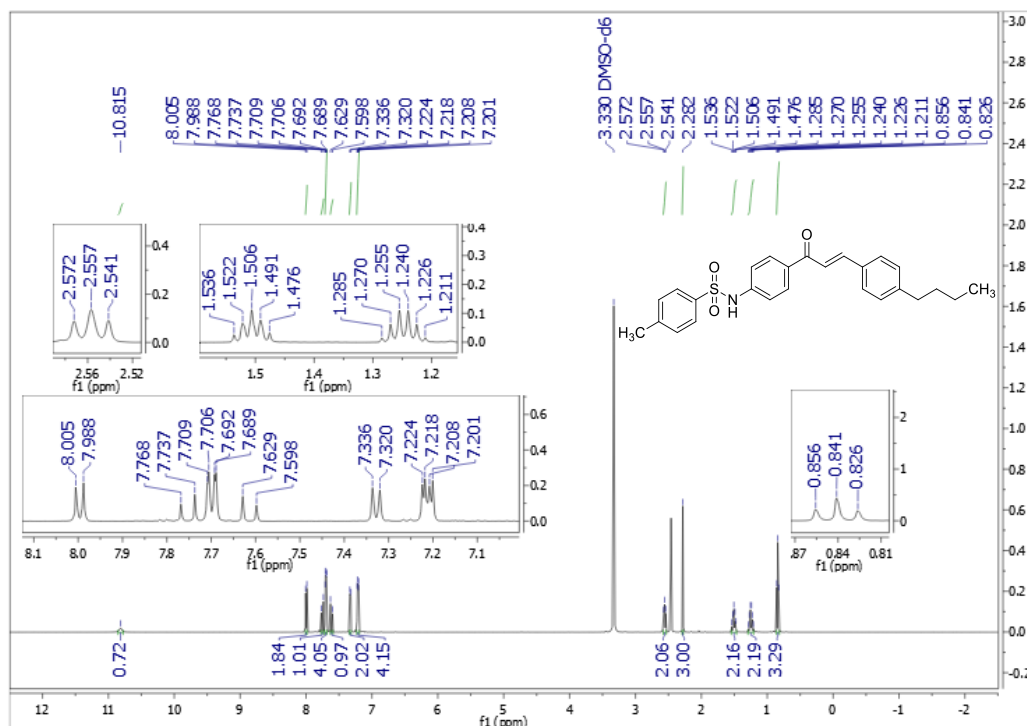


Figure A.27 The ^1H NMR spectrum (DMSO- d_6 , 500 MHz) of 70

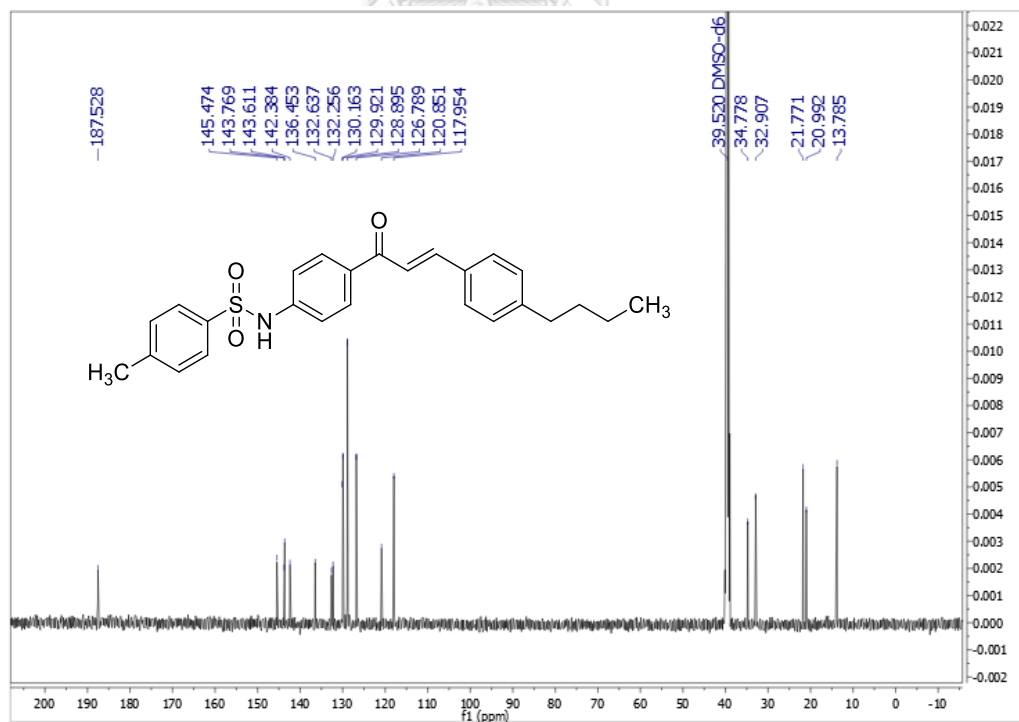


Figure A.28 The ^{13}C NMR spectrum (DMSO- d_6 , 125 MHz) of 70

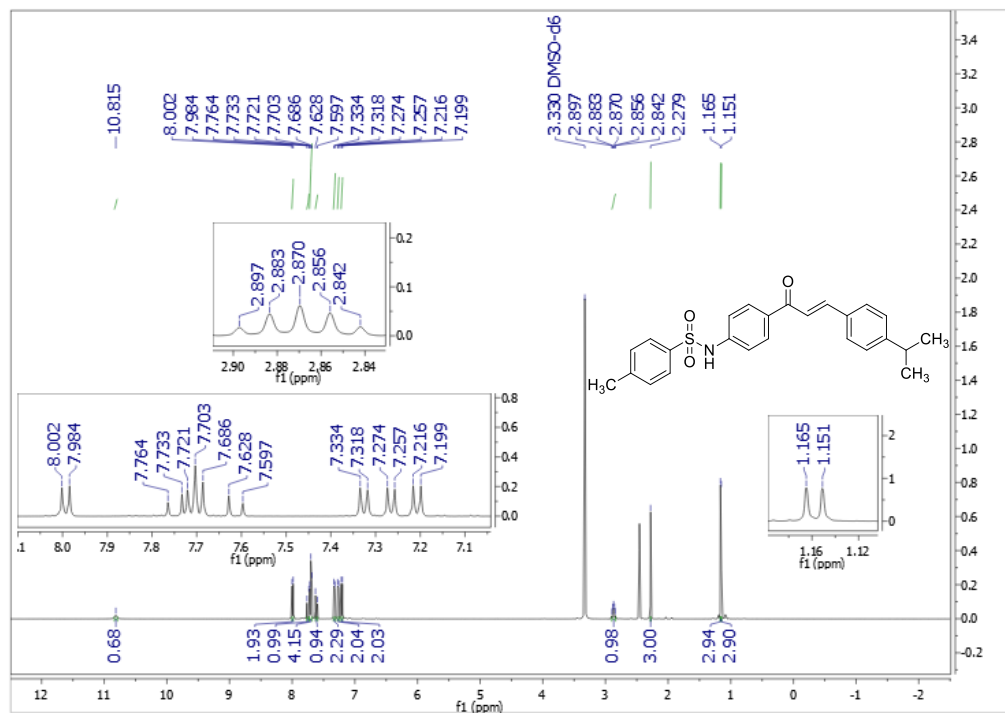


Figure A.29 The ¹H NMR spectrum (DMSO-d₆, 500 MHz) of 71

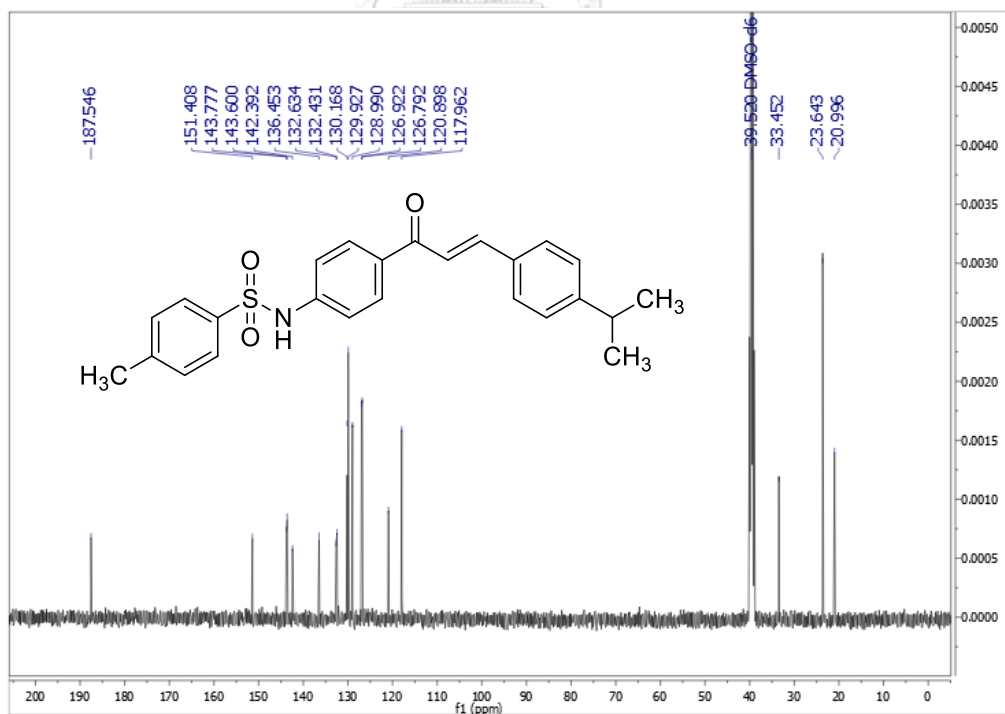


Figure A.30 The ¹³C NMR spectrum (DMSO-d₆, 125 MHz) of 71

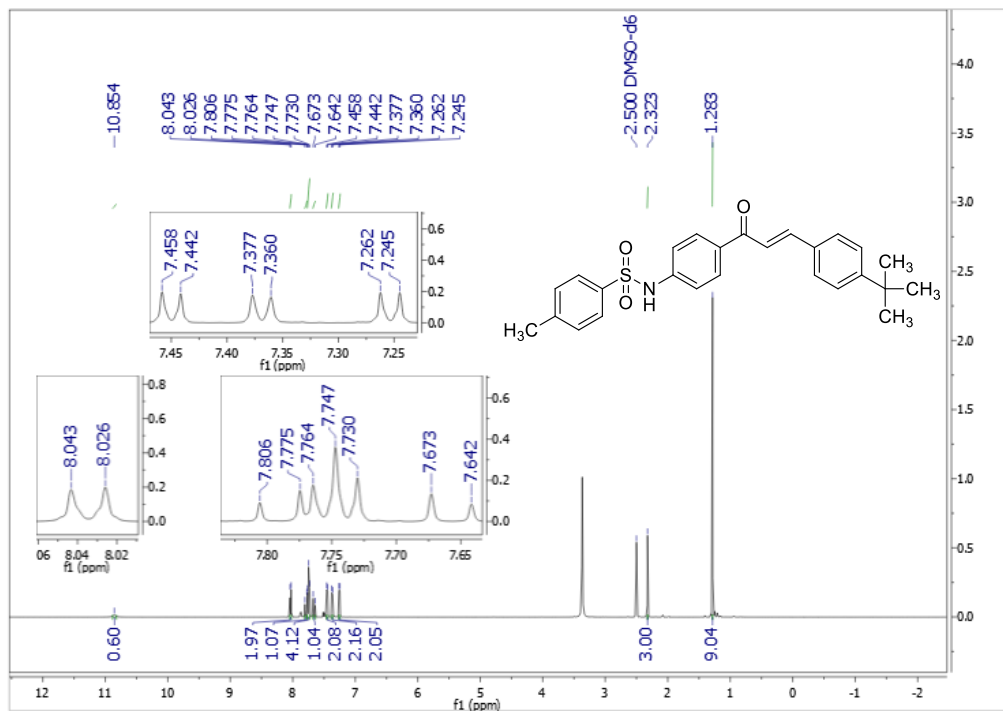


Figure A.31 The ^1H NMR spectrum (DMSO- d_6 , 500 MHz) of 72

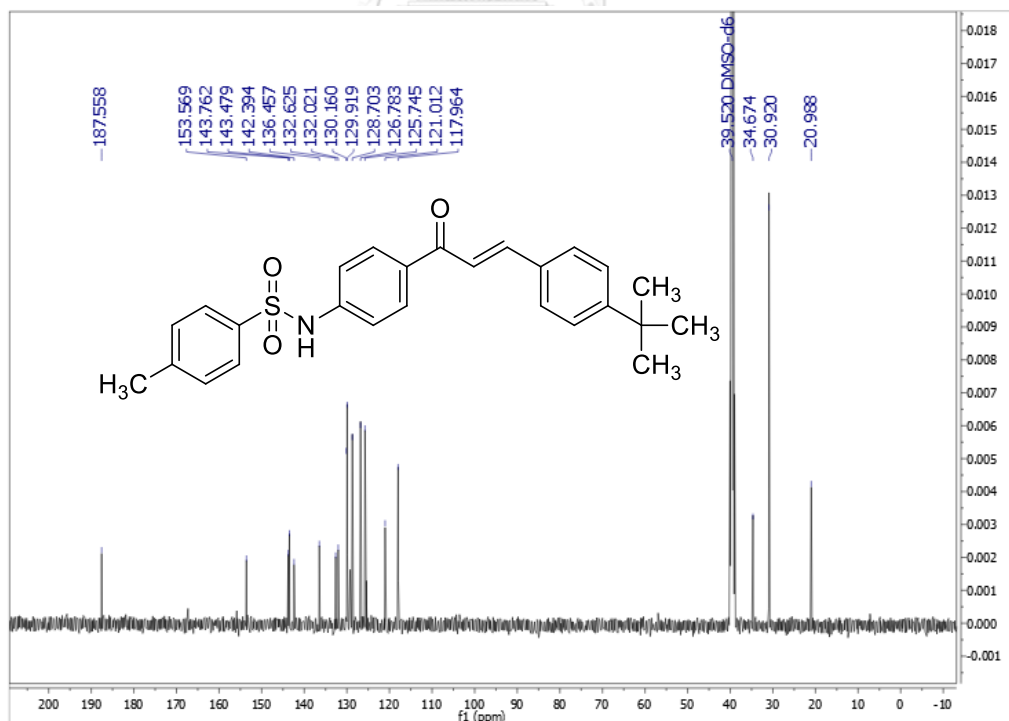


Figure A.32 The ^{13}C NMR spectrum (DMSO- d_6 , 125 MHz) of 72

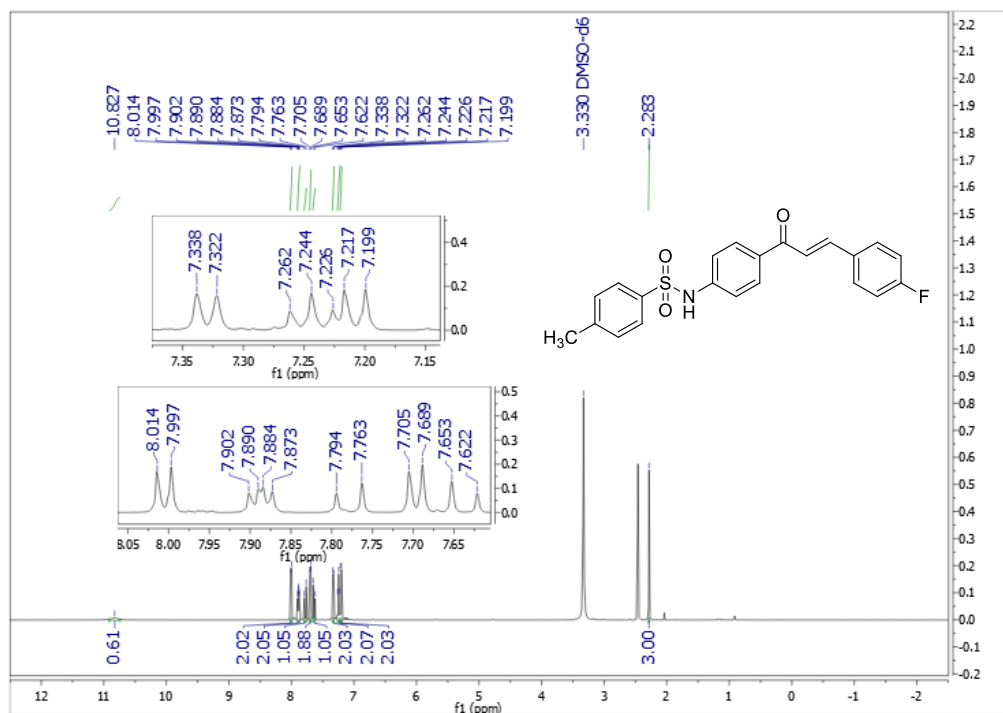


Figure A.33 The ^1H NMR spectrum (DMSO- d_6 , 500 MHz) of 73

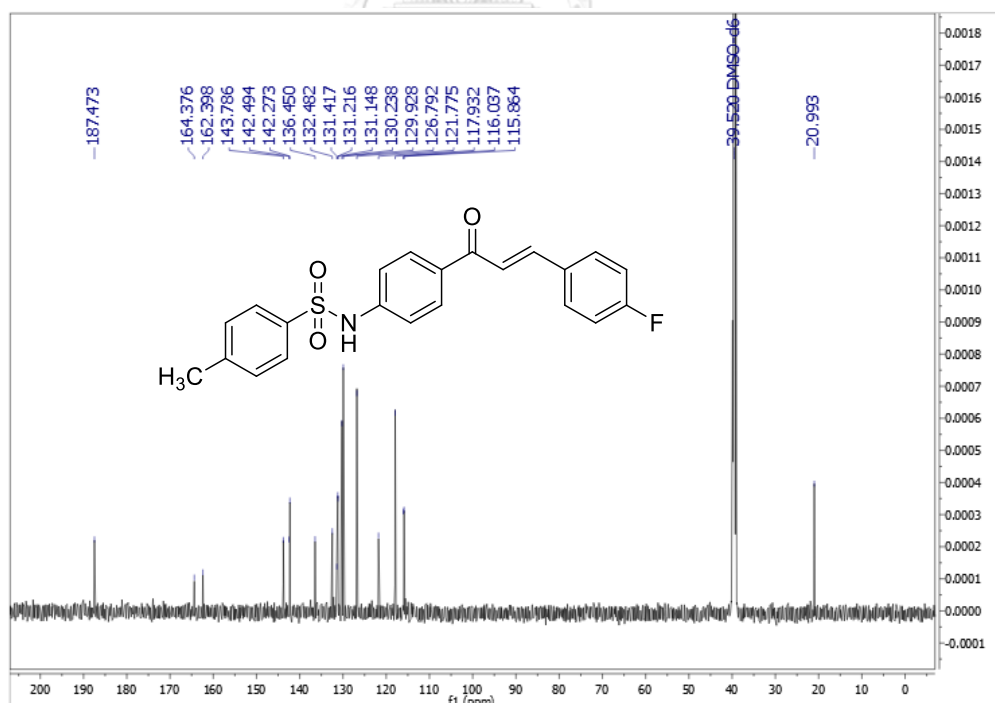


Figure A.34 The ^{13}C NMR spectrum (DMSO- d_6 , 125 MHz) of 73

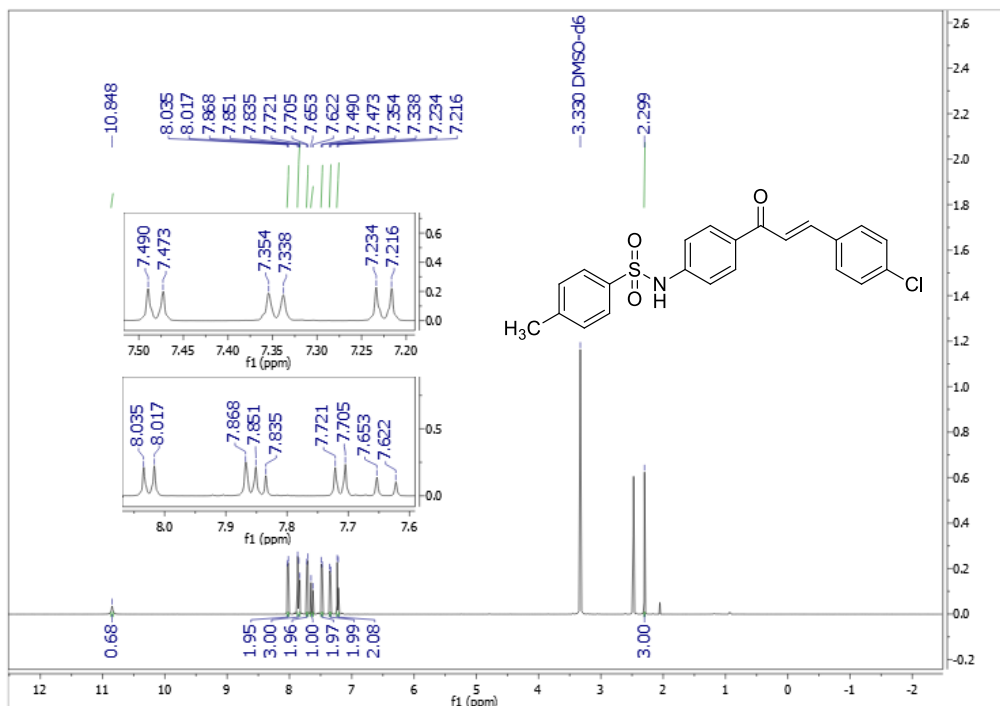


Figure A.35 The ¹H NMR spectrum (DMSO-d₆, 500 MHz) of 74

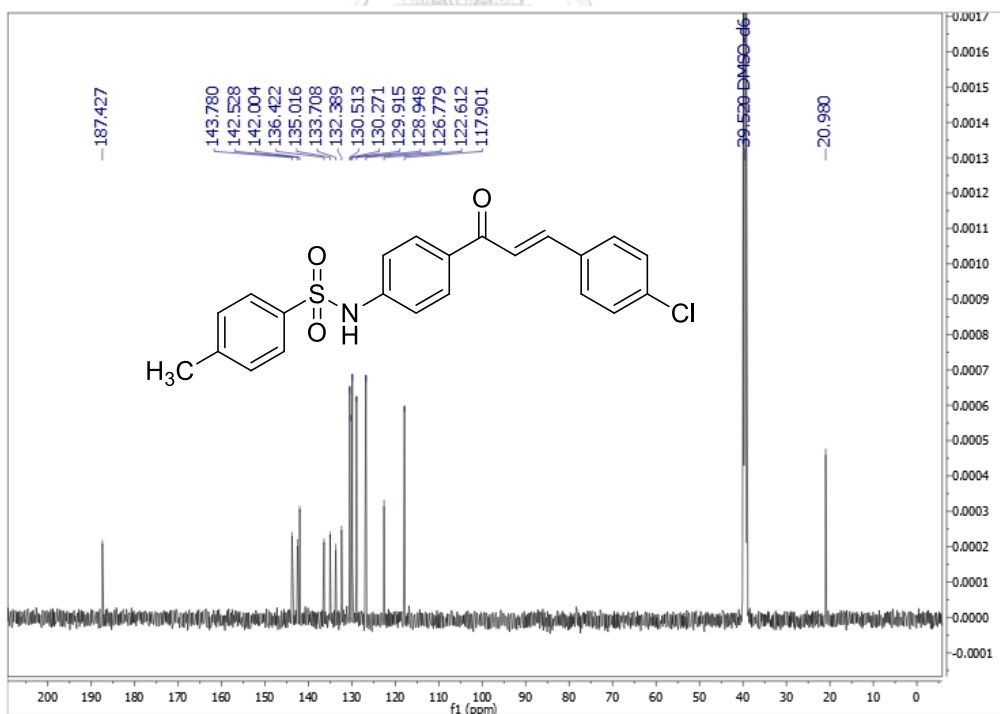


Figure A.36 The ¹³C NMR spectrum (DMSO-d₆, 125 MHz) of 74

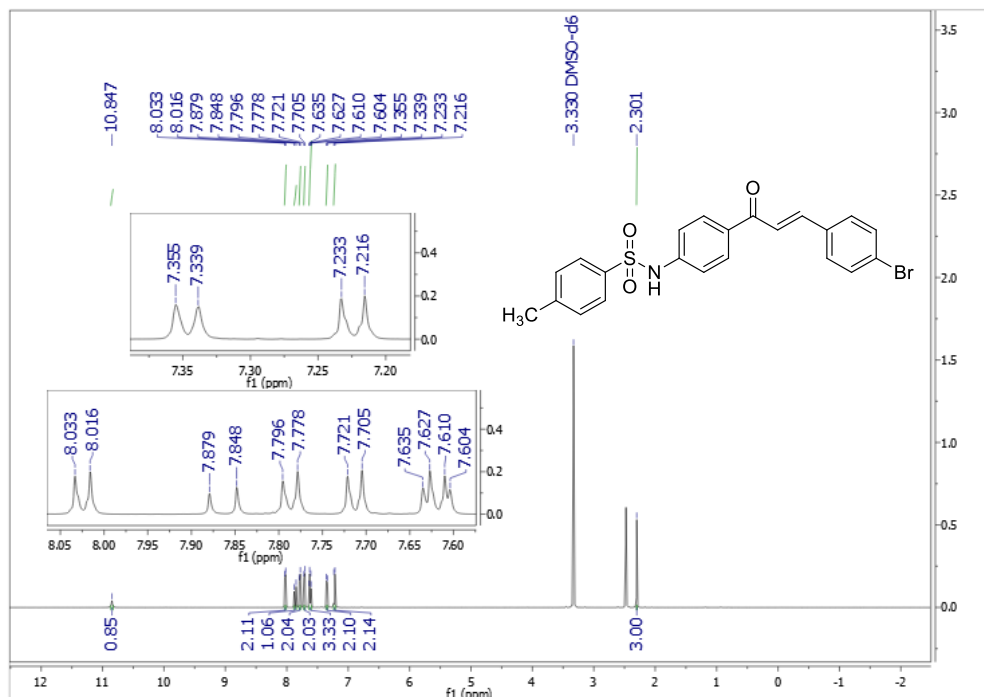


Figure A.37 The ¹H NMR spectrum (DMSO-*d*₆, 500 MHz) of 75

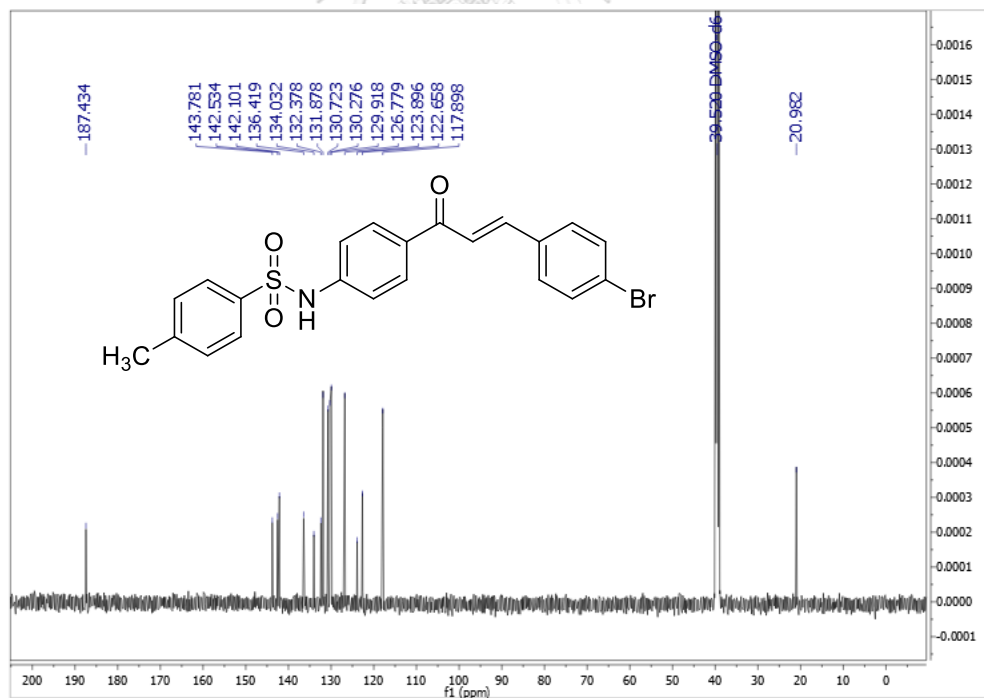


Figure A.38 The ¹³C NMR spectrum (DMSO-*d*₆, 125 MHz) of 75

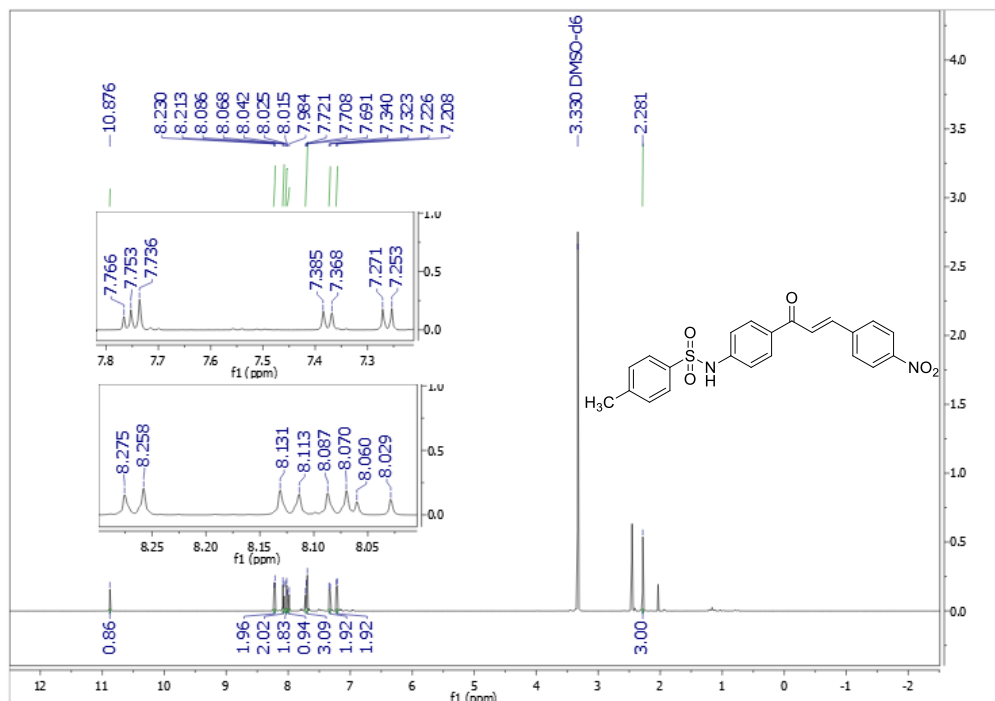


Figure A.39 The ¹H NMR spectrum (DMSO-*d*₆, 500 MHz) of 76

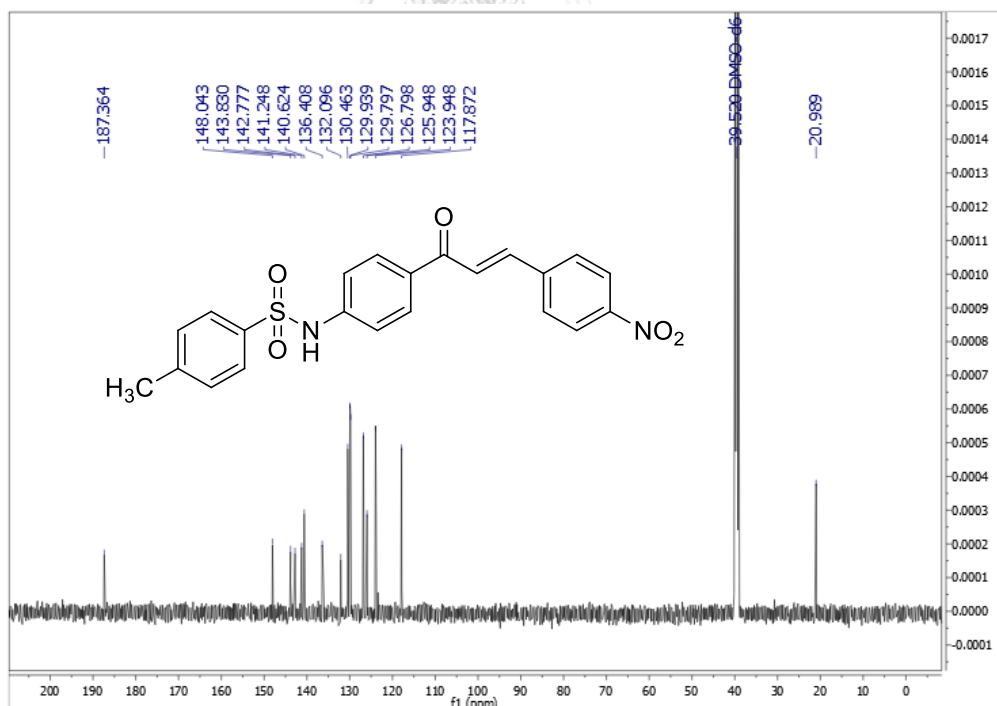


Figure A.40 The ¹³C NMR spectrum (DMSO-*d*₆, 125 MHz) of 76

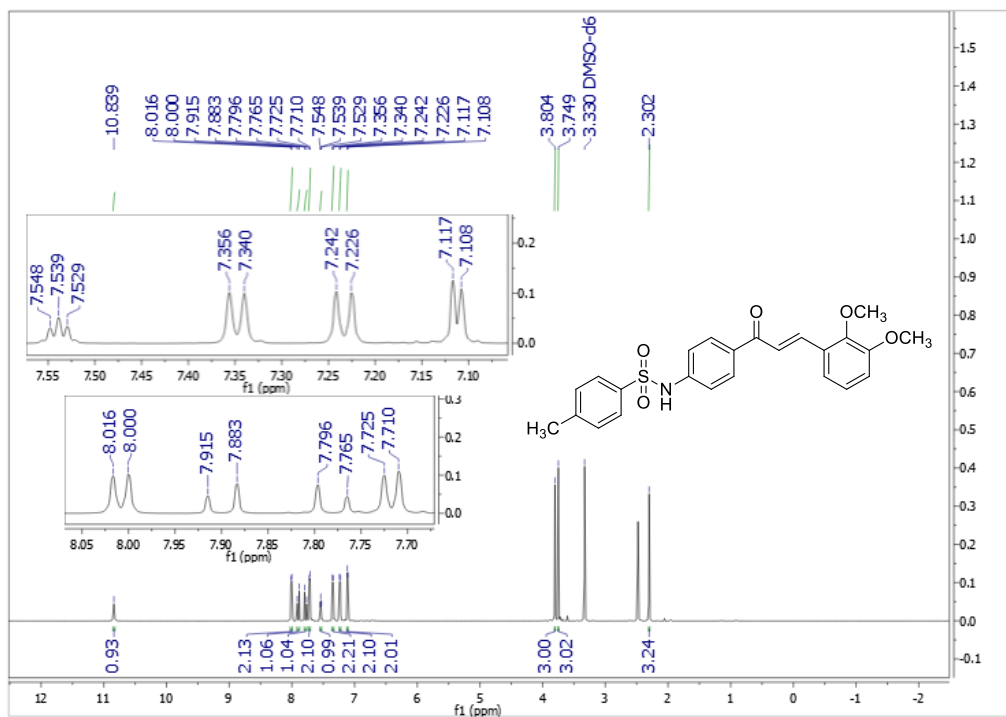


Figure A.41 The ¹H NMR spectrum (DMSO-*d*₆, 500 MHz) of 77

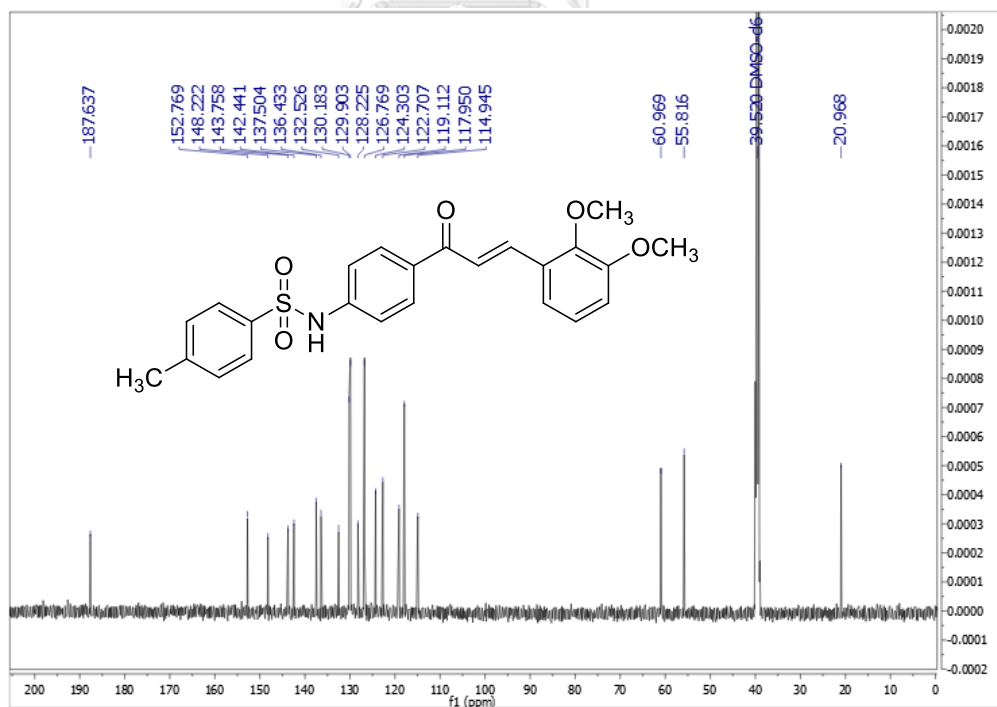


Figure A.42 The ¹³C NMR spectrum (DMSO-*d*₆, 125 MHz) of 77

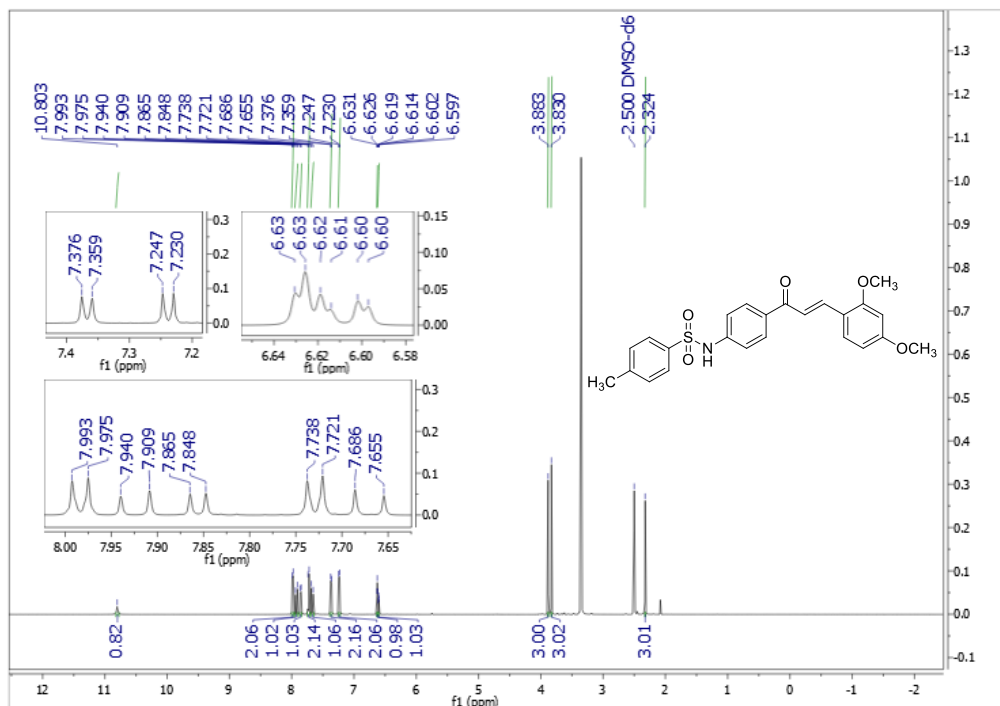


Figure A.43 The ^1H NMR spectrum (DMSO- d_6 , 500 MHz) of **78**

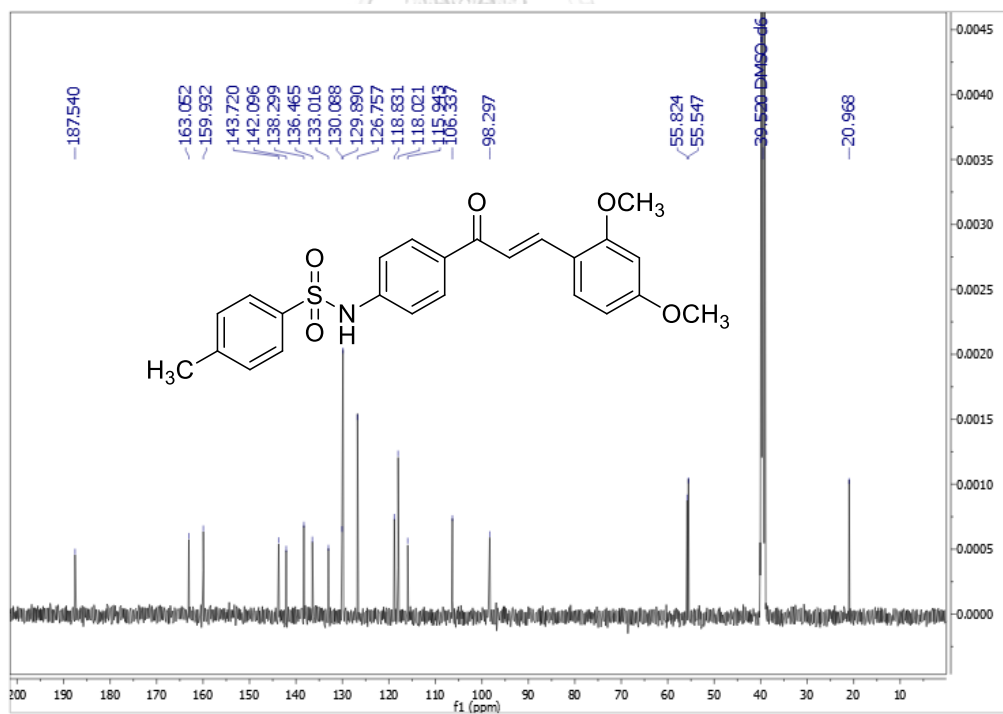


Figure A.44 The ^{13}C NMR spectrum (DMSO- d_6 , 125 MHz) of **78**

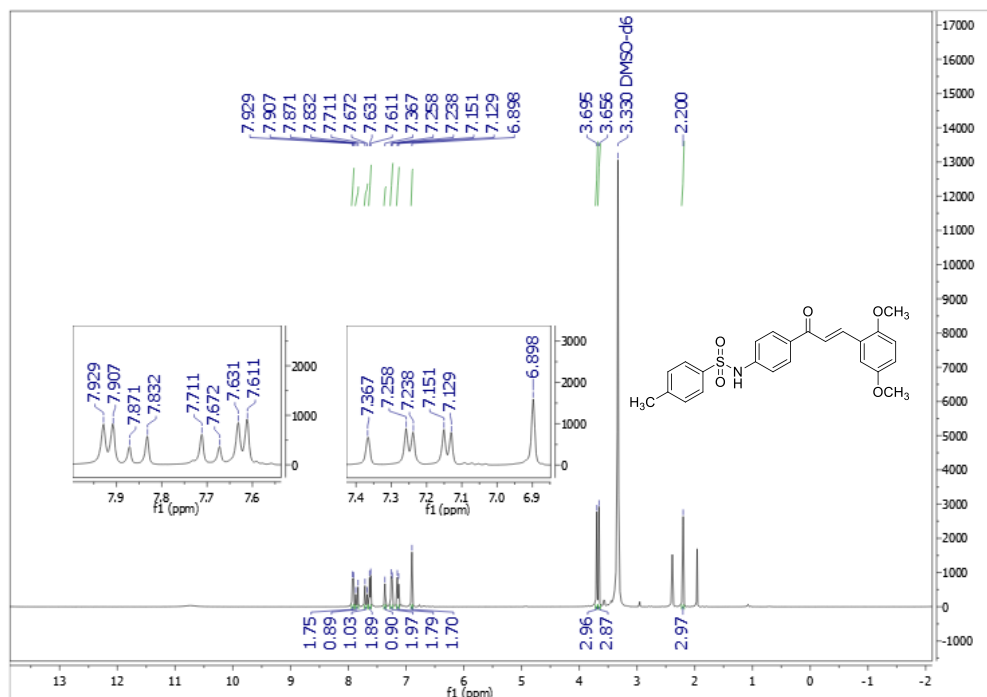


Figure A.45 The ¹H NMR spectrum (DMSO-*d*₆, 400 MHz) of **79**

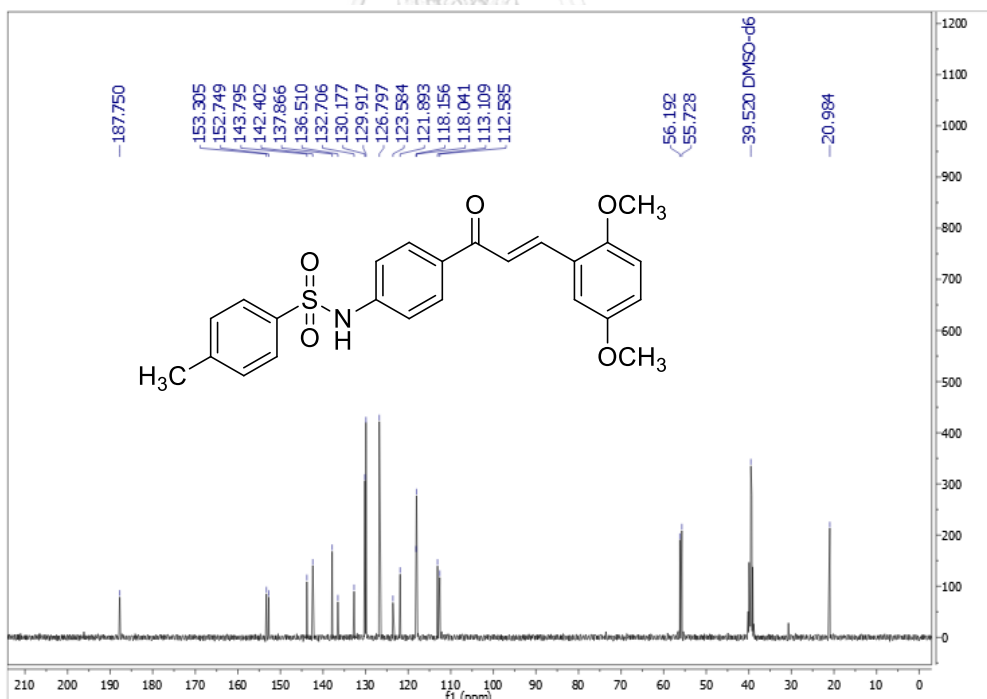


Figure A.46 The ¹³C NMR spectrum (DMSO-*d*₆, 100 MHz) of **79**

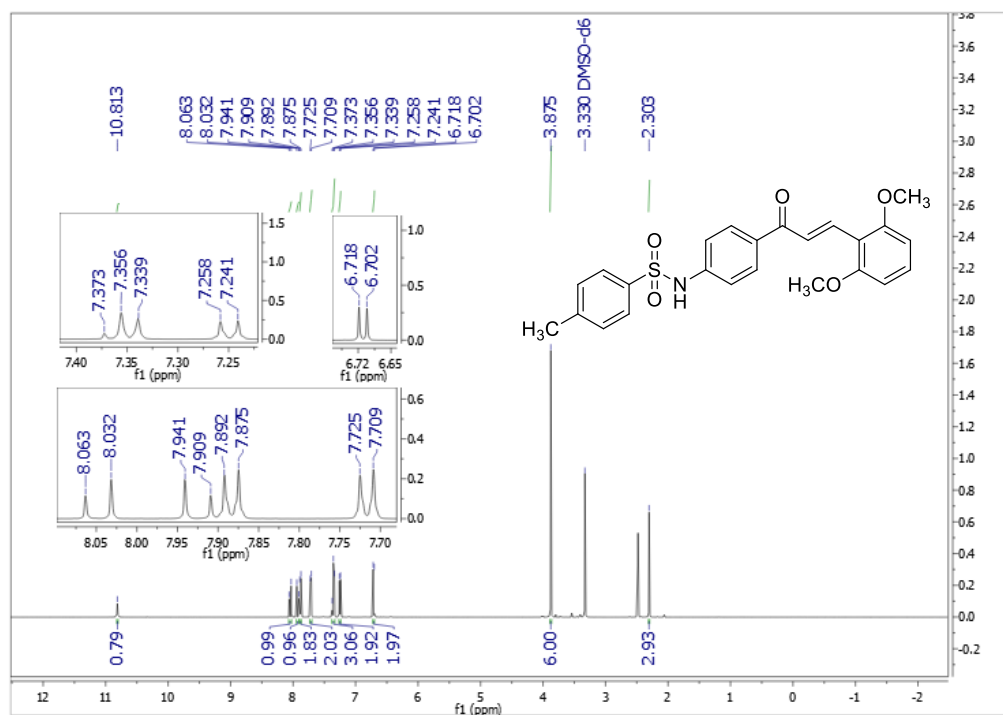


Figure A.47 The ^1H NMR spectrum (DMSO- d_6 , 500 MHz) of 80

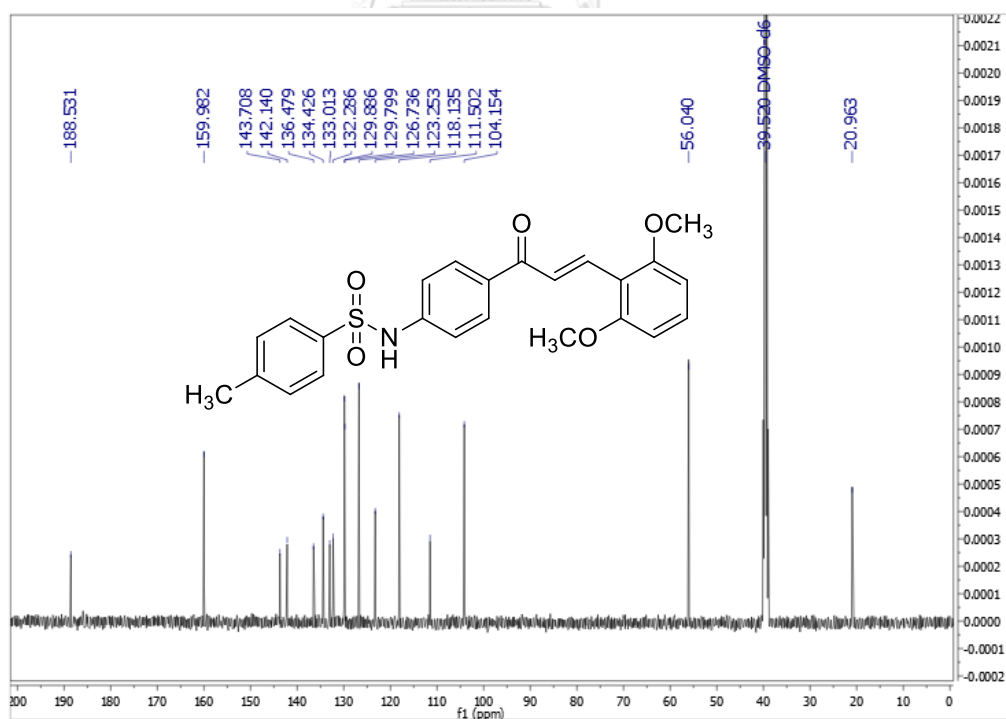


Figure A.48 The ^{13}C NMR spectrum (DMSO- d_6 , 125 MHz) of 80

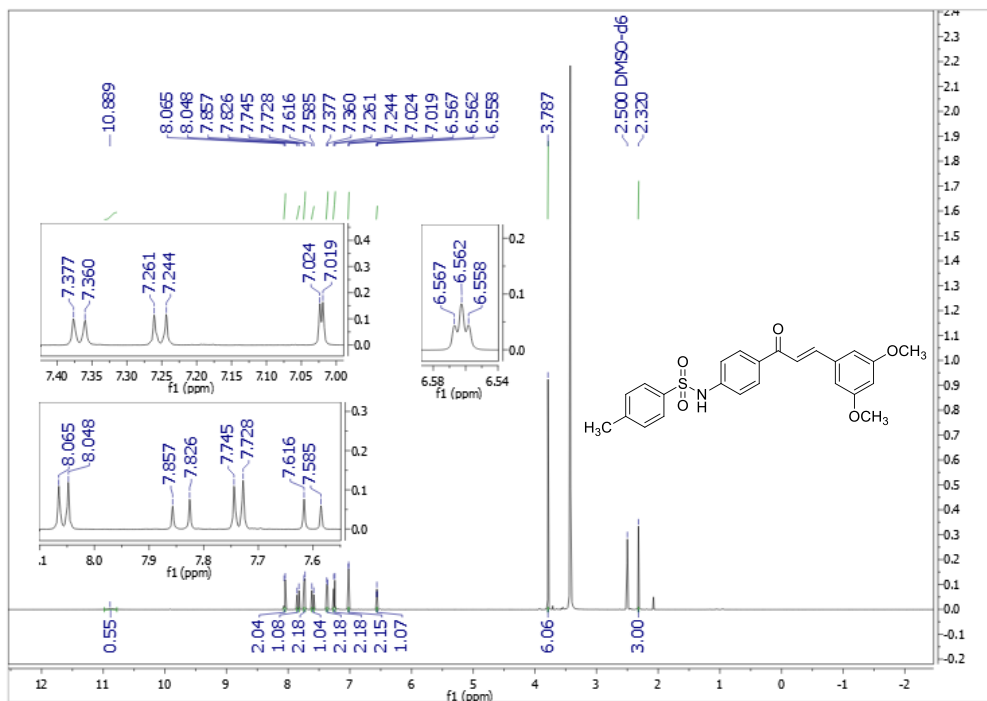


Figure A.49 The ^1H NMR spectrum (DMSO- d_6 , 500 MHz) of **81**

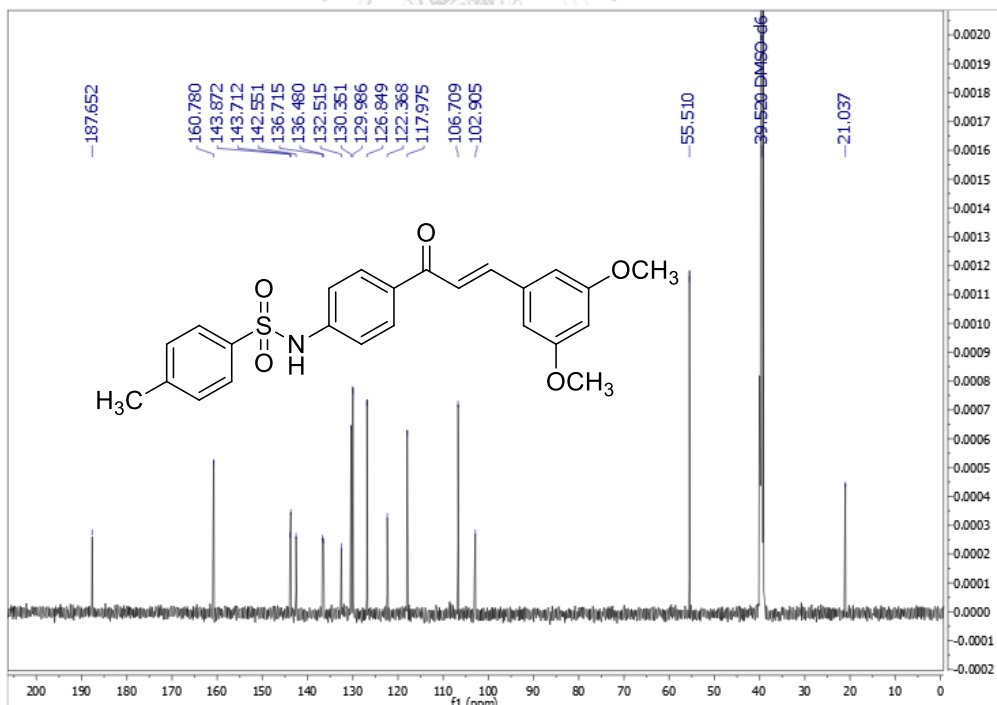


Figure A.50 The ^{13}C NMR spectrum (DMSO- d_6 , 125 MHz) of **81**

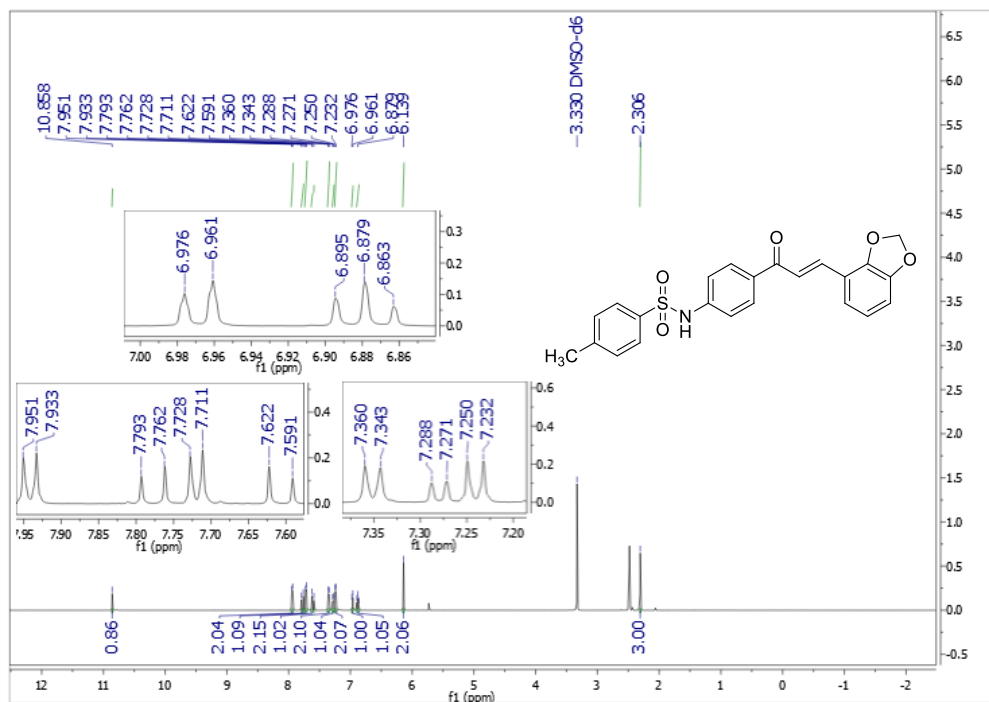


Figure A.51 The ^1H NMR spectrum (DMSO- d_6 , 500 MHz) of 82

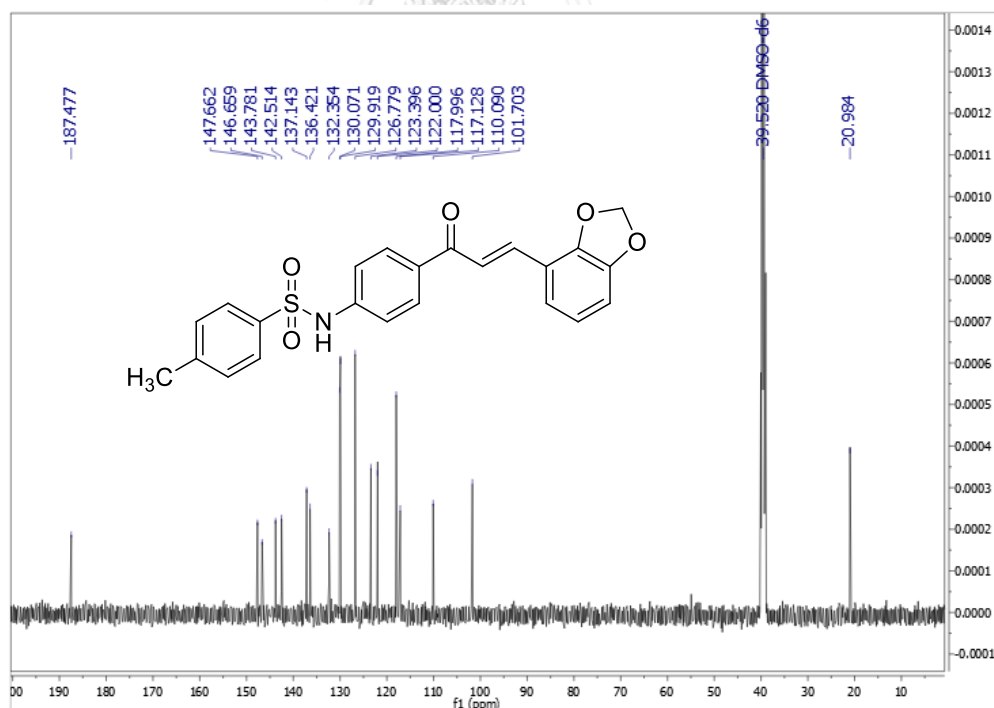


Figure A.52 The ^{13}C NMR spectrum (DMSO- d_6 , 125 MHz) of 82

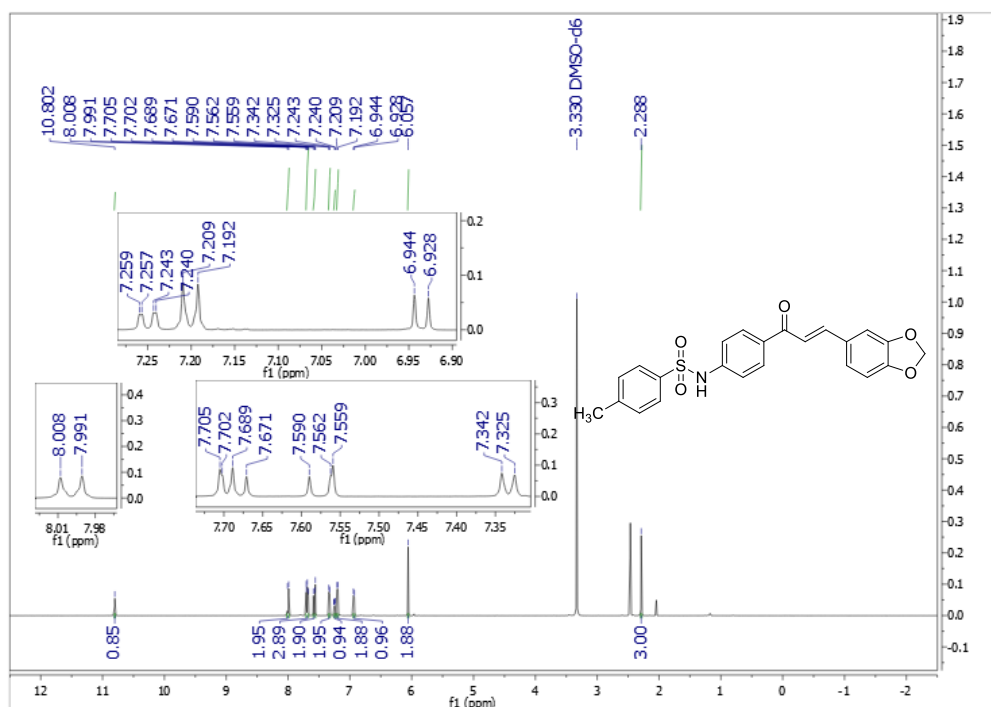


Figure A.53 The ^1H NMR spectrum ($\text{DMSO-}d_6$, 500 MHz) of **83**

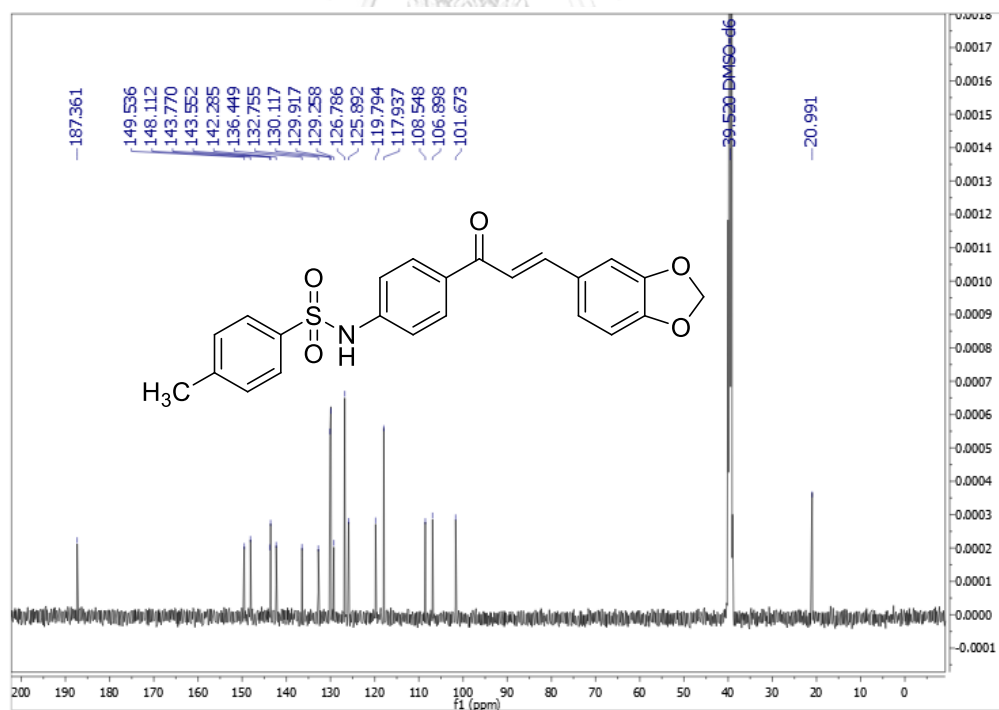


Figure A.54 The ^{13}C NMR spectrum ($\text{DMSO-}d_6$, 125 MHz) of **83**

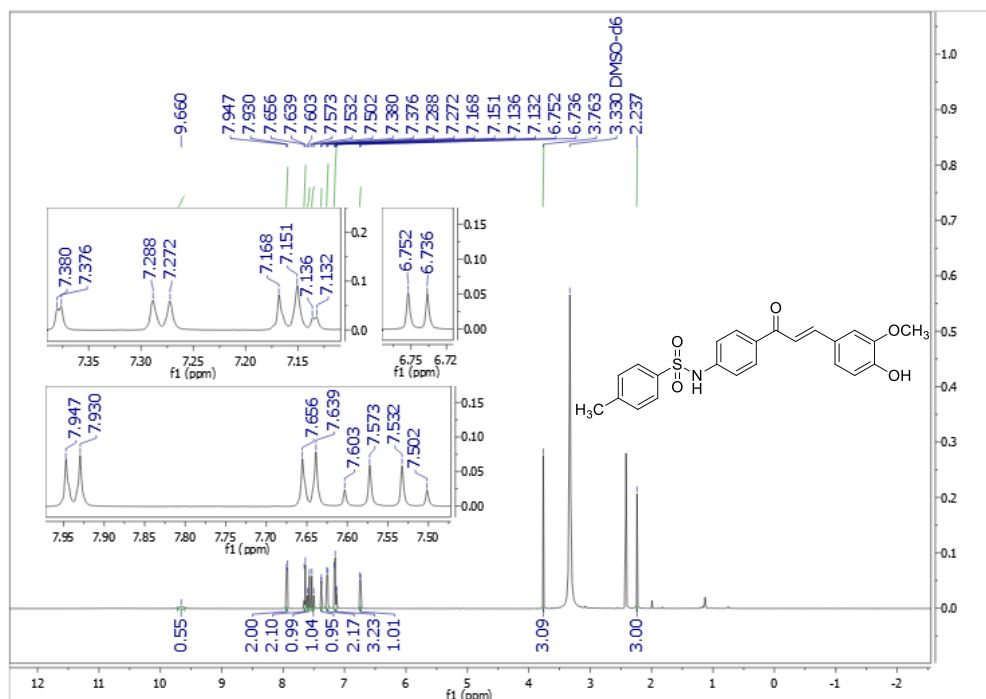


Figure A.55 The ^1H NMR spectrum (DMSO- d_6 , 500 MHz) of **84**

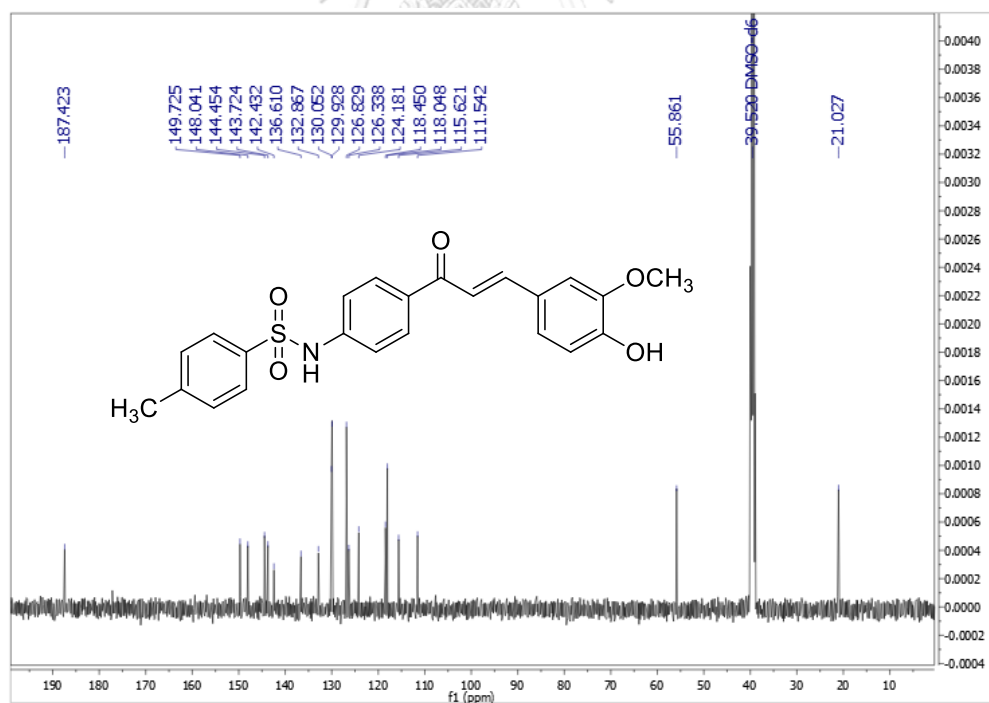


Figure A.56 The ^{13}C NMR spectrum (DMSO- d_6 , 125 MHz) of **84**

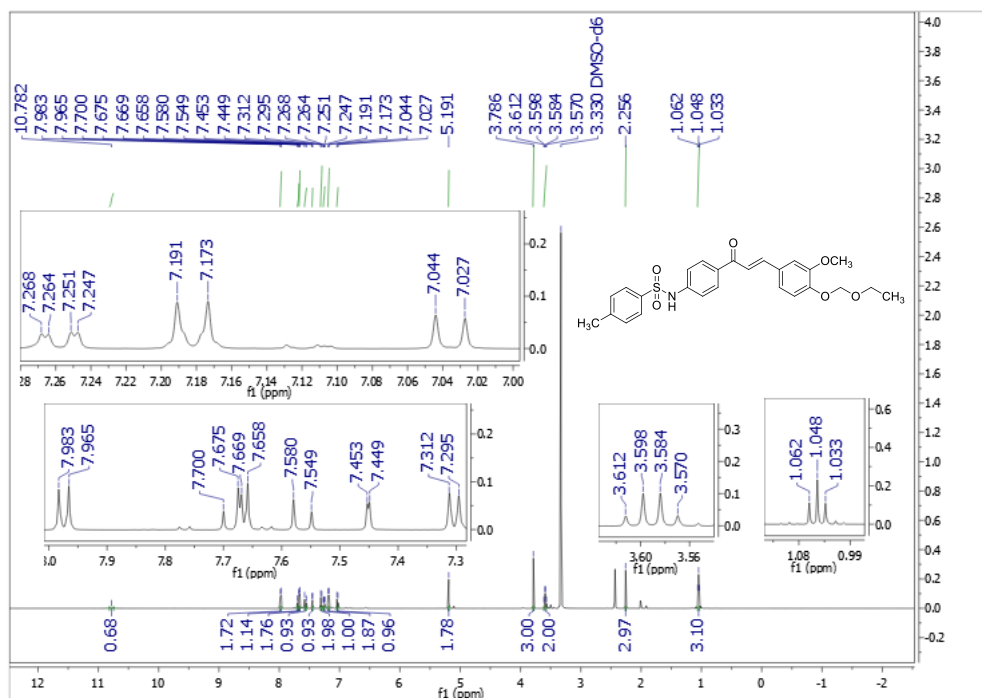


Figure A.57 The ^1H NMR spectrum (DMSO- d_6 , 500 MHz) of **85**

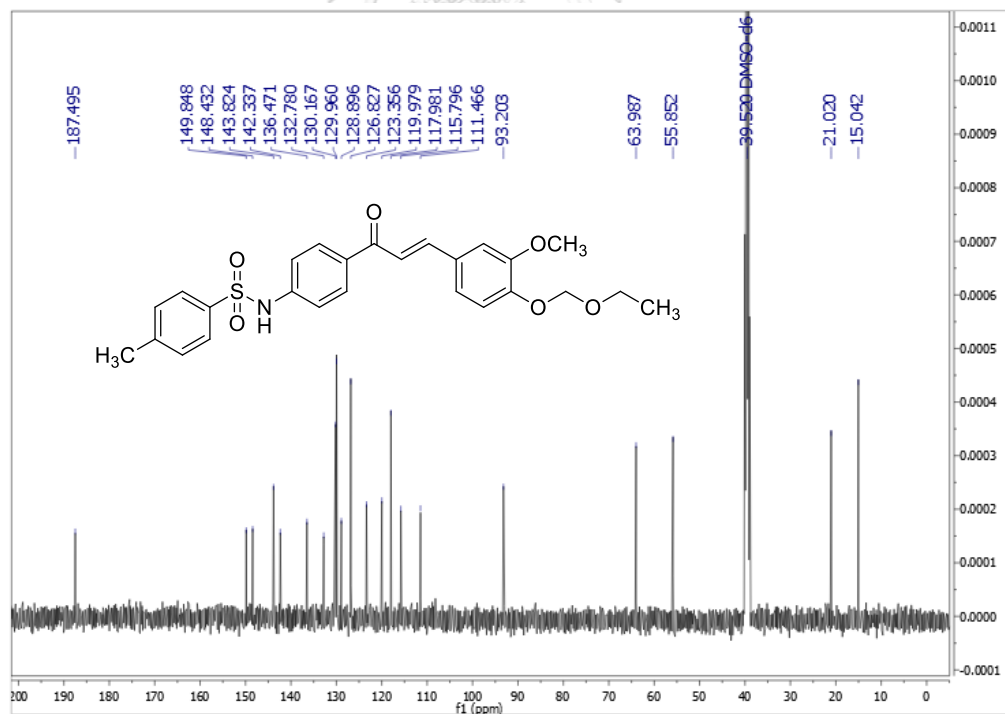


Figure A.58 The ^{13}C NMR spectrum (DMSO- d_6 , 125 MHz) of **85**

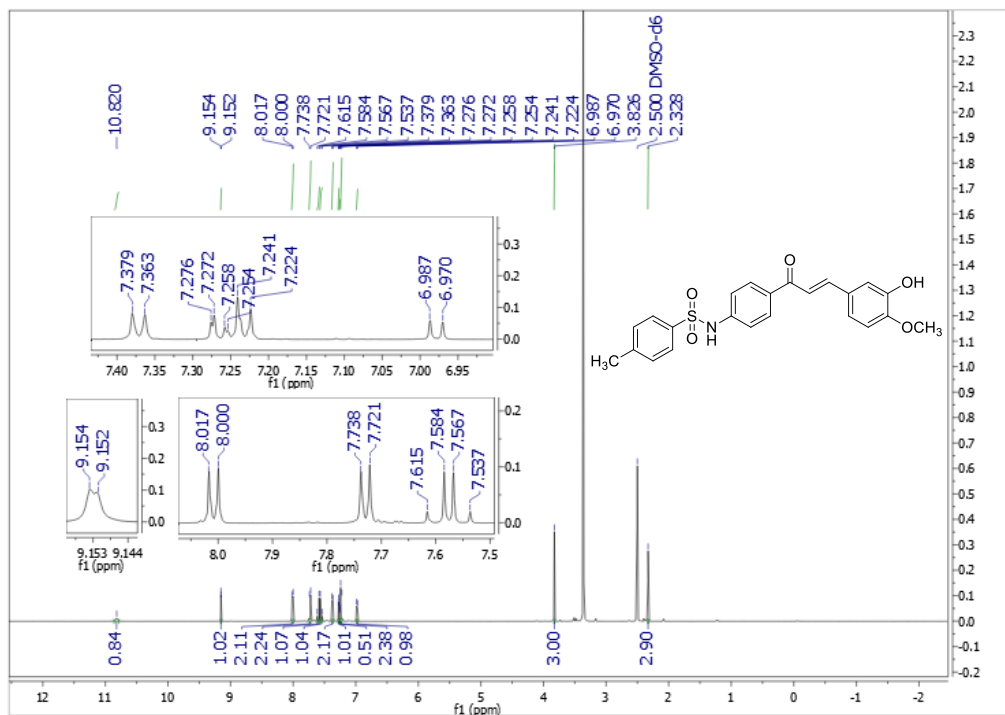


Figure A.59 The ¹H NMR spectrum (DMSO-*d*₆, 500 MHz) of **86**

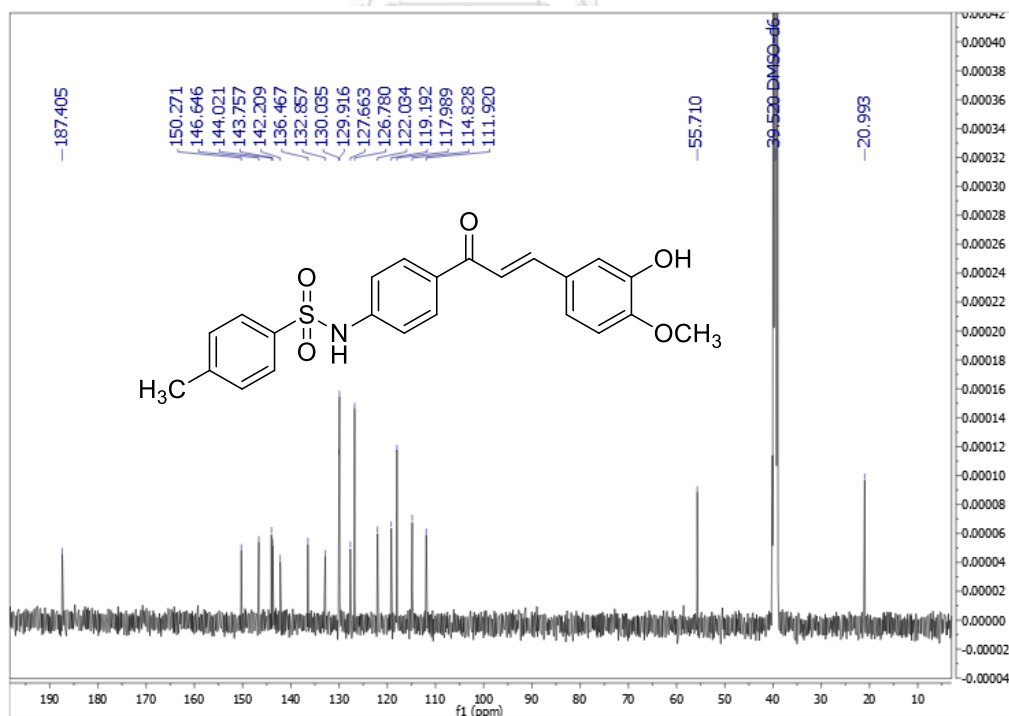


Figure A.60 The ¹³C NMR spectrum (DMSO-*d*₆, 125 MHz) of **86**

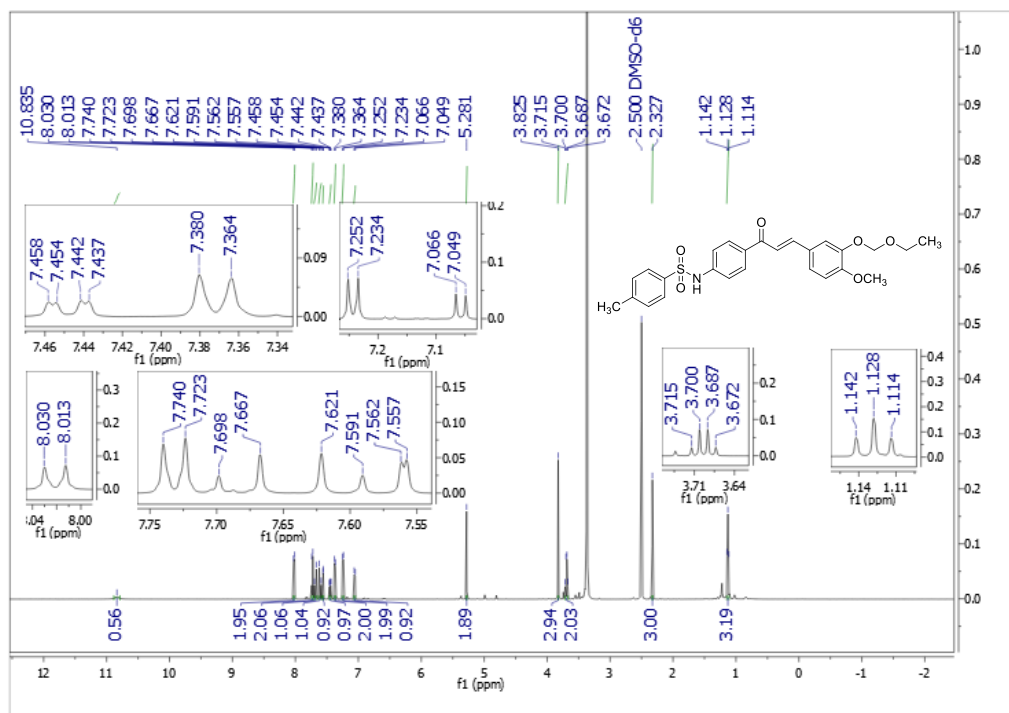


Figure A.61 The ^1H NMR spectrum (DMSO- d_6 , 500 MHz) of 87

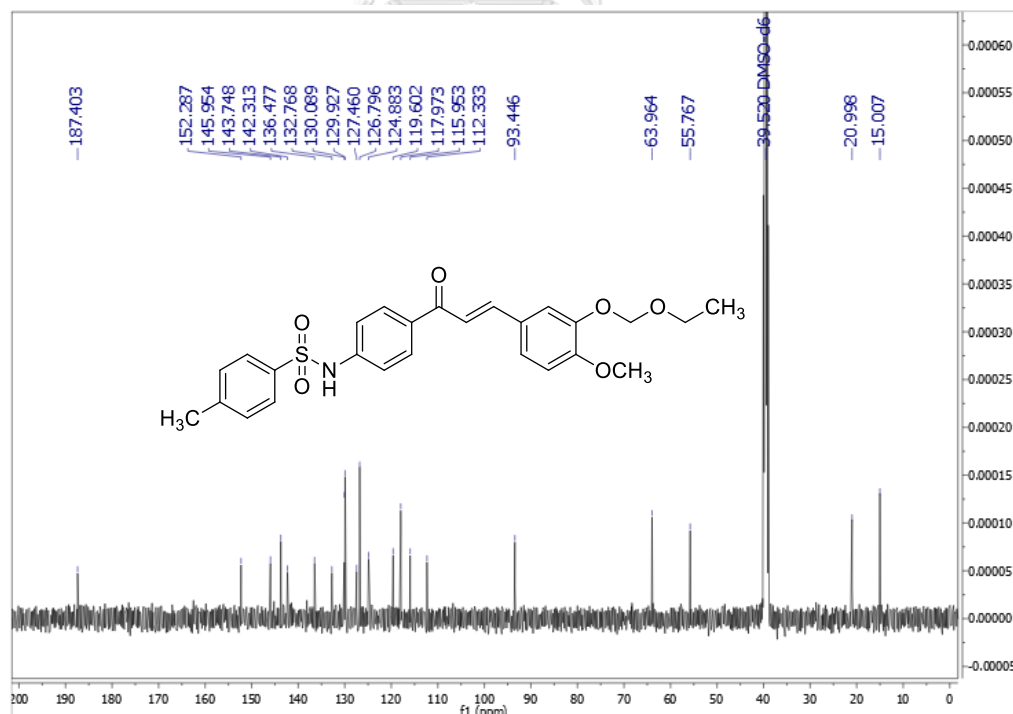


Figure A.62 The ^{13}C NMR spectrum (DMSO- d_6 , 125 MHz) of 87

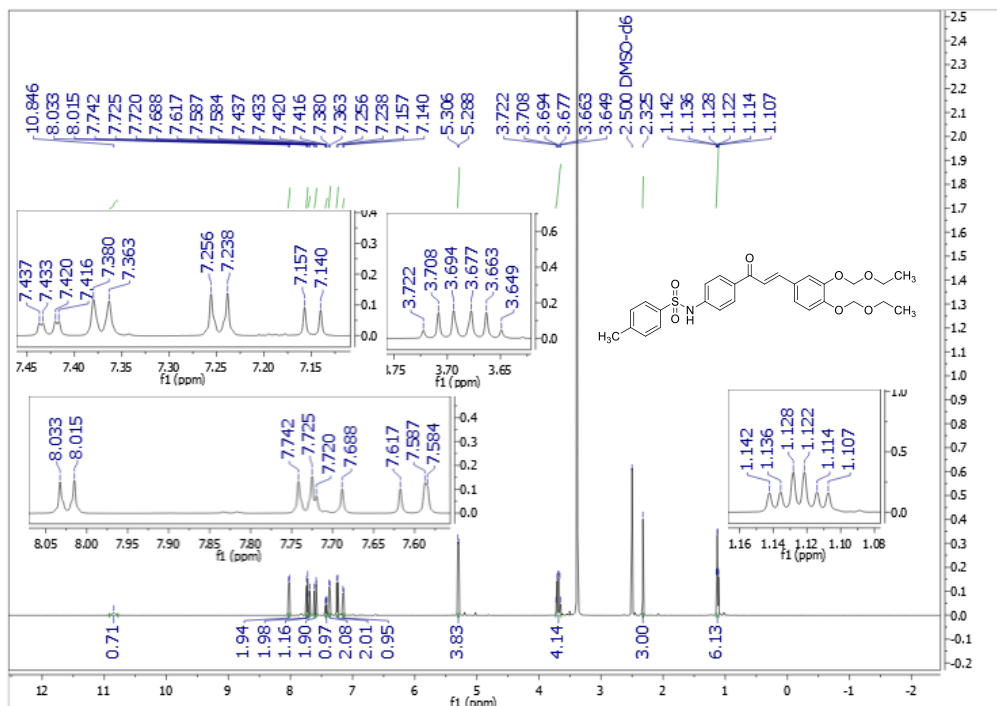


Figure A.63 The ¹H NMR spectrum (DMSO-*d*₆, 500 MHz) of 88

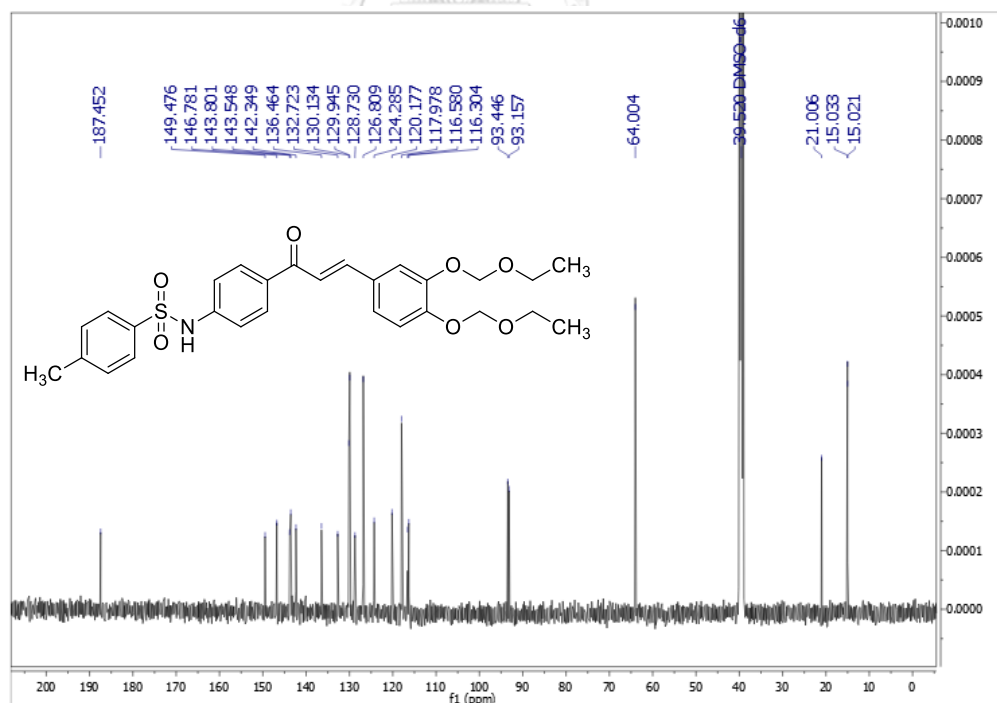


Figure A.64 The ¹³C NMR spectrum (DMSO-*d*₆, 125 MHz) of 88

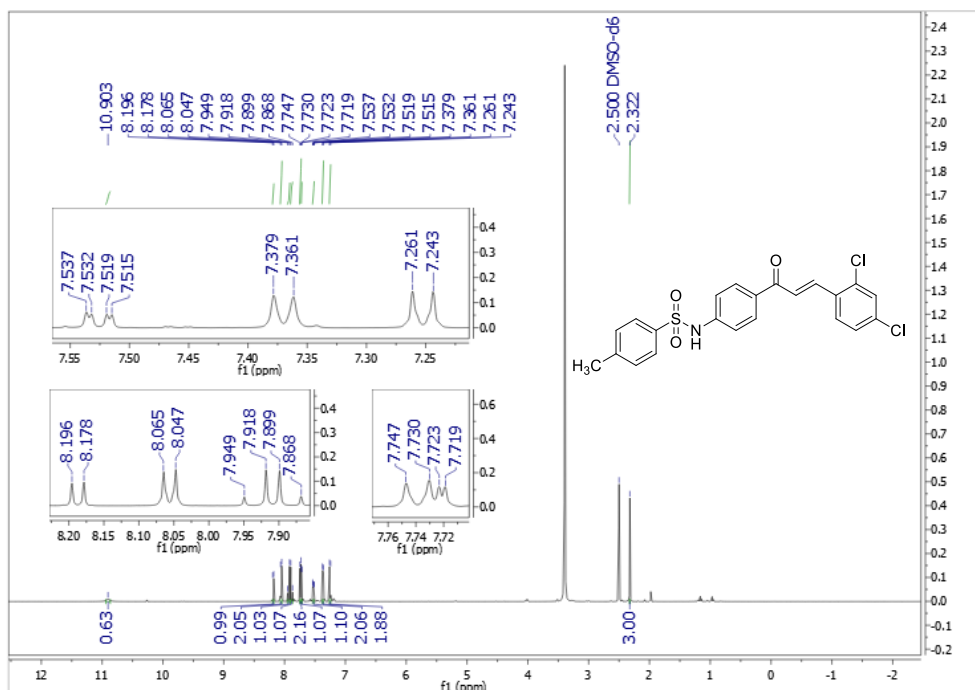


Figure A.65 The ^1H NMR spectrum (DMSO- d_6 , 500 MHz) of **89**

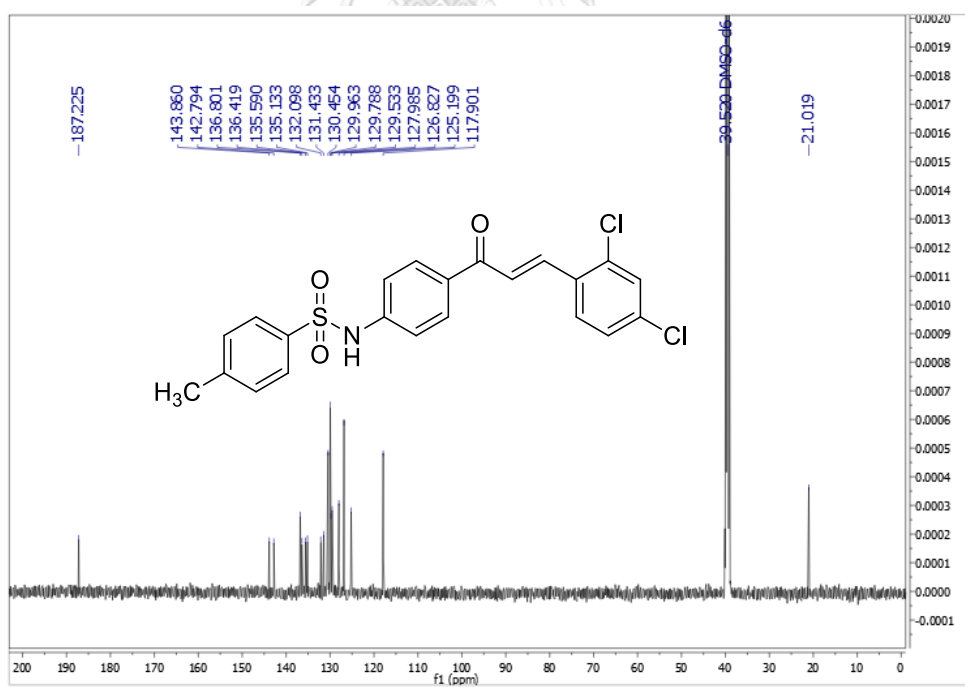


Figure A.66 The ^{13}C NMR spectrum (DMSO- d_6 , 125 MHz) of **89**

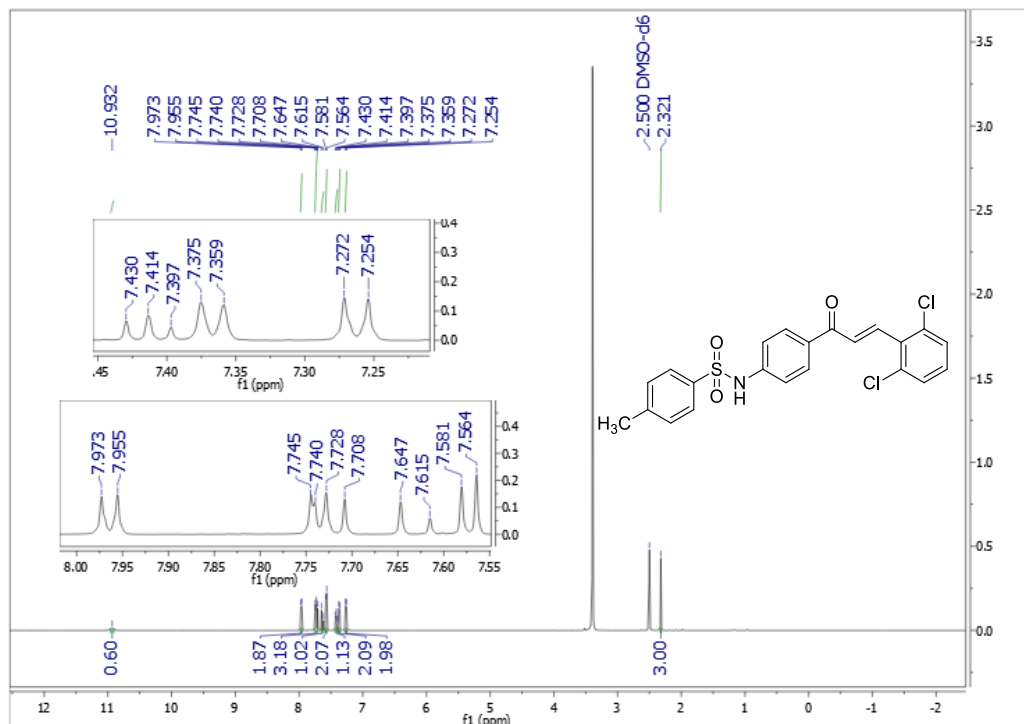


Figure A.67 The ^1H NMR spectrum (DMSO- d_6 , 500 MHz) of 90

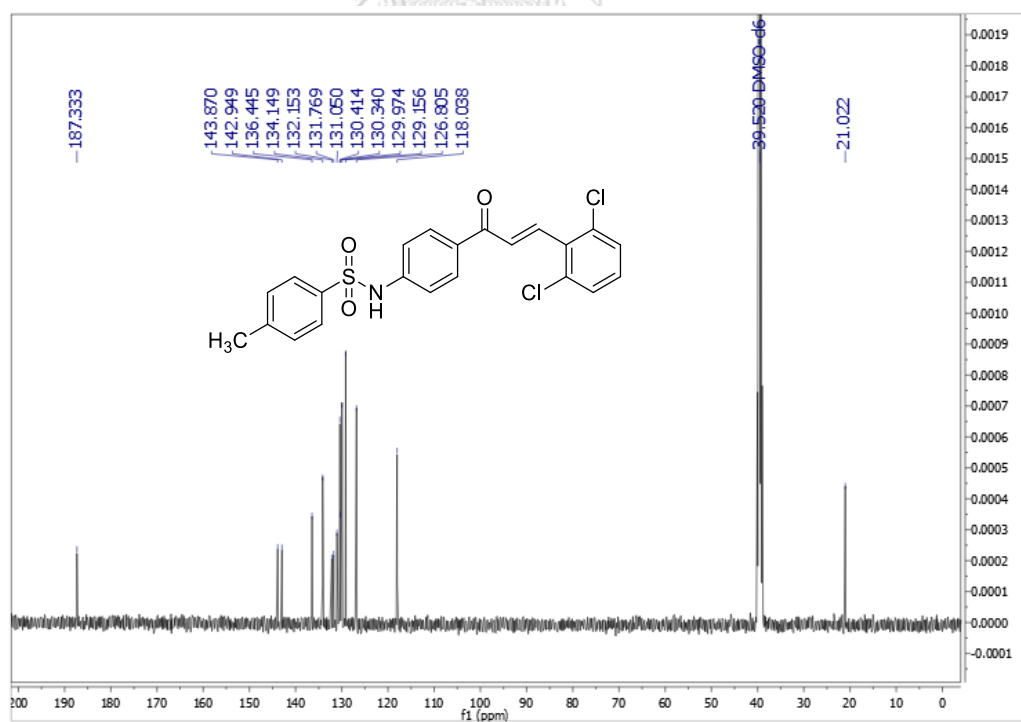


Figure A.68 The ^{13}C NMR spectrum (DMSO- d_6 , 125 MHz) of 90

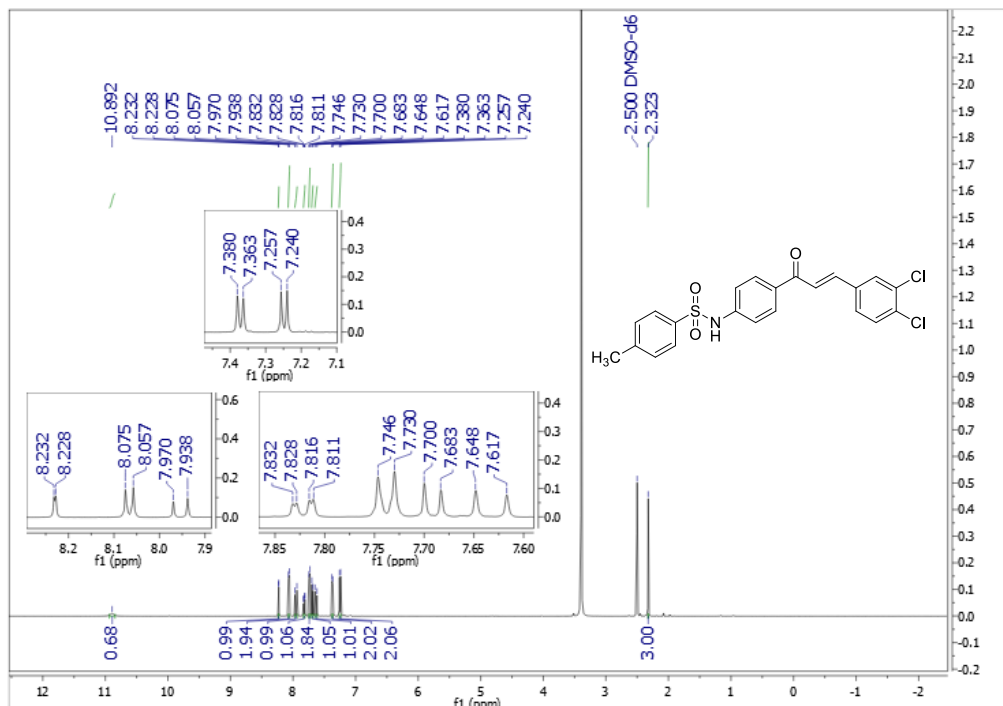


Figure A.69 The ¹H NMR spectrum (DMSO-*d*₆, 500 MHz) of **91**

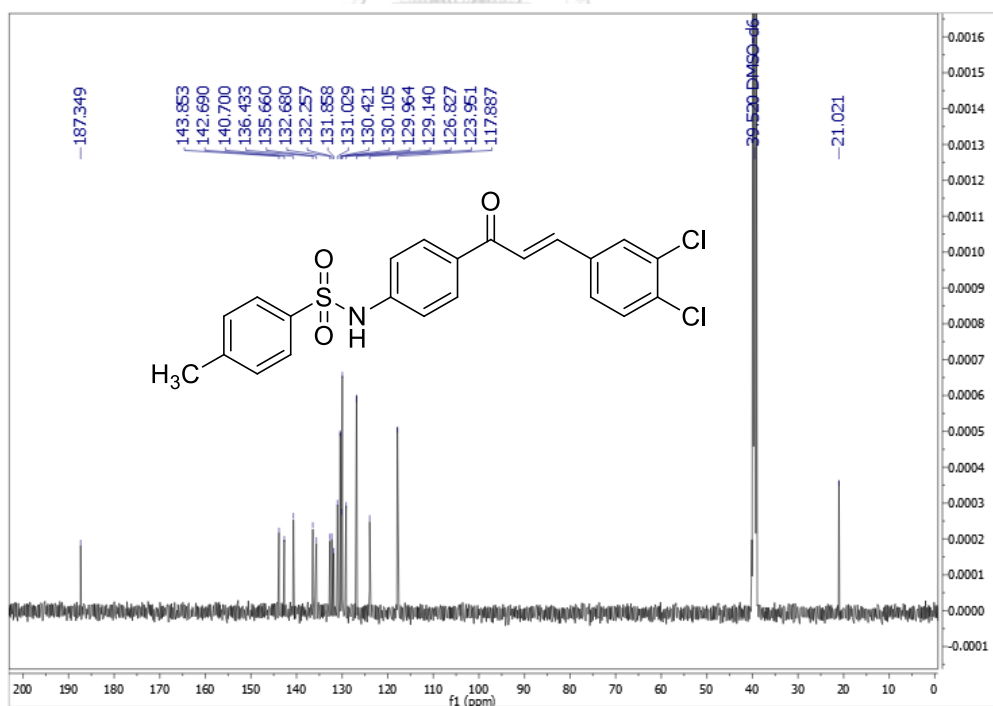


Figure A.70 The ¹³C NMR spectrum (DMSO-*d*₆, 125 MHz) of **91**

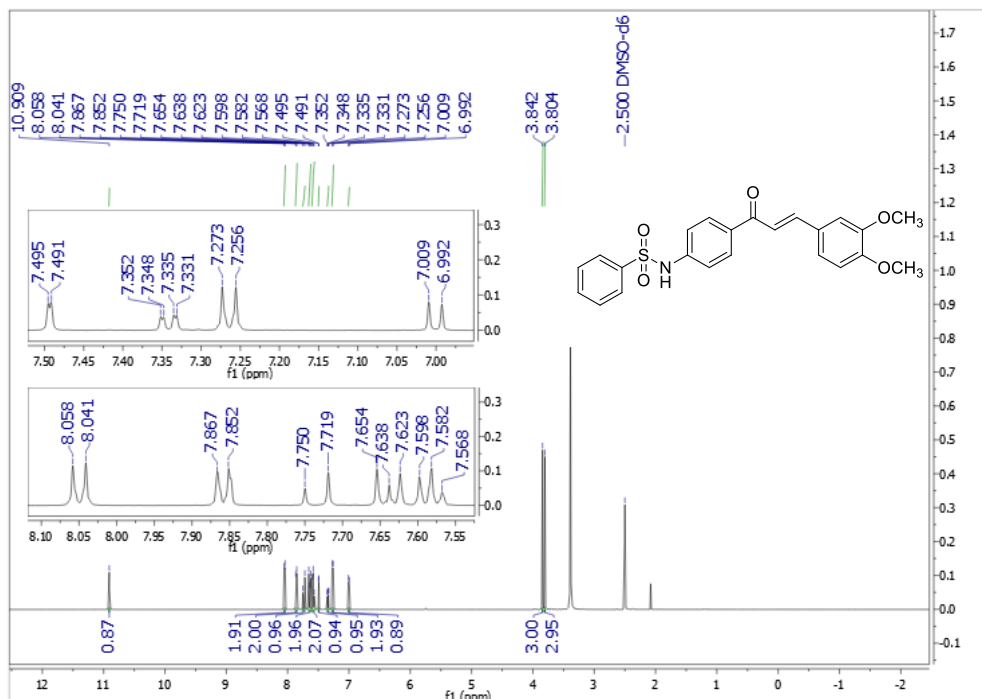


Figure A.71 The ^1H NMR spectrum (DMSO- d_6 , 500 MHz) of **92**

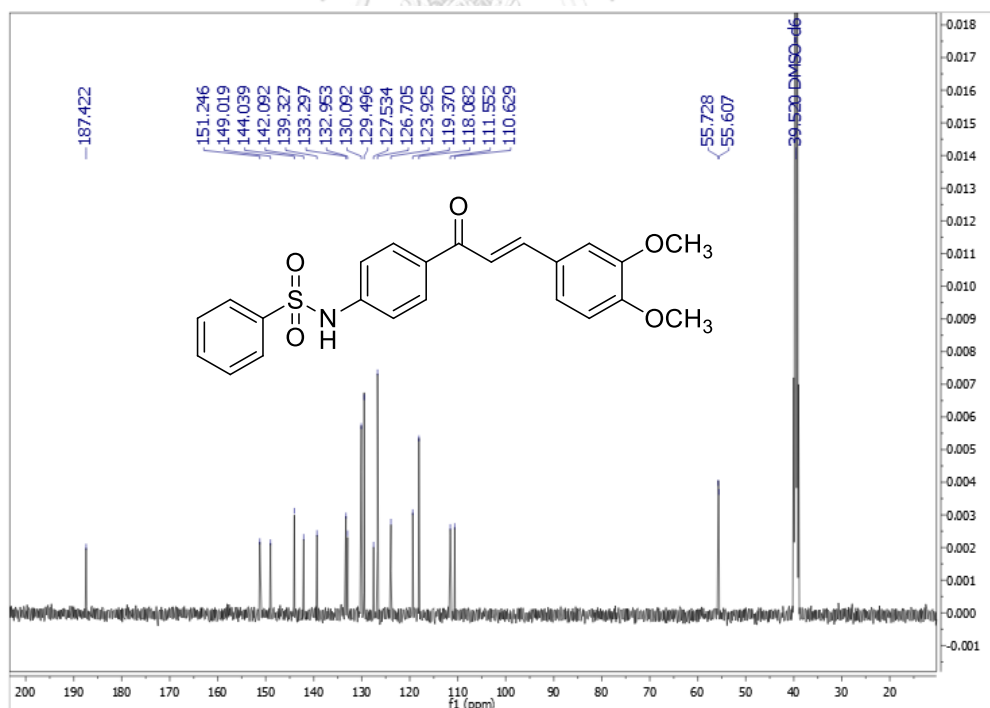


Figure A.72 The ^{13}C NMR spectrum (DMSO- d_6 , 125 MHz) of **92**

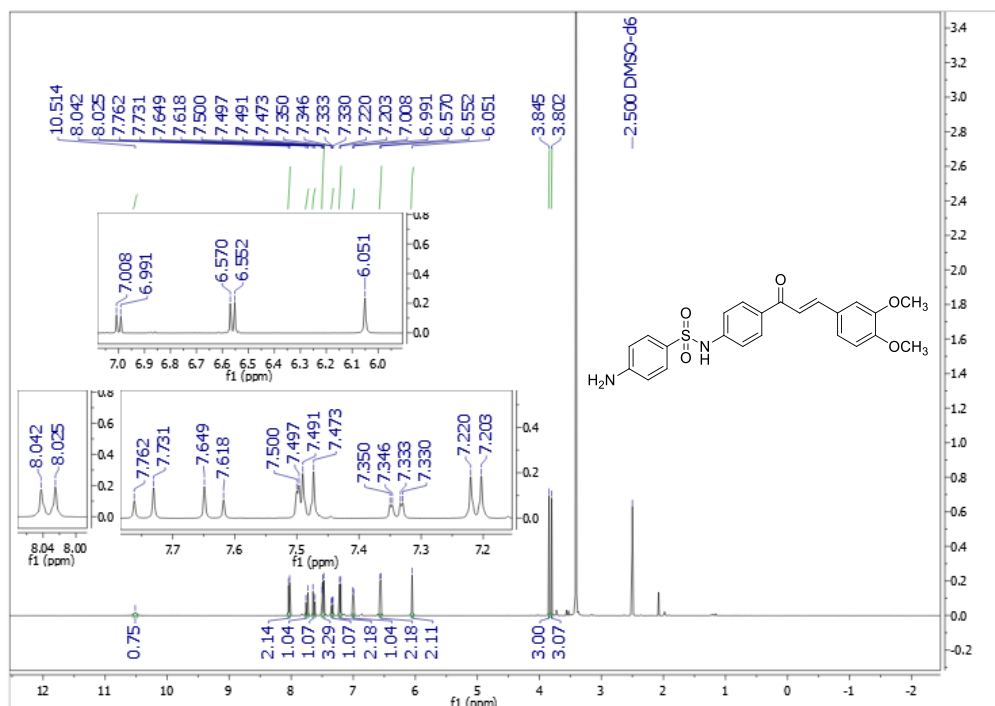


Figure A.73 The ¹H NMR spectrum (DMSO-*d*₆, 500 MHz) of **93**

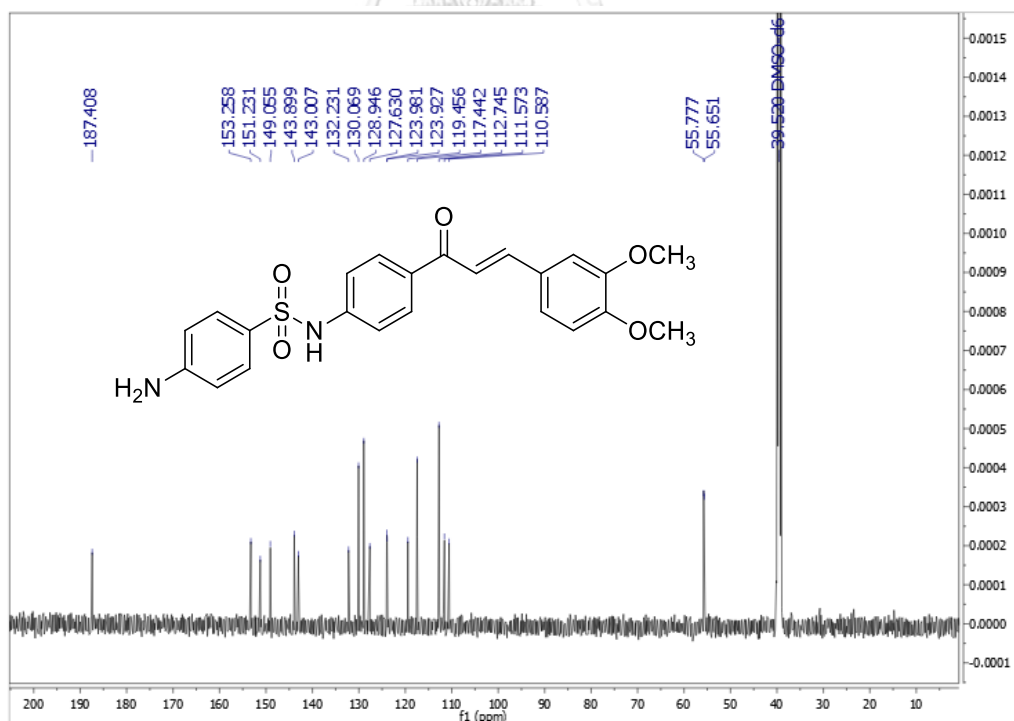


Figure A.74 The ¹³C NMR spectrum (DMSO-*d*₆, 125 MHz) of **93**

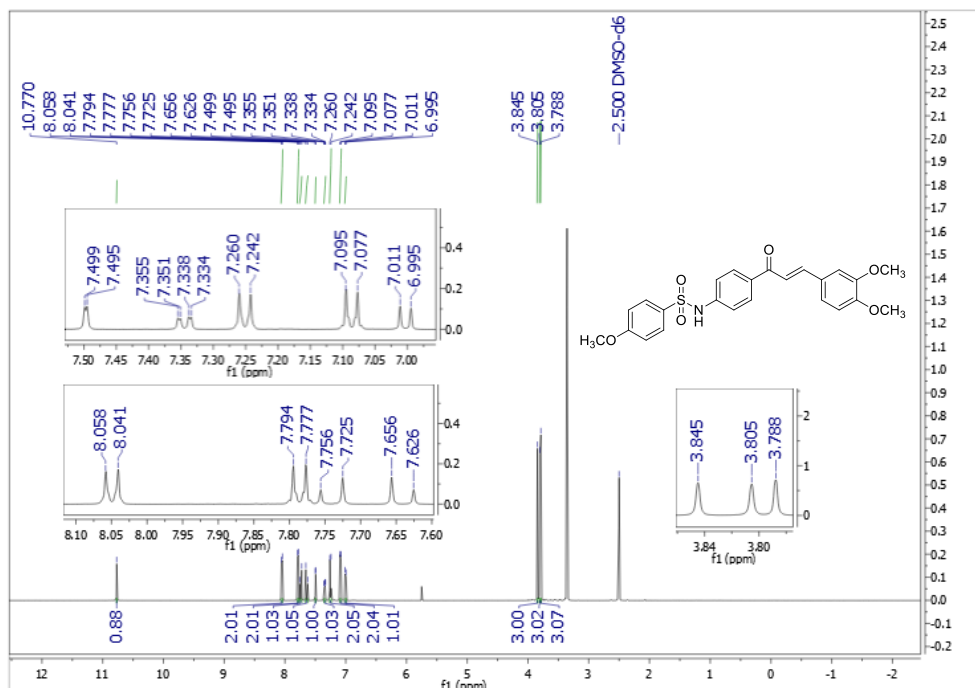


Figure A.75 The ^1H NMR spectrum (DMSO- d_6 , 500 MHz) of 94

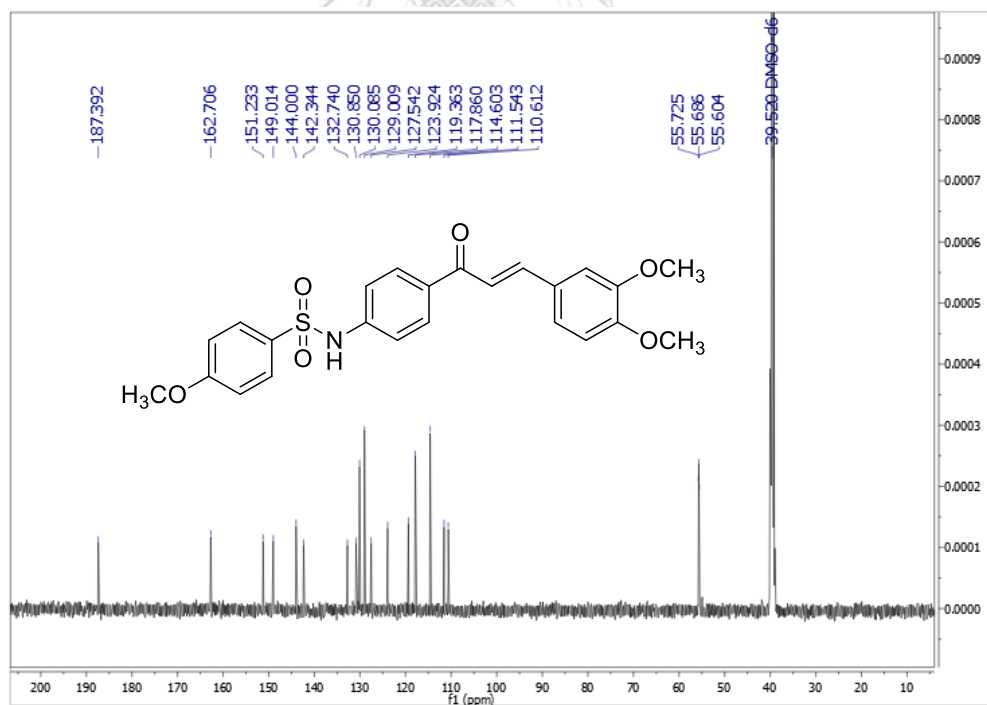


Figure A.76 The ^{13}C NMR spectrum (DMSO- d_6 , 125 MHz) of 94

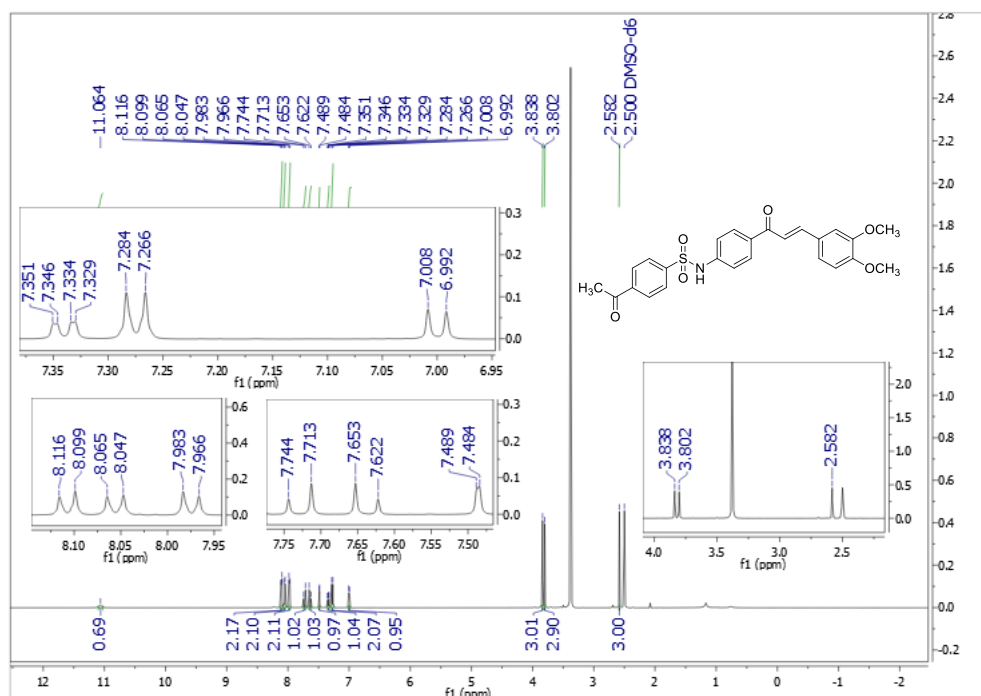


Figure A.77 The ^1H NMR spectrum (DMSO- d_6 , 500 MHz) of **95**

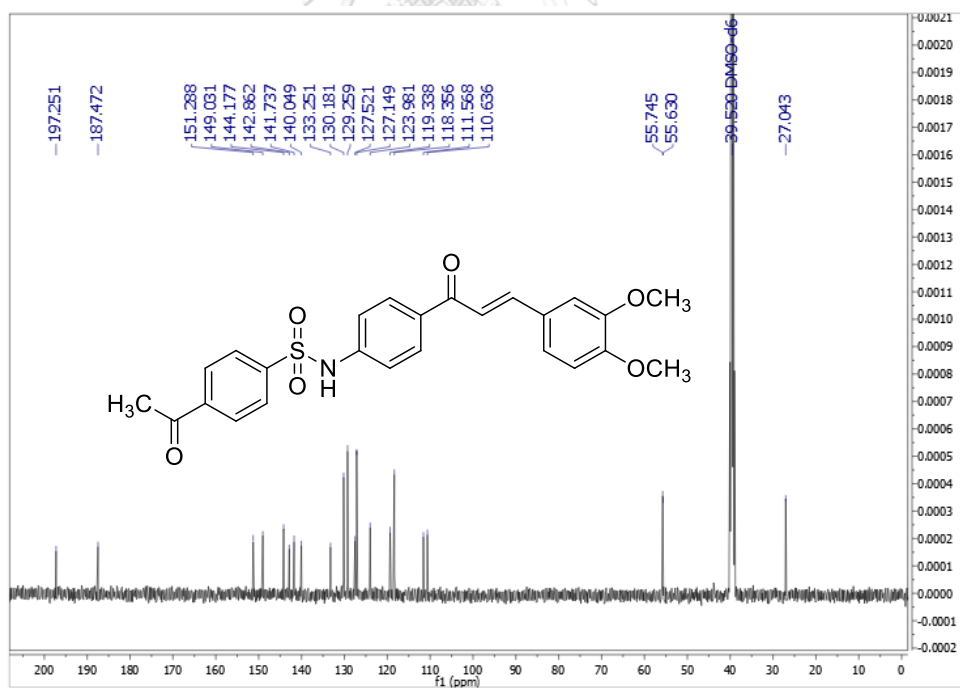


Figure A.78 The ^{13}C NMR spectrum (DMSO- d_6 , 125 MHz) of **95**

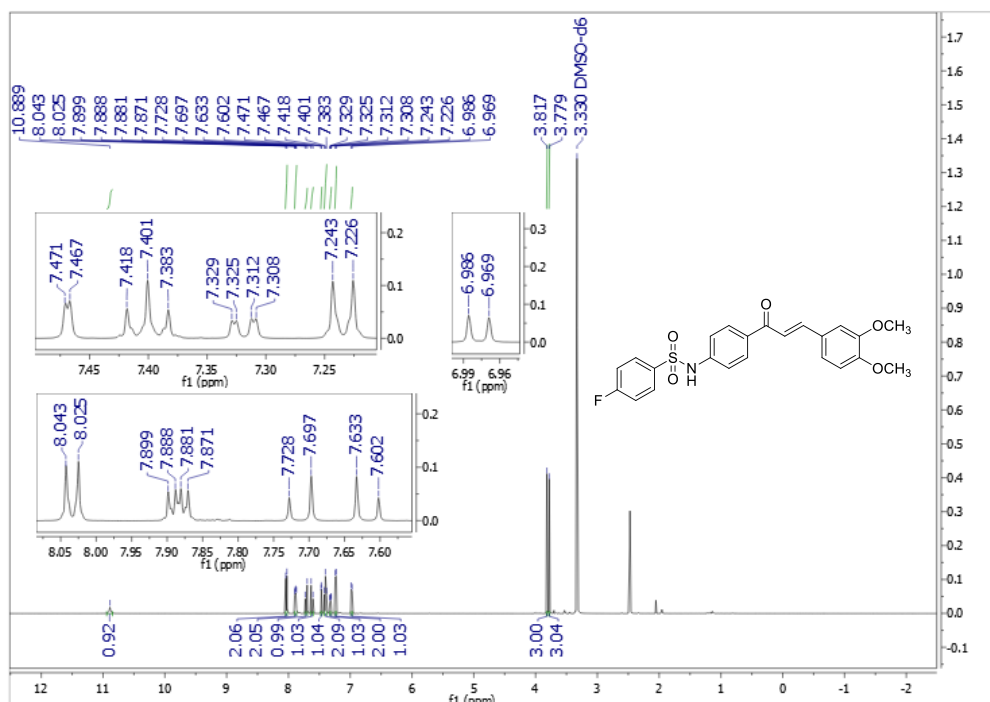


Figure A.79 The ¹H NMR spectrum (DMSO-*d*₆, 500 MHz) of **96**

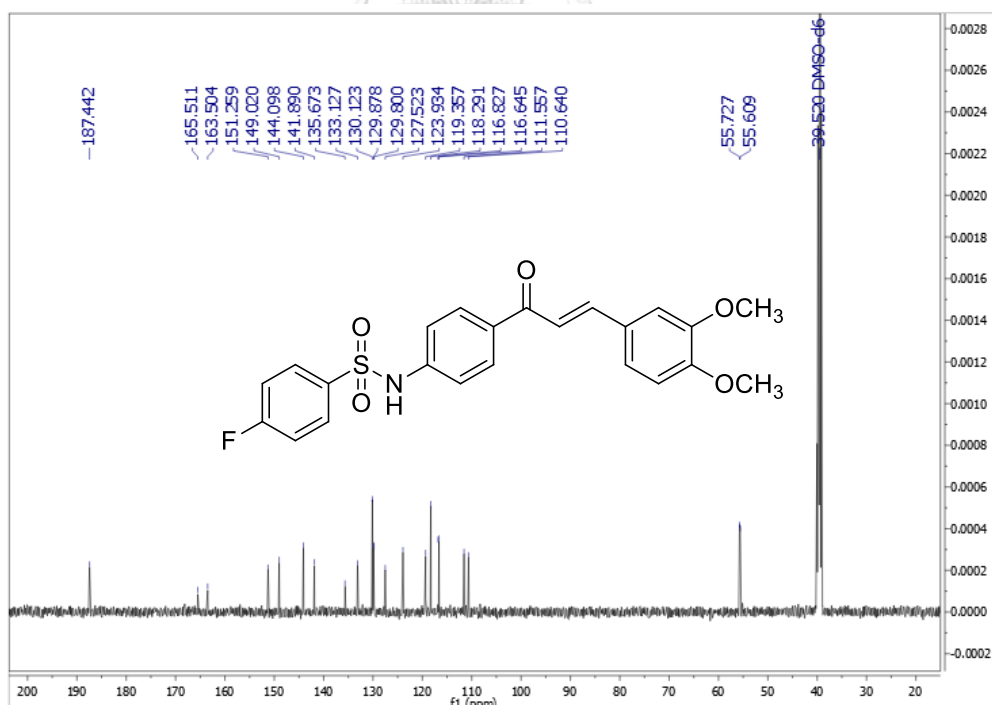


Figure A.80 The ¹³C NMR spectrum (DMSO-*d*₆, 125 MHz) of **96**

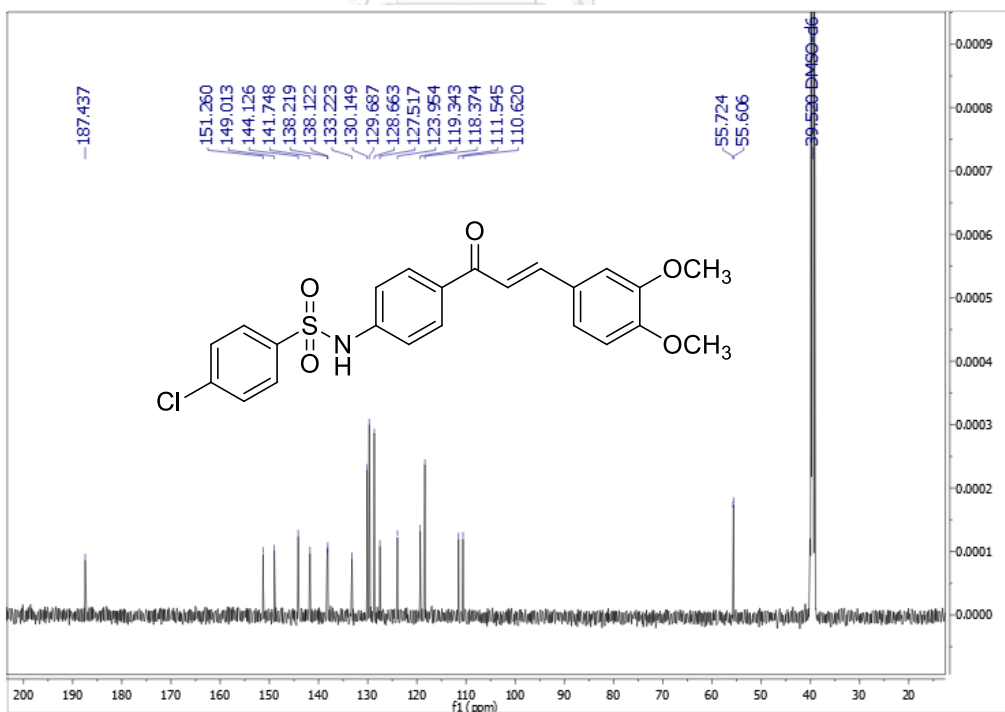
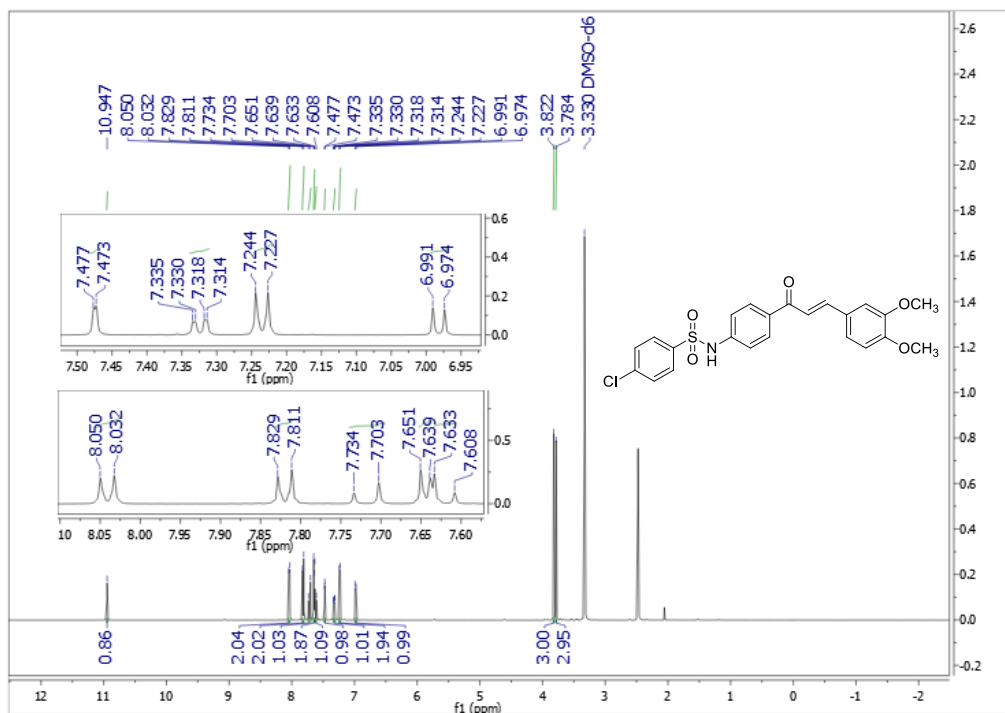


Figure A.82 The ^{13}C NMR spectrum (DMSO- d_6 , 125 MHz) of **97**

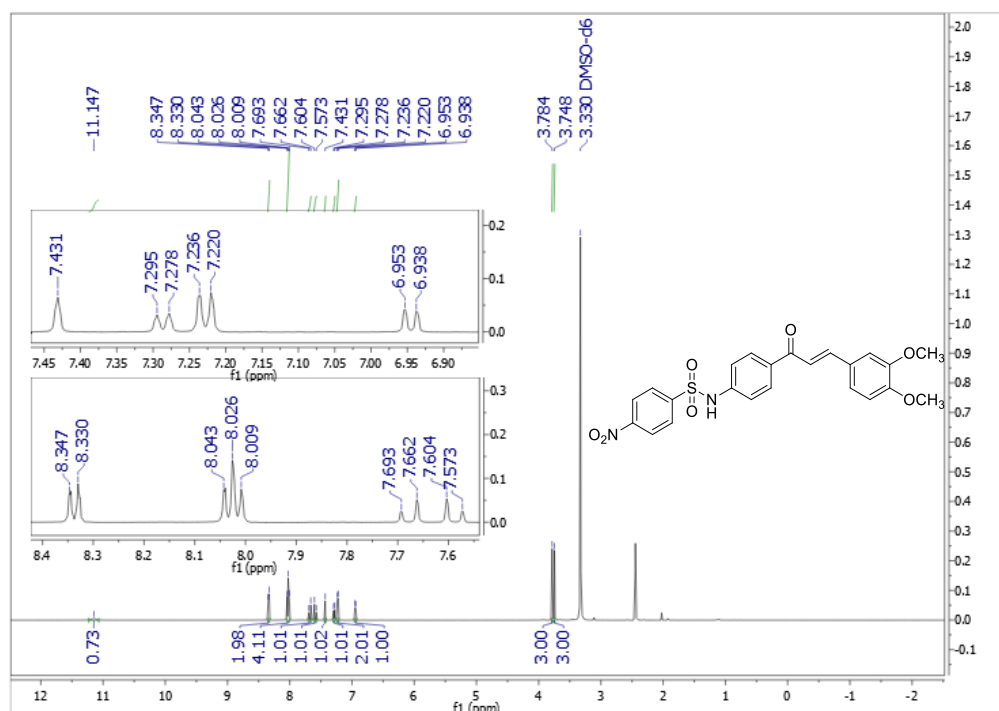


Figure A.83 The ¹H NMR spectrum (DMSO-d₆, 500 MHz) of **98**

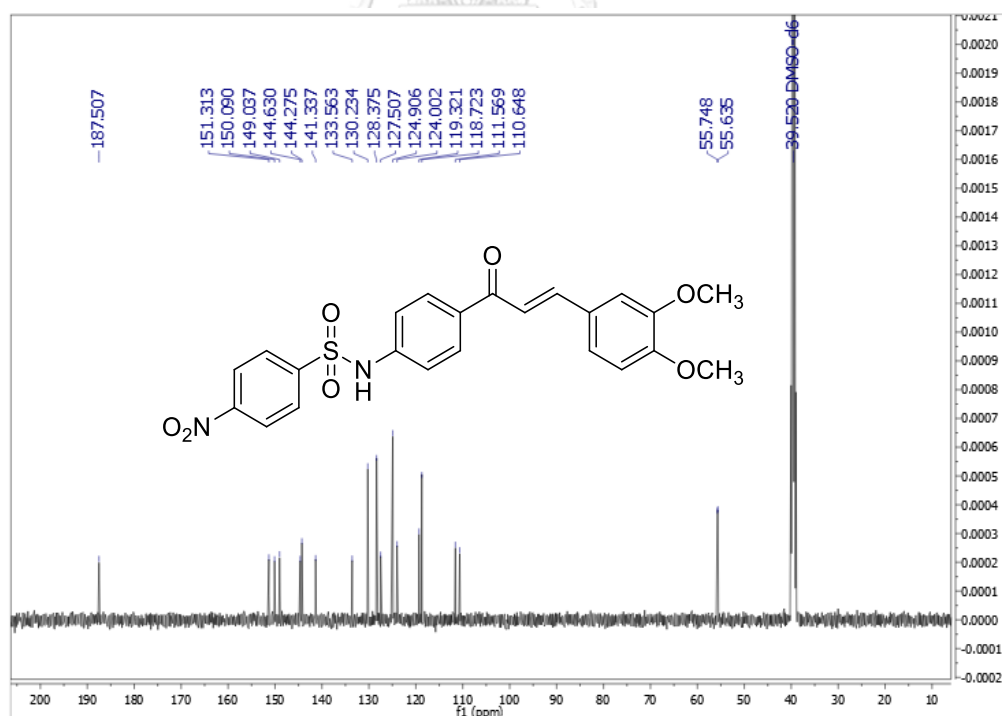


Figure A.84 The ¹³C NMR spectrum (DMSO-d₆, 125 MHz) of **98**

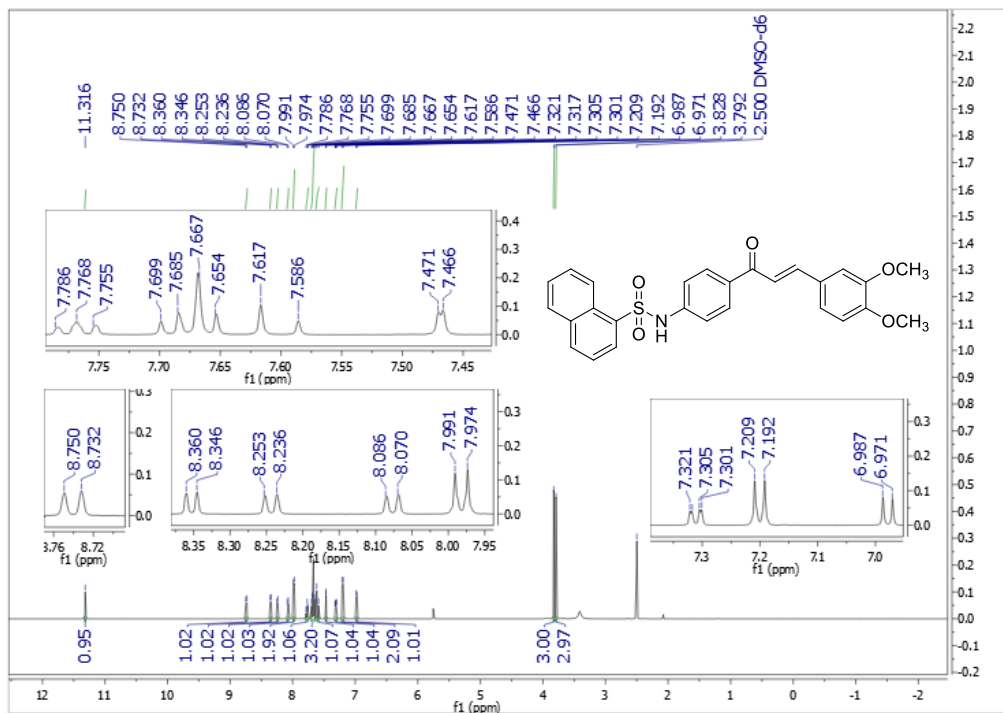


Figure A.85 The ^1H NMR spectrum (DMSO- d_6 , 500 MHz) of **99**

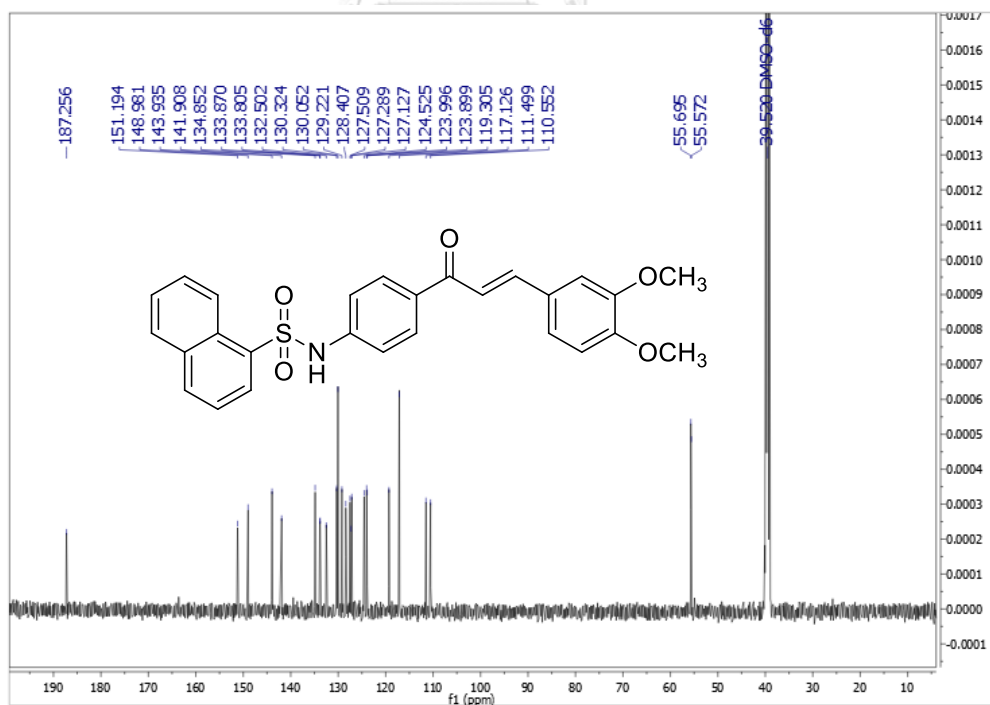


Figure A.86 The ^{13}C NMR spectrum (DMSO- d_6 , 125 MHz) of **99**

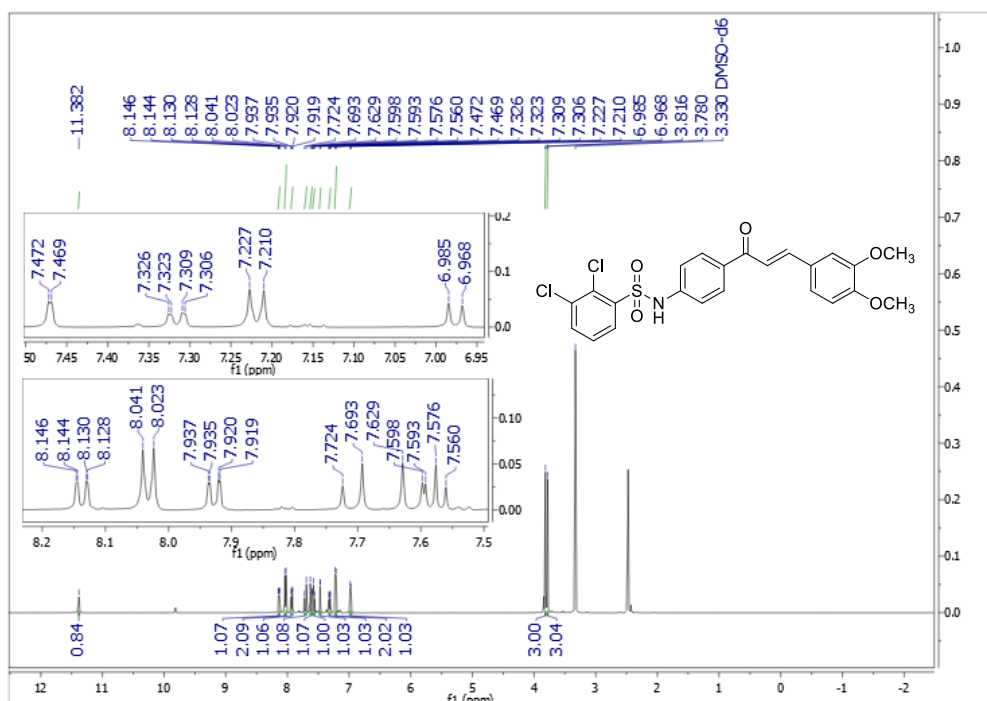


Figure A.87 The ^1H NMR spectrum (DMSO- d_6 , 500 MHz) of 100

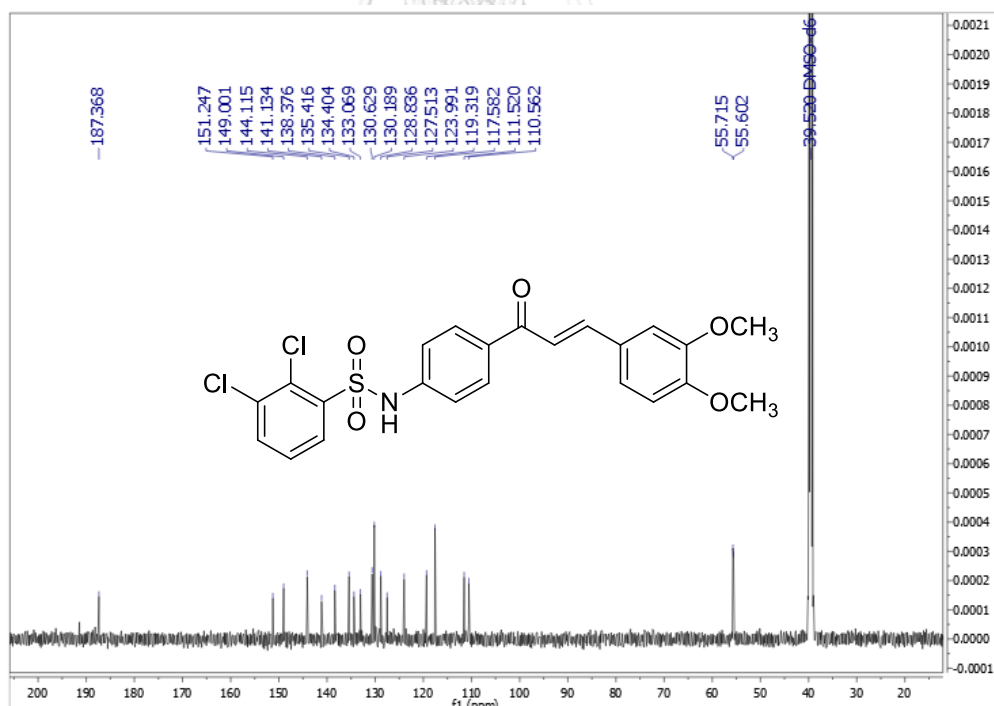


Figure A.88 The ^{13}C NMR spectrum (DMSO- d_6 , 125 MHz) of 100

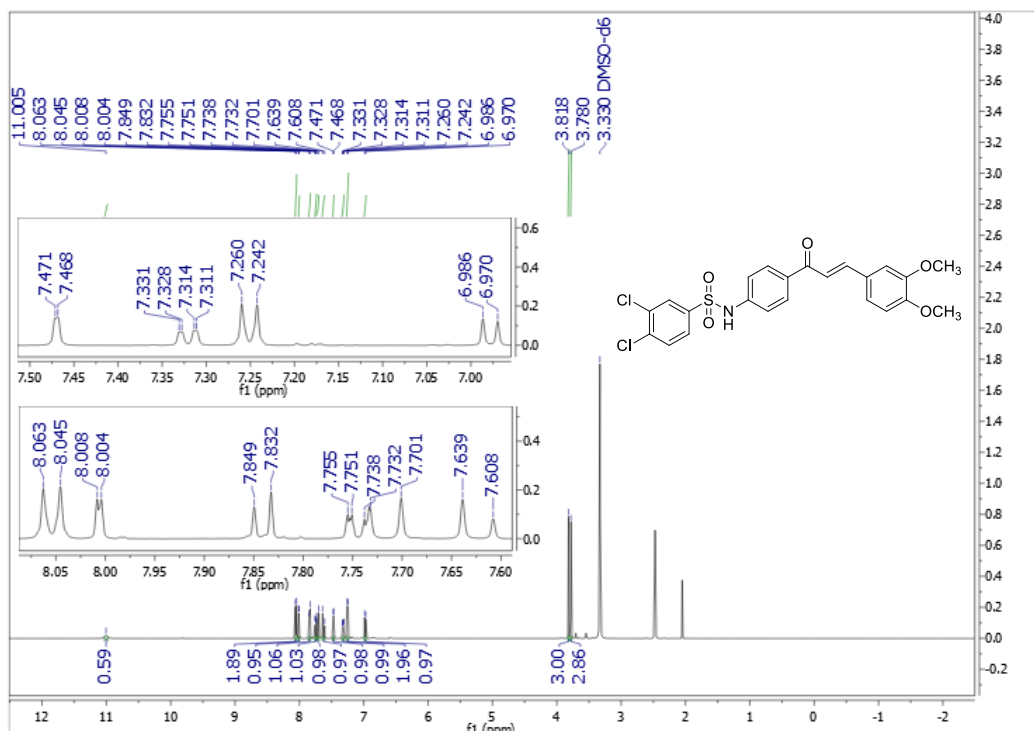


Figure A.89 The ^1H NMR spectrum (DMSO- d_6 , 500 MHz) of **101**

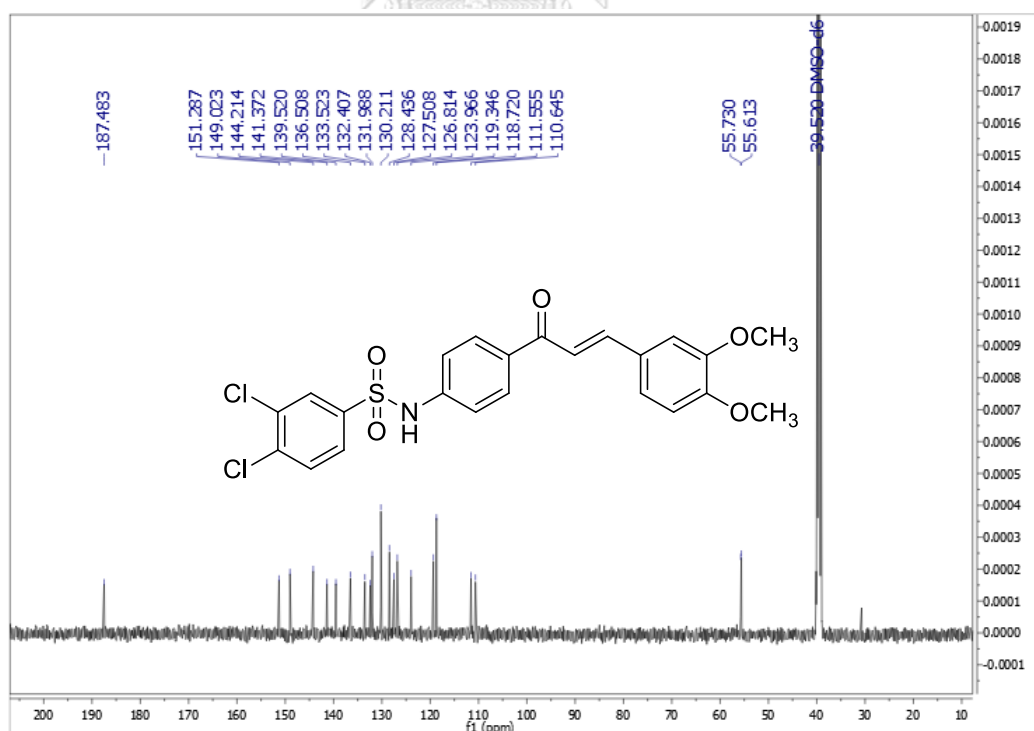


Figure A.90 The ^{13}C NMR spectrum (DMSO- d_6 , 125 MHz) of **101**

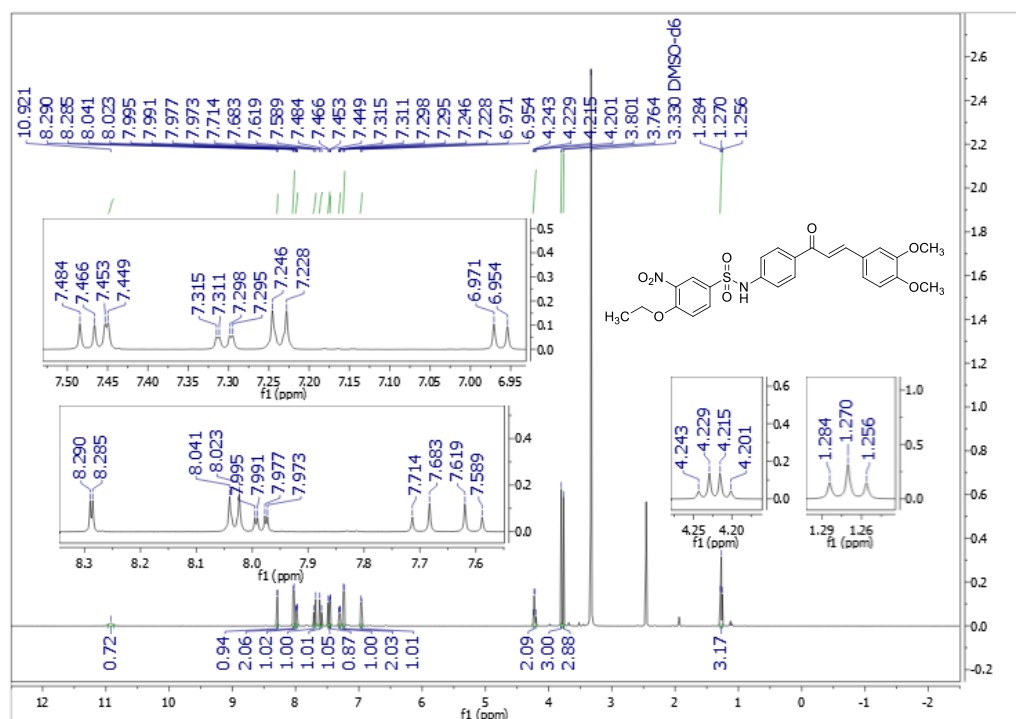


Figure A.93 The ¹H NMR spectrum (DMSO-d₆, 500 MHz) of 103

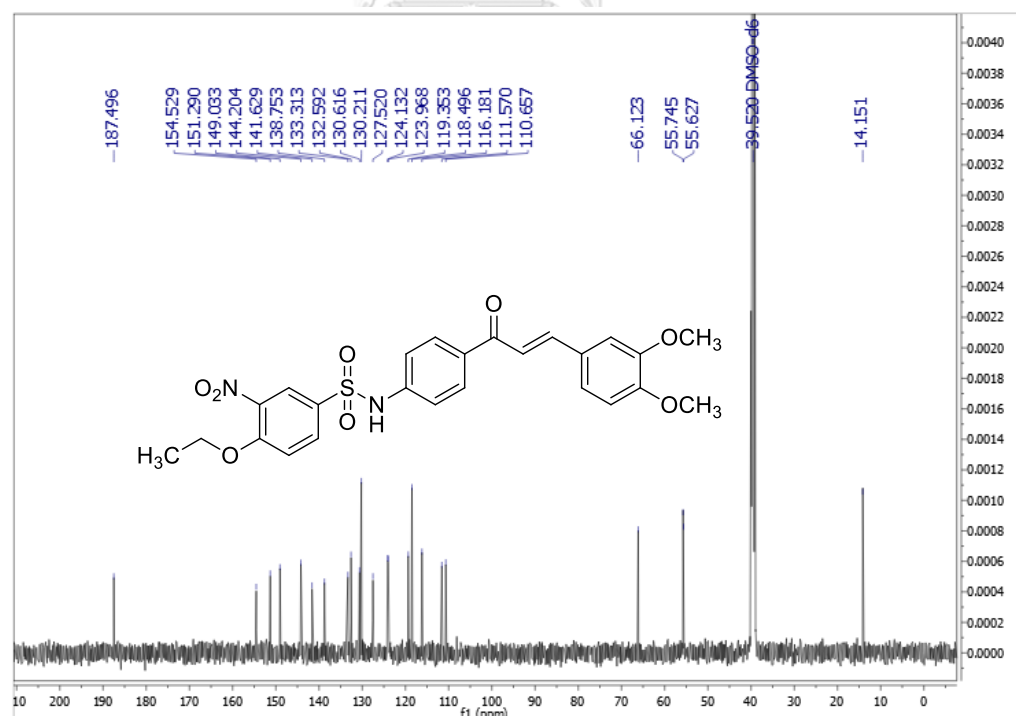
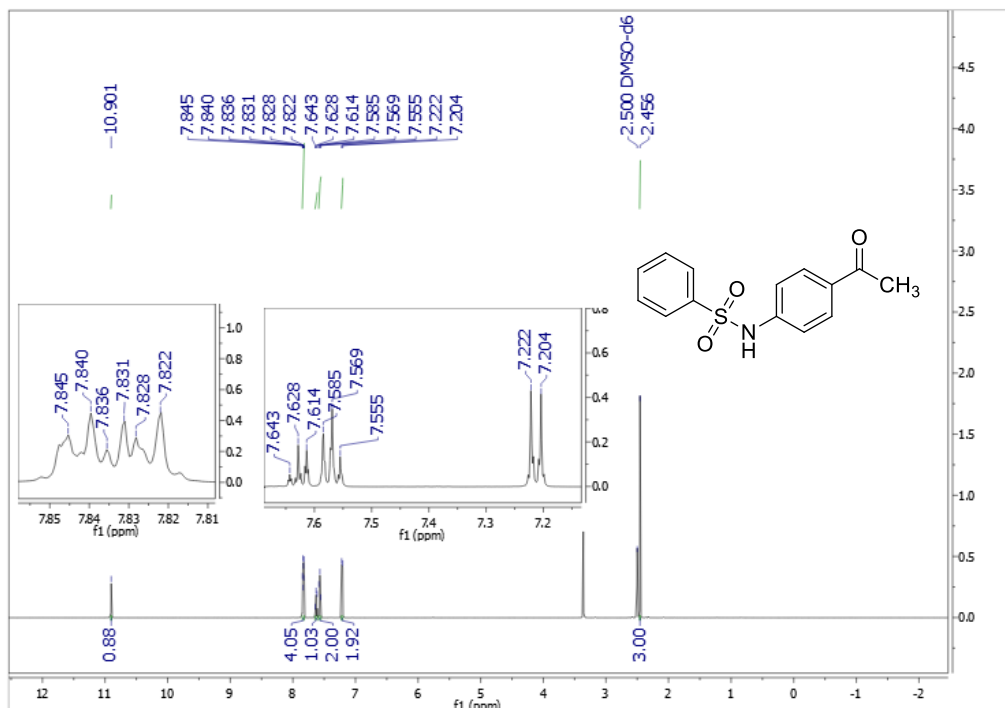
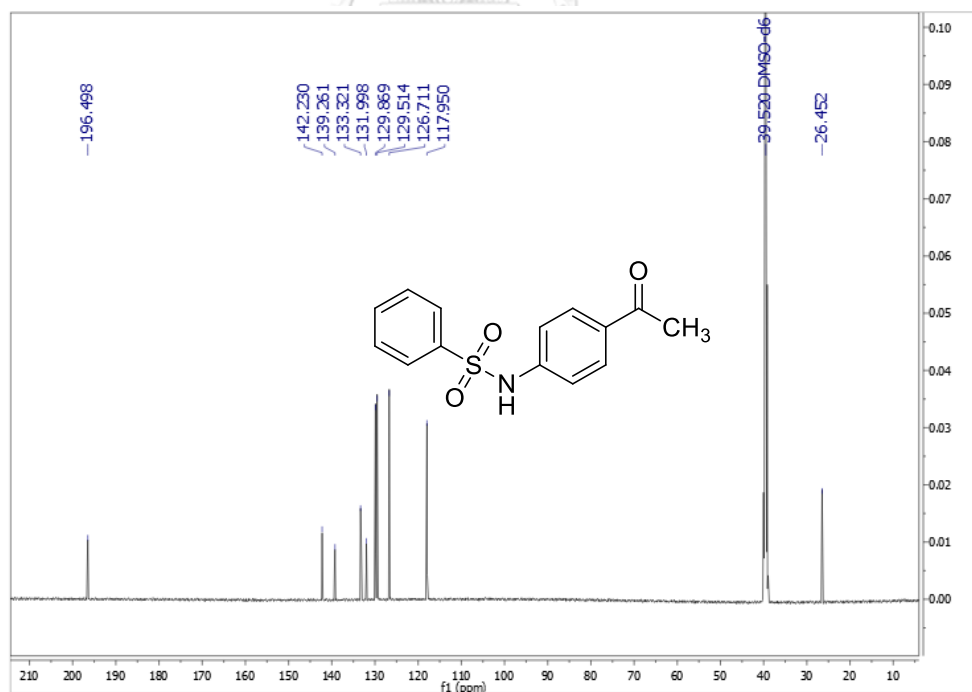
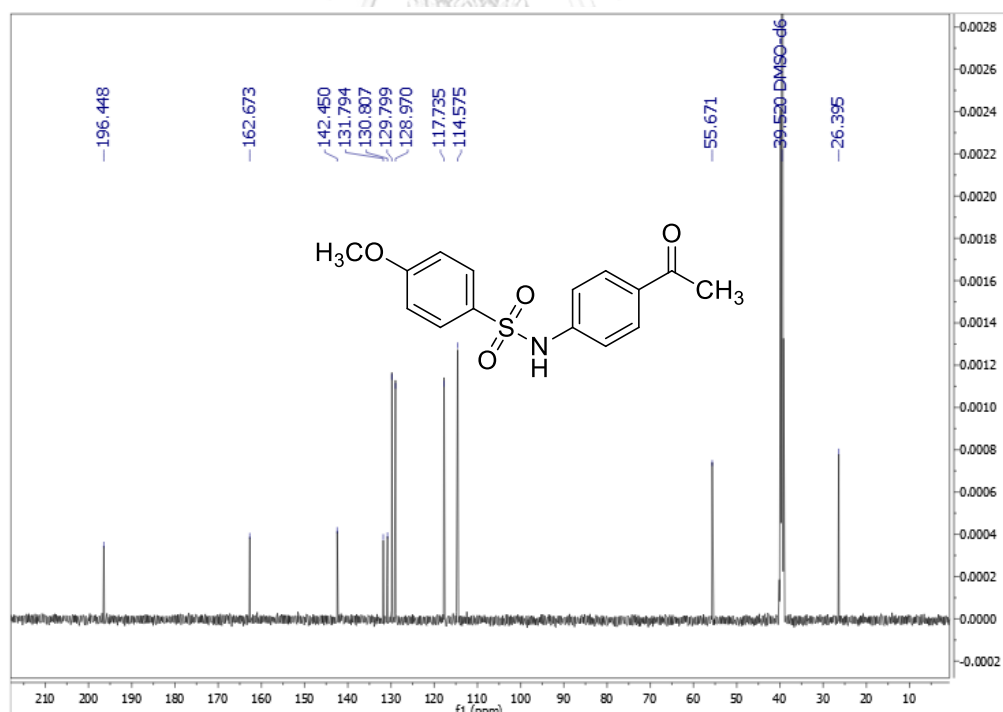
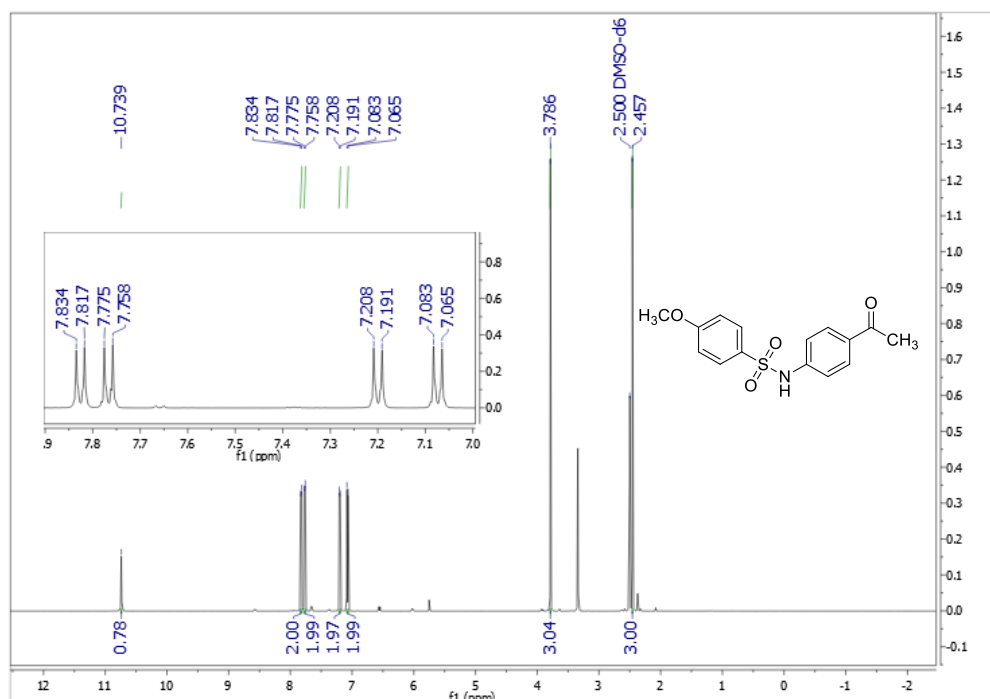
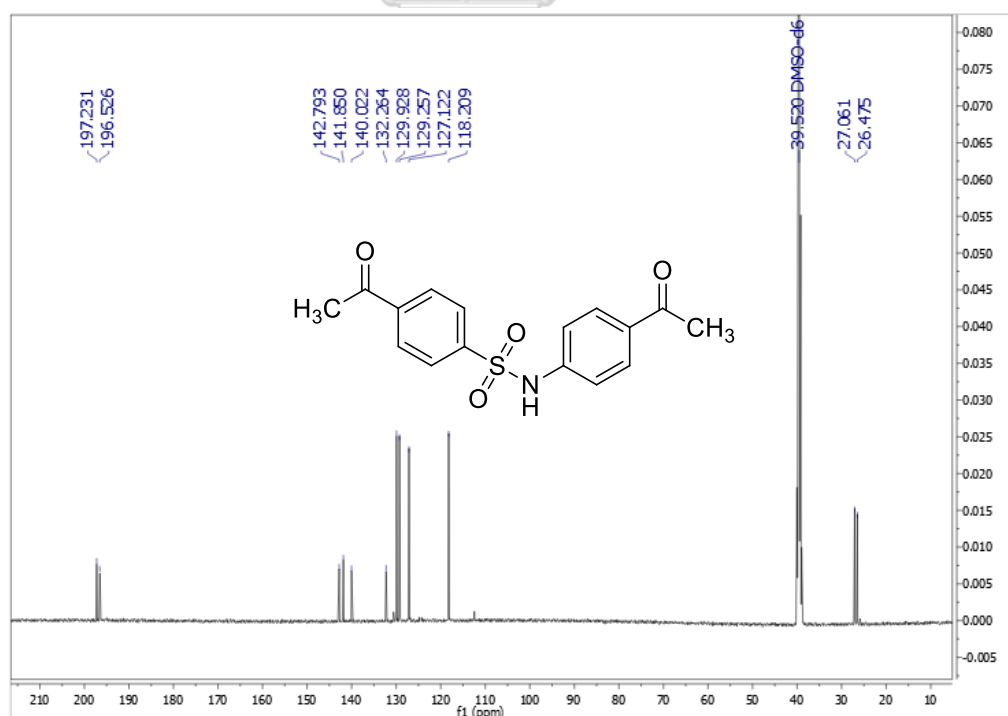
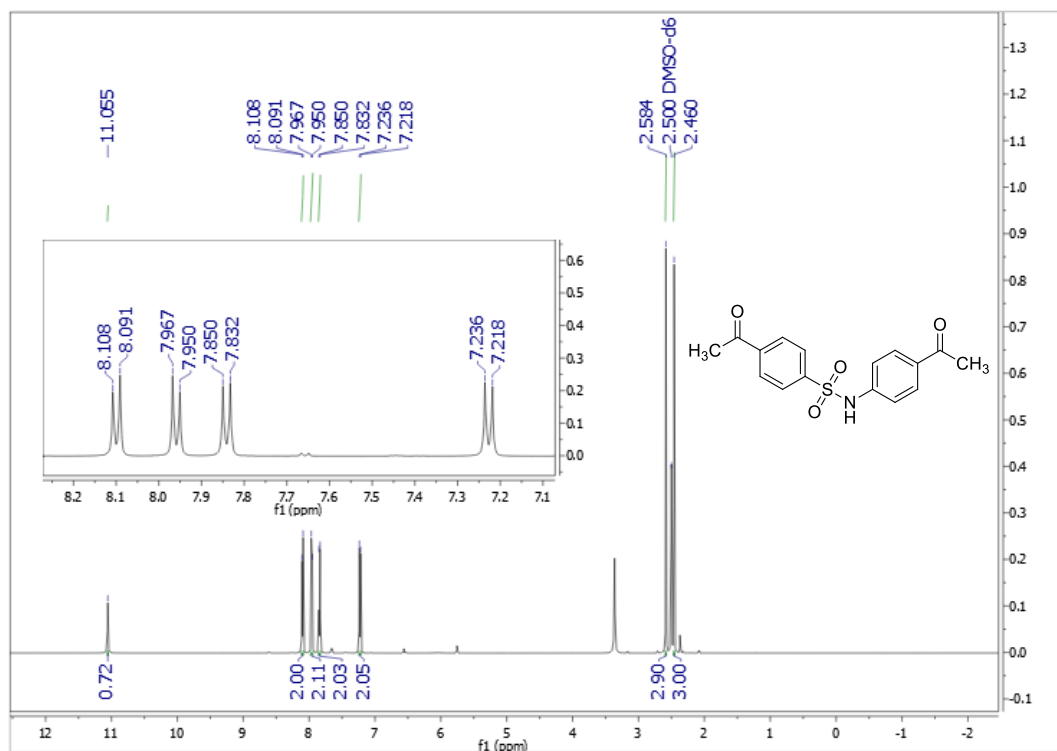


Figure A.94 The ¹³C NMR spectrum (DMSO-d₆, 125 MHz) of 103

Figure A.95 The ^1H NMR spectrum (DMSO- d_6 , 500 MHz) of **104**Figure A.96 The ^{13}C NMR spectrum (DMSO- d_6 , 125 MHz) of **104**





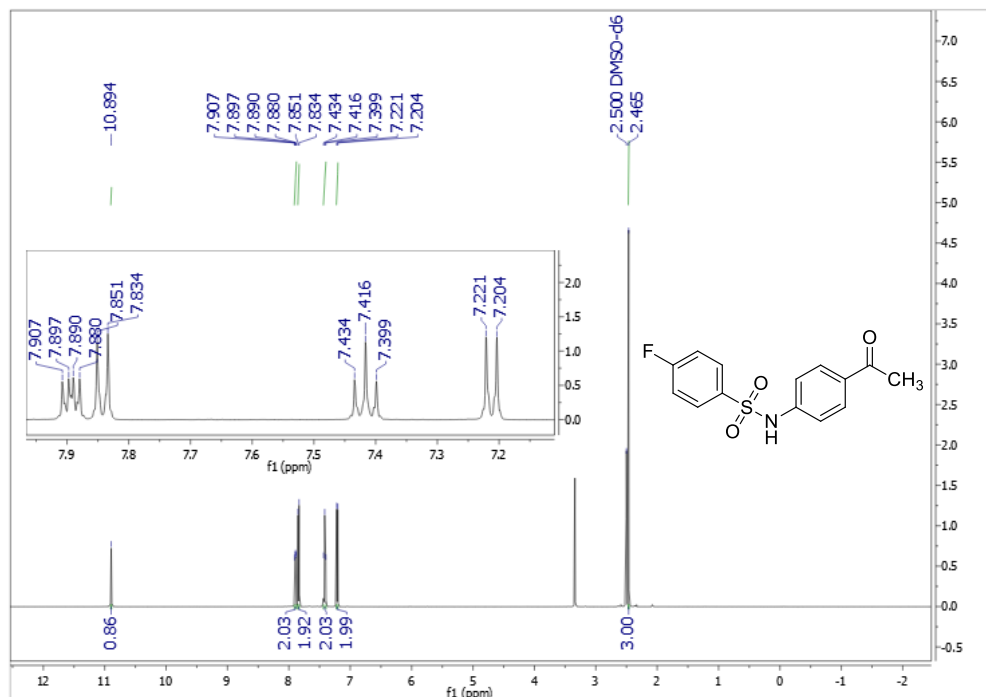


Figure A.101 The ^1H NMR spectrum (DMSO- d_6 , 500 MHz) of **107**

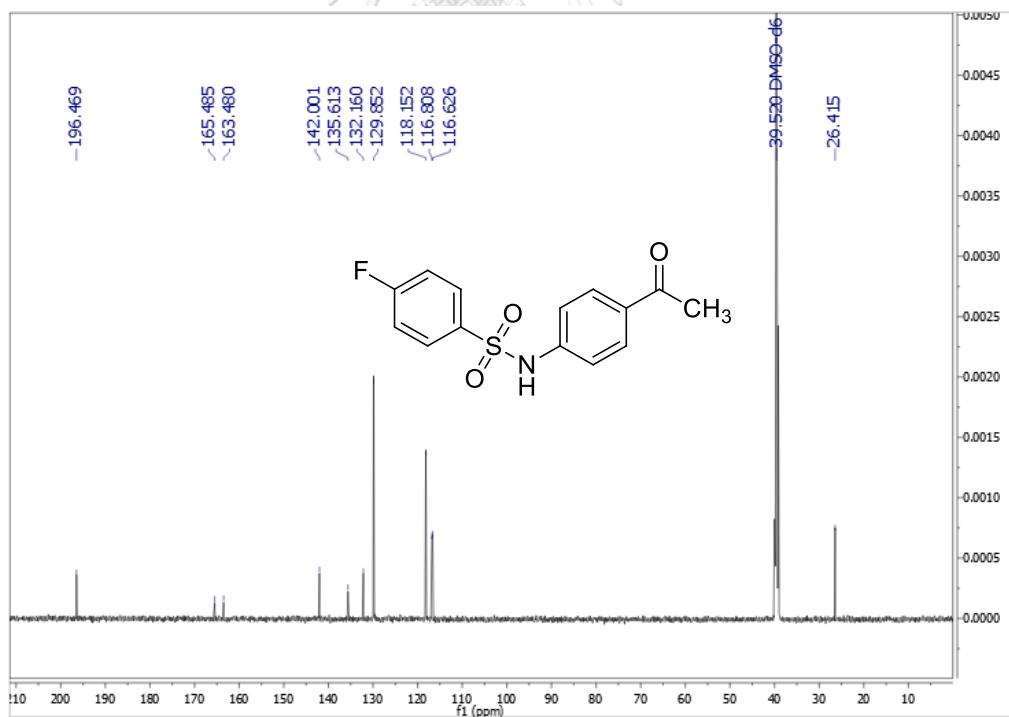
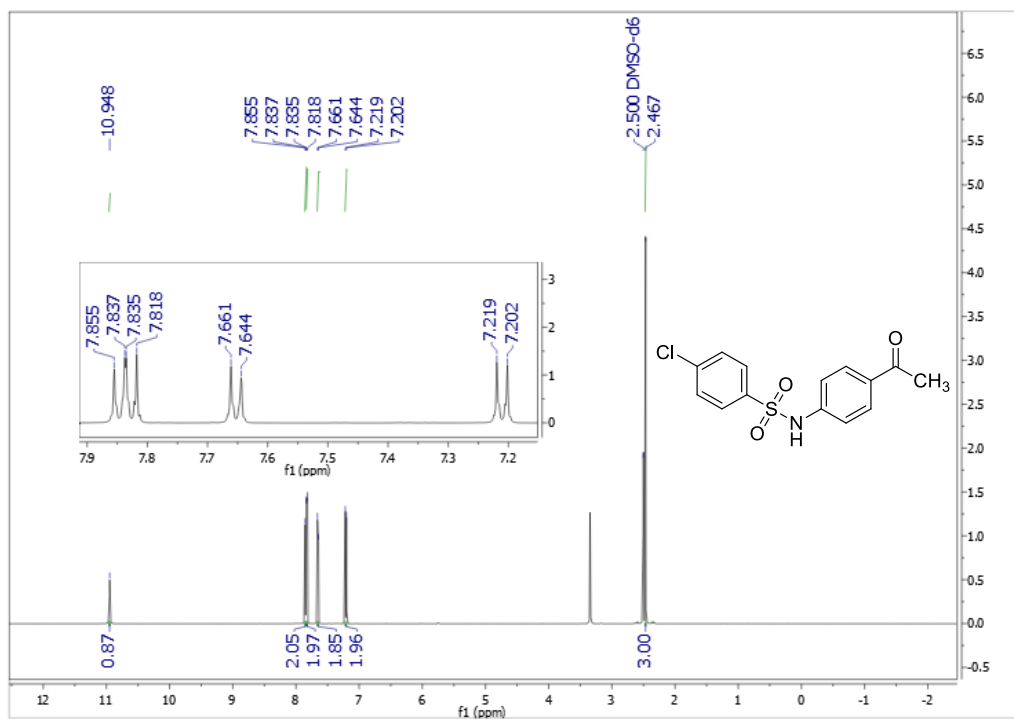
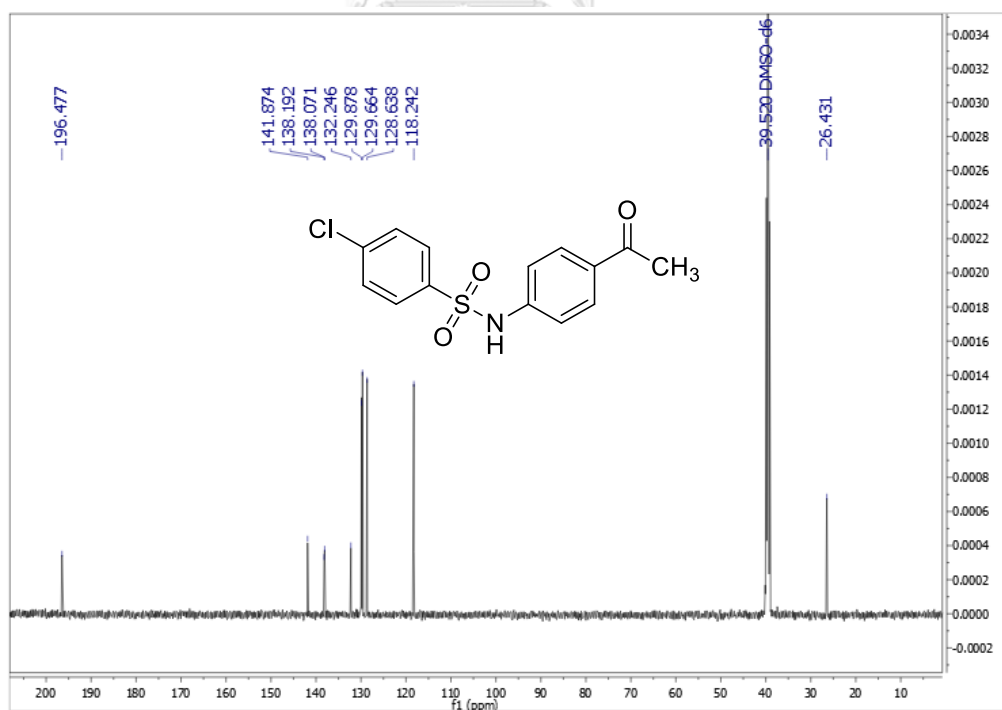


Figure A.102 The ^{13}C NMR spectrum (DMSO- d_6 , 125 MHz) of **107**

Figure A.103 The ^1H NMR spectrum (DMSO- d_6 , 500 MHz) of **108**Figure A.104 The ^{13}C NMR spectrum (DMSO- d_6 , 125 MHz) of **108**

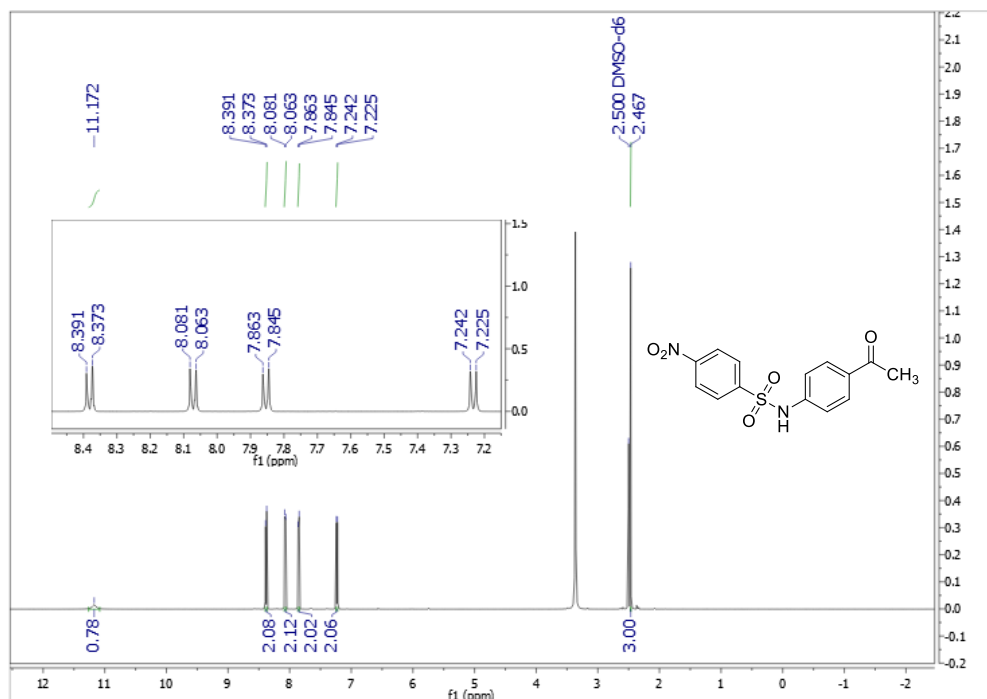


Figure A.105 The ^1H NMR spectrum (DMSO- d_6 , 500 MHz) of 109

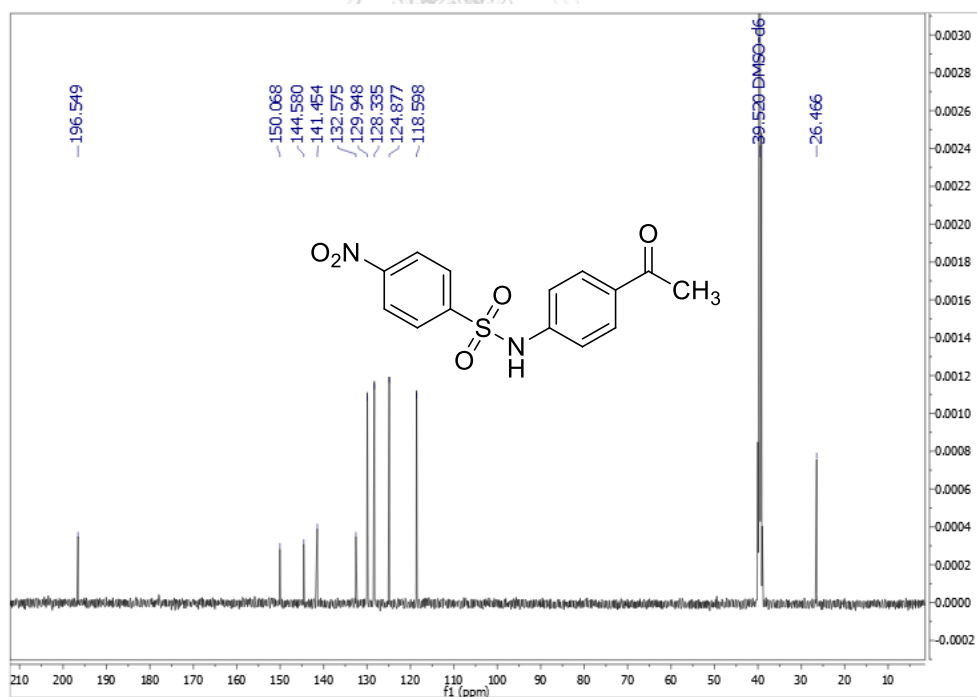


Figure A.106 The ^{13}C NMR spectrum (DMSO- d_6 , 125 MHz) of 109

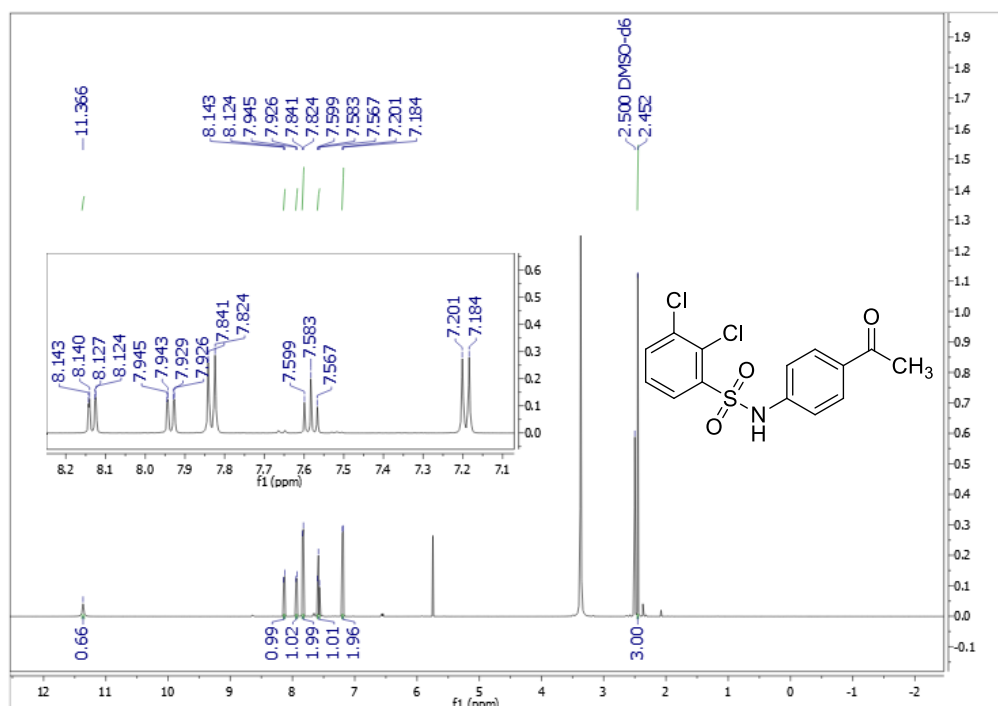


Figure A.107 The ^1H NMR spectrum (DMSO- d_6 , 500 MHz) of **110**

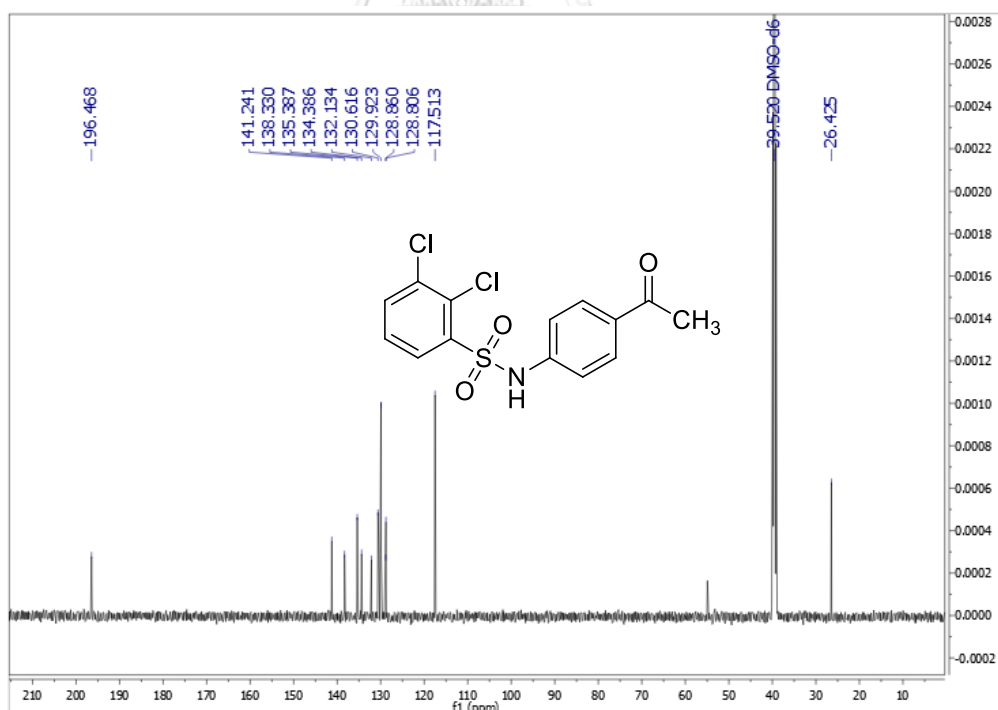
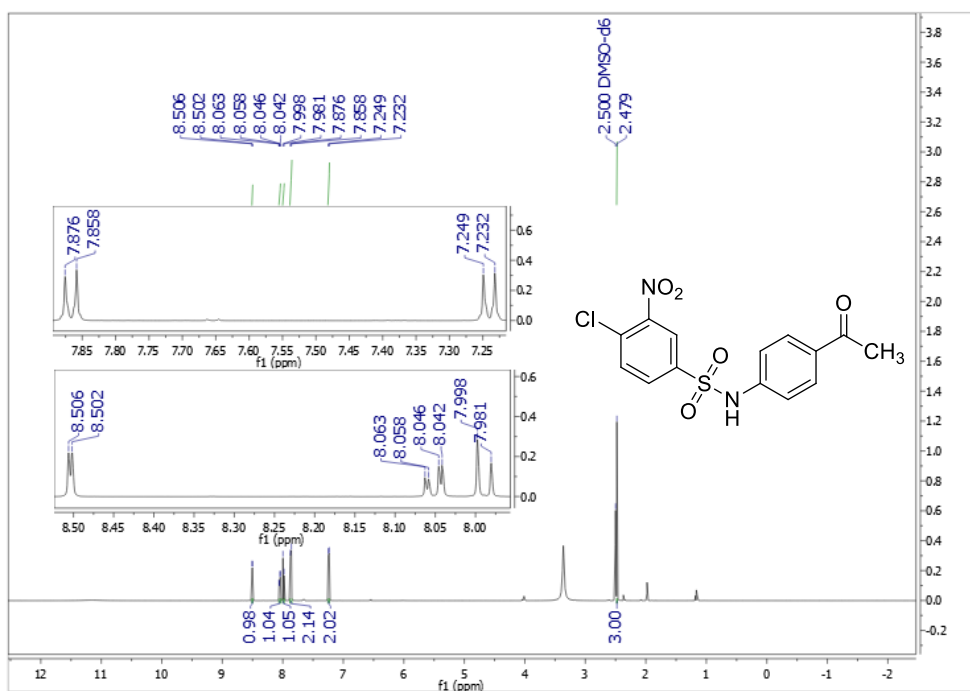
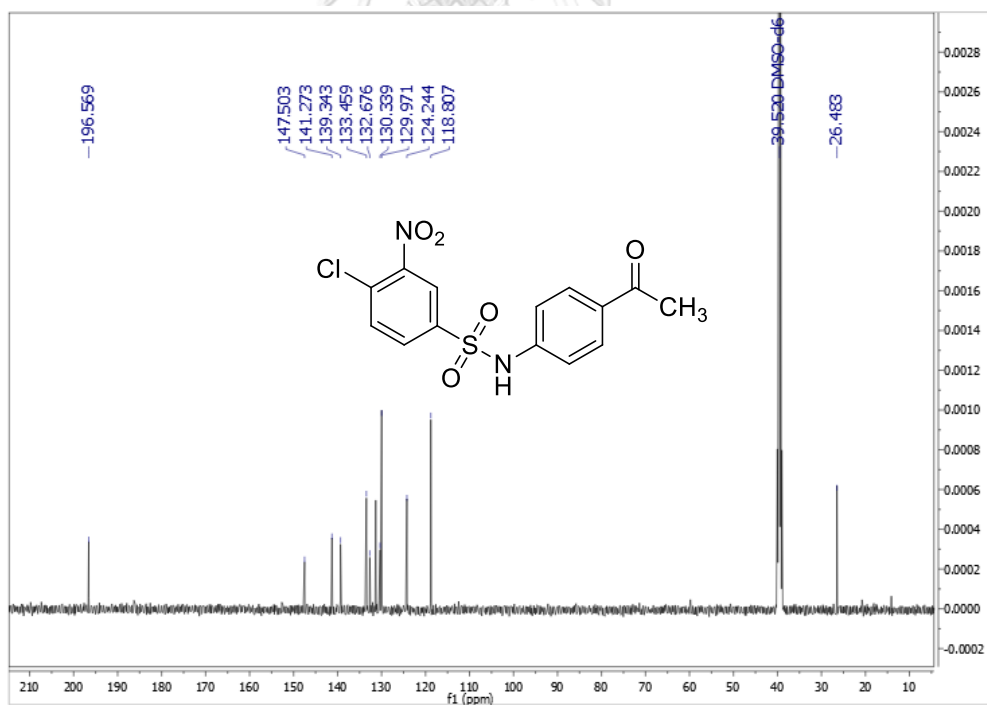


Figure A.108 The ^{13}C NMR spectrum (DMSO- d_6 , 125 MHz) of **110**

Figure A.109 The ¹H NMR spectrum (DMSO-*d*₆, 500 MHz) of 111Figure A.110 The ¹³C NMR spectrum (DMSO-*d*₆, 125 MHz) of 111

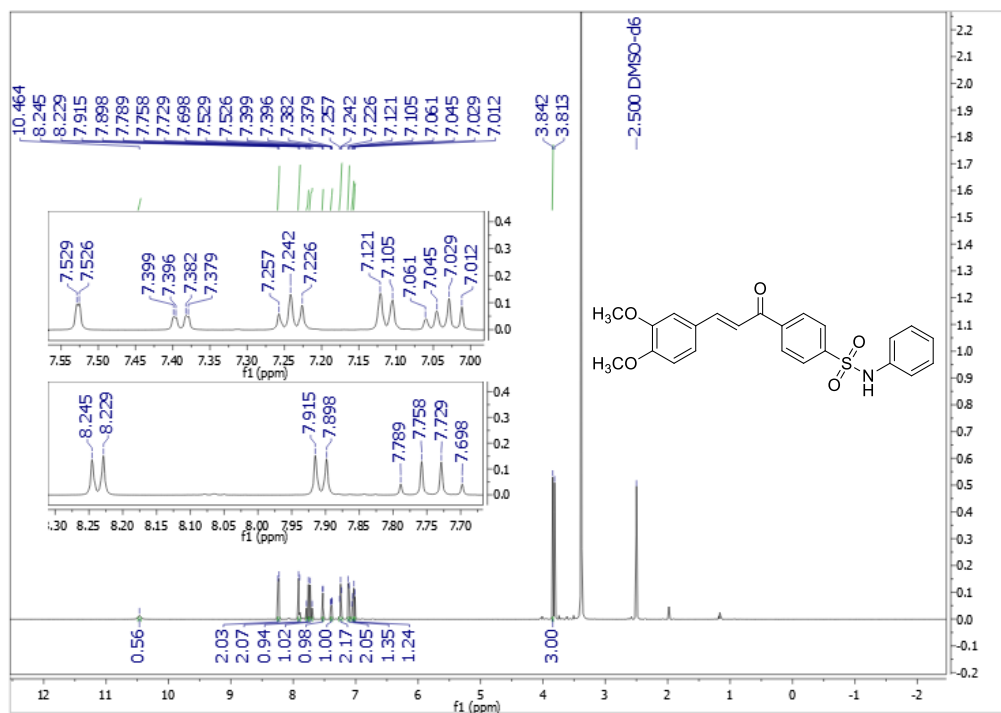


Figure A.111 The ¹H NMR spectrum (DMSO-*d*₆, 500 MHz) of 112

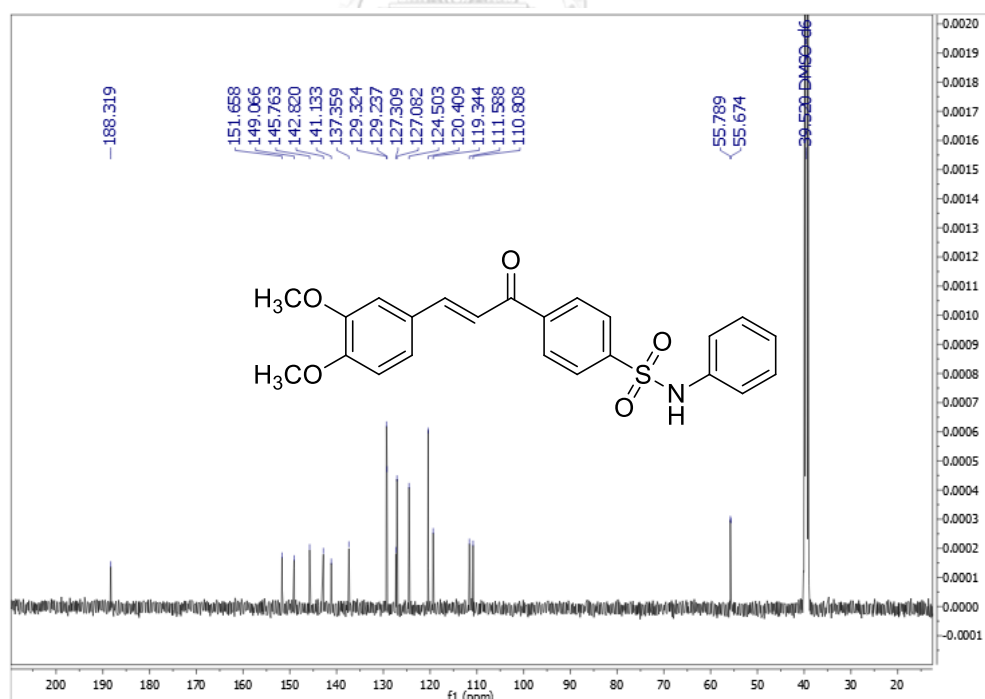


Figure A.112 The ¹³C NMR spectrum (DMSO-*d*₆, 125 MHz) of 112

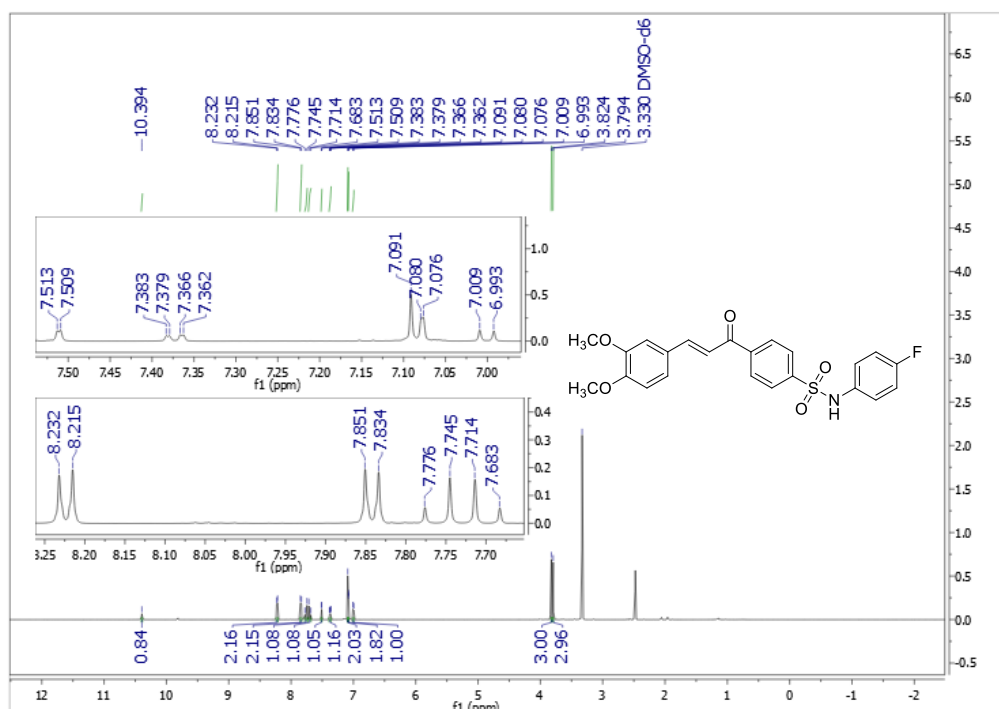


Figure A.113 The ¹H NMR spectrum (DMSO-*d*₆, 500 MHz) of 113

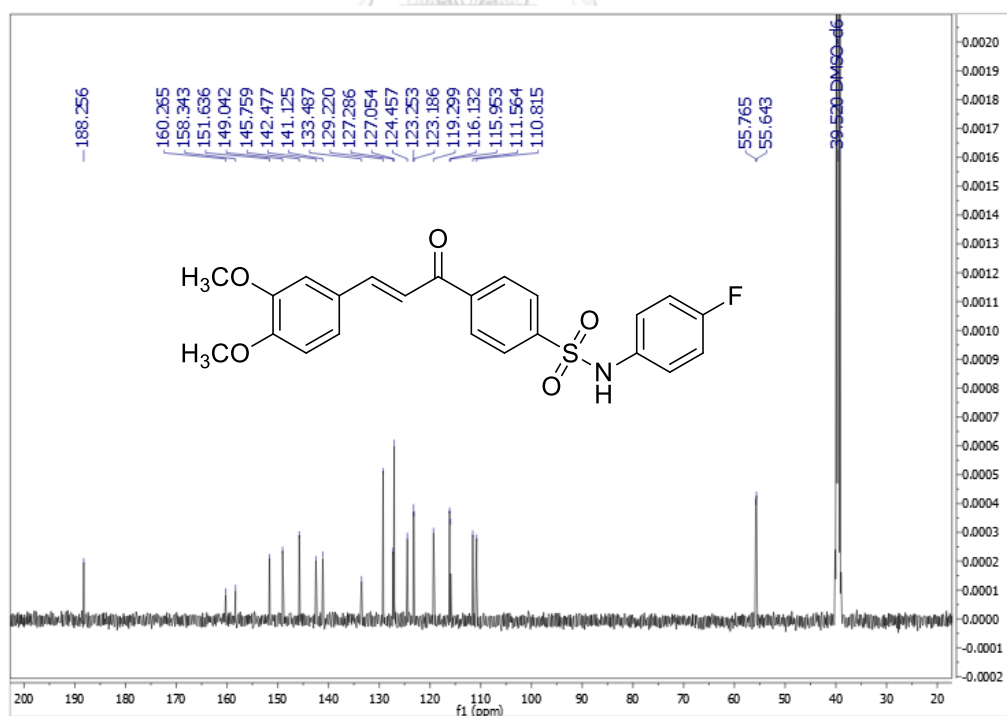


Figure A.114 The ¹³C NMR spectrum (DMSO-*d*₆, 125 MHz) of 113

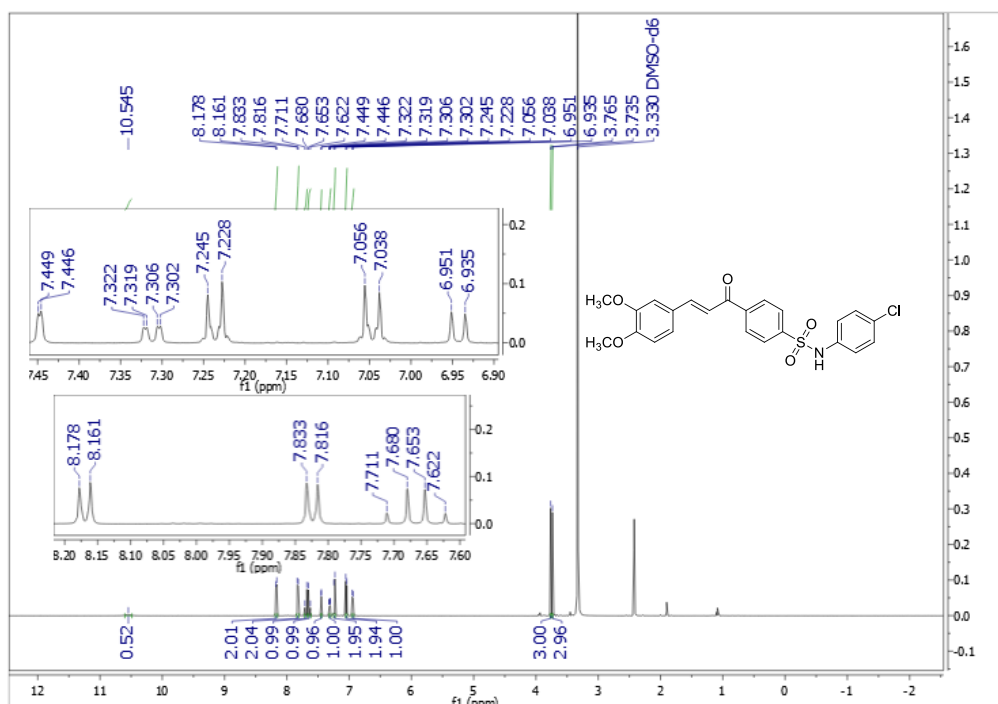


Figure A.115 The ¹H NMR spectrum (DMSO-*d*₆, 500 MHz) of **114**

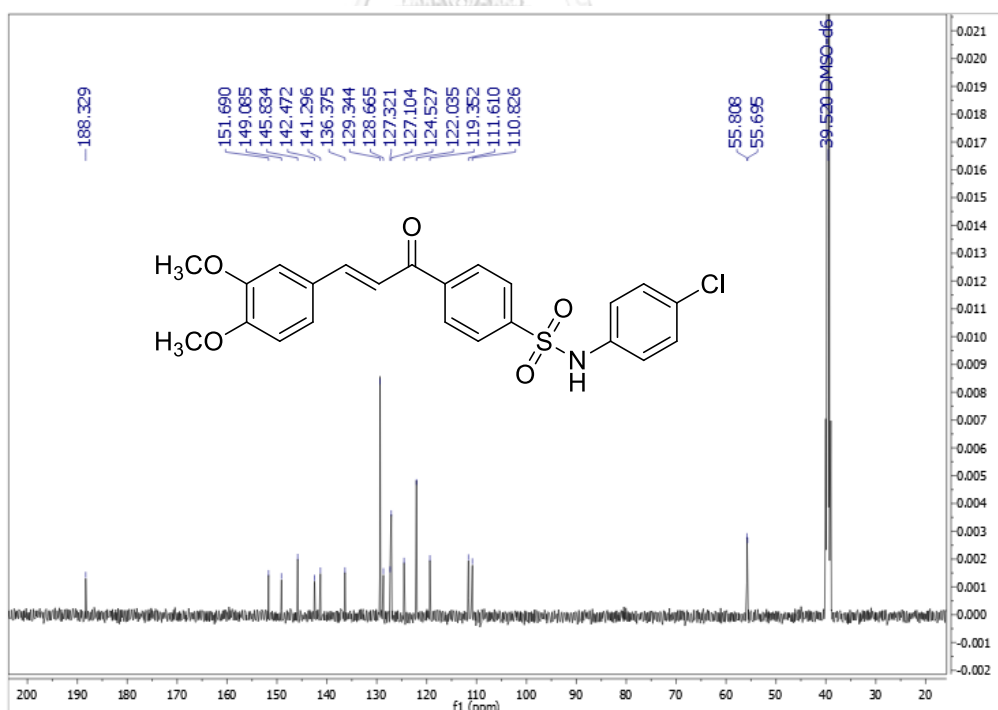


Figure A.116 The ¹³C NMR spectrum (DMSO-*d*₆, 125 MHz) of **114**

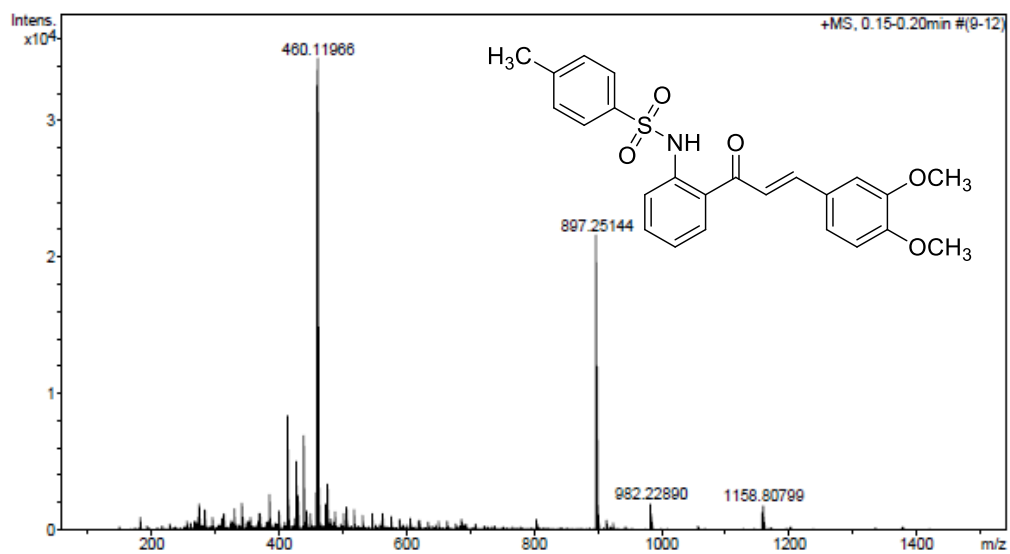


Figure A.117 The HR-MS (ESI) of 60

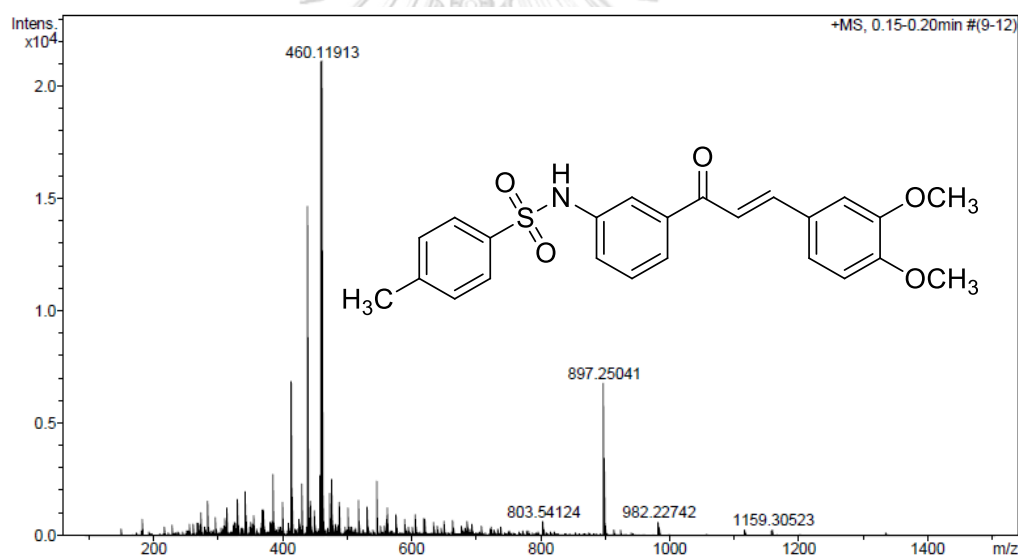


Figure A.118 The HR-MS (ESI) of 61

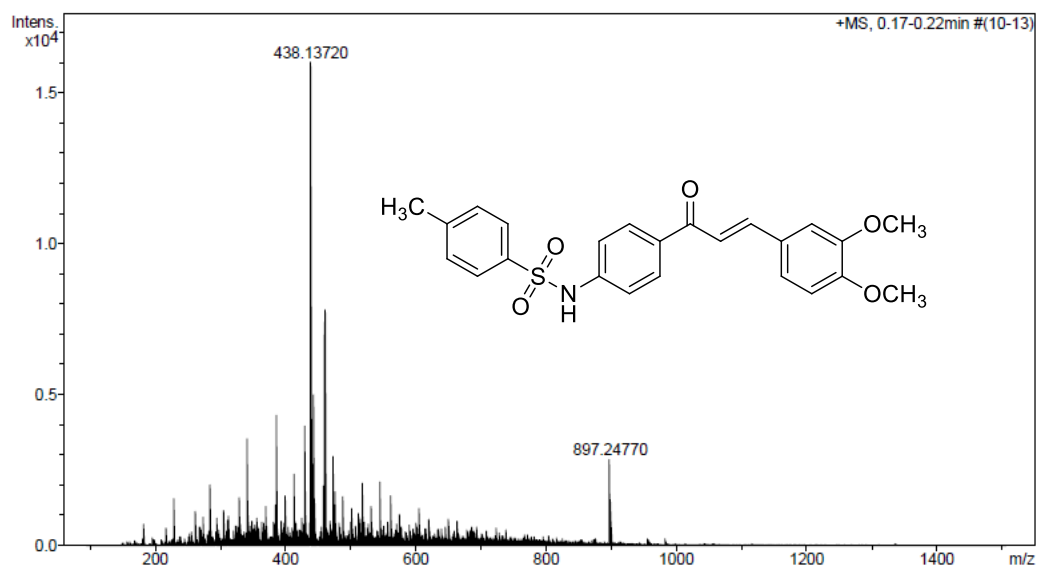


Figure A.119 The HR-MS (ESI) of 62

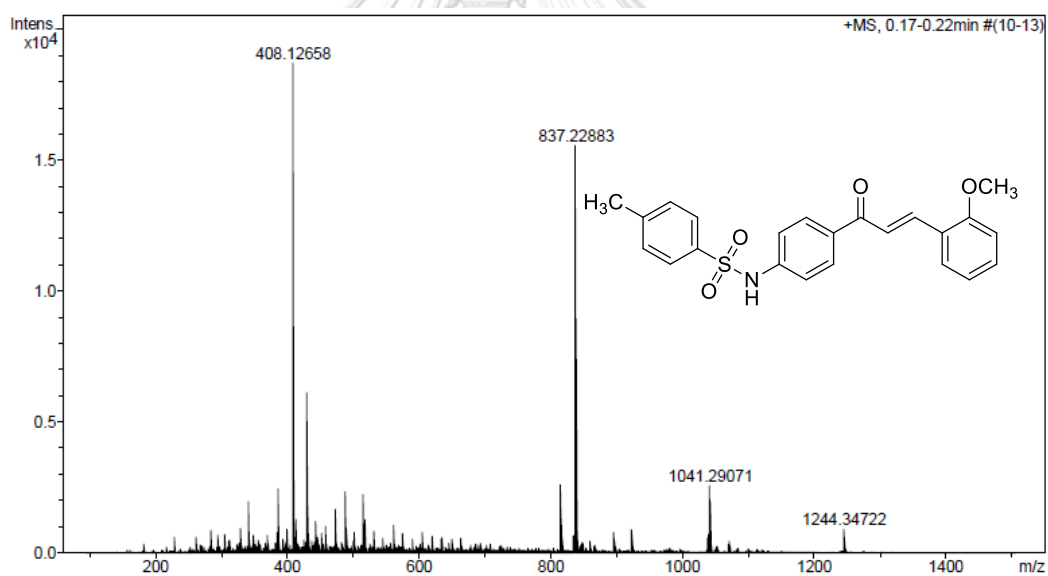


Figure A.120 The HR-MS (ESI) of 64

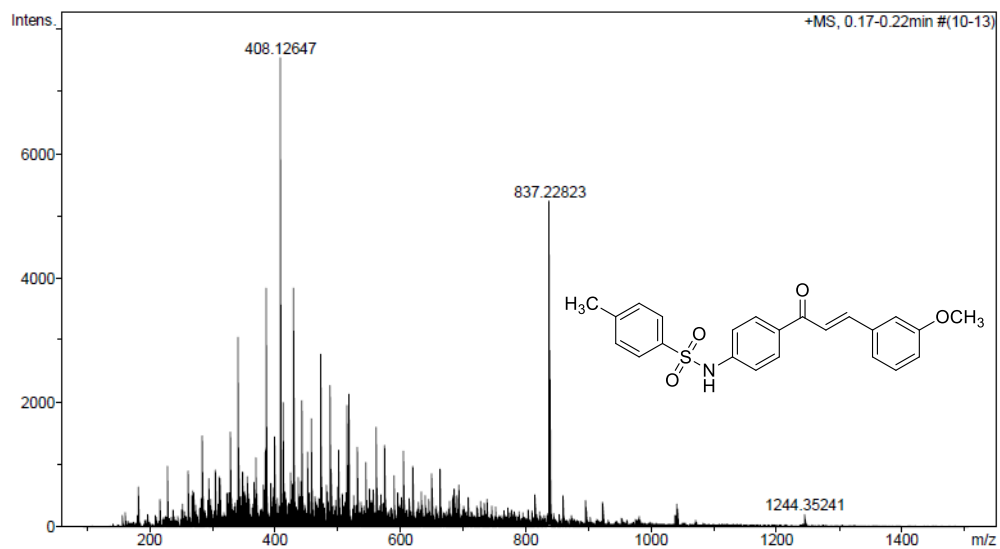


Figure A.121 The HR-MS (ESI) of 65

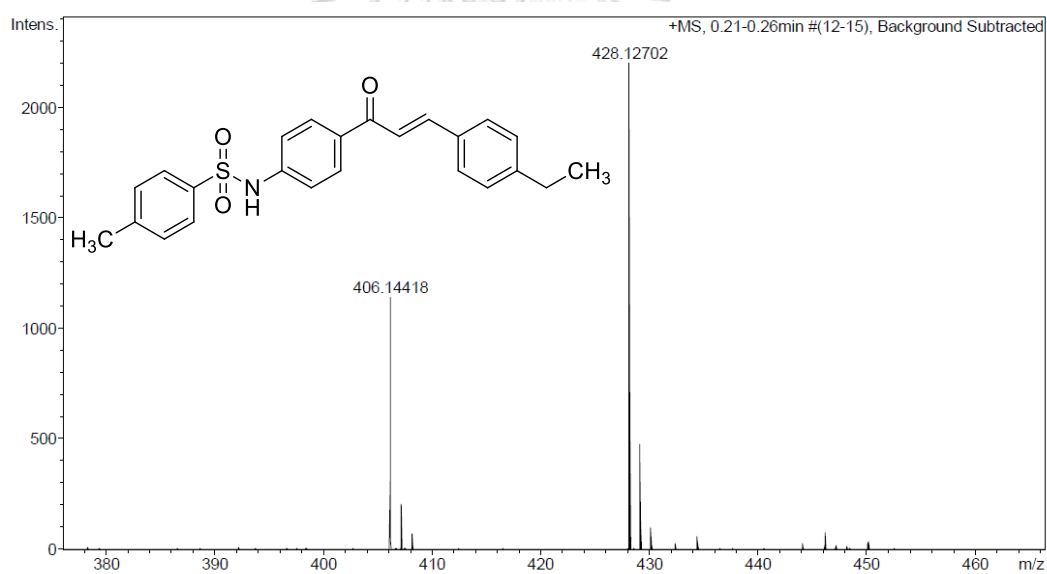


Figure A.122 The HR-MS (ESI) of 68

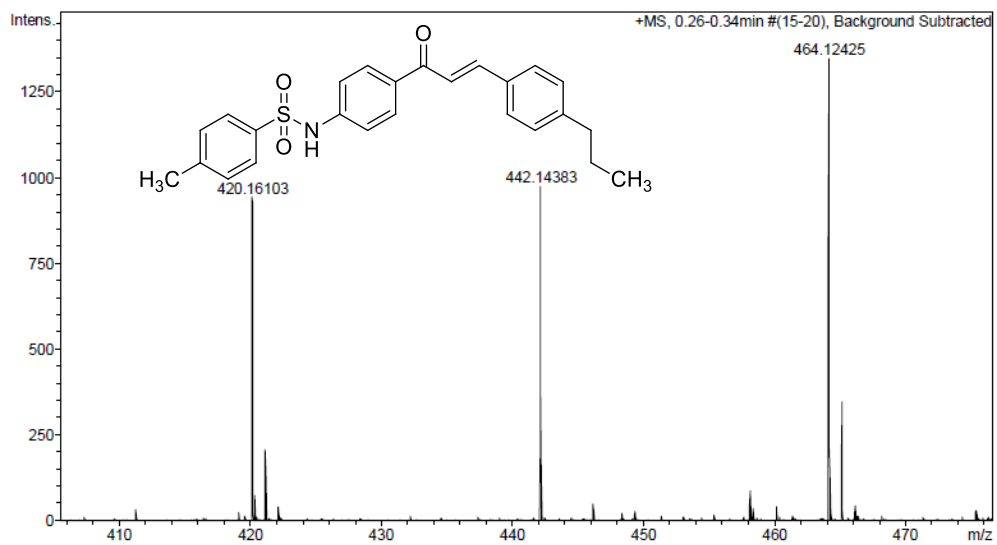


Figure A.123 The HR-MS (ESI) of 69

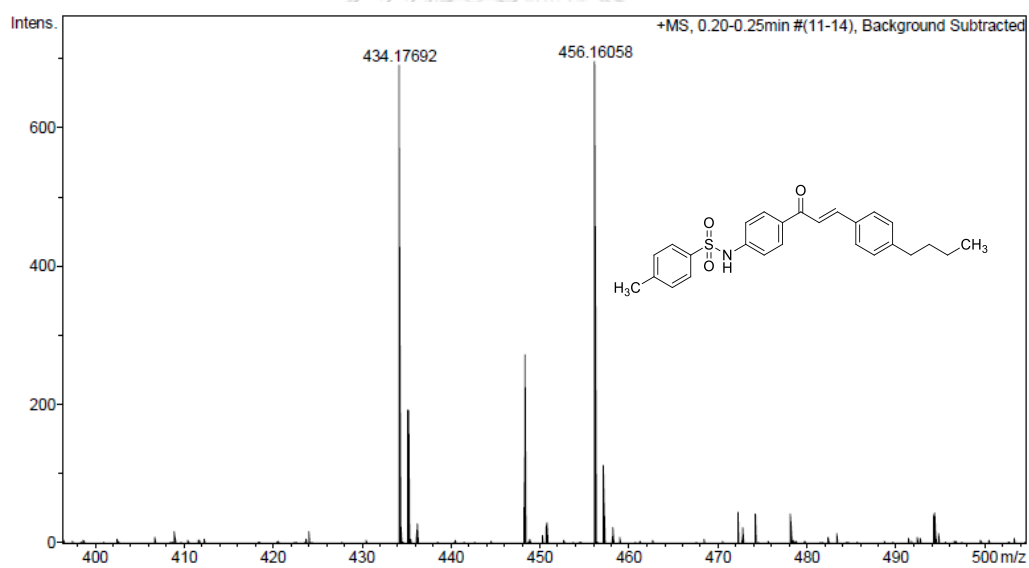


Figure A.124 The HR-MS (ESI) of 70

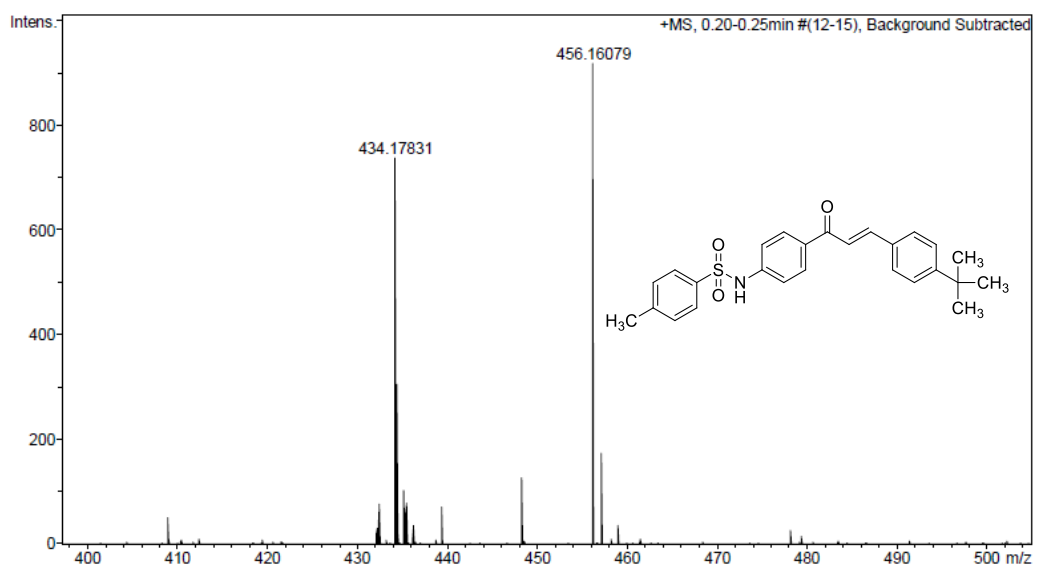


Figure A.125 The HR-MS (ESI) of 72

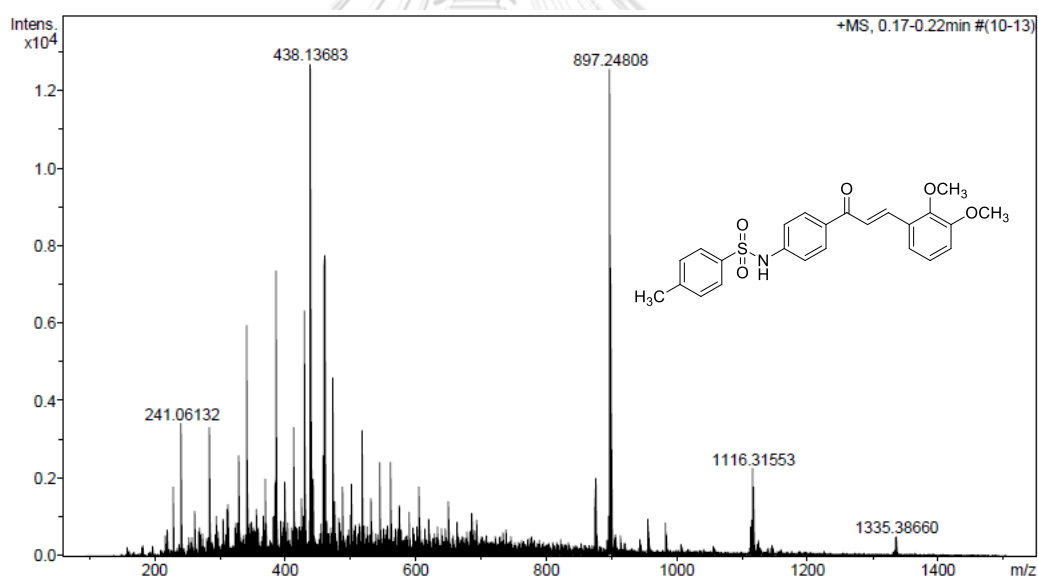


Figure A.126 The HR-MS (ESI) of 77

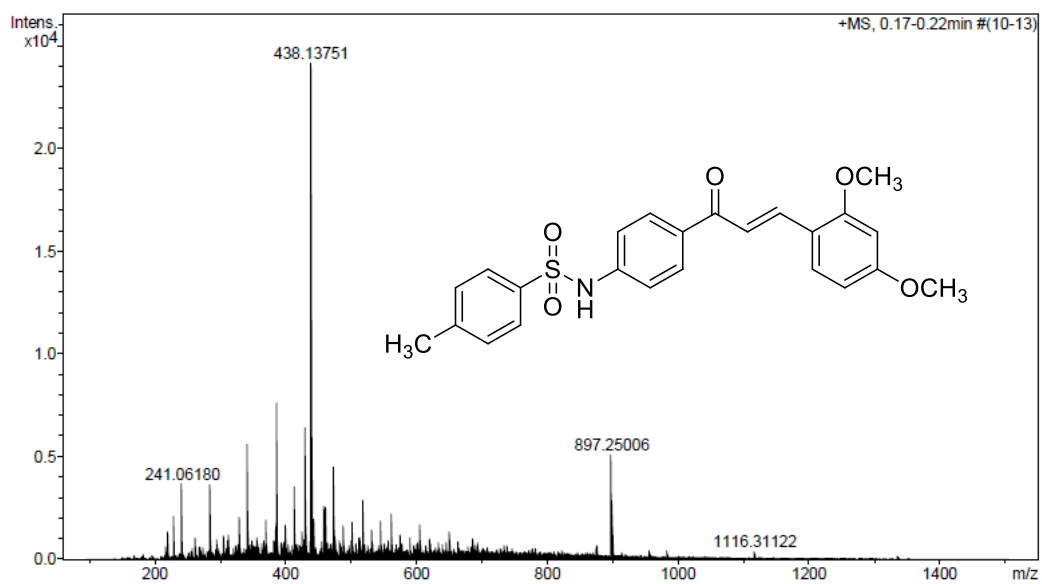


Figure A.127 The HR-MS (ESI) of 78

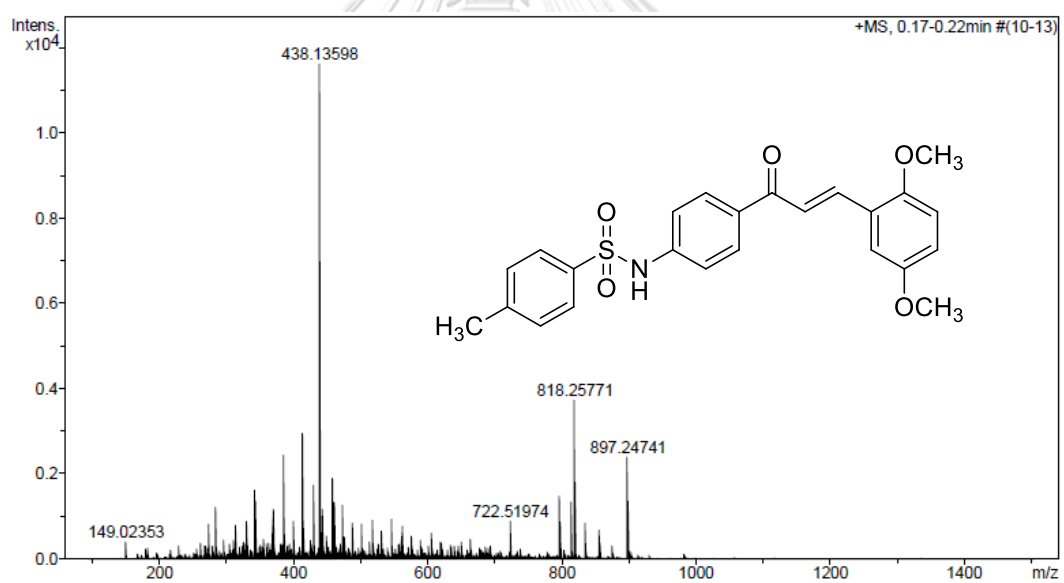


Figure A.128 The HR-MS (ESI) of 79

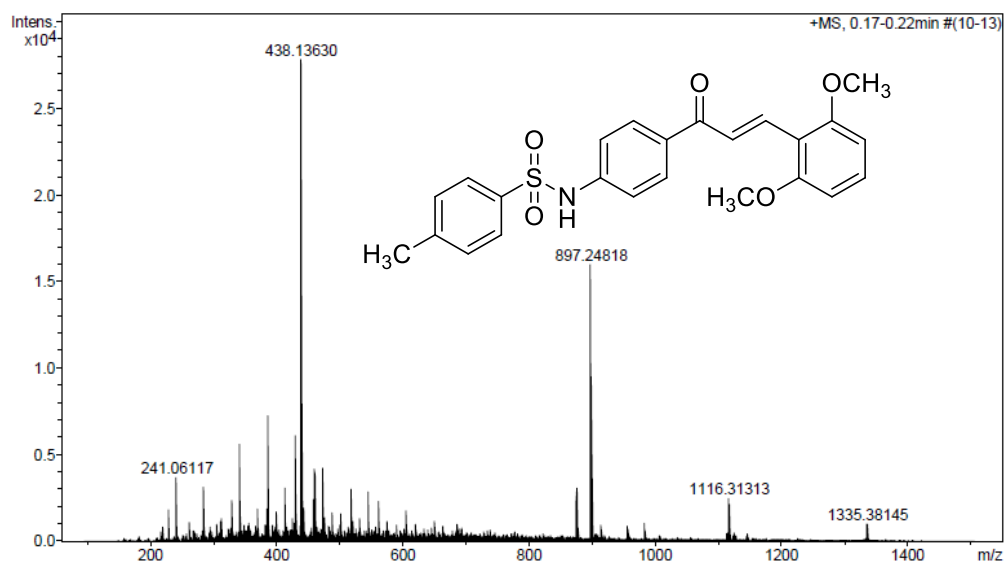


Figure A.129 The HR-MS (ESI) of 80

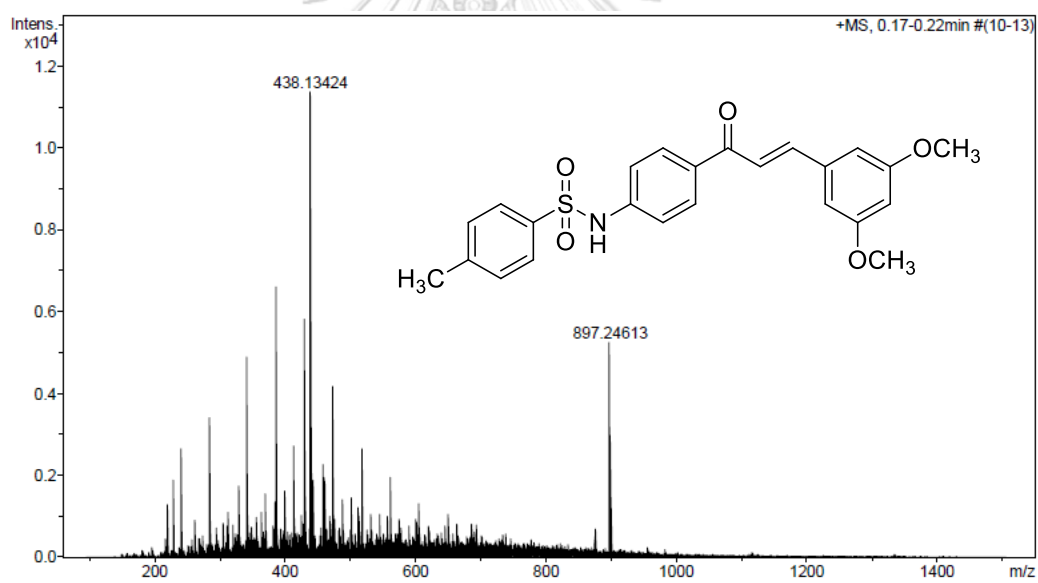


Figure A.130 The HR-MS (ESI) of 81

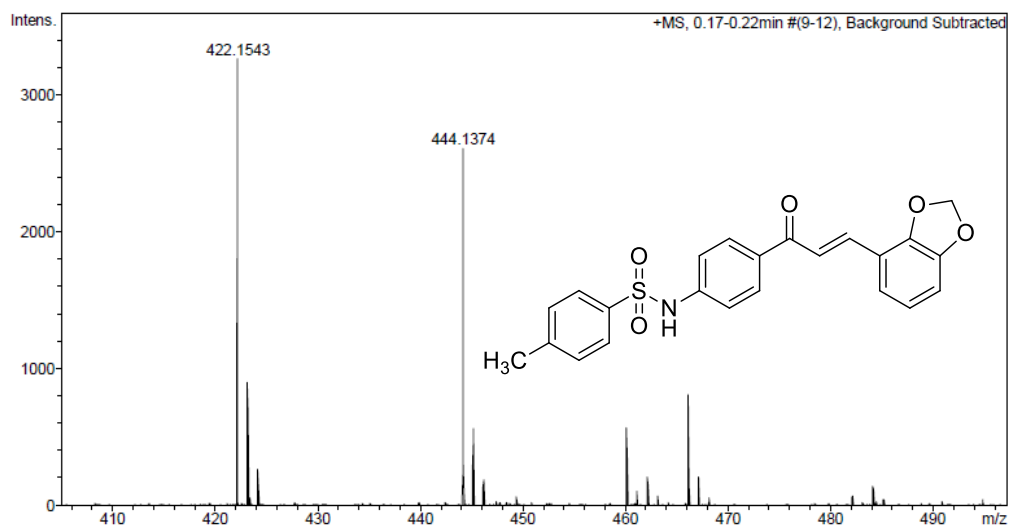


Figure A.131 The HR-MS (ESI) of 82

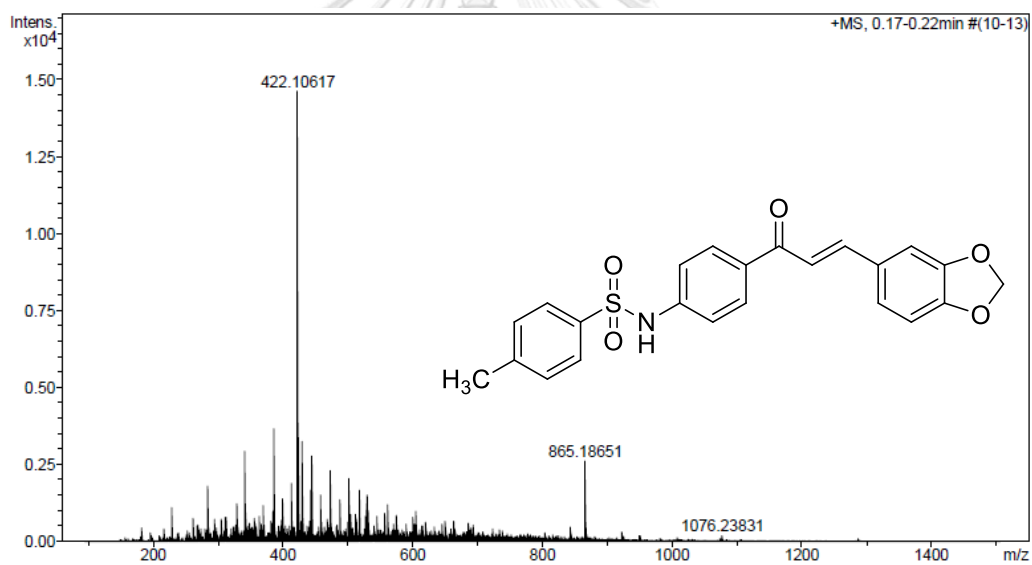


Figure A.132 The HR-MS (ESI) of 83

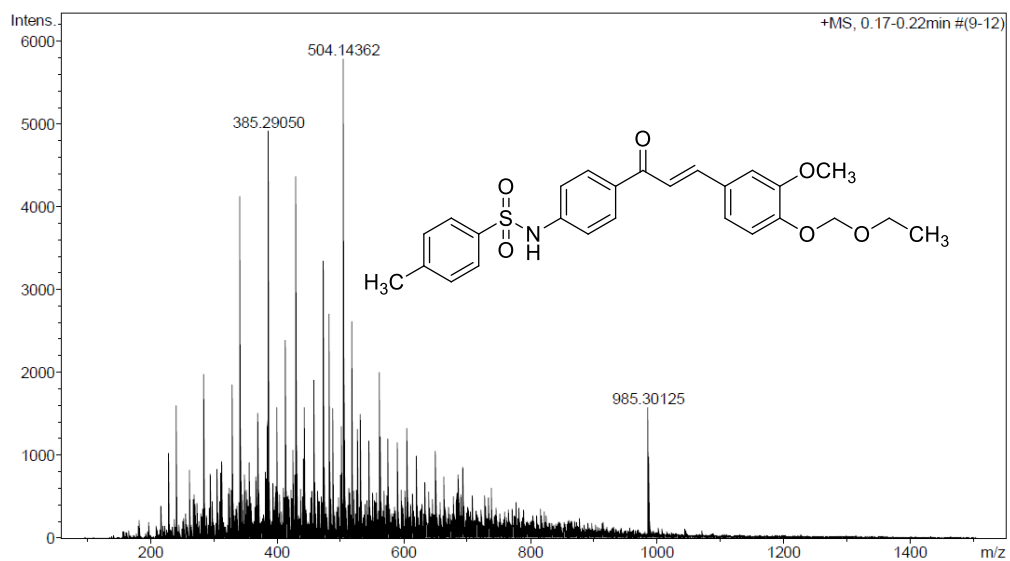


Figure A.133 The HR-MS (ESI) of 85

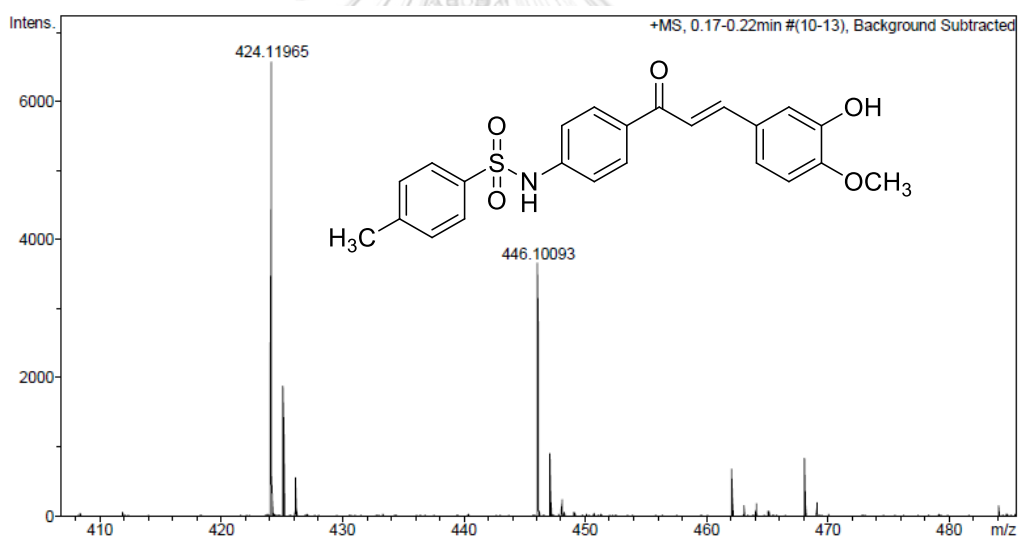


Figure A.134 The HR-MS (ESI) of 86

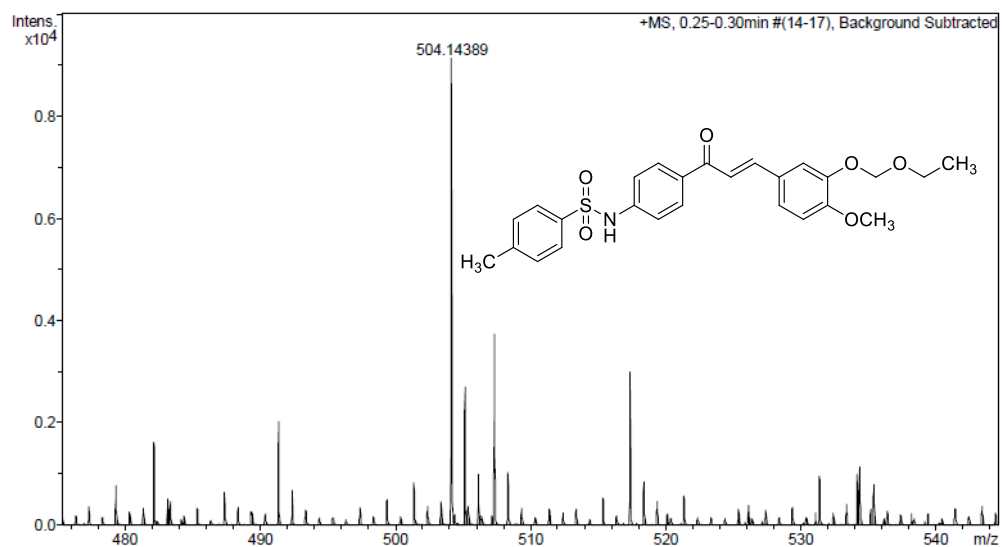


Figure A.135 The HR-MS (ESI) of 87

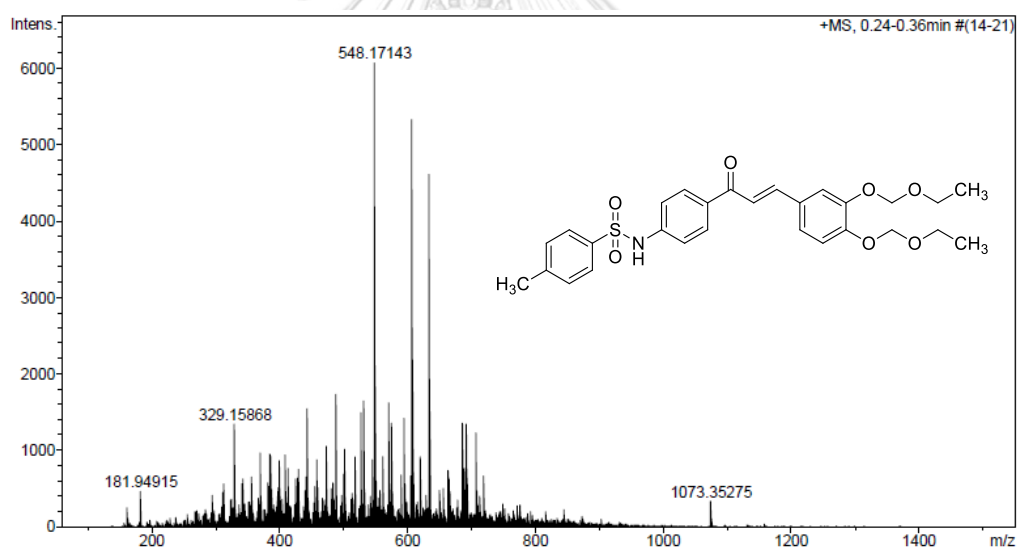


Figure A.136 The HR-MS (ESI) of 88

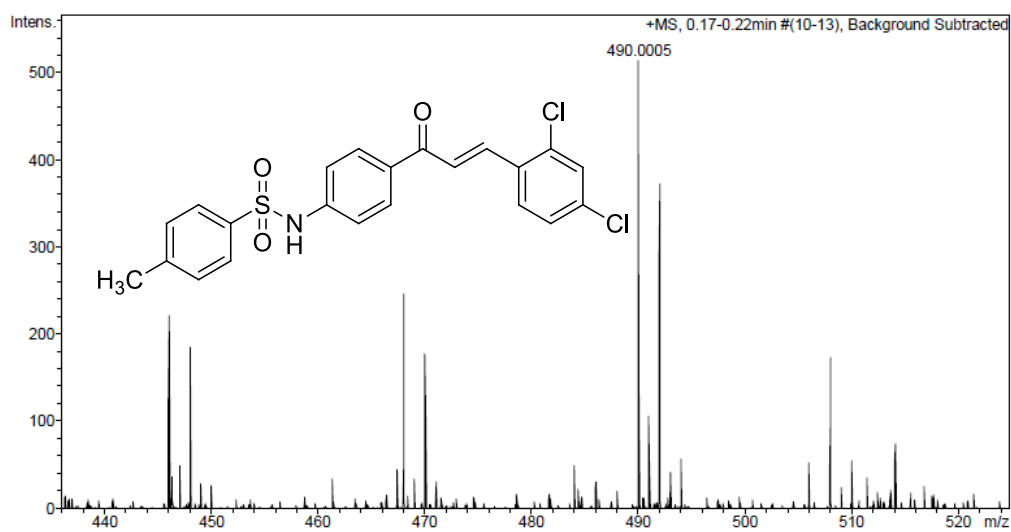


Figure A.137 The HR-MS (ESI) of 89

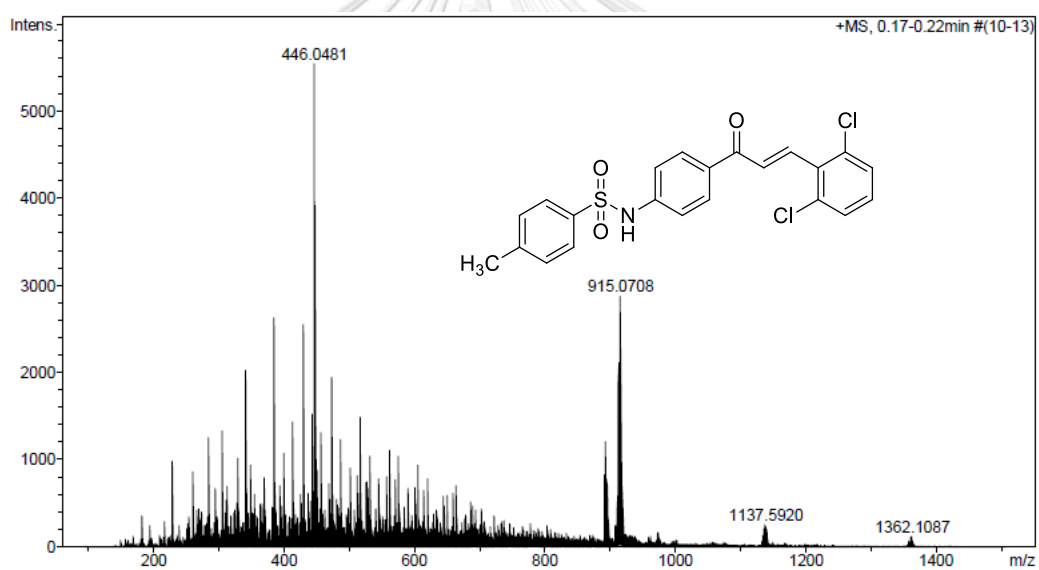
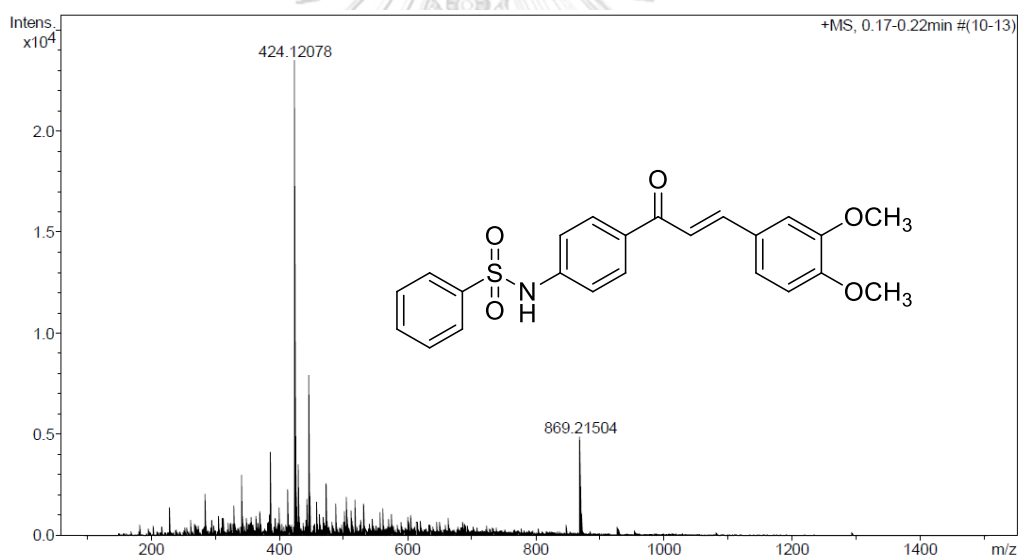
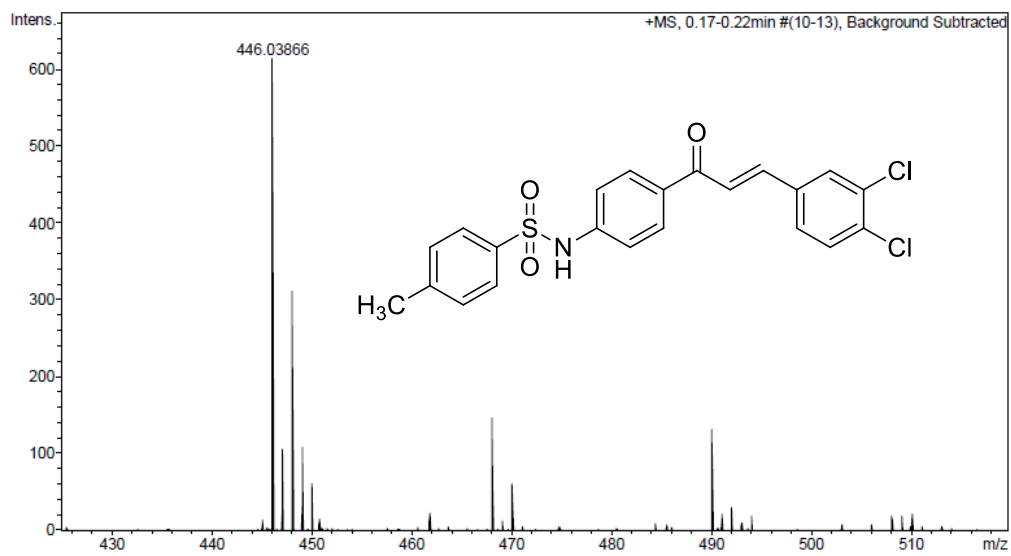


Figure A.138 The HR-MS (ESI) of 90



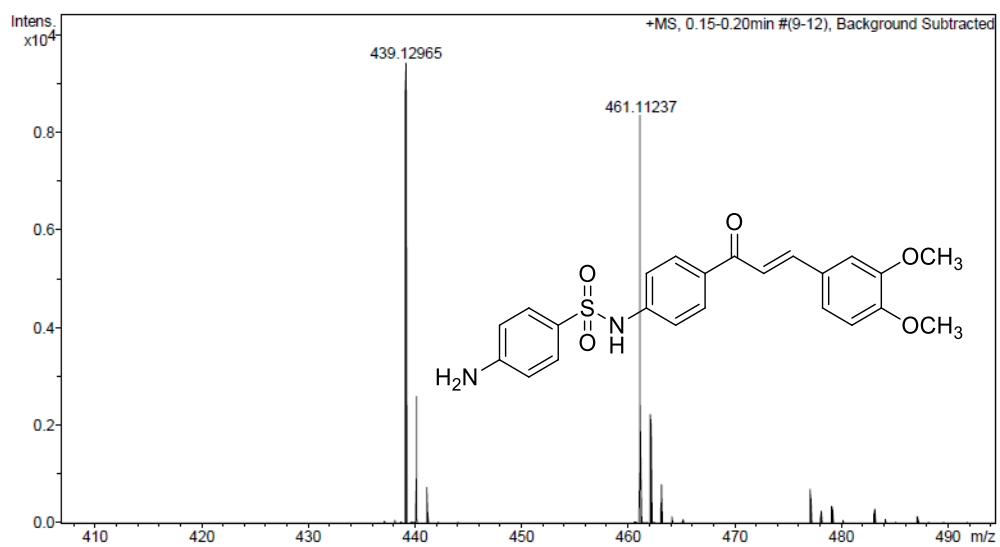


Figure A.141 The HR-MS (ESI) of 93

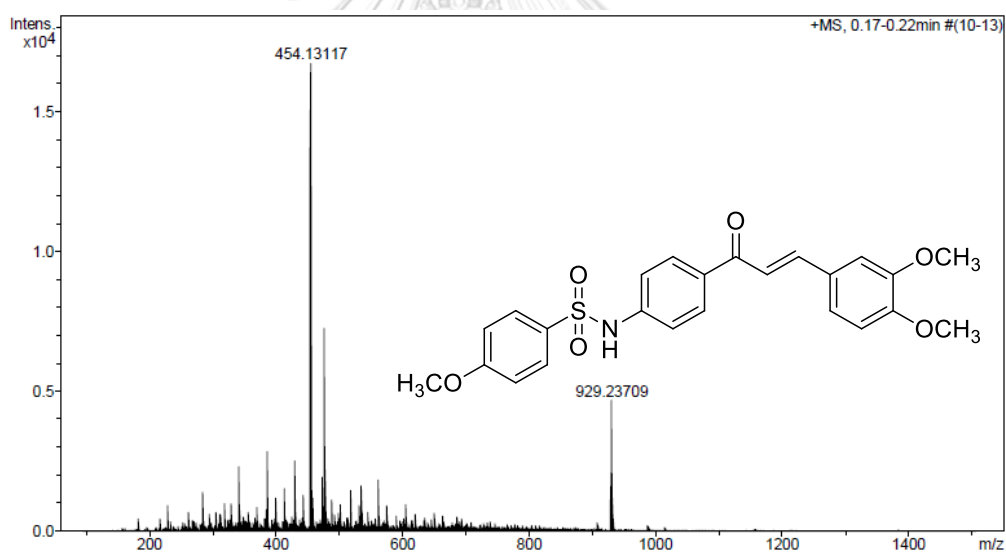
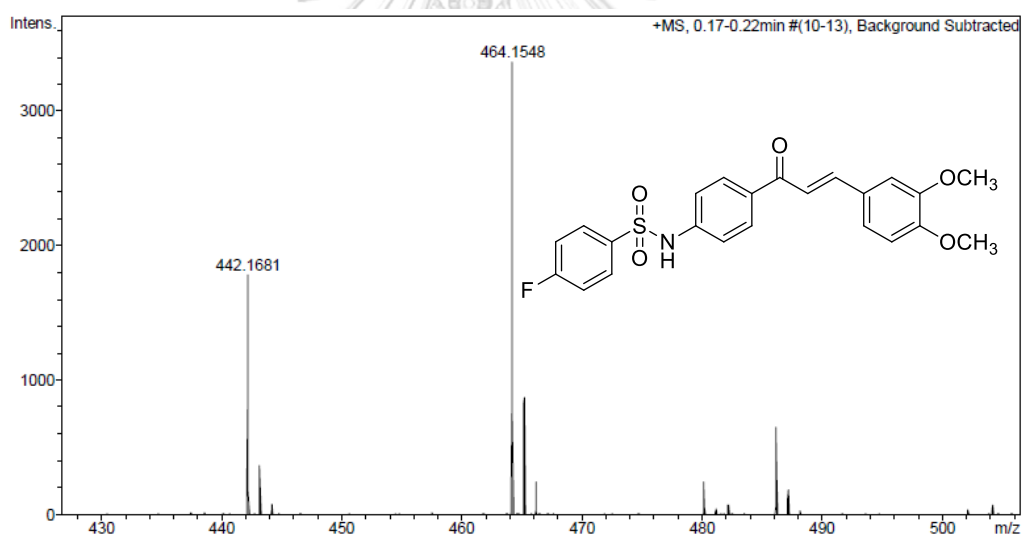
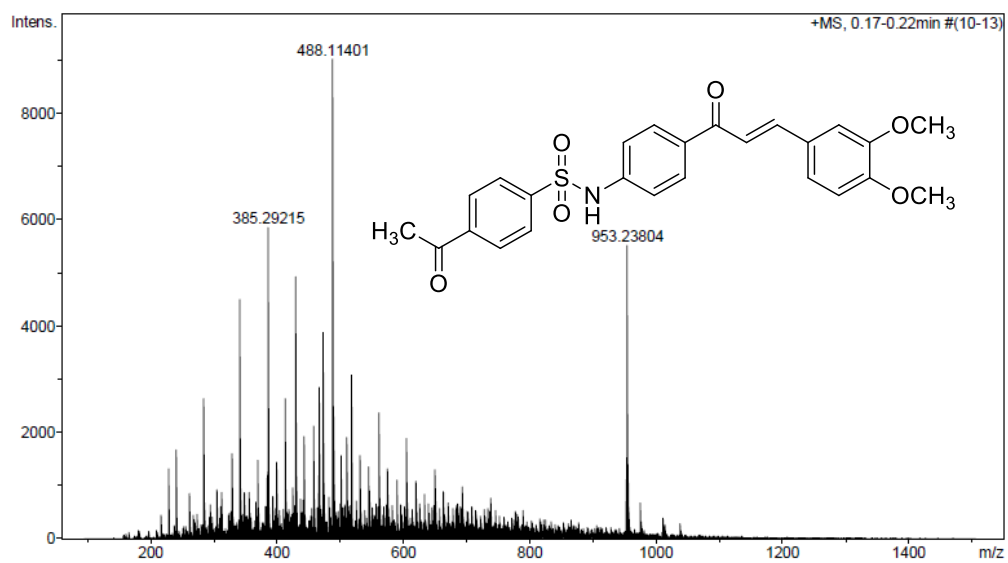


Figure A.142 The HR-MS (ESI) of 94



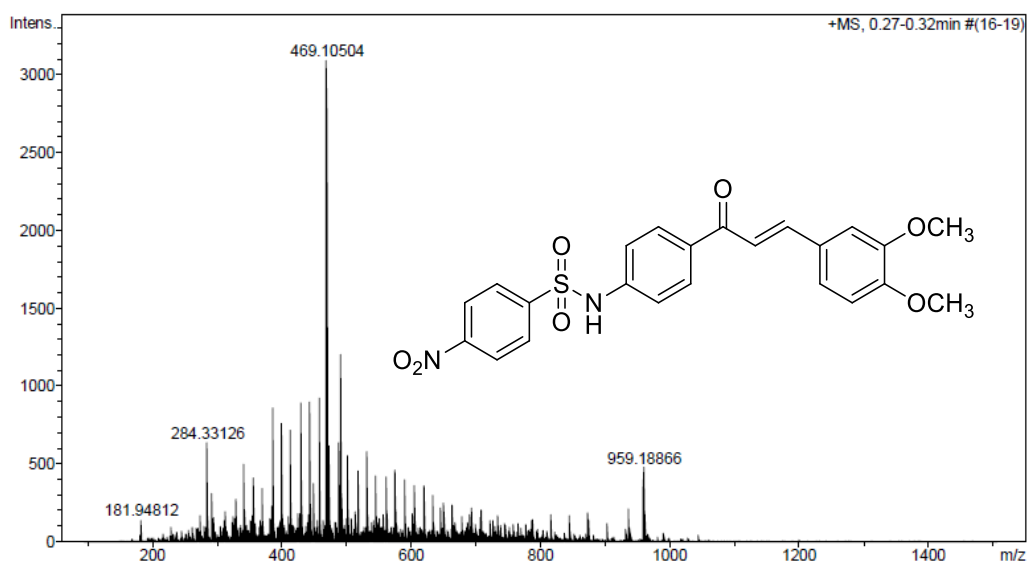


Figure A.145 The HR-MS (ESI) of 98

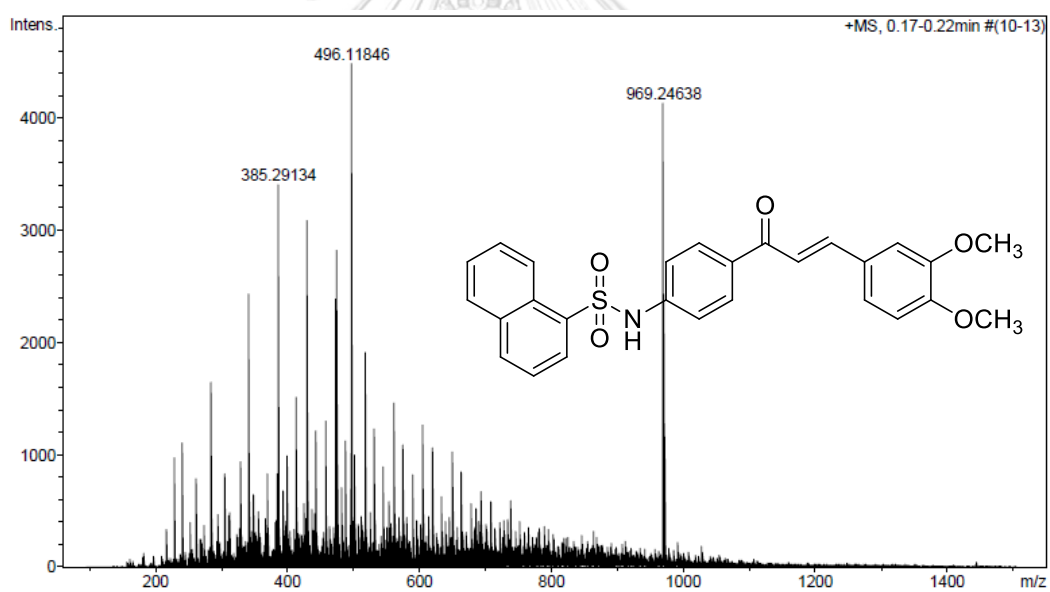


Figure A.146 The HR-MS (ESI) of 99

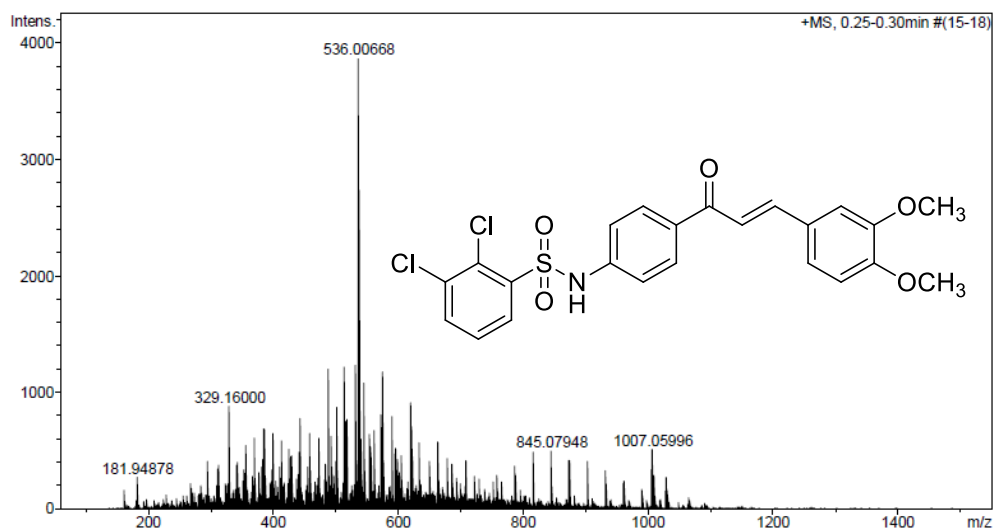


Figure A.147 The HR-MS (ESI) of 100

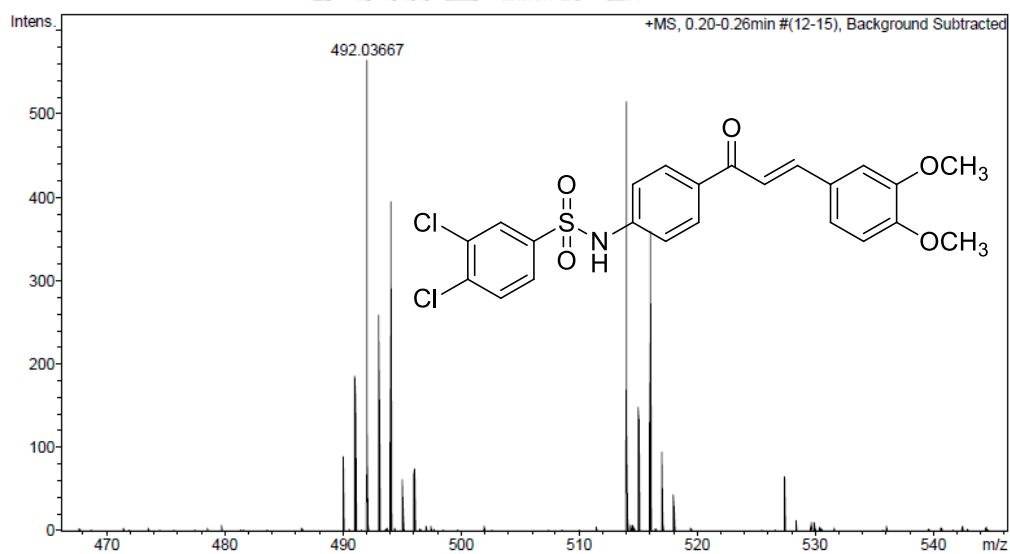


Figure A.148 The HR-MS (ESI) of 101

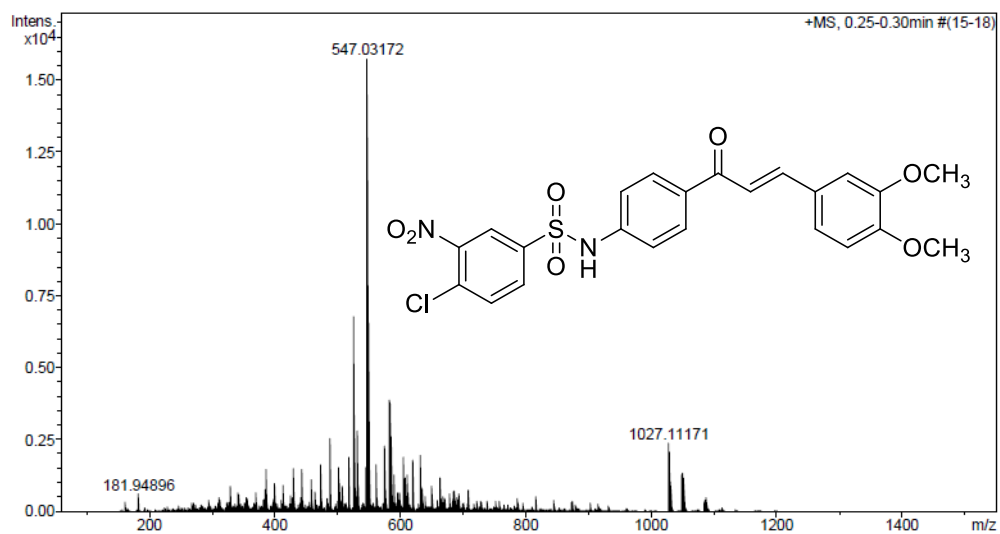


Figure A.149 The HR-MS (ESI) of 102

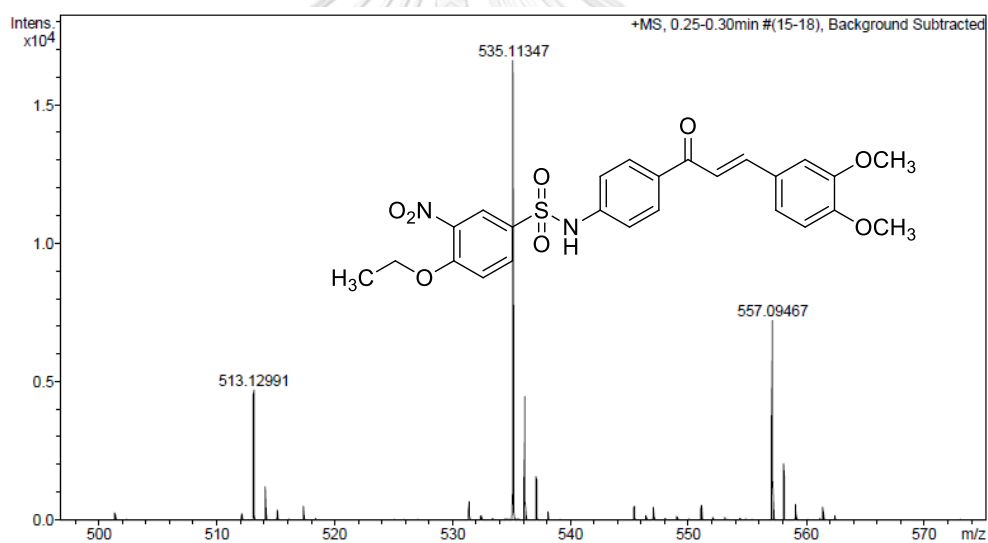


Figure A.150 The HR-MS (ESI) of 103

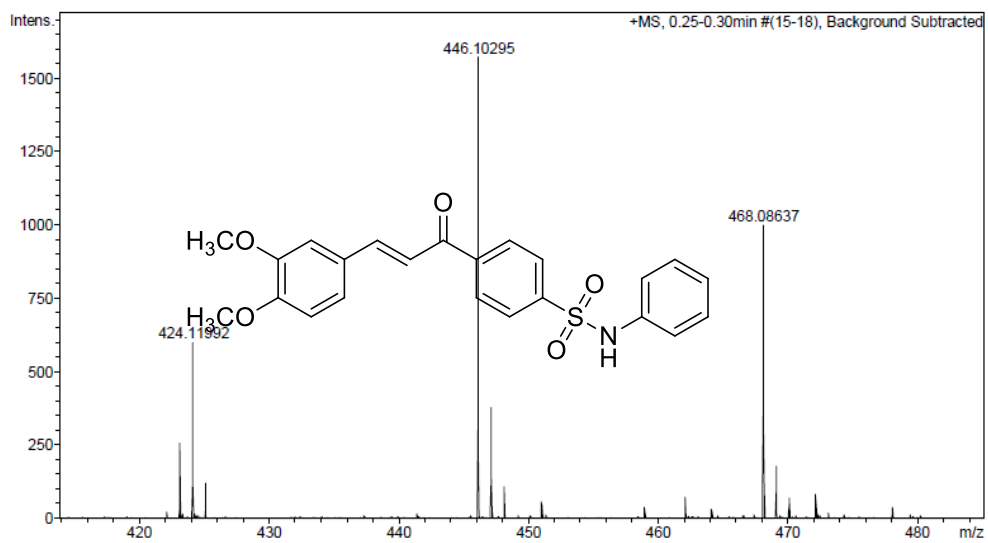


Figure A.151 The HR-MS (ESI) of 112

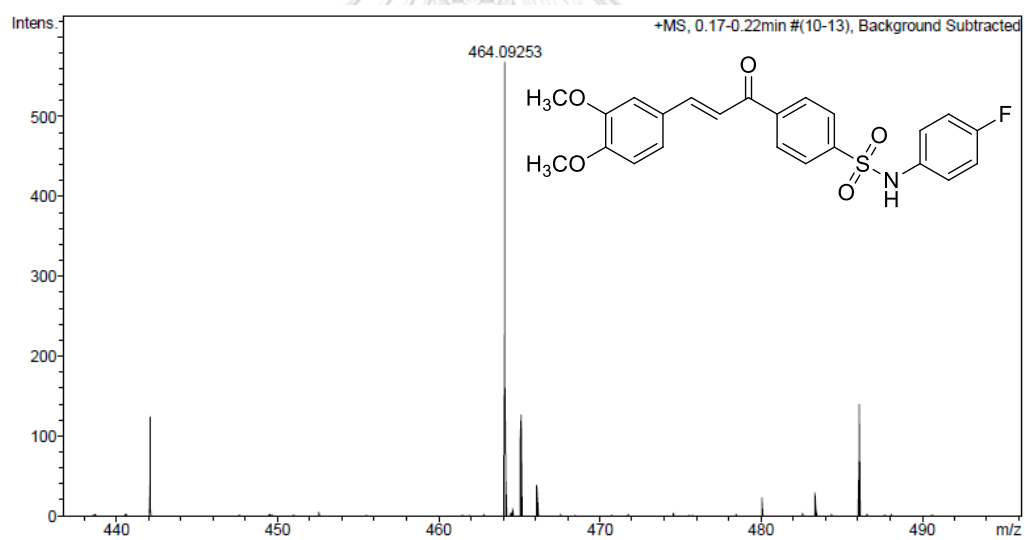


Figure A.152 The HR-MS (ESI) of 113

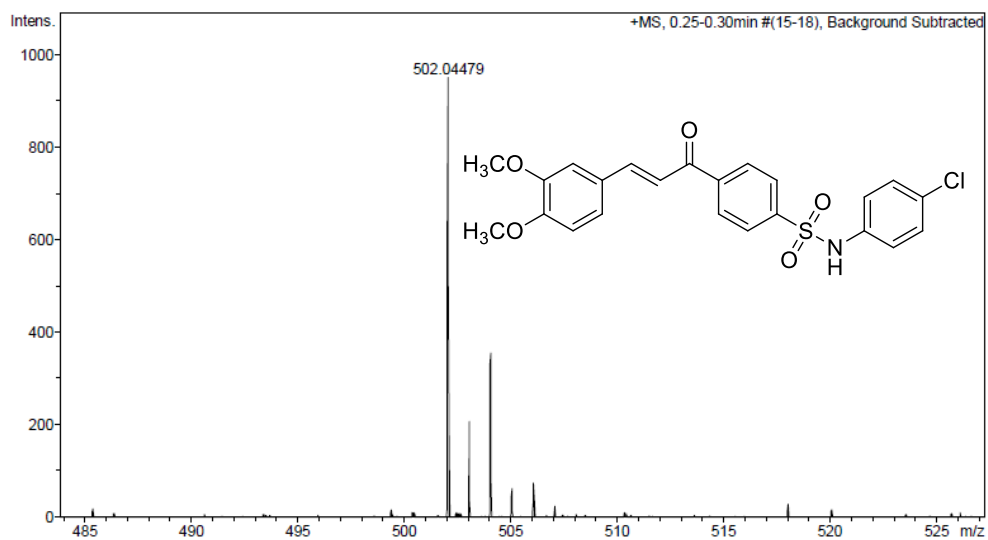


Figure A.153 The HR-MS (ESI) of 114



REFERENCES



จุฬาลงกรณ์มหาวิทยาลัย
CHULALONGKORN UNIVERSITY

1. Zhuang, C.; Zhang, W.; Sheng, C.; Zhang, W.; Xing, C.; Miao, Z., Chalcone: a privileged structure in medicinal chemistry. *Chem. Rev.* **2017**, *117*, 7762-7810.
2. Ayabe, S.; Uchiyama, H.; Aoki, T.; Akashi, T., Plant phenolics: phenylpropanoids. *Comprehensive Natural Products II* **2010**, 929-976.
3. Sun, H.; Li, Y.; Zhang, X.; Lie, Y.; Ding, w.; Zhao, X.; Wang, H.; Song, X.; Yao, Q.; Zhang, Y.; Ma, Y.; Wang, R.; Zhu, T.; Yu, P., Synthesis, α -glucosidase inhibitory and molecular docking studies of prenylated and geranylated flavones, isoflavones and chalcones. *Bioorg. Med. Chem. Lett.* **2015**, *25*, 4567-4571.
4. Cai, C.-Y.; Rao, L.; Rao, Y.; Guo, J.-X.; Xiao, Z.-Z, Cao, J.-Y.; Huang, Z.-S.; Wang, B., Analogues of xanthenes-chalcones and bis-chalcones as α -glucosidase inhibitors and anti-diabetes candidates. *Eur. J. Med. Chem.* **2017**, *130*, 51-59.
5. Rocha, S.; Sousa, A.; Ribeiro, D.; Correia, C. M.; Silva, V. L. M.; Santos, C. M. M.; Silva, A. M. S.; Araoo, A. N.; Fernandes, E.; Freitas, M., A study towards drug discovery for the management of type 2 diabetes mellitus through inhibition of the carbohydrate-hydrolyzing enzymes α -amylase and α -glucosidase by chalcone derivatives. *Food Funct.* **2019**, *10*, 5510-5520.
6. Hisieh, C.; Hisieh, T.; Ei-Shazly, M.; Chuang, D.; Tsai, Y.; Yen, C.; Wu, S.; Wu, Y.; Chang, F., Synthesis of chalcone derivatives as potential anti-diabetic agents. *Bioorg. Med. Chem. Lett.* **2012**, *22*, 3912-3915.
7. Wu, J.; Li, J.; Cai, Y.; Pan, Y.; Ye, F.; Zhang, Y.; Zhao, Y.; Yang, S.; Li, X.; Liang, G., Evaluation and discovery of novel synthetic chalcone derivatives as anti-inflammatory agents. *J. Med. Chem.* **2011**, *54*, 8110-8123.
8. Israf, D. A.; Khaizurin, T. A.; Syahida, A.; Lajis, N. H.; Khozirah, S., Cardamonin inhibits COX and iNOS expression *via* inhibition of p65NF- κ B nuclear translocation and IK-B phosphorylation in RAW 264.7 macrophage cells. *Mol. Immunol.* **2007**, *44*, 673-679.
9. Srinivasan, B.; Johnson, T. E.; Lad, R.; Xing, C., Structure-activity relationship studies of chalcone leading to 3-hydroxy-4,3',4',5'-tetramethoxychalcone and its analogues as potent nuclear factor κ B inhibitors and their anticancer activities. *J. Med. Chem.* **2009**, *52*, 7228-7235.

10. Sugii, M.; Ohkita, M.; Taniguchi, M.; Baba, K.; Kawai, Y.; Tahara, C.; Takaoka, M.; Matsumura, Y., Xanthoangelol D isolated from the roots of *Angelica keiskei* inhibits endothelin-1 production through the suppression of nuclear factor κ B. *Biol. Pharm. Bull.* **2005**, *28*, 607-610.
11. Kim, H. D.; Li, H.; Han, E. Y.; Jeong, H. J.; Lee, J. H.; Ryu, J.-H., Modulation of inducible nitric oxide synthase expression in LPS-stimulated BV-2 microglia by prenylated chalcones from *Cullen corylifolium* (L.) Medik. through inhibition of I- $\text{KB}\alpha$ degradation. *Molecules* **2018**, *23*, 109.
12. Lahsasni, S. A.; Al Korbi, F. H.; Aljaber, N. A.-A., Synthesis, characterization and evaluation of antioxidant activities of some novel chalcones analogues. *Chem. Cent. J.* **2014**, *8*, 32-41.
13. Mok, B.L., The synthesis of functionalised sulfonamides. *ProQuest LLC* **2013**.
14. Skillman, T. G.; Feldman, J. M., The pharmacology of sulfonyleureas. *Am. J. Med.* **1981**, *70*, 361-372.
15. Riaz, S.; Khan, I. U.; Bajda, M.; Ashraf, M.; Qurat-ul-Ain; Shaukat, A.; Rehman, T. U.; Mutahir, S.; Hussain, S.; Mustafa, G.; Yar, M., Pyridine sulfonamide as a small key organic molecule for the potential treatment of type-II diabetes mellitus and Alzheimer's disease: *In vitro* studies against yeast α -glucosidase, acetylcholinesterase and butyrylcholinesterase. *Bioorg. Chem.* **2015**, *63*, 64-71.
16. Wang, G.; Chen, M.; Wang, J.; Peng, Y.; Li, L.; Xie, Z.; Deng, B.; Chen, S.; Li, W., Synthesis, biological evaluation and molecular docking studies of chromone hydrazone derivatives as α -glucosidase inhibitors. *Bioorg. Med. Chem. Lett.* **2017**, *27*, 2957-2961.
17. Taha, M.; Irshad, M.; Imran, S.; Chigurupati, S.; Selvaraj, M.; Rahim, F.; Ismail, N. H.; Nawa, F.; Khan, K. M.; Synthesis of piperazine sulfonamide analogs as diabetic-II inhibitors and their molecular docking study. *Eur. J. Med. Chem.* **2017**, *141*, 530-537.
18. Nassir, N.; Yatimah, A.; Zanariah, A.; Raied, M. S.; Ekhlass, M. T.; Aidil, A. H., Synthesis and antibacterial evaluation of some novel imidazole and benzimidazole sulfonamides. *Molecules* **2013**, *18*, 11978-11995.

19. Bano, S.; Javed, K.; Ahmad, S.; Rathish, I.G.; Singh, S.; Alam, M.S., Synthesis and biological evaluation of some new 2-pyrazolines bearing benzene sulfonamide moiety as potential anti-inflammatory and anti-cancer agents. *Eur. J. Med. Chem.* **2011**, *46*, 5763-5764.
20. Muzammi, T. P.; Khetani, D.B., Synthesis and characterization of Schiff base m-nitro aniline and their complexes. *Res. J. Chem. Sci.* **2015**, *5*, 52-55.
21. Oana M. D.; Florentina, L.; Cornelia, V.; Mihai, M.; Valentin, N.; Romona, F.; Dragos, P.; Lenuta, P., Synthesis and biological evaluation of new 2-azetidinones with sulfonamide structures. *Molecules* **2013**, *18*, 4140-4157.
22. Lobb, K.L.; Hipskind, P.A.; Aikins, J.A.; Alvarez, E.; Cheung, Y.; Considine, E.L.; Dios, A.D.; Durst, G.L.; Ferritto, R.; Grossman, C.S.; Giera, D.D.; Hollister, B.A.; Huang, Z.; Iversen, P.W.; Law, K.L.; Li, T.; Lin, H.; Lopez, B.; Lopez, J.E.; Cabrejas, L.M.M.; McCann, D.J.; Molero, V.; Reilly, J.E.; Richett, M.E.; Shih, C.; Teicher, B.; Wikel, J.H.; White, W.T.; Mader, M.M., Acyl sulfonamide anti-proliferatives: benzene substituent structure-activity relationships for a novel class of antitumor agents. *J. Med. Chem.* **2004**, *47*, 5367-5380.
23. Seo, W.D.; Kim, J.H.; Kang, J.E.; Ryu, H.W.; Curtis-Long, M.J.; Lee, H.S.; Yang, M.S.; Park, K.H. Sulfonamide chalcone as a new class of α -glucosidase inhibitors. *Bioorg. Med. Chem. Lett.* **2005**, *15*, 5514–5516.
24. Thomas, R. L.; Halim, S.; Sivaprasad, S.; Owens, D. R., IDF Diabetes Atlas: A review of studies utilising retinal photography on the global prevalence of diabetes related retinopathy between 2015 and 2018. *Diabetes research and clinical practice* **2019**, *157*, 107840.
25. Eisenbarth, G.S., Type I diabetes mellitus. A chronic autoimmune disease. *J. Med.* **1986** *314*, 1360–13682.
26. Atkinson, M. A.; Eisenbarth, G.S.; Michels, A. W., Type 1 diabetes. *Lancet* **2014**, *383*, 69–82.
27. Diabetes prevention trial–type 1 diabetes study group. Effect of insulin in relatives of patients with type 1 diabetes mellitus. *J. Med.* **2002**, *346*, 1685–1691.
28. Insel, R. A.; Dunne, J. L.; Atkinson, M. A.; Chiang, . L.; Dabelea, D.; Gottlieb, P. A.; Greenbaum, C. .; Herold, K. C.; Krischer, . P.; Lernmark, A.; Ratner, R. E.; Rewers, M;

- Schatz, D. A.; Skyler, . S.; Sosenko, J. M.; Ziegler, A., Staging presymptomatic type 1 diabetes: a scientific statement of JDRF, the Endocrine society, and the American Diabetes Association. *Diabetes Care* **2015**, *38*,1964–1974.
29. Seino, Y.; Nanjo, K.; Tajima, N. Kadowaki, T.; Kashiwagi, A.; Araki, E.; Ito, C.; Inagaki, N.; Iwamoto, Y.; Kasuga, M.; Hanafusa, T.; Haneda, M.; Ueki, K., Report of the committee on the classification and diagnostic criteria of diabetes mellitus. *J. Diabetes Invest.* **2010**, *1*,212–228.
30. Yagihashi, S., Clinical staging of type 2 diabetes: the time has come. *J. Diabetes Invest.* **2010**, *3*, 1-2.
31. DeFrono, R. A.; Ferrannini, E.; Groop, L.; Henry, R. R.; Herman, W. H.; Holst, J. J.; Hu, F. B.; Kahn, C. R.; Ra, I.; Shulman, G. I.; Simonson, D. C.; Testa, M. A.; Weiss, R., Type 2 diabetes mellitus. *Nat. Rev. Dis. Primers* **2015**, 15019.
32. DeFronzo, R. A.; Abdul-Ghani, M. A., Preservation of β -cell function: the key to diabetes prevention. *J. Clin. Endocrinol. Metab.* **2011**, *96*, 2354–2366.
33. Holman, R.R.; Cull, C.A.; Turner, R.C., A randomized double-blind trial of acarbose in type 2 diabetes shows improved glycemic control over 3 years. *Diabetes Care* **1999**, *22*, 960.
34. Kimura, K.; Lee, J.H.; Lee, I.S.; Lee, H.S.; Park, K.H.; Chiba, S., Two potent competitive inhibitors discriminating alpha-glucosidase family I from family II. *Carbohydr. Res.* **2004**, *339*,1035.
35. Lebovitz, H. E., α -Glucosidase inhibitors. *Endocrinol Metab. Clin. North.* **1997**, *26*, 539-551.
36. Wehmeier, U.F.; Piepersberg, W., Biotechnology and molecular biology of the alpha-glucosidase inhibitor acarbose. *Microbiol. Biotechnol.* **2004**, *63*, 613.
37. Park, K. H.; Kim, J. H.; Seo, W. D.; Ryu, Y. B.; Ryu, H. W.; Lee, W. S.; Gal, S. W., Preparation of chalcone derivatives as glycosidase inhibitors. PCT/KR2006/001227. WO 2007/11453. **2007**.
38. Bahekar, S.P.; Hande, S.V.; Agrawal, N.R.; Chandak, H.S.; Bhoj, P.S.; Goswami, K.; Reddy, M.V.R., Sulfonamide chalcones: Synthesis and *in vitro* exploration for therapeutic potential against *Brugia malayi*. *Eur. J. Med. Chem.* **2016**, *124*, 262-269.

39. Kim, B.-T.; Chun, J.-C.; Hwang, K.-J., Synthesis of dihydroxylated chalcone derivatives with diverse substitution patterns and their radical scavenging ability toward DPPH free radicals. *Bull. Korean Chem. Soc.* **2008**, *29*, 1125-1130.
40. Ramadhan, R.; Phuwapraisirisan, P., New arylalkanones from *Horsfieldia macrobotrys*, effective antidiabetic agents concomitantly inhibiting α -glucosidase and free radicals. *Bioorg. Med. Chem. Lett.* **2015**, *25*, 4529-4533.
41. Alrubaie, L. A.; Muhasin, R. J.; Mousa, M. N., Synthesis, characterization and evaluation of anti inflammatory properties of novel α , β -unsaturated ketones. *Trop. J. Pharm. Res.* **2020**, *19*, 147-154.
42. Bharatham, K.; Bharatham, N.; Park, K. H.; Lee, K. W., Binding mode analyses and pharmacophore model development for sulfonamide chalcone derivatives, a new class of α -glucosidase inhibitors. *J. Mol. Graph. Model.*, **2008**, *26*, 1202-1212.
43. Gani, R.S.; Timanagouda, K.; Madhushree, S.; Joshi, S. D.; Hiremath, M. B.; Mujawar, S. B. H.; Kudva, A. K., Synthesis of novel indole, 1,2,4-triazole derivatives as potential glucosidase inhibitors. *J. King Saud Univ. Sci.* **2020**, *32*, 3388-3399.
44. Nipun, T. S., Khatib, A.; Ibrahim, Z.; Ahmed, Q. U.; Redzwan, I. E.; Saiman, M. Z.; Supandi, F.; Primaharinastiti, R.; El-Seedi, H. R., Characterization of α -glucosidase inhibitors from psychotria malayana Jack leaves extract using LC-MS-based multivariate data analysis and *in-silico* molecular docking. *Molecules* **2020**, *25*, 5885-5901.
45. Jenis, J.; Baiseitova, A.; Yoon, S. H.; Park, C.; Kim, J. Y.; Li, Z. P.; Lee, K. W.; Park, K.H., Competitive α -glucosidase inhibitors, dihydrobenzoxanthenes, from the barks of *Artocarpus elasticus*. *J. Enzyme Inhib. Med. Chem.* **2019**, *34*, 1623-1632.
46. Brylinski, M., Aromatic interactions at the ligand-protein interface: implications for the development of docking scoring functions. *Chem. Biol. Drug Des.*, **2017**, *91*, 380-390.
47. McGaughey, G. B.; Gagné, M.; Rappé, A. K., π -Stacking Interactions. *J. Biol. Chem.*, **1998**, *273*, 15458-15463.

48. Roskoski, R., Modulation of enzyme activity. *xpharm: the comprehensive Pharmacology Reference* **2007**, 1-11.



VITA

NAME I Putu Sukanadi

DATE OF BIRTH 24 June 1994

PLACE OF BIRTH Sampaka

INSTITUTIONS ATTENDED Chulalongkorn University

HOME ADDRESS Matahari Street, Bumi Sejahtera Village, Kaliorang Sub-district, Kutai Timur District, Kalimantan Timur, Indonesia, 75384

